UNDERGROUND ICE IN PERMAFROST, MACKENZIE

DELTA-TUKTOYAKTUK PENINSULA, N.W.T.


by


WILLIAM ALAN GELL

B.Sc., Liverpool University, 1971
M.A., University of British Columbia, 1973


A THESIS SUBMITTED IN PARTIAL FULFILMENT OF

THE REQUIREMENTS FOR THE DEGREE OF

DOCTOR OF PHILOSOPHY


in the Department

of

Geography


We accept this thesis as conforming to
the required standard

In presenting this thesis in partial fulfilment of the requirements for an advanced degree at the University of British Columbia, I agree that the Library shall make it freely available for reference and study. I further agree that permission for extensive copying of this thesis for scholarly purposes may be granted by the Head of my Department or by his representatives. It is understood that copying or publication of this thesis for financial gain shall not be allowed without my written permission.

Department of _GEOGRAPHY_

The University of British Columbia
2075 Wesbrook Place
Vancouver, Canada
V6T 1W5

Date _30 MARCH 1976_

ABSTRACT

A study was made of the petrology of a variety of underground ice types in permafrost on the Tuktoyaktuk Peninsula and Pelly Island, Mackenzie Delta, N.W.T. Ice bodies of a considerable range of ages occur, including some deformed in the Wisconsin glaciation; also permafrost and ice is growing ab initio beneath recently drained lake bottoms. The spectrum of ice body size is also wide, extending from pore-sized particles to beds 25 m thick.

The major objective of the study was an understanding of the growth and deformation of such ice bodies from a petrologic viewpoint. Thus several bodies of known, recent, age were analyzed in order to enumerate features typical of growth. This was possible for icing mounds, tension cracks and active layer ice which grew in winter 1973-74. Growth conditions were inferred in terms of water supply, freezing directions and rates, solute rejection (bubble formation) and crystal size, shape, lattice and dimensional orientation.

On the basis of this knowledge of growth features, older and larger ice bodies were studied, and post-solidification characteristics were analyzed. Some near-surface ice gave evidence of thermomigration of bubbles, but the major changes in fabric were due to thermally and mechanically induced stresses. In the case of wedge ice, progressive changes in crystal size, shape, lattice and dimensional orientation were recognized from the centre to the boundary of the wedge, due to recrystallization and grain growth associated with wedge development.

Segregated ice was studied in pingos and an involuted hill. A pingo core with steeply-dipping beds showed little evidence of flow while a broader pingo with a greater pore ice content had undergone some flow in the segregated ice layers. A range of fabrics was found in the involuted hill, optic axis orientations becoming increasingly concentrated normal to compositional layering while dimensional orientations tended towards parallelism with the layering in anticlines in the ice. The influence of bubbles on deformation is pointed out in that larger crystals occur in clear ice and thus have greater intracrystalline slip than in bubbly ice. Where a wedge penetrated such a fold, the fabric changed along the fold limb in a manner symmetrically related to the wedge.

Additionally, several near-surface ices were studied and showed evidence of multiple growth periods, and multiple freezing directions, indicating that the ice grew in enclosed water in frozen material. Thus the complexity of freezing and melting histories may be recognized petrographically while it is not readily apparent in the field.

LIST OF CONTENTS

LIST OF CONTENTS (cont'd)

LIST OF TABLES

LIST OF FIGURES

LIST OF FIGURES (cont'd)

LIST OF FIGURES (cont'd)

LIST OF FIGURES (cont'd)

LIST OF FIGURES (cont'd)

# ACKNOWLEDGEMENTS

# Chapter 1

## INTRODUCTION

Permafrost is a temperature condition of soil and rock materials where these materials have been maintained below $0^{\circ}$C for a minimum of two years. Two broad zones of permafrost are recognized, (a) continuous, (b) discontinuous. (a) In the continuous zone permafrost is present everywhere beneath the surface, except below large water bodies. A temperature of $-5^{\circ}$C exists at the southern boundary, at the depth of zero annual amplitude (about 15 m) and permafrost may reach 1000 m in thickness, under Baffin Island for example. (b) In the discontinuous zone permafrost may be locally absent; where present it is thinner than in the continuous zone, and variable in thickness.

From the temperature conditions it is evident that water in permafrost may be in the solid form, but this is not necessarily the case as substantial amounts of liquid water may be adsorbed on clays (Williams 1967), and also saline permafrost has been reported.

Where ground ice occurs it may be in one of a wide range of forms; coatings on sediment particles, pore cement, individual grains, veins, infils in cracks, or massive beds. In the continuous permafrost zone all types may be actively growing, whereas in the discontinuous zone ice bodies are generally smaller and inactive. In particular, ice wedges are inactive in the discontinuous zone (Brown and Péwé 1973). Ice may grow and melt annually in the seasonally freezing and thawing layer, or active layer, above permafrost. Thus some forms are transient. In the thick continuous permafrost zone, permafrost aggradation and associated ground ice growth is being monitored (Mackay 1973a) beneath recently drained lake bottoms adjacent to very old

permafrost and contained ice. Some of these old bodies have been deformed by Wisconsin ice sheets (Mackay, Rampton and Fyles 1972). Thus ice bodies in permafrost are of widely ranging ages and histories.

The permafrost literature has abundant references to surficial forms underlain by ice, for example a range of ice-cored mounds has been recognized (French 1971). However, there has been less advance in understanding mechanisms of growth and deformation of ground ice. Some aspects of the petrology of ice wedges (Black 1953; Corte 1962a) and beds (Corte 1962a; Mackay and Stager 1966a) including ice in submarine permafrost (Mackay 1972a) have been studied, but no comprehensive theory of growth and subsequent history of such ice bodies from a petrologic viewpoint is at hand.

Valuable contributions to our knowledge of a range of ground ice types have come from papers by Mackay (1966, 1971, 1973a). Heat conduction theory has been applied to the freezing of massive ice bodies, and the results tested by detailed field measurement of pingo growth (Mackay 1973a). The cracking patterns of ice wedges have been studied at several sites over a period of years (Mackay 1974a). Also a discussion has been presented of the development of reticulate ice veins in fine-grained materials (Mackay 1974b, 1975c).

The above work has been based largely on observations of exposed ice bodies and ice grown under known conditions. Such exposures and monitoring are rare and criteria for recognizing ice type and growth and deformation history from limited samples are needed.

In the past 13 years there have been two international conferences on permafrost, which included papers on ground ice. The First International

Conference on Permafrost was held in 1963 and the proceedings were published

in 1966, which contained little reference to the petrology of ground ice

although it was mentioned as an aid in ice classification. The moderator's

report of that conference included the following statements concerning

ground ice (p. 550):

> Shumskii and Vtiurin present a classification based on genetic
> principles. Unfortunately the origins of many ground ice masses
> are not yet well enough known to place them in such a classifica-
> tion. There is an immediate need for more detailed knowledge of
> the physical properties and structural peculiarities of the various
> types of massive ground ice... At present two types of massive
> ground ice can be distinguished: (1) Pingo ice - characterized
> by translucent, large-size, simple shaped crystals and by the
> occasional scarcity or more often the complete absence of internal
> structures. (2) Ice-wedge ice - consisting of small size crystals
> and showing a distinct vertical to inclined foliation. A consid-
> erable amount of mineral and organic material is aligned with the
> foliation.
>
> So far all other varieties of massive ground ice must be lumped
> together with only the certainty that there are more types to be
> distinguished when more complete descriptions and quantitative
> data are available. The possible Taber ice is in this group.
> The thick tabular sheets of ground ice characterized by horizontal
> layering with frequent dirty ice layers reported from the Mackenzie
> Delta, northeast Greenland, and various places in Siberia may be
> another distinct type.

In presenting suggestions for future research on massive ground ice, it

was stated that (p. 551):

> ...Perhaps the greatest present need in the study of massive ground
> ice is for quantitative information on the ice bodies and the ice
> itself... Information should also be collected on bubble size,
> shape, and distribution... A further concentrated application of
> petrofabrics to all types of massive ground ice is needed.

The above statements were made in 1963, but by the time the Second

International Conference on Permafrost took place in Yakutsk in 1973, little

such work had been carried out. In a review paper on the origin, composition

and structure of perennial frozen ground and ground ice, Mackay and Black
(1973) referred to the inclusion characteristics of ices, but the only mention
of c-axis distributions was based on the early work of Black (1954). Thus
it appeared that no new studies on the petrology of ground ice had been
carried out in North America in the years 1963-1973. Again the recommenda-
tion was made (Mackay and Black 1973, p. 190) that:

> A descriptive classification and unified terminology of all ground
> ice types and of related morphologic forms should be adopted
> before the Third International Permafrost Conference meets.

This summarized the state of ground ice petrology at that time. In
1974, the Ad Hoc Study Group on Permafrost of the Committee on Polar Research,
NRC-NAS, produced a survey of "Priorities for Basic Research on Permafrost."
This included the following statement:

> Specific studies of the petrology, geochemistry, and physical
> characteristics of ground ice are rare and grossly insufficient
> to provide the understanding necessary for detecting, delimiting,
> and identifying ground ice by indirect means such as airborne
> and satellite sensors and geophysical techniques. In fact, ground
> ice as it appears in cores has not been sufficiently studied to
> permit identification as to origin or to compare its chemistry,
> except rarely, with that of adjoining waters (pp. 31-32).

In addition it was pointed out that crystal characteristics are important
in determining rheological properties of ice bodies and permafrost. From a
terminological point of view it was stated that for ground ice:

> No generally unified terminology exists, since each discipline
> and country uses its own with only certain words common to many.
> A standardized terminology should be developed (p. 31).

In terms of classifications of ground ice, the committee concluded that:

> A variety of ground-ice classifications exist(s) for specific
> purposes, but there is neither a generally accepted descriptive

morphometric classification, nor a genetic classification. These
should be developed and accompanied by a standardized system of
symbols for field mapping and laboratory studies. Such a task
can best be implemented by a cooperative international effort
(p. 31).

A brief review of classifications is given in Chapter 2 of this thesis,

the point being made here is that the need for studies of the structure and

petrology of ground ice has been recognized, but very few papers have been

produced in North America.

The major objective of this study is an understanding of the growth

and deformational characteristics of ice bodies in permafrost. In terms of

ice growth, petrologic and petrofabric techniques are employed to determine

the mode of water supply to the freezing front, the growth directions and

growth rates, and mechanism of inclusion incorporation and its influence on

crystal characteristics. Post-freezing phenomena are investigated from a

petrologic viewpoint: thermomigration, flow and fracture. No field

measurements of flow and fracture are attempted.

Chapter 2

BACKGROUND TO THE PRESENT STUDY

1. Permafrost in the outer Mackenzie Delta - Tuktoyaktuk Peninsula Area

The modern Mackenzie Delta is generally a low, flat area, but on the distal boundary are islands of Pleistocene age reaching 50 m in altitude, due to glacier ice thrusting (Mackay 1971). Tuktoyaktuk Peninsula, of Pleistocene age, is predominantly low-lying but with abundant positive relief features in the form of involuted hills, and pingos which may reach up to 50 m.

The principal study area lies on the coast of the Beaufort Sea within a 30 km radius of Tuktoyaktuk, and a secondary area includes Pelly Island, one of the outer islands beyond the modern Delta (Fig. 1). The Pleistocene coastal plain in the Tuktoyaktuk area has been classified as "Undifferentiated coastlands" by Mackay (1963, p. 137). Parts of the coast are receding rapidly, especially where abundant ground ice occurs. The entire area is in continuous permafrost which may exceed 370 m (Jessop 1970) but locally depressions or through taliks in the permafrost occur below extensive water bodies which do not freeze to the bottom in winter. Drainage of such lakes provides conditions for permafrost aggradation. Examples have been monitored and described by Mackay (1973a). In one case coastal recession caused lake drainage, permafrost and then pingo growth. Thus old permafrost and contained ground ice is being degraded and removed in some areas, while new permafrost and ground ice grow nearby.
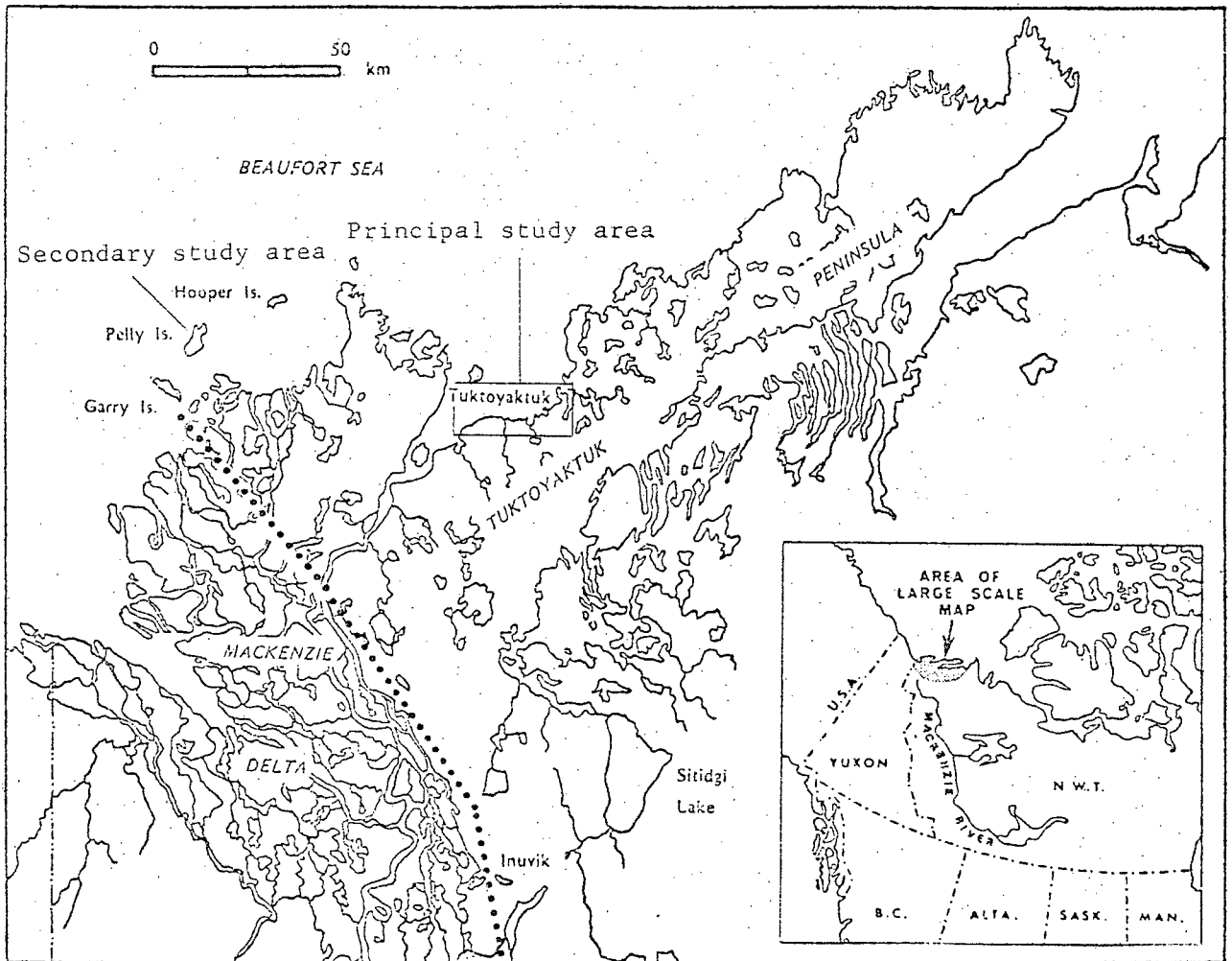
Figure 1a
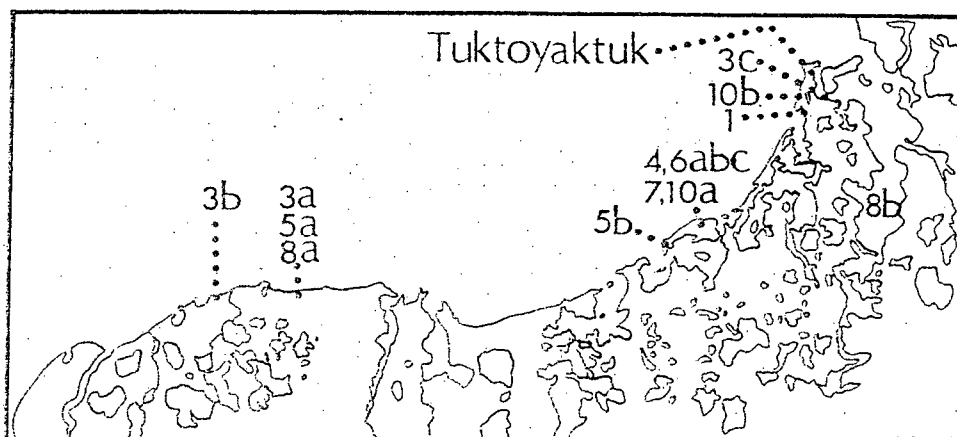


Figure 1b

Principal study area and sample sites

## 2. Thermal Characteristics

Detailed temperature data for the area are becoming available. The mean annual soil surface temperature is taken as -8° C (Mackay 1974c). However, variations in surface temperature are important in that thermal tension and compression occur annually, sometimes tensions are sufficient to cause fracture and the growth of ice wedges. Additionally the creep behaviour of ice is temperature dependent, and thermal gradients may cause thermomigration.

## 3. Ground Ice Types

Several ice types have been observed in the area; these have been enumerated by Mackay (1972b, p. 4): open cavity ice, wedge ice, vein ice, tension crack ice, closed cavity ice, epigenetic segregated ice, aggradational ice, sill ice, pingo ice and pore ice. These ice types have been studied by inspection of slump faces, probing of ice wedges, and drill-hole analysis.

From exposures and drill-hole records it is evident that ice underlies all major topographic highs. Thus ice is important in the geomorphic evolution of the area. However, exposures also show that there is no simple relation between surface form and the presence of ice at depth; for example large ice wedges may have no surface expression in the form of troughs, and abundant ice may underlie low-lying areas (Rampton and Walcott 1974). Also, mesoscopic features of ice bodies in chance exposures may not readily indicate the growth or deformation mechanisms which have operated. Few workers have employed standard petrologic techniques on ground ice; these methods are applied here to aid in understanding ice in permafrost.

Several classifications of underground ice types have been prepared (Shumskii and Vtiurin 1966; Vtiurina and Vtiurin 1970; Mackay 1972c). The classifications are based on such factors as place of development, origin of water, phase composition and modification of water (Vtiurina and Vtiurin 1970) or origin of water prior to freezing, principal transfer process and ground ice forms (Mackay 1972c). The petrology of the resulting ice was not included in such classifications; the present study will attempt to show the value of the approach.

4. <u>Previous Ground Ice Petrology Studies</u>

The pioneers in this field were Shumskii in the U.S.S.R. and Black in Alaska, who carried out their field work in the late 1940s. Black's work on ice wedges was published in 1963; more extensive results are available in his Ph.D. thesis (Black 1953) and an unpublished manuscript (1954). A wide range of ice types was studied by Shumskii whose research was translated into English in 1964.

The only later work outside the U.S.S.R. has been that of Corte (1962a), based on Greenland studies, Müller (1963) and some Japanese reports. Extensive work has been continued in Russia and Vtiurina and Vtiurin (1970) have summarized recent results. The proceedings of the First and Second International Conferences on Permafrost contain reference to ground ice petrology. Some of the major results of these studies are discussed below.

Shumskii (1964) grouped underground ice types under the heading of "congelation ice," including perennial vein ice (wedge ice), segregation ice and injection ice. The primary (growth) texture of wedge ice was

termed "allotriomorphic-granular" or "hypidiomorphic-granular"; also in-active, or "fossil" wedges were observed. The texture of segregation ice was described by Shumskii (1964, p. 222) as "hypidiomorphic-granular" and "allotrimorphic-granular" with crystals being elongated parallel to the freezing direction, and normal to the layering; air inclusions were also observed, and it was pointed out that there is a range of forms from pore ice to segregated ice. "Injection ice" was considered by Shumskii to be important in pingo growth. However, "injection" ice textures and petro-fabrics were not analyzed in detail, but studies showed very large grains with random lattice orientations. These data and the inclusion patterns were taken to indicate the freezing of large masses of intruded water.

The three ground ice types of wedge ice, segregation ice and injection ice were discussed by Shumskii; on the other hand, Black (1953) studied only ice wedges, but in greater detail. His field areas were near Fair-banks and Barrow, Alaska. Black defined some of the main fabrics to be expected in surface and buried wedges, and demonstrated that contraction and expansion of the ground caused flow and fracture of ice in wedges. Deformation fabrics were found to be superimposed on growth fabrics; the origin of some fabrics was not understood. Black pointed out the presence of inclusion "foliations" subparallel to the wedge sides, containing vertically oriented inclusions. Crystal size ranged from 0.1 mm to 100 mm; shapes were equidimensional, prismatic or irregular; and boundaries straight to sutured. Seven types of c-axis distribution were recognized, the three most widespread being (1) vertical, (2) normal to the wedge axis and horizontal, (3) normal to the wedge axis and inclined to one or both sides. Black recognized the importance of temperature gradients, the lateral stress system, and basal glide in fabric development.

Corte (1962a) investigated four patterned ground types at Thule, Greenland, and made correlations among surface pattern, grain size and structure of the active layer, and type and distribution of ground ice for the patterns investigated. Fabric analysis was performed on four ground ice types: - ice wedges, relict ice, ice mass and ice lens, and on contacts of ice wedges with relict and mass ice, and fabric criteria were found to be helpful in distinguishing ice types.

Vtiurina and Vtiurin (1970) summarized Russian work on ground ice development. They included discussion of the growth of pore ice, lens ice, injection ice, wedge ice and the burial of surface ice such as naleds and glacier ice. Little reference was made to petrologic aspects of the ice types; no petrofabric diagrams were presented, but crystal shape received some consideration.

Müller (1963) studied some crystal characteristics of pingo ice in the Tuktoyaktuk area, and compared this ice with wedge and glacier ice. Crystal size was measured and rubbings displayed crystal shape and contained bubbles. The bubbles were unusual in that they were parallel in a given crystal, but not in adjacent crystals. As no c-axis measurements were made in that study, the planes of bubbles could not be related to crystal structure; however it seems likely that they were in the basal plane. Crystal size was $>10$ mm mean diameter for pingo ice, and $<6$ mm for wedge ice. As pointed out by Müller crystal shapes differed markedly from those in glacier ice, either active or stagnant.

Some petrofabric analysis of a segregated ice body was carried out by Mackay and Stager (1966a); Mackay (1972b, p. 21) described a thin section of ice from a drill core from below the Beaufort Sea.

5. Terminology

The few papers concerned with the petrology of ground ice have no consistent terminology for fabric properties. Black (1953, p. 64) discusses the application of igneous and metamorphic rock terms in ice wedges, and points out that this should not be attempted as many such terms are genetic in connotation. Elsewhere Black (1953, p. 43) lists terms for types of dimensional lineation of crystals: holocrystalline, anhedral (zenomorphic), subhedral (hypautomorphic), euhedral (automorphic), equi-dimensional and elongated.

In contrast, Corte (1962a) did not employ such textural terminology, but used the terms "irregular" and "elongate" for crystal shape. Shumskii (1964) developed a more complex nomenclature (Table 1), and also gave a series of terms for frozen soil texture which is discussed in a later section.

Considering deformation textures, we find that Black (1953) discussed the transformation of growth "fabrics" by ground expansion in the summer causing horizontal stresses. Previous cracks with air bubbles and hoar infils become shear planes whereas cracks with clear ice are strong and shear takes place adjacent to them. Initial hoar crystals are recrystal-lized and reoriented. Black pointed out the importance of temperature and stress in determining the response of crystals (p. 76):

> Rapid flow or shear at low temperatures seems to produce small
> rectangular grains, but at high temperatures large sutured
> grains seem to result.
>
> ... optic axis lineations... seem to be due to the response of
> individual crystals to shear, in which crystals rotate to
> permit gliding on the basal plane...

| TERM | PAGE | CRYSTAL CHARACTERISTICS | ICE TYPES |
|---|---|---|---|
| Euhedral | 131 | Crystals bounded by regular faces. | |
| Allotriomorphic-granular | 171 | Isometric, anhedral, random c-axes. | Extruded ice; Perennial vein ice. |
| Hypidiomorphic-granular | 171 | Columnar, in a zone of geometric selection; also called crystalline granular; intermediate between allotriomorphic-granular and prismatic-granular. | Extruded ice; Perennial vein ice; segregation ice. |
| Prismatic-granular | 160 | Parallel-fibrous oriented growth; also called Panidiomorphic-granular. | Vein ice, naleds, segregated ice and possibly injected ice. |
| Intersertal | 178-9 | Rejected impurities arranged on grain boundaries (term also employed for frozen ground texture). | Congelation ice. |
| Poikilitic | 175,179 | Crystals containing insoluble solid impurities or fine air inclusions. | Congelation ice. |
| Cataclastic | 203,349 | Large primary crystals remain among fine crushed granules. | Perennial vein ice. |

Table I.   Shumskii's textural terminology.

Corte (1962a, p. 38) summarized his results on wedge ice as:

The smaller grains are those formed recently in a thermal
contraction crack, while those at each side (of the wedge)
are older grains formed by recrystallization from small ones.

## Soil texture

Interrelationships between ice and sediment have been considered
by Shumskii (1964) and Linell and Kaplar (1966). Shumskii distinguished
textures of frozen ground from ice textures: (1) intersertal - refers to
the in situ freezing of water without migration - ice grains fill the pores
and are usually smaller than the skeletal particles (Shumskii 1964, p. 214);
(2) poikilitic (p. 215) describes skeletal particles included in the large
crystals of the ice cement which has grown along the pores.

Linell and Kaplar (1966) produced a classification system of frozen
soils, and gave some descriptions on the basis of ice content, ice distribu-
tion and ice type ranging from ice coatings on particles to lenses.

From the above discussion it is evident that more work is needed on
the growth and deformation of ground ice with varying inclusion contents.
Since the publication of the above studies much experimental work on ice
has been performed, which is reviewed in the next section.

## 6. Ice Growth: A Review

### (a) Introduction

It is obvious that underground ice bodies have grown under widely
varying conditions of temperature, soil type, water supply, and time.
Petrologic data on solidification features of such ice are lacking. The
intention in this section is to review work on the growth of ice in lakes

and under experimental conditions. Consideration is given firstly to bulk

growth of ice from pure water; secondly to the redistribution of solutes

at an advancing ice-water interface; and thirdly to the rejection of solid

particles at the interface. The third case is the closest approach avail-

able in the literature, to ice growth in a porous medium. In the present

study we are concerned with such optically recognizable factors as grain

size, grain shape, dimensional orientation, substructure and crystallo-

graphic orientation relative to the growth direction; these factors are

important in the inference of growth directions, and also determine the

mechanical and other properties of a given ice body.


(b)  The Freezing of Bulk Water

Studies of lake ice and ice grown in the laboratory (Perey and

Pounder 1958) have shown that polycrystalline aggregates display at least

two texturally distinct zones:  (a) a zone of competitive growth at the

cooling surface (lake-air interface or laboratory cell wall); and (b) a

zone of elongated crystals aligned parallel to the heat flow direction.

A similar banding occurs in other materials, such as metal castings. In

the case of ice the textural zonation is accompanied by an increase in

lattice preferred orientation in the columnar zone. Numerous workers have

investigated crystal orientations in lake ice and preferred orientations

were usually found, although the orientations reported by different authors,

and in some cases the orientations in different parts of the same water

body varied from c-axis horizontal to c-axis vertical, to random. Michel

and Ramseier (1971) found vertical, random and horizontal preferred

orientations, but vertical columnar crystals had horizontal c-axes. Lab-

oratory controlled studies were also inconclusive (Perey and Pounder 1958;

Pounder 1963; Harrison and Tiller 1963) but a general tendency was found for c-axes normal to the growth direction. Several theories have been proposed to explain the appearance of preferred orientations. Most theories explain some experimental and field results, but not all. Ketcham and Hobbs (1957) studied the growth of two thousand grain pairs and established that the conditions for one grain (A) to encroach upon the other (B) are that: (1) B must have its c-axis tilted towards the line formed by the intersection of the grain boundary between A and B and the ice-water interface called "Line L", (2) the projection on the ice-liquid interface of the c-axis of B must be perpendicular to line L.

The major points to be extracted here are that in ice grown from the melt the initial growth is in a zone of randomly oriented crystals from which develops a zone of columnar crystals elongated parallel to the heat flow or freezing direction, but with c-axis orientations normal to that direction. Thus if these results can be applied to ice growth in permafrost we have useful criteria for determining growth directions. However, under naturally occurring conditions, ice growth does not usually occur in pure bulk water, and water supply is normally drawn through a porous medium. Thus we must consider these factors and their influence on growth conditions.

(c) Redistribution of Solutes

The growth of ice from aqueous solutions is more complex than for pure water because of the redistribution of solutes that occurs during solidification. Weeks and Assur (1964) presented a theory for sea ice based on the metals literature, but ground ice, except in unusual circumstances, has impurity concentrations far lower than in sea ice.

Solid solubility in ice is very low (Glen 1974) and as ice crystals grow there is rejection of solute at the interface into the liquid. Since redistribution is primarily by diffusion, concentration gradients are established in the liquid with the highest solute concentrations at the interface. Consequently an initially planar interface becomes unstable to changes in shape. Any ice projections into the zone of lower solute tend to grow and interdendritic spaces are rich in solute, thus irregularities appear on the columnar crystals. Although much of the solute content is rejected at the interface, some incorporation occurs at zones of disorder such as grain boundaries and lattice defects. In the case of insoluble foreign particles, dislocations are nucleated when particles are grown into the crystal. Where the crystal grows around the impurity, the dislocations are propagated into the growing crystal. When dendritic growth occurs, the interdendrite spaces eventually close, often with a misorientation, and joining occurs by dislocations. Other mechanisms of dislocation formation, and their mechanical significance are discussed later.

An important type of solute in water in the field situation is that which forms bubbles on freezing. The presence of gas bubbles in massive ground ice bodies has been pointed out by Mackay (1971), in ice lenses by Gold (1957) and Penner (1961) but no detailed discussion of their characteristics has been given.

Bubbles may be characterized by their size, shape, orientation, layering and changes in those properties. But firstly we must consider the nucleation of bubbles; this is approached through standard models of solute rejection at an advancing solid-liquid interface (Pohl 1954). The

distribution coefficient for air in the ice-water system is taken as 0.01, thus a strong concentration is established ahead of the interface in an air saturated liquid. Nucleation may occur on particles, but in experimental studies, Maeno (1967) and Bari and Hallett (1974, p. 508) showed that wetted particles did not produce this effect. Such would always be the case in the field situation; there nucleation probably occurs at points of high solute concentration. After nucleation, slow growth gives large spherical bubbles; intermediate growth gives a cylindrical shape parallel to the growth direction; in rapid freezing, bubbles are entrapped by advancing crystal so a small spherical form is retained (Chalmers 1959). Very rapid freezing gives insufficient time for bubble growth. The shapes are from theory; in practice differing shapes may occur close together, as depicted by Vasconcellos and Beech (1975 p. 83, Fig. 3), whose controlled experiments were performed on the water-ice-$CO_2$ system. In the field the situation is more complex, water supply through soil may vary, rates of heat extraction may vary, and freezing may be multidirectional for example in the active layer.

(d)  Substructure

Substructure is here defined as optically recognizable variations in lattice properties within a given crystal. Usually this is confined to differences in lattice orientation.

Dislocation formation and propagation due to dendritic growth and incorporation of foreign atoms has already been discussed. In addition, small angle boundaries can occur by the amalgamation of dislocations by climb. The sub-boundaries so formed intersect the solid-liquid interface and are propagated parallel to the growth direction, with misorientations

of several degrees.

Substructures may be produced during growth by mechanically, thermally, or compositionally induced stresses. Thermal gradients, especially non-uniform gradients, can produce stresses which will generate dislocations. As discussed above compositional changes occur with variations in freezing rate. The resultant fluctuations in lattice constant can produce dislocations. The concentration of dislocations is of fundamental importance to the deformation of ice crystals in post-solidification stress systems.

(e)  Laboratory Growth of Ice in Sediments

The growth of ice in porous media, especially soils, has been investigated for over 45 years. Early studies of soil freezing and associated ice growth were carried out by Taber (1930) and Beskow (1935). Taber pointed out that several factors were involved in ice segregation: size and shape of soil particles, availability of water, size and percentage of voids, rate of cooling, and resistance to heaving. A major contribution was Taber's demonstration (p. 308) that growing ice crystals are in contact with a water film adsorbed on mineral particles, and water flows through the film to nourish the growing crystals.

The results of Taber and Beskow were supported by the work of Corte (1962b). The base of a water-filled box was subjected to freezing temperatures while the top was maintained above 0° C. Some particles placed on the ice surface rose with the growing ice, indicating the presence of a water layer between the ice and soil particles. Such a process is analagous to freeze-back from the top of permafrost. If the experimental

system is inverted, the mechanism of ice lens growth is represented. In the case where a range of particle sizes is present, sorting occurs, the ice excluding those particles which can migrate through the pores.

Higashi (1958) performed experimental studies of frost heaving, and related ice segregation types to heaving. He classified three types of ice segregation:- (a) ice filament layer, (b) sirloin-type freezing, (c) concrete-type freezing. Types (a) and (b), with high ice content, occurred under conditions of slow freezing boundary penetration. Concrete freezing (c) did not show any degree of ice segregation and occurred under fast freezing conditions.

Penner (1961) grew ice lenses in soil with carefully controlled environment of temperature, pressure and water supply, and found that the structure of the lenses was not as uniform as anticipated. Ice grains were elongated in the direction of heat flow, but optic axis orientation in adjacent crystals was often markedly different. Also, crystal orientation was usually different above and below the soil occluded in the ice lens. This was probably a result of non-unidirectional heat flow around the contained soil. Penner's sample was restricted to only a few grains, so no statistical analysis could be applied.

Unpublished work by Kaplar and Goodby at CRREL (Kaplar, personal communication, 1974) produced results similar to those of Penner, but with a stronger concentration of optic axes parallel to the heat flow direction.

(f)  Rejection of Insoluble Particles at the Freezing Interface

The supply of water to ice bodies such as lenses is through a porous medium of sand or clay. Thus the ice-water interface is more complicated

than in the freezing of bulk water. Mackay (1973a) has pointed out the

major distinction between pore ice and segregated ice, which both form in

porous media. In addition, experimental studies (Uhlmann et al. 1964;

Hoekstra and Miller 1967) have been performed on the interaction between

insoluble suspended particles and the solid-liquid interface. These are

briefly reviewed. Uhlmann et al. (1964) used ice-water and other transparent

materials at varying freezing rates, and various suspensions, including

silt, with irregular-shaped particles, size ranging from 1 micron to several

hundred microns. At low growth velocities, particles were rejected at the

interface, and pushed for several centimetres. With closely spaced par-

ticles, as in soil, the process continued, impinging particles being pushed

together. (In the field there is a limit to the space available for

rejected particles.) With increasing freezing rate, a critical velocity

was found at which the particles ceased to be rejected and were incorporated

into the interface. There was, however, a dependence on particle size.

The critical velocity for particles less than $15\mu$ in diameter was inde-

pendent of size, whereas for larger particles, the larger the size the

lower the critical velocity for trapping.

Hoekstra and Miller (1967) performed experiments on the ice-water-

particle system, employing Pyrex-glass spheres and soft-glass cylinders

as foreign particles. With an upward-moving freezing interface, the

critical velocity was inversely proportional to the particle radius. They

also found that adding NaCl to the water caused reductions in the critical

velocity.

Uhlmann et al. (1964) and Hoekstra and Miller (1967) interpret the

rejection of particles as being due to an imbalance of surface tension

forces between the particle, water and ice. In order to satisfy the energy requirements and keep the particle ahead of the interface, liquid replenished the ice behind the particles. It was argued that the particle-interface separation decreased with increased freezing rate, and the critical velocity corresponded to the point at which further decrease of particle-interface separation would lower the chemical potential of the system, rendering the pushing configuration unstable and allowing incorporation of the particle. Grooves or depressions on the interface tended to trap the particles at lower growth rates. Thus it is to be expected that grain boundaries would trap solid particles.

Ketcham and Hobbs (1967) described an experiment whereby a piece of fine copper wire was placed in a sample of polycrystalline ice and observations were made of the ice surface as it grew into the water. It was found that grain boundaries moved away from the vicinity of the wire, which was ascribed to the wire forming a more efficient heat sink than the ice, thus causing the grains adjacent to the wire to protrude further into the water than the surrounding grains. Such variations in temperature across the ice interface due to inclusions would be expected to affect relative crystal growth.

(g) Conclusion

Few studies have been performed on the petrology of underground ice; however, the results of the more detailed studies of ice growth in laboratories and surface ice types (sea, lake, river) may be applied to permafrost conditions. Review of ice growth in bulk water has shown that freezing directions may be inferred in terms of zonation of crystal size and shape, bubble zones and bubble elongation direction. Bubble type

depends on freezing rate, as well as the amount of dissolved air in the water. In naturally occurring field situations freezing rates and solute contents are usually unknown, thus rigorous application of theory is impossible, but where bulk water freezes the general principles may be expected to hold. Under permafrost conditions water supply is generally through a permeable medium. From the review of rejection of insoluble particles at an ice-water interface, it is apparent that preferential rejection of fine-grained particles may occur but during rapid interface advance, all particles may be engulfed. Thus crude estimates of freezing rate may be gained from sediment content, although this also depends on water availability. Additionally during freezing, dislocations are incorporated in the crystal growth mechanism, and also at inclusions. Arrays of dislocations are of fundamental importance in deformation processes. It appears that the major differences in ice grown in sediment from ice grown in bulk water are crystal size, dislocation content and sediment incorporation which all influence flow characteristics.

7. Post-Freezing Phenomena

(a) Introduction

Some of the features resulting from freezing are subject to several thermally and mechanically induced phenomena, which must be recognized.

(b) Thermomigration

For the moment let us consider the thermal field and its effects. In permafrost conditions the upper 10 to 20 m of earth materials are subject to appreciable annual temperature variations. The resulting temperature gradients may give rise to thermomigration of inclusions. For example,

Stehle (1967) and Kheisin and Cherepanov (1969) have reported bubble migra-
tion and the breakup of cylindrical bubbles into strings of spherical bubbles
in lake ice. In addition the migration of saline inclusions in ice has been
observed. The migration of such droplets was observed in experiments by
Harrison (1965) as follows:- (a) droplet elongation in the migration direc-
tion, (b) diagonal migration -- due to migration parallel to the c-axis rather
than in the heat flow direction. It is evident that while a vertical temper-
ature gradient prevails in permafrost, migration might occur parallel to c-axes.
Thus thermomigration is a problem to be considered in ice petrology.


(c)   The Deformation of Ice

   (i)   Introduction

   Under natural permafrost conditions ice bodies are subject to various
stress fields, e.g. thermally induced stresses associated with annual expan-
sion and contraction of the upper ground layers; additionally some massive
ice bodies have thick cores (Mackay 1973b) which have suffered differential
uplift and may be expected to creep.

   Thus a review is made of the deformation mechanisms in ice,
based on laboratory and glacier studies, emphasis being given to petro-
graphic and petrofabric features. The most common experimental technique
in the study of the deformation of ice has involved exerting compressive,
tensile, or torsional stresses on a cylindrical sample of polycrystalline
ice. Frequently the experiments have been directed toward a quantitative
analysis of the flow, but often the results are interpreted in terms of
intracrystalline and intercrystalline sliding, etc. Some workers have

prepared thin sections from the initial and deformed ice in order to examine changes in crystal size, shape, orientation, substructure, and to relate these changes to the stress field. By this method bulk relationships are obtained, but detailed knowledge of individual crystals is not always available. Similarly, studies on glacier samples have been performed, but in these cases the stress and strain fields are poorly known, thus interpretation of fabric diagrams is difficult. In the present study no field measurements of strain were possible, but gross estimates are available from the theoretical work of Lachenbruch (1962) and comparison with glacier studies.

(ii)  Deformation mechanisms in ice

The major work in this field has been by Gold (1963, 1972), and by Kamb (1972) who performed long-term, high-temperature (-5°C to 0°C) experiments on polycrystalline ice, and presented photomicrographs and petrofabric diagrams representative of several stages of the flow. Earlier Steinemann (1954) and Shumskii (1958) deformed and annealed polycrystalline ice, and analyzed the recrystallization.

Kamb (1972) studied petrofabric and textural changes during flow, and showed that grain size and shape changed from 0.5 - 0.9 mm equant, straight sided grains to coarser, highly interlocking shapes by a grain boundary migration mechanism. The size increase was enhanced nearer the melting point. Strain shadows, frequent at all temperatures, were thought to indicate kinking during translation gliding on the basal plane. The initial petrofabric pattern of the ice was approximately random, but orientations became strongly preferred during recrystallization. Two maxima developed in simple shear, the stronger maximum being normal to the shear

plane and the second inclined at about 20° to the direction of shear. Shumskii (1958) found a similar pattern in a shear experiment, and argued that the major maximum comprised relatively unstrained grains grown during deformation, but Kamb (1972) found no such distinction.

An important result of Kamb's work was to show the dependence of petrofabrics on shear stress, by comparing petrofabrics of two samples deformed to the same total shear strain but at different stresses. He went on to discuss the relationship of grain size and shape to flow. The increase in grain boundary irregularity would be expected to decrease the role of grain boundary sliding, and grain coarsening should increase the creep rate. Intracrystalline plastic flow caused strain shadows, but these did not increase with total strain indicating that undistorted crystalline material was generated during recrystallization. It was found that the shape changes occurred much more rapidly than petrofabric changes, also texture is temperature-sensitive in that the higher the temperature the coarser the grain size. Conversely, petrofabrics show no such sensitivity.

If an attempt is made to relate textural changes to stress, there is the problem of temperature dependence, and the wide range of temperatures employed by different workers. But it is apparent from Kamb's (1972) work that grain boundary migration occurs over a wide range of stresses, including those below 1 kg cm$^{-2}$. Although polygonization and primary recrystallization were reported by Shumskii (1958) and Gold (1963) the two processes were not distinguished petrologically, nor were the stresses given. Kamb's (1972) results are helpful in that lattice orientations were measured, which showed that stresses > 1 kg cm$^{-2}$ are necessary for new crystal growth.

(d)  The Influence of Impurities on Deformation

### (i)  Introduction

Ice bodies in permafrost may contain inclusions in the solid, liquid or gaseous states.  Therefore as some deformation mechanisms depend on uninterrupted movement of boundaries and dislocations, foreign atoms or gross defects will affect the deformation process.

### (ii)  Solid Inclusions

The inclusions which are of primary interest in the study of the petrology of underground ice are sediment particles, rather than solid solutions, as only optical methods were employed in the present field study. Several workers have studied the creep of frozen soils and ice containing dispersed sand (Goughnour and Andersland 1968; Hooke et al 1972; Ladanyi 1972) but no thin section analyses were performed.  Thus the relationship of inclusions to grain characteristics is unknown.

The effect of immobile second phases on grain boundary motion is determined by the boundary type and position on the boundary.  High boundary curvature indicates the possibility of more rapid movement, and thus the inclusion will have little effect, whereas pinning of boundaries of lower curvature is likely.  The influence of second phases at crystal triple points has not been considered in the literature.

### (iii)  Gaseous Inclusions

A high concentration of gas bubbles occurs in all natural ices - glacier, lake, sea and permafrost ice - but the available literature contains no reference to field studies of the influence of such bubbles on deformation.

Also, the experimental work on the effect of bubbles on the deformation of ice is far from conclusive.

It is interesting to compare the results of Steinemann (1958), Kamb (1972) and Kuon and Jonas (1973) in terms of the influence of air bubbles on recrystallization and grain growth. Kamb (1972, p. 233) has pointed out that

> Since the changes in texture and fabric here in specimens
> containing abundant air bubbles were comparable to the
> changes observed by Steinemann (1958) in air-free samples,
> it follows that the air bubbles do not substantially
> inhibit the processes of recrystallization and grain growth.

On the other hand, Kuon and Jonas (1973) found a distinct influence of the air bubbles in retarding grain boundary motion, and thus influencing the grain growth process. The results of Kuon and Jonas (1973) are in agreement with other results in the materials science literature (Gleiter and Chalmers 1968) and in the absence of more detailed work on ice, are accepted here.

(e)     The Fracture of Ice

(i)     Introduction

Fracture occurs when the lattice loses cohesion. Fracture in columnar grained ice under compressive stress has been reviewed comprehensively by Gold (1972) but he did not treat the thermal contraction mechanism which is discussed below. Gold (1961) discussed the crystallographic dependence of cracks produced by thermal shock.

### (ii)  Thermal Stresses

The temperature of the upper few metres of permafrost varies sea-
sonally.  In particular, a steep vertical temperature gradient becomes
established in winter.  Thermal contraction is largely constrained, and
tensile strains arise, which are a function of the temperature difference
between the ground surface and an "average" temperature, and the coefficient
of thermal contraction over that temperature range.  There may be, however,
a rapid dissipation of thermal strain with time.

### (iii)  Factors Influencing Fracture

Crack patterns developing under thermal shock in ice plates were shown
by Gold (1961) to be dependent on the crystallographic orientation of the
ice with respect to the shocked surface.  A preference was found for the
surface trace of cracks to be parallel to the planes containing 'a' and
'c' directions.  Abrupt changes in crack direction in passing from one grain
to the next were observed.

In the failure experiments of Gold (1972) and others the ice samples
have been fairly pure or at least deaerated.  By comparison, permafrost
ice usually has a high bubble, sediment and solute content.  Also ground
ice may have a well-developed crystal substructure and varying crystal size
and shape, compared with the more uniform laboratory samples.  Further, all
ice bodies near the ground surface have complex cyclic stress histories and
may have been subject to substantial recrystallization, with an effect on
subsequent fracture characteristics.

(f)   Conclusion

Mackay (1971, 1972b) has pointed out the wide range of conditions to which various ground ice types are subject.   In the present review of post-solidification phenomena we have considered the response of ice to the experimental imposition of thermal gradients and mechanical loading, and pointed out petrologic criteria which may be applied to the field situation.

Chapter 3

TECHNIQUES

## 1. Introduction

The major objective of this study is an understanding of mechanisms of growth and deformation of ice bodies in permafrost in relation to their thermal, stress and geomorphic environments. To this end a sampling plan was established for exposed ice bodies such that stratigraphic and structural relations were known, and crystal and inclusion characteristics could be related to those data. Field and laboratory techniques are discussed separately.

## 2. Field Techniques

Maps of physiographic provinces were presented by Mackay (1963) and of sediment distribution by Rampton (1972 a,b); the distribution of ice bodies in the field area has not been given and mapping is not attempted here.

### Sampling

Sampling was restricted to those ice bodies exposed on coastal sections or subject to easy drilling. As an example, consider the case of an involuted hill, near Tuktoyaktuk. Here a massive ice core has been exposed for many years. It is apparent on 1935 air photographs (air photo #A 5023-87R). A sampling plan was devised to investigate:

(1) the relationship among crystal and inclusion characteristics and depth in core samples of relatively undeformed ice;

(2) the relationship of crystal and inclusion characteristics to

fold symmetry where differential uplift has occurred;

(3) the influence of wedge penetration in a fold.

Additionally core samples were taken from a 6 m deep pit for comparison with samples from the cliff exposures to investigate the effect on texture and petrofabrics of load release and changed thermal regime due to coastal recession. Elsewhere similar principles were employed in order to examine texture and petrofabrics with reference to macroscopic symmetry, e.g. foliations in ice wedges.

For the purpose of understanding post-solidification changes in a given ice type, bodies of known age (i.e. those which grew between the two field seasons of 1973 and 1974) were compared with older bodies. This was possible for tension crack ice, where crack ice in the active layer of 1973 was sampled in 1974. Also icing mounds which grew after freezeback of the 1973 active layer were sampled by Dr. J.R. Mackay; this provided information concerning solidification features and the response of early crystal layers to heave. Active layer ice was also studied.

In the case of ice grown in fractures the only ice of known age was the tension crack ice, mentioned above. No example of 1973-1974 wedge crack ice was obtained, although recent thermal contraction crack ice was found and the prograde fabrics of wedges penetrating sediment and massive ice were compared. Thus it was possible to compare ice growth in the two major fracture types: tension cracks (mechanically induced) and ice wedge cracks (thermally induced).

Lake ice was also studied in order to investigate the possibility of buried lake ice being mistaken for ice grown in situ.

A SIPRE corer and a chain saw were employed for sampling; this has been a standard method on other ice types, e.g. glaciers, sea and lake ice. It provided a rapid means of obtaining good core lengths of 75 mm diameter and was used with a power unit when cold storage facilities were nearby. Hand drilling was carried out in an underground pit and samples were stored there for transfer by helicopter to the laboratory.

Where coring was not possible, as around folds on cliffs, a chain saw was employed; this method was previously used on ground ice by Corte (1962a) and on glaciers by Colbeck and Evans (1973). As ice on the cliffs had suffered changes in loading and thermal conditions due to coastal retreat, a channel was first cut into the cliff and samples taken from the back of the channel and local variations in crystal and inclusion character- istics were sought, for example Tyndall figures. Additionally samples of cores from a man-made pit were compared with cliff samples. Sawn samples were transferred as quickly as possible, usually $< \frac{1}{2}$ hour, in freezer boxes to cold storage at -20° C.

The effect of storage on crystal characteristics has been studied by Carte (1961b) who showed that thin sections could be stored at -20° C for months without major adjustment of grain boundaries. Kamb (1972) stored thin sections at a similar temperature, and Bari and Hallett (1974) sug- gested storage at or below -20° C to avoid changes in bubble characteris- tics. In the present study most core and block samples were analyzed within a few days of sampling, but some were stored at $< -20°$ C for about 8-10 months. Thick sections were prepared and sandwiched between glass

slides with a vaseline seal around the edge, to prevent sublimation, and stored with the samples; photographic slides taken before and after storage showed no recognizable change. Thus it is concluded that stored samples are reasonably representative of the field situation.

3. Laboratory Techniques

Thin section preparation varied with the ice type, in terms of inclusion content and crystal size.

In the case of clean, fine crystalline ice, a microtome was used, as described by Langway (1958) and Michel and Ramseier (1971).

For coarsely crystalline ice, a more rapid method was employed, namely freezing a smoothed thickly sawn section to a slide, then thinning with a flat metal plate, and sand- and emery-paper. This is standard practice in glacier studies, and Kreitner (1969) showed, in a study of aufeis, that smoothing of sections with a warm iron produced no change in crystal characteristics.

In some ices there were bands of high sediment content, and the above two methods were impractical. In such cases gradual thinning was possible using emery paper and carborundum; sediment particles were removed with a point. As found by Black (1953) and Corte (1962a) the best temperature for thin section preparation was about -10°C.

As the study was field-based, only optical methods were employed. Thin section analysis and universal stage technique is standard, and no discussion is given here. Ice crystal c-axes were measured and in some cases a-axis orientations were found by etching, although this was not

widely employed. Where possible, at least 100 c-axes were measured and

plotted on equal area, lower hemisphere projections. In general, scatter

diagrams are given together with component diagrams based on such crystal

characteristics as size, shape, substructure, inclusion content and rela-

tionship to layerings. Most of the patterns show a high degree of pre-

ferred orientation and contouring is not always employed; but in order to

emphasize progressive changes in fabric some diagrams have been contoured

by Kamb's (1959) method. The method indicates the statistical significance

of orientation maxima. In the present work, contour intervals of $2\sigma$ are

used, where $\sigma$ is the standard deviation from the expected density of a

uniform population. Inclusion layerings, foliations, etc., are included

to show symmetry relationships. Crystal dimensional orientations are

given in separate diagrams.

Chapter 4

RESULTS

Permafrost conditions in the field area, the variety of contained ground ice types and their relationships to surficial form have been pointed out. It is the intention in the present chapter to discuss the growth and deformation of ice bodies largely from a petrologic viewpoint. Thus ice bodies of known ages ( < 1 year) were analyzed in order to enumerate typical growth features. Growth conditions are discussed in terms of water supply, freezing directions and rates, solute rejection (bubble formation) and crystal size, shape and lattice and dimensional orientation. With this knowledge as a foundation, consideration is given to older ice bodies, and post-solidification features are discussed in relation to deformation associated with, for example, growing ice wedges.

A summary diagram, based on Mackay's (1972b) classification of underground ice is given in Appendix 1. The diagram is an attempt at showing interrelationships among ice types, surface form, and water source and transfer mechanisms. Extra categories are included to indicate inclusion, textural and petrofabric features signifying growth and later conditions.

## Chapter Outline

An examination of lake ice introduces the discussion of ice types. The ice grew during winter 1973-74 and represents growth in bulk water. This is followed by consideration of several topographic rises of various sizes, underlain by ice with different inclusion contents. Such ice bodies, and also frozen sediment, may be fractured. Thus a discussion is given of mechanically- and thermally-induced fractures. This is followed by inves-

tigation of other ice types which differ in form and in relation to surface
expression. The importance of multiple growth and melt periods are pointed
out.

1. Lake Ice

Introduction

The possible existence of a variety of surface ices, which became
buried and preserved within permafrost, has been pointed out (Mackay 1972a,
p. 5) although they are thought to be uncommon in North America. The case
against a buried origin of massive ice bodies has been given by Mackay (1971,
1973b) in terms of ice body thickness, topographic position, stratigraphic
position, water quality, ice fabrics and bubble patterns. It is to be
expected that small ice bodies may have originated from buried snow banks,
lake ice or sea ice where coasts are actively slumping. It is the intention
in this section to examine non-buried lake ice, as an aid in distinguishing
such ice from underground ice grown in situ.

Field Characteristics

A site was chosen on a small shallow lake near Tuktoyaktuk. The
coring position was nearshore but not liable to slumping. A core 0.68 m
long was obtained, including dark ice at the top and the contact with
sediment and organic matter at the base.

Ice Characteristics

The upper 0.08 m comprised dark ice and the remainder had long
vertical bubbles. No disturbance of the pattern was observed, either in
terms of growth conditions or post-solidification structures.

## Bubble Characteristics

In the upper 0.08 m is a high concentration of apparently randomly scattered bubbles which are spherical and $< 0.5$ mm diameter together with some fine vertical bubbles. At 0.08 m depth the bubble pattern changes; large, 15 mm long, 3 mm diameter vertically elongated bubbles appear, superimposed on the upper pattern. Additionally there are vertical trains of small ($< 1$ mm) spherical bubbles separated by 2-3 mm. This pattern continues to the basal contact with sediment.

## Crystal Characteristics

Figure 2 (a)-(e) demonstrates the change in crystal size and shape with depth. The horizontal sections (Fig. 2(a), (b), (c)) are at depths 0.015 m, 0.3 m and 0.5 m. In the upper section crystals are generally relatively small, 6 mm x 3 mm; there is an increase in size downwards to 30 mm x 20 mm at 0.5 m depth (in horizontal sections). Crystal shape is anhedral and serrated, giving an interdigitating but not complexly interlocking pattern, as found by Ragle (1963). Vertical sections show the vertical dimensional orientation typical of the freezing of bulk water (Fig. 2 (d), (e)). A marked zone of wedging out of competing crystals exists in the upper 100 mm, and at 200 mm depth crystals have widened to $> 10$ mm and may exceed 200 mm in length. There are no lateral irregularities in crystal shape. This pattern continues to the base of the core, and individual crystals were traceable for over 0.35 m. There is no pronounced substructure throughout.

The relationship between bubbles and crystal characteristics is such that in the upper zone of high bubble concentration, bubbles are both

(a) Horizontal Section,
    top of core.

    10 mm grid ⊢———⊣
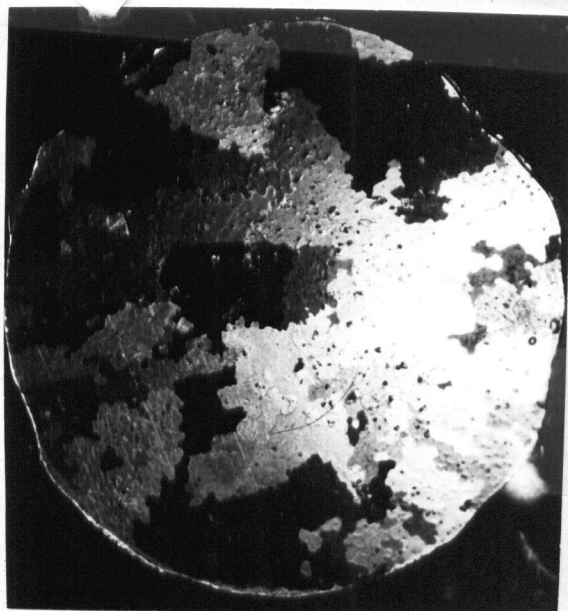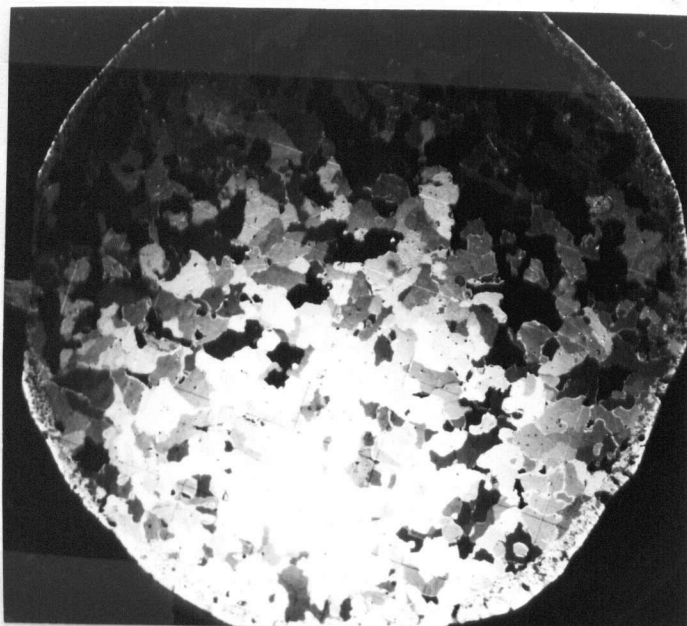
(b) Horizontal Section,
    0.3 m depth.

    10 mm grid ⊢———⊣

(c) Horizontal Section,
    0.5 m depth.

    10 mm grid ⊢———⊣
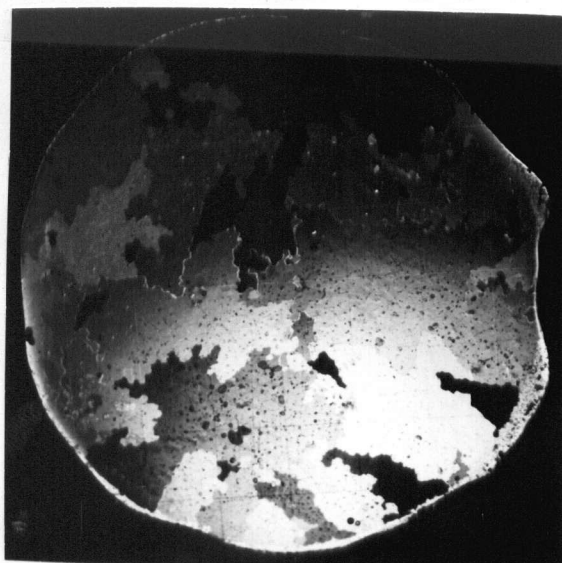
Figure 2.  Thin sections of lake ice.

Crossed polarizers

Top



(d) Vertical Section
0.02-0.12 m depth.

10 mm grid ⊢——⊣
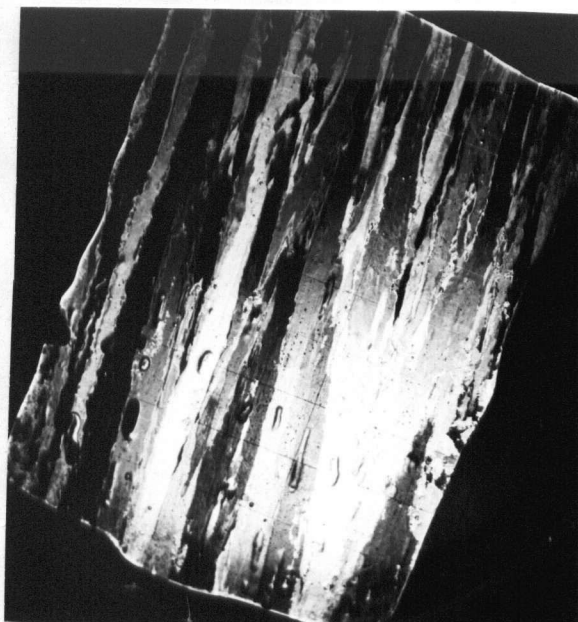
Top



(e) Vertical Section
0.32-0.42 m depth.

10 mm grid ⊢——⊣

Figure 2.    (Continued)
Crossed polarizers

intergranular and intragranular; at depth the larger elongated bubbles are frequently on vertical boundaries. At 0.5 m elongate bubbles are not always vertical although groups are parallel within individual crystals, which indicates lattice control.

Lattice orientations are shown in Figure 3. A horizontal c-axis preferred orientation is evident throughout, but with a progressive decrease in spread about the horizontal with depth. The small number of c-axes plotted for the petrofabric diagrams of deep ice is due to the small number of long crystals. The concentration of c-axes represents a high selectivity of lattice orientations.

## Interpretation

The ice is known to have grown over one winter (1973-74). The body was not observed during growth, nor were any major surface structures visible at the time of sampling owing to presence of a small snow cover.

The bubble and crystal characteristics are typical of lake ice from other areas (Knight 1962a; Lyons and Stoiber 1962; Ragle 1963). There is evidence for only one period and direction of growth; downward from the top, as a competitive zone of crystal growth occurs there, with a progressive downward increase in lateral size of vertically elongated crystals. C-axis orientations are horizontal throughout indicating basal plane growth; the range of variability around the horizontal decreases with depth. Bubble patterns are also indicative of vertical growth. There is no evidence for interruptions of the growth, or later fracture. It is interesting to compare this ice with the icing mound ice, discussed elsewhere, in which heave caused a modification of crystal characteristics in the upper ice, and a
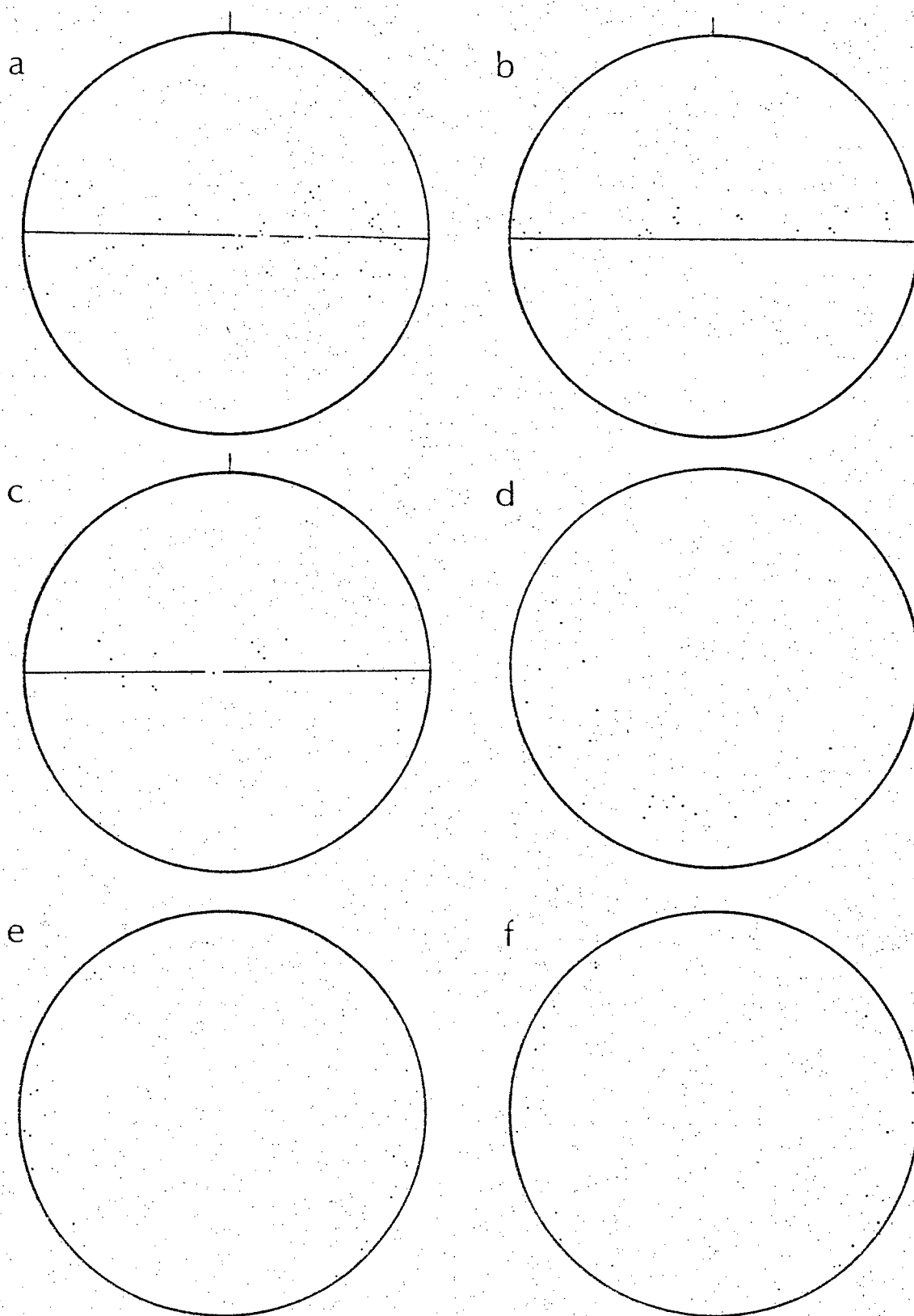
Figure 3. (a),(b),(c) are from progressively deep vertical sections;
(d),(e),(f) are from progressively deep horizontal sections;
(d) is from above (a);(e) is from above (b);(f) is from above (c).

Diagrams in plane of samples

fracture became infilled with ice of differing features from the primary growth. On such evidence icing mound ice and lake ice could be distinguished if the latter became buried. Also lake ice is quite distinct from lens ice and wedge ice in terms of inclusions, crystal size and shape, and lattice orientations. Further, if lake ice became buried by slumping the overlying material would be dissimilar in sedimentary features and later freezing texture from non-slumped or otherwise undisturbed material which froze in situ. Thus on such stratigraphic and petrologic criteria, in addition to those enumerated by Mackay (1971, 1973b), it should be possible to distinguish buried ice from ice grown underground.

## 2. Icing Mound Ice

### Introduction

An icing is a mass of fresh water ice which has frozen at or near the ground surface, from spring or river water. Where the water passes through frozen ground, the forcing mechanism is artesian pressure. The water does not always reach the ground surface; some may spread laterally into or between sediment horizons, thus uplifting the overburden to form an icing mound. Although icings are fairly frequent in permafrost (and non-permafrost) areas (Carey 1973) they have not been studied in detail in North America. Few have been reported in the field area (Mackay 1975b) but in view of their surficial nature, possible extent, geomorphic form and water source, it is important to be able to distinguish the ice type from, say, pingo ice which grows by a different mechanism. Gradational forms exist between icing mounds and those of segregated ice. Two such mounds (Fig. 4) grew in winter 1973-1974 on the Tuktoyaktuk peninsula

Figure 4.    Field position (Photo by Dr. J.R. Mackay)
             Liverpool Bay icing mound


Top




Figure 5.                    Bubble characteristics
                             10 mm grid ⊢————⊣

and provided an opportunity to inspect ice bodies of known age before
major post-solidification changes could occur.

## (a) Tuktoyaktuk Icing Mound

### Field Characteristics

A small icing mound (3 m high) grew over the winter 1973-1974
on the side of a pingo (Mackay 1973a, Fig. 18, Pingo No. 13; 1975b)
20 km east of Tuktoyaktuk. The mound was not present in August
1973, and was first observed in July 1974, thus its maximum age is
known. Drilling on the lake bottom has shown that artesian pressures
have developed in sub-permafrost ground water by pore water expulsion
during permafrost aggradation in sands (Mackay 1972b). The icing
mound grew from water moving up a tension crack from depth and being
injected into the active layer. A crack was still visible, with
water flowing in July 1974 and flow continued into late August 1974,
and was observed in March and August 1975 (Mackay, personal communica-
tion).

### Ice Characteristics

A 0.5 m thick sample was taken (by J.R. Mackay) from the upper
part of the mound, to include the contact with the active layer.
Structures in the sample were slight folding of the compositional
layering due to heaving, and a later fracture. The compositional
layering was determined by bubble content (no sediment or organic
matter being present); the bubbles occur in distinct bands parallel
to the mound surface. Bubble sizes and shapes were uniform within
a given band, but varied from band to band (Fig. 5). A detailed

bubble stratigraphy is given in Figure 6. Near the contact with the organic matter, the ice had a milky appearance due to the high content of very small air bubbles followed below by a bubble-free zone, then bubbles, a pattern which continued to depth.

## Crystal Characteristics

Crystal size varies down the sample. Adjacent to the organic matter is a zone of small crystals indicating a chill zone (Fig. 7(a)). Where bubble layering appears, small crystals (2.0 x 1.0 mm) occur below bubbles. Below this depth, grain size becomes more consistent, crystals being very elongated, >80 mm and widening from 2 mm to as much as 8 mm in the depth range 80 mm to 160 mm. Crystals become longer than the thin section (80 mm) and average 5 mm in width to a depth of 0.4 m, then widen to 10 to 15 mm at the base (Fig. 7(b)).

Crystal shape varies with depth. In the upper zone, crystals are anhedral, some having slightly serrated boundaries. Many terminate abruptly, being wedged out by adjacent crystals. At the small bubble bands, grain shape becomes more interlocking. Below, in the zone of elongate crystals, shapes are anhedral, with some serrations in the upper part which become more gently curved at depth. The gently curved boundaries continue to depth. The only major shape changes are at some bubble bands, where one crystal grows laterally at the expense of its neighbour.

Substructure, in the form of variation in extinction angle within a crystal, is confined to the upper part of the sample, which froze most rapidly. Also, it has suffered the most heaving and

Figure 6.

Bubble Band Sequence
Depths in metres.
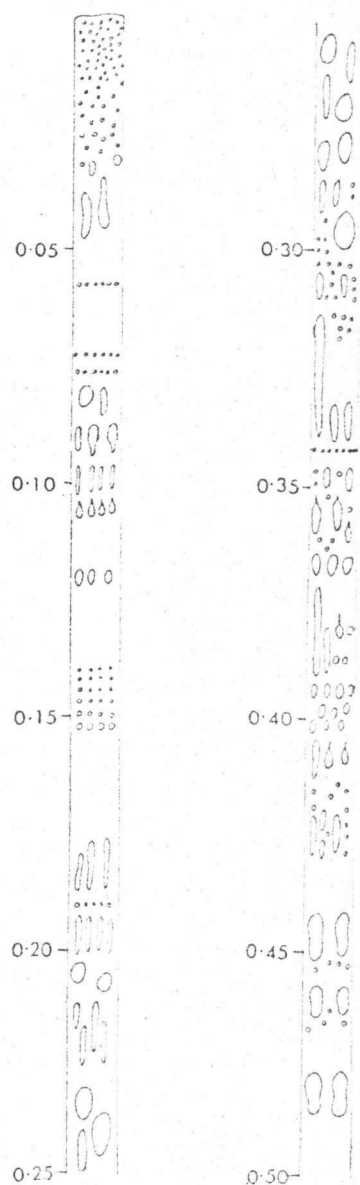


Figure 7.

(a) Crystal characteristics
Upper part of mound,
10 mm grid. ⌐⎯⌐
Vertical section

Top



(b) Crystal characteristics
Lower part of mound,
10 mm grid. ⌐⎯⌐
Vertical section

Top
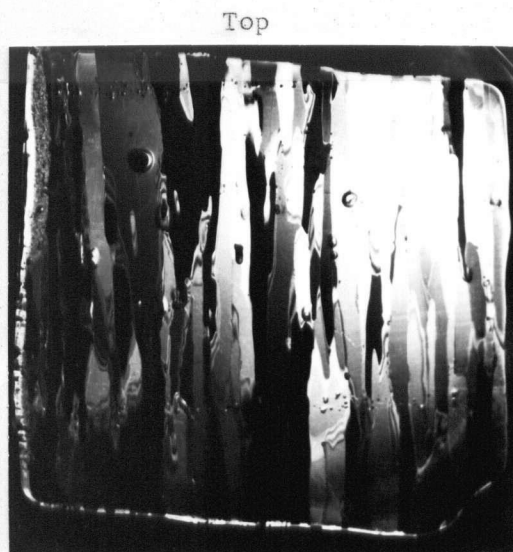
folding of layers and grain boundaries are most irregular. Dimensional orientation is consistent throughout the body, being orthogonal to the bubble banding, and parallel to the freezing direction.

The relationship of bubbles to crystal characteristics is as follows:

(a) In the upper, milky zone, bubbles are frequently near grain boundaries.

(b) Bubbles are consistent in size and shape within given bands throughout the section, not all are associated with a grain boundary position. Thus a widespread nucleating event occurred, regardless of texture. Such an event could be supersaturation of gas at an essentially planar interface. Thus bubbles occur in both intercrystalline and intracrystalline positions.

(c) Further from the chill zone, the freezing rate decreased and bubble nucleation occurred preferredly at grain boundaries. At such sites there is increased gas concentration in the liquid where two interfaces are advancing. Filament-like bubbles lie in the boundaries, then widen downwards into bulbous shapes, as more gas is expelled at the rest of the interface. Gas moves along the concentration gradient, thus the bubbles become fewer but larger. Some such bubbles have small bulbous zones on the filaments, or the filaments are detached, or are in 2 parts (Fig. 5). These features indicate local variations in supply of gas to individual bubbles, which are surrounded by "normal" bubbles. Similar bubbles have been observed in experimental ice growth (Carte 1961a). If more "abnormal" bubbles occurred, it might

be indicative of post-solidification break up (Kheisin and Cherepanov 1969), but this process seems less likely. The inverse form of bubble, with the filament at the base was never observed, so that we have a useful 'way-up' indicator for freezing direction.

(d) A local effect occurs where many crystals terminate at a horizontal band of small bubbles and a larger number of crystals grow below, indicating that crystals did not grow between bubbles, but nucleation occurred on the distal side of the band.

The usual pattern of type (c), above, returns below. It is possible that bubble nucleation occurs within the liquid or at an upward advancing interface if ice is also growing upward due to freezing at the base of the intrusion. Such bubbles could become detached and rise through the liquid to become attached to the upper interface. No samples were obtained from the base of the icing mound.

In the intermediate zone where some bubbles are intracrystalline, formation may have been enhanced by small gas bubbles in suspension produced during turbulent flow up the fracture, or by submicroscopic foreign particles which have different surface energies and roughnesses from crystal surfaces. However, growth is parallel to the basal plane, and Knight (1971) found that $\Theta$, the equilibrium contact angle, tends to zero for air bubbles in water contacting the basal plane, so nucleation would be relatively easy.

It has been noted above that filament-like growth was sometimes interrupted locally before larger, cylindrical bubbles developed.

This is interpreted as indicating a transient state in which bubble diameter increases but conditions are very critical in terms of gas concentration in the water and solidification rate. A change in solidification rate may cause either a diameter increase or a growth stoppage. When the diameter increases a steady state may be attained, which gives cylindrical bubbles parallel to the freezing direction. In comparison with the non-reproducibility of experimental bubble growth, it is surprising that bubble characteristics are so constant in a given layer in the icing mound. Vasconcellos and Beech (1975) discussed the development of bubbles in the ice/water/$CO_2$ system and demonstrated that three adjacent bubbles grew: (a) for the most part in the transient state, with the diameter increasing, (b) initially transient, then steady state, (c) in steady state all the time. Thus in the same cell, the solidification rate varied with position, rate (a) $<$ rate (b) $<$ rate (c). In comparison bubble bands in the icing mound ice display little lateral variability in bubble size and shape.

Petrofabric diagrams were prepared for a series of vertical samples (Fig. 8). A strongly developed girdle is evident, showing c-axes to be parallel to the compositional layering. This is characteristic of rapid ice growth into bulk water.

Crystals at the contact of ice with organic matter were not measured due to the difficulty of making thin sections of ice containing solid inclusions and the small crystal size typical of the chill zone. However, the uppermost measured crystals show a wider girdle (Fig. 8(b)) than succeeding lower sections (Fig. 8(c)).
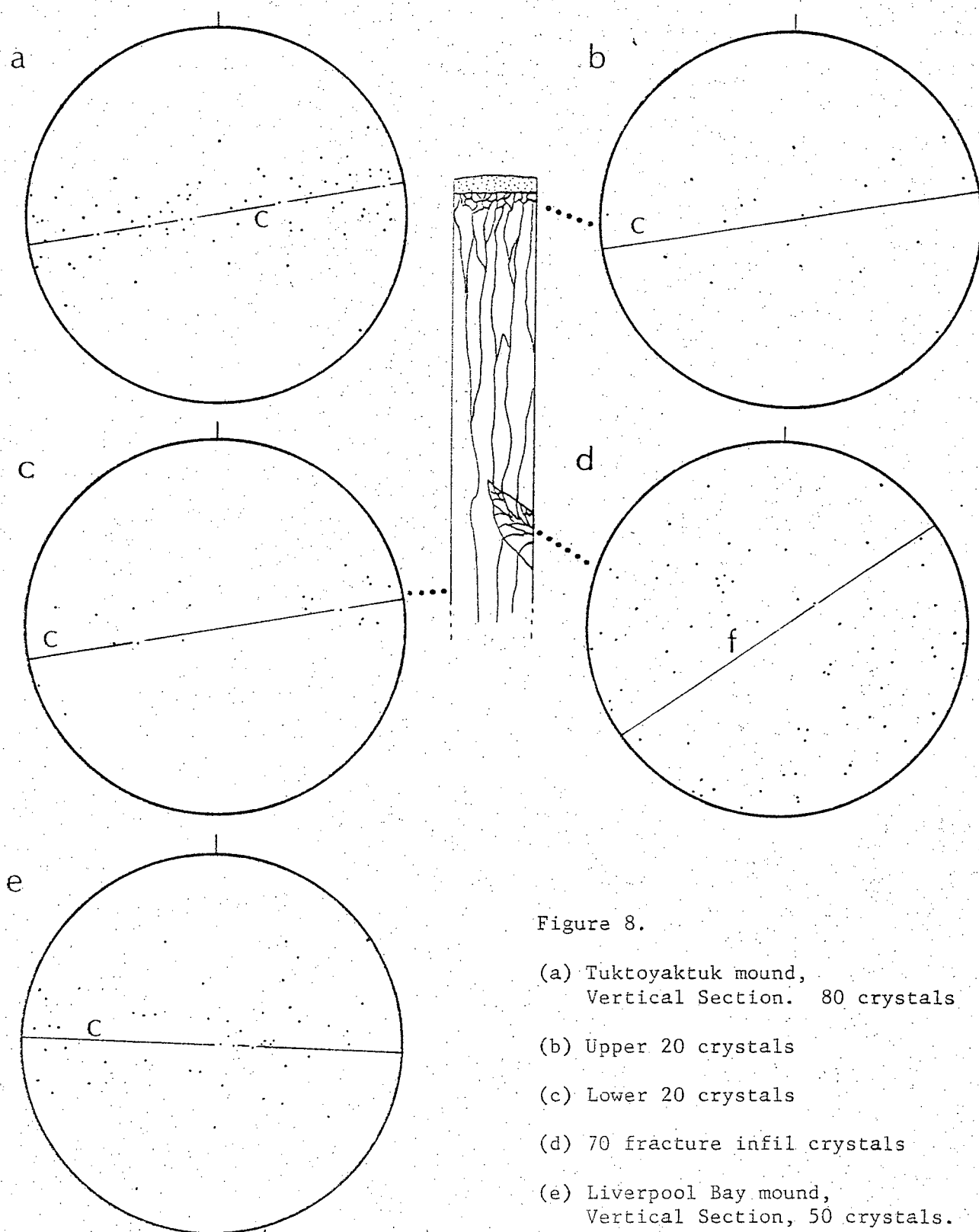
Figure 8.

(a) Tuktoyaktuk mound,
    Vertical Section.  80 crystals

(b) Upper 20 crystals

(c) Lower 20 crystals

(d) 70 fracture infil crystals

(e) Liverpool Bay mound,
    Vertical Section, 50 crystals.
    Diagrams in plane of samples

    c = compositional layering
    f = fracture surface

This is to be expected on the basis of selective growth of crystals with basal planes parallel to the freezing direction.

## Fracture Zone

The above pattern was disturbed in the centre of the sample, where the bubble layering was interrupted by a zone of irregularly shaped bubbles of various sizes. This zone was oblique to the general layering and veered parallel to that layering near the top of the sample. The upper sections show a texture similar to that of the previous series, but an abrupt change occurs in the fracture zone (Fig. 9). Bubble shape varies considerably, but with a general trend away from the surfaces of the fracture zone. Thread-like bubbles are short (2-3 mm), narrow ($<$ 1 mm), and interspersed with spherical (1 mm) bubbles. Crystal size varies widely, from $<$ 3 mm to $>$ 25 mm long axis, in contrast to the previous elongate pattern. Crystal shapes are anhedral with much more complex shapes than in the banded ice, having serrations, cusps, and intergrowths. Substructure (i.e. extinction variation) is not developed, but a cellular microstructure parallel to basal planes, as in sea ice occurs. There is a tendency toward a dimensional orientation trending into the zone (Fig. 9).

Petrofabric diagrams for the zone are shown in Fig. 8(d), the contrast with Fig. 8(a) being evident. There is no horizontal girdle pattern, instead c-axes are more dispersed relative to the freezing directions.

Figure 9.

Tuktoyaktuk icing mound,
Fracture infil crystals,
Vertical Section, 80 mm across.
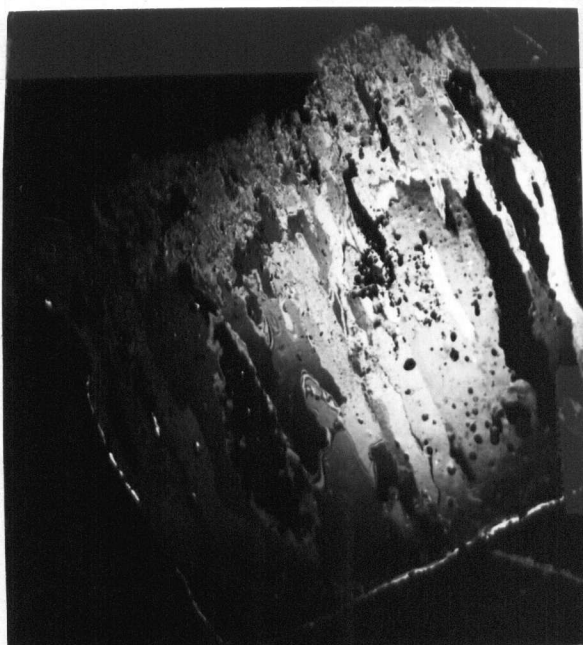


Figure 10a.

Liverpool Bay icing mound,
Vertical Section, contact with
overlying soil.  Note chill zone,
elongated crystals.
Section 80 mm square.



Figure 10b.

Liverpool Bay icing mound,
Lower, vertical section.
10 mm grid. └────┘



All sections under crossed polarizers

Interpretation

The icing mound resulted from water under artesian pressure at depth moving up a tension crack and inserting itself into the active layer on the side of the pingo probably in late autumn or early winter. The active layer was cold, and copious nucleation produced a chill zone, from which grew very elongate crystals. Alternating bubbly and bubble-free layers occur regularly, bubble shape being consistent in orientation, size and shape within individual bands. Filaments occur on the upper ends of elongate bubbles, a useful way-up criterion. C-axis preferred orientation is orthogonal to the growth direction. As growth continued, updoming occurred, folding the upper layers. A later fracture became infilled with ice with markedly differing texture and petrofabrics.

The texture and petrofabrics of the fracture zone are interpreted as indicating the fracture of the regular pattern and later infilling. Some growth took place in lattice continuity with previously existing crystals, but nucleation of new crystals also occurred (Fig. 9). The elongate crystals are oblique to the pattern of the surrounding ice, and reflect multidirectional growth into a cavity. Dimensional orientation is locally parallel to freezing directions. A cellular substructure in this ice suggests a higher chemical content.

It is interesting to compare crystal growth in the main mass of the mound with that in the fracture. In the main mass crystals are very elongate parallel to the freezing direction which changed very little. In comparison the thermal gradient varied around the

fracture. Thus for a columnar grain to survive over any great
distance necessitates considerable curvature, due to the progressive
change in the favoured growth direction. As the grain's crystallo-
graphic orientation remains constant, the curvature must be generated
by lateral branching. At some stage this may become more difficult
than the initiation and growth of a new grain oriented more suitably
for continued growth. Hence the variation in lattice orientation
in the petrofabric diagrams.

The petrology of such mounds has not been discussed elsewhere
in the literature. It is apparent that they differ markedly from
segregated ice in the cases described. The mounds may be temporary,
depending on the overburden thickness and water supply.

(b)  Liverpool Bay Icing Mound

Field Characteristics

A second icing mound was found by Dr. J.R. Mackay in July 1974.
It occurred on the side of a pingo (Mackay 1973a, Fig. 19, Pingo
No. 15) near Liverpool Bay, Tuktoyaktuk Peninsula. The mound was
2.3 m high. The mechanism of growth is believed to be the same as
that of the previous example; water was bubbling up in a pool in
July 1974 (Mackay, personal communication). The growth period is
known to have been during or after the freeze-back of the active
layer in the winter 1973-74, as the site was surveyed in summer 1973,
and ice growth took place at the base of the active layer. A sample
of the upper portion of the mound including part of the overburden
was collected by Dr. J.R. Mackay.

### Ice Characteristics

The contact with the overburden was abrupt but not planar.
This represented the initial contact - i.e. there had been no
melt-through of the active layer at the time of sampling. There
were also some thin ($<$ 5 mm) ice lenses up to 50 mm long in the
overburden, which was mainly organic matter with some sediment.
Inclusions of this material occurred in the top 50 mm of the ice,
in particles from 1 mm to 10 mm in diameter, decreasing in concen-
tration downwards. The very few bubbles which occurred in the top
50 mm tended to be small ($<$ 1 mm), spherical in trains, or slightly
elongated. Below and throughout the whole sample was a pattern of
very irregular sub-vertically elongated bubbles, generally $\leqslant$ 25 mm
long, but a few reached 75 mm. No structures such as fractures were
observed.

A series of vertical thin sections was prepared. The over-
burden at the contact has a low ice content, and the contact with
the ice is abrupt and irregular at two scales, i.e. sinuous at hand
specimen scale (Fig. 10(a)) and at microscopic scale. Sediment
content in the ice tends to decrease downward from the contact. The
bubble pattern differs markedly from that in the previously discussed
mound, there being no well developed layering. There is a general
increase in bubble concentration downwards. Few bubbles occur at
the contact, and below the pattern is essentially random, with
locally higher concentrations. Shapes range from spherical ($\leqslant$ 1 mm),
to elongate irregular (8 mm long, 3 mm wide) - these bubble charac-
teristics continue downwards. A cellular substructure increases in

concentration with depth in the form of a series of locally parallel cells, which are probably zones of higher chemical content parallel to the basal plane.

## Crystal Characteristics

Differences from the previous icing mound continue in textural properties. Grain size ranges from <1 mm at the contact (Fig. 10(a)) through an intermediate zone (5 mm x 2 mm) to an elongate zone (>65 mm long by 20 to 30 mm wide). This elongate crystal zone extends for another 80 mm, some crystals exceeding 80 mm in length (Fig. 10(b)). Smaller crystals (10 mm x 5 mm) occur interspersed or in groups among the larger.

Crystal shape is anhedral throughout the sample. In the competitive growth zone at the overburden contact, boundaries lack strong curvatures or serrations. The zone of intermediate crystals contains both vertical and horizontal serrations unrelated to inclusions. The elongated crystals have irregular boundaries (Fig. 10(b)). Intergrowth is demonstrated by repetition of extinction angle in nearby crystal segments and also by serrations which are mainly horizontal, but may have secondary promontories. Dimensional orientation in the two sections (Fig. 10a,b) is markedly vertical, i.e. parallel to the freezing direction.

Substructure in the form of differing extinction bands occurs in the large columnar crystals, defined by irregular sub-boundaries. This type of substructure decreases with depth, to be replaced by a cellular substructure, small pockets (≪1 mm) parallel in a given

crystal, indicative of saline inclusions. Superimposed on this is a tendency to varying extinction position.

No relationship of bubbles to crystal characteristics exists in the upper ice, neither spherical nor elongated bubbles being preferredly sited in crystals or on boundaries. Farther from the contact, small elongate bubbles are aligned on sub-boundaries and boundaries, while large irregular bubbles have no apparent relationship to texture. Sediment is mainly at or near to boundaries.

Two horizontal sections were prepared from the top of the ice body, one in the competitive zone and the second 25 mm below. Crystal size changed from 2 mm x 1 mm to 8 mm x 5 mm in this distance. Crystal shape at the top was anhedral with most boundaries being essentially straight but with minor serrations locally. This changed below to more serrated, complex shapes in the larger crystals. In the upper crystals, no substructure is apparent, but in the lower section low angle boundaries occur, meeting boundaries in serration grooves. Dimensional orientation is nowhere well developed. Most bubbles occur on grain boundaries, but the concentration decreases downward, in the large crystal zone.

Petrofabric diagrams were prepared only for the vertical sections (Fig. 8(e)). The horizontal girdle is characteristic of rapid ice growth in bulk water, rather than in a porous medium.

Interpretation

The overall form and the gross pattern of crystal size and shape are similar in both icing mounds. In detail the second mound

lacks a well developed bubble layer pattern, bubble shapes are irreg-
ular, grain boundaries have more serrations, and the cellular sub-
structure is apparent in the whole body, compared with its occurrence
in fracture ice only in the previous mound.  It appears that the
melt had higher solute content which produced the serrated pattern
and cellular substructure.  This also contributed to the complex
bubble shapes.

## Topographic Expression and Ice Characteristics

The icing mounds were not observed in the field by the author,
but detailed descriptions were supplied with the samples by Dr.
J.R. Mackay (personal communication 1974, 1975).

From these descriptions and those of other authors (Shumskii
1964) it is apparent that such mounds may range widely in lateral
extent and height.  Growth may continue as long as water is available,
and fractures are common.  The mounds thus resemble small pingos.

The ice characteristics enumerated above demonstrate clearly
the difference from pingo ice (discussed in section 3 ).  The evi-
dence from ice petrology is that icing mound ice in the above cases
is typical of the freezing of bulk water, rather than of segregated
ice.

## 3.  Pingo Ice

## Introduction

Although very limited in their spatial distribution, pingos are
dominant geomorphic features and have long attracted attention.  Several

theories of origin have been proposed (Porsild 1938; Müller 1963; Shumskii 1964; Mackay 1962, 1972b, 1972e, 1973a, 1975b; Mackay and Stager 1966b) and a detailed understanding of many associated phenomena is now at hand. In his 1962 paper Mackay applied heat conduction theory to the freezing of a lake basin in permafrost with boundary conditions applicable to the Mackenzie Delta - Tuktoyaktuk Peninsula area. In addition, theory and laboratory experimental knowledge of ice lensing conditions was employed to explain the variable ice contents in exposed pingo cores. This initial theory of pingo growth has been tested by detailed surveys of actively growing pingos, and has been modified to include artesian pressures at the base of permafrost, pulsating growth, tension crack patterns and a tentative link between growth rate and climatic parameters (Mackay 1973a, 1975b). Despite these developments, there has been no concomitant advance in our understanding of the petrological aspects of ice within the cores of pingos. As reviewed previously, almost no laboratory controlled work has been performed on ice growth in sediment, from a crystallographic viewpoint. In particular the influences of pore water pressure and inclusions have not been investigated. In terms of field study of core ice, no reports of petrologic analysis have appeared since 1966. Müller (1963) compared pingos in Greenland and the Mackenzie Delta area and included some discussion of crystal size and shape, but no petrofabric diagrams were presented.

A field inspection of exposed pingo ice in a cave on Richards Island was carried out by Mackay and Stager (1966b) who found that:

> The ice was usually bubble free. Although crystal sizes varied
> from site to site few were less than one-third of an inch across
> and many were 1 inch to 2 inches in diameter, 8 inches being the
> largest dimension noted. Worm-like bubble tubes, as much as

0.1 inch in diameter and 5 inches long, were sometimes found
along intercrystal faces. An examination of many tens of
bubbles, from several localities, showed a preference for two axial
orientations: the first was toward the pingo centre, the second
toward the outer base (p. 367).

Additionally an unspecified number of crystal optic axes was measured in

a sample from one ice layer, and

... an estimated 80 per cent of the optic axes were horizontal
and lay parallel to the ice-clay contact; that is, the axes
pointed toward the geometric centre of the pingo (p. 367).

Thus it is apparent that in this case both the optic axes and elongate

bubbles were generally orthogonal to the adjacent sediment bands, despite

the dip of the layering, and it seems reasonable to conclude that the

lineations represent the freezing direction.

Shumskii (1964) also considered pingo ice, and as is found elsewhere

in the Russian literature (Sumghin 1940) he referred to injection of water

at the freezing front to cause rapid freezing and uplift. Mackay (1973a,

p. 1000) discounted injection ice as a major factor in pingo growth but

pointed out that it may occur temporarily. Thus one aspect of the present

study is to determine the mode of growth. In our discussion of icing

mound ice the characteristics of ice grown from water intruded beneath a

thin overburden have been enumerated. Owing to the lack of laboratory and

field data on segregation ice some of the following discussion on growth

of pingo cores in terms of segregation or injection and the influence of

heaving and overburden pressure on growth features must be considered

speculative.

In the present work, three pingos were studied:

(a) a small pingo, one of a suite studied by Mackay (1973a, Fig. 14, Pingo No. 11);

(b) Whitefish Summit Pingo;

(c) a hollowed-out pingo in Tuktoyaktuk.

(a)  Pingo No. 11 (69° 23'N, 133° 30'W)

A drained lake near Tuktoyaktuk contains three large growing pingos and one small non-growing pingo (Mackay 1973a, Fig. 14, Pingo No. 11). The small pingo ceased to grow as it was centred near the edge of the former lake and permafrost aggradation cut off growth. It thus provides an example of early pingo growth which has not been disturbed greatly by later heaving, although general lake-bottom heave is occurring. Also its approximate age is known, so post-solidification changes can be dated.

### Field Characteristics

The pingo is 1.5 m high with a well developed vegetation cover. Two vertical cores were removed, one from the summit and one from the side, each core being about 3.1 m long. 1.2 m of ice-free peat overlies 0.8 m of alternating peat and ice layers grading into a pure ice core with a few peat inclusions at the top. Coarse sediment underlies the core.

### Ice Characteristics

Ice layers within the peat are lens-shaped, the thickest are 20 mm and taper laterally. Ice-peat boundaries are irregular and peat inclusions up to 3 mm occur within the ice (Fig. 11). Otherwise

Figure 11.

Pingo No. 11, Vertical
section.   Ice lenses
in peat.   10 mm grid.
Crossed polarizers



Figure 12.

Pingo No. 11, Vertical
section.   Crystals in ice
core.   10 mm grid.
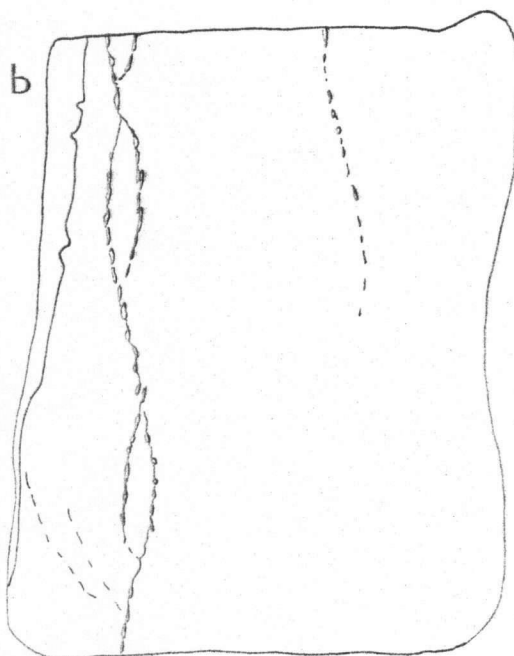Crossed polarizers



a

b
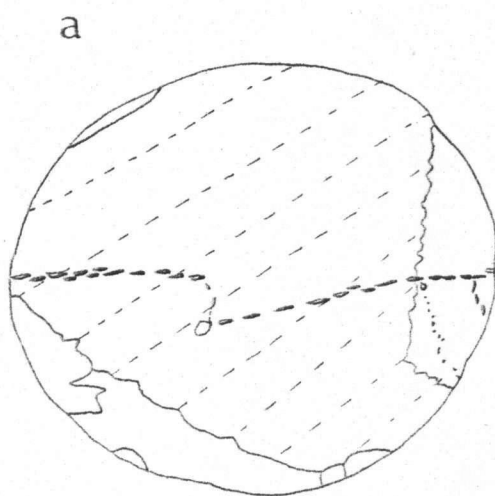
Figure 13.   Fractures in core ice, Pingo No. 11.
(a) Horizontal section, (b) Vertical section.

the ice is clear except for cylindrical bubbles and strings of spherical bubbles, arranged vertically with diameters up to 1 mm and lengths of 3 mm.

## Crystal Characteristics

Individual crystals cross the ice layers, and have grown to 2 cm vertically and laterally. Peat inclusions are contained in single crystals, thus the peat did not encourage further crystal growth. Elongate bubbles occur both in crystals and on boundaries. Grain boundaries are generally straight to gently curved, and vertical serrations mark the wedging out of a crystal by its neighbours. No pronounced substructure occurs in the crystals.

Within the ice core, peat inclusions become fewer and smaller with depth. Here, peat affects crystal shape, boundaries trending horizontally below peat pockets, but vertically where peat is absent, which indicates selective growth at the impurity, due to differential heat flow. Bubbles occur in vertical trains, decreasing downwards in size from 2 mm. They occur on or close to crystal boundaries.

Crystals are very elongated, being greater than 160 mm long and widen downwards to 30-40 mm wide. Shape is anhedral with curved and serrated boundaries. These boundaries have a general trend on which are superimposed dendritic shapes (Fig. 12).

This pattern continues for 0.3 m depth, where crystals are still elongate and narrow, but more complexly intergrown. Also some grains display alternating extinction. From a depth of 2.3 to 2.8 m

the ice is essentially inclusion-free. Crystals are anhedral with boundary shapes ranging from simple curvature to highly serrated. These major serrations occur on each side of a crystal at a given depth, but become more frequent and less pronounced downwards where several crystals are wedged out. Horizontal sections show crystals to be anhedral in that plane also. These more regular crystals continue downward for 0.2 m where more complex shapes occur, crystals are intergrown and contain bands differing in extinction angle by several degrees. These result from branches of a crystal growing together along a misfit boundary.

The second core, from the side of the pingo, had the same general characteristics but with some nearly vertical fractures between depths of 2.05 and 2.33 m. At 2.33 m occurs a 20 mm thick peat layer. The lower peat-ice interface is gradational, and vertical, discontinuous trains of peat fragments descend for 120 mm. Bubbles are few; those which do occur are mainly within the peat, and at the bottom of the ice core, where a mass of fine bubbles gives the ice a milky appearance.

Fractures are approximately vertical and are indicated by flattened voids, unlike any bubble (Fig. 13). In horizontal sections the fractures meet at right angles. There is no change in fractures at crystal boundaries but two fractures often meet at such a boundary. In vertical sections fractures are seen to be sinuous, merge and bifurcate and to terminate upwards or downwards. They do not reach to the ground surface and have not been subject to lateral offset or new crystal growth; however a small crystal grows at a junction of two cracks (Fig. 13).

A change in texture occurs at a horizontal peat layer. Small crystals occur in the peat, but large crystals grow immediately at the lower peat-ice interface. Such growth of large crystals is unlikely to be new nucleation, and in the absence of evidence of melt-back of earlier crystals, it seems likely that these are horizontal extensions of crystals from beyond the peat layer which is known to be laterally discontinuous. These crystals grow competitively and at the base of the core (3.06 m) there is only one crystal in a thin section. This crystal has a well developed substructure at the base, associated with a high bubble content. The inclusions have given rise to trains of dislocations, and alternating extinction.

Crystal dimensional orientation is dominantly vertical throughout, except in upper lenses where crystal long axes are controlled by lens shape. C-axis orientations (Fig. 14) in these lenses show a concentration in the horizontal, and a diffuse vertical grouping (Fig. 14(a)). No other crystal characteristics correlate with the differing lattice orientations. In the ice core (Fig. 14(b)-(f)), c-axes tend to lie in a horizontal plane, which contains point maxima, crystals in other orientations being wedged out. Thus growth has been mainly in the basal plane. This pattern is interrupted in the discontinuous peat layers, where small crystals show more dispersed c-axes, but the c-axis horizontal pattern is found immediately below the peaty layer.

## Interpretation

The pingo began to grow between 1950 and 1957 (minimum date from willows, Mackay 1973a, p. 987) in a "residual pond" in a drained
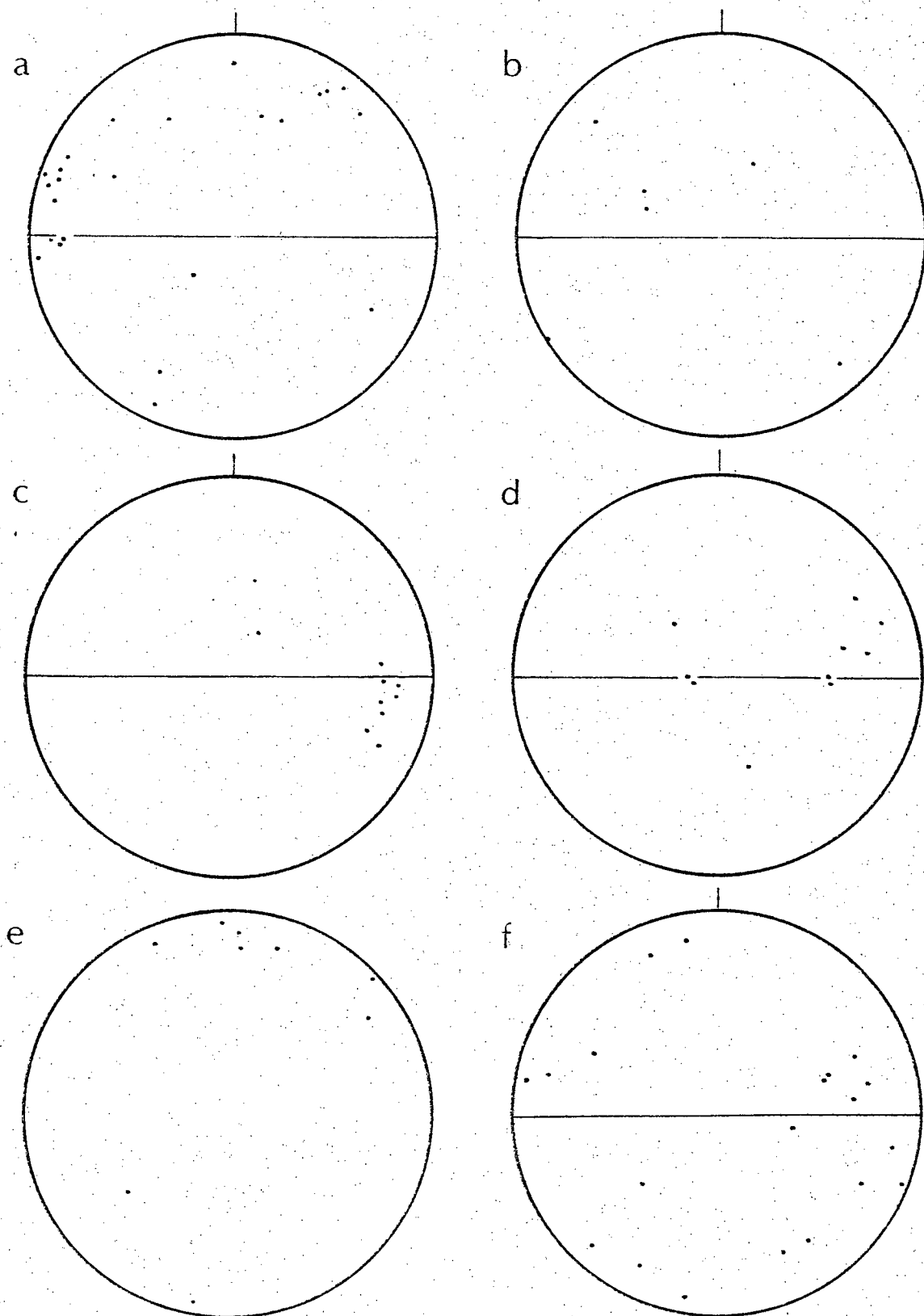
67



Figure 14. Pingo No. 11
  (a) vertical section, crystals in lenses in peat, core 1;
  (b),(c),(d) successively deep vertical sections in core;
  (e) Horizontal section, lower ice;
  (f) vertical section, crystals in peaty layer, core 2.

Diagrams in plane of samples

lake. Early growth was in the form of lenses within peat below which crystal characteristics suggest growth in bulk water. The vertical columnar shape with horizontal irregularities and horizontal c-axes are typical of much growth. There is no evidence for freezing upward from the base of the ice body, so in this case water was not injected into already frozen material, rather bulk water existed temporarily at the freezing front.

(b) Whitefish Summit Pingo (69° 23'N, 133° 33'W)

During June 1973 this 16 m high coastal pingo was subject to wave attack which exposed the ice core. Samples were taken as shown in Fig. 15: a series in the upper ice layer and a second series approximately ver- tically through the core. Slumping quickly buried the ice core.

Field Characteristics

The exposed stratigraphy comprised, from the top down:
(a) 3.5 m of stoney clay, which is widespread in the area (Rampton 1972b). This is structureless in terms of both primary depositional structures and features produced by freezing. No reticulate ice veins were observed in 1973. An ice wedge, 1 m long and 50 mm wide at the shoulder, penetrated the top of the pingo;

(b) 0.35 m of fine sand displays laminations 3 mm to 50 mm thick, with pockets of ironstained sand;

(c) ice core, 3 m thick;

(d) pore ice (in sand) of unknown thickness.
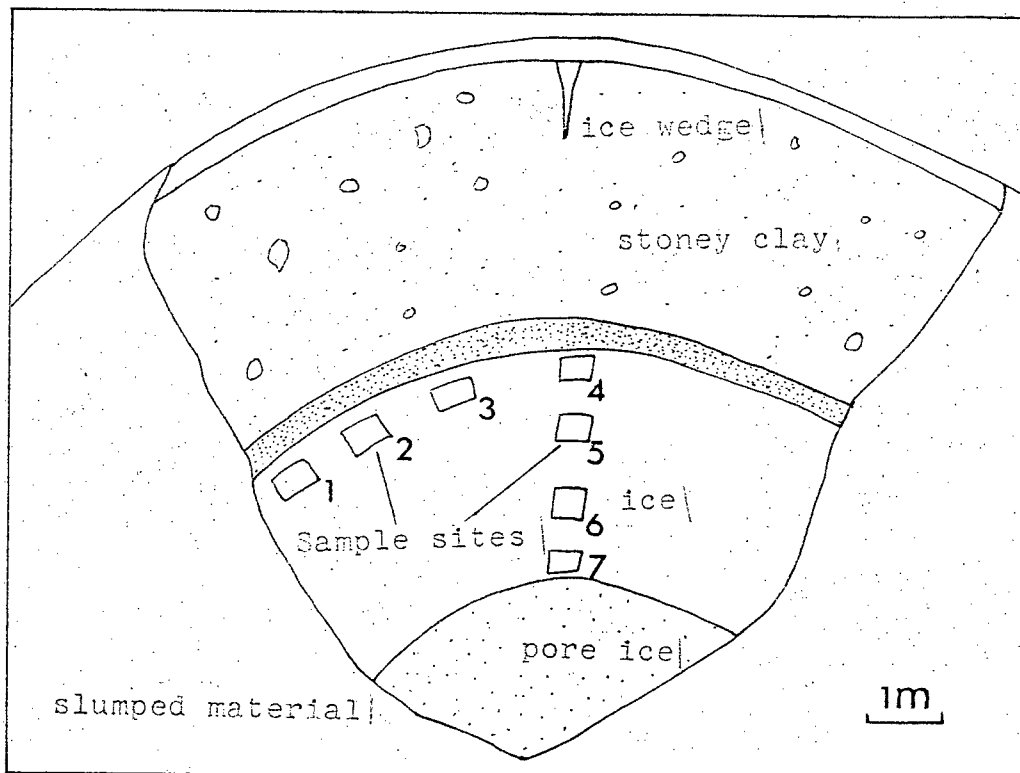
Figure 15.   Whitefish Summit Pingo, stratigraphy and sample positions.
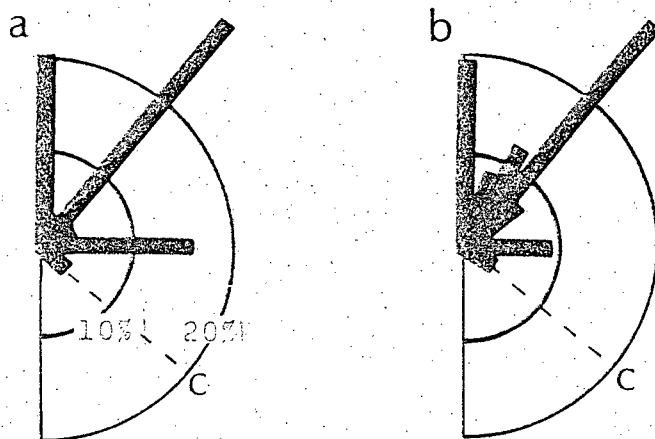


Figure 16.   Dimensional orientation, basal crystals, Whitefish
             Summit core.
             Diagrams in vertical plane containing maximum dip of layering

## Ice Characteristics

The pure ice part of the core was 3 m thick, and underlain by fine sand containing some pore ice. It is possible that a further ice layer underlies the pore ice, but was not exposed, and drilling was not attempted through the frozen sand. However, the steepness of the compositional layering and ice-icy sediment contact suggests excess ice growth at depth.

The only compositional layering is determined by bubble content, in terms of the presence or absence of bubbles and their size and shape. The layers are approximately parallel to the upper surface of the core and to the interface with the underlying sediment-rich ice. Very little sediment occurs in the upper banded ice.

## Bubble Characteristics

Few bubbles occur in the upper part of the core. They are apparently randomly positioned, and spherical, 1 mm in diameter or slightly elongated parallel to the banding. Minor fractures associated with the uplift of the core have their positions indicated by bubbles and voids in subvertical trains.

Additionally a 90 mm zone of melt figures was observed in the ice at the slump surface, and parallel to that surface. The high concentration of figures within crystals contrasted strongly with the adjacent bubble-poor ice where the few bubbles were mainly on crystal boundaries. Many figures were linked by intercrystalline threads, indicating a melting origin.

One meter above the pore-ice begin zones of higher bubble content. A zone of large bubbles overlies a zone of small bubbles, the boundary being abrupt. Bubbles in the upper zone are more widely separate and vary in shape: (i) elongate bubbles are orthogonal to the banding, but are not simple cylinders. Upper ends are often pointed, in contrast to the lower ends. Bulbous and inverted U shapes are common. These elongate bubbles range up to 15 mm in length. The retention of these bubble shapes suggests that no strong deformation of the ice has taken place; (ii) spherical shapes are rare, occur in groups, and are less than 1 mm in diameter; (iii) flattened figures occur, usually less than 2 mm in diameter. These are confined to the slump surface, which suggests they are melt figures, although similar figures were reported by Müller (1963) in deeper ice. Bubble size in the small bubble zone is restricted to 3 mm, spherical bubbles do not exceed 1 mm diameter.

Closer to the contact with the sediment-rich ice, bubble size generally decreases. Worm bubbles decrease to 5 mm in length, 0.5 mm diameter, spherical are less than 0.3 mm.

### Crystal Characteristics

Crystal size is strongly related to bubble content. As bubble content increases with depth, so crystal size decreases from $680 \pm 40$ mm$^2$ at the top of the core to $120 \pm 20$ mm$^2$ at the base. Locally bubble bands occur in the upper ice, with associated small crystals. The general relationship of crystal size and bubble content and the presence of sediment-rich ice at depth indicates an increase in freezing rate with depth, relative to rate of water supply.

Considering crystal shape, it is found that small crystals tend toward an equigranular shape with no strong curvatures or embayments, while large crystals are more irregular with deep embayments and multiple curvatures. Straight compromise boundaries are rare. Strain shadows occur throughout the ice body, but in less than 30% of the crystals. Crystal dimensional orientation is orthogonal to the layering at the base of the ice body (Fig. 16) and becomes more nearly parallel to the layering near the top.

Bubble positions relative to crystals are such that the majority occur on crystal boundaries, although near the slump surface a zone of melt figures occurs parallel to that surface, the included figures being parallel in an individual crystal. This feature and the presence of threads linking some figures indicate a melting origin.

The preferred dimensional orientation of elongate bubbles at the base of the ice body is parallel to that of crystals, and orthogonal to the compositional layering. This indicates the heat flow direction during growth, and that no change in the patterns has occurred since growth, i.e. no major flow has occurred to produce a crystal dimensional orientation parallel to the layering, as occurred in the involuted hill ice.

Many minor fractures are recognized in the ice core, these are both intergranular and intragranular. No new crystal growth is present, but voids occur which are frequently flat and orthogonal to the fracture surface.

Petrofabric diagrams for samples around the top of the core and in a vertical series are shown in Figure 17(a)-(o). Because of great variability, each thin section is given separately: (a)-(g) are from the upper layer, (h)-(j) from 1.5 m depth, (k)-(m) from 3.0 m depth, and (n), (o) from 4.5 m. The tendency is for c-axis orientations to be more concentrated with depth into a girdle parallel to the compositional layering. The c-axis pattern is not typical of segregated ice in experimentally grown lenses (Penner 1961, Kaplar, personal communication 1974) or in other large pingos (see Tuktoyaktuk pingo, next section) or involuted hill ice. The girdle patterns occur in the zones of bubbly ice which have smaller but elongate crystals, rather than columnar crystals as was the case in icing mounds, and Pingo No. 11.

### Interpretation

The compositional layering throughout the ice body was parallel to the freezing front at the time of growth. Crystals and bubbles near the base of the ice core have a dimensional preferred orientation orthogonal to the layering which indicates that no major flow has occurred, a conclusion which is supported by the lattice orientations which have c-axes parallel to the layering. Higher up the ice body the dimensional orientations are less well pronounced and c-axes are more dispersed, which contrasts with the involuted hill, where more uplift has occurred, and basal planes are parallel to the compositional layering. In the early growth stage, freezing was slow, as indicated by the low bubble content and large crystal size. An increase in freezing rate is indicated by successively: ice containing large bubbles orthogonal to the banding
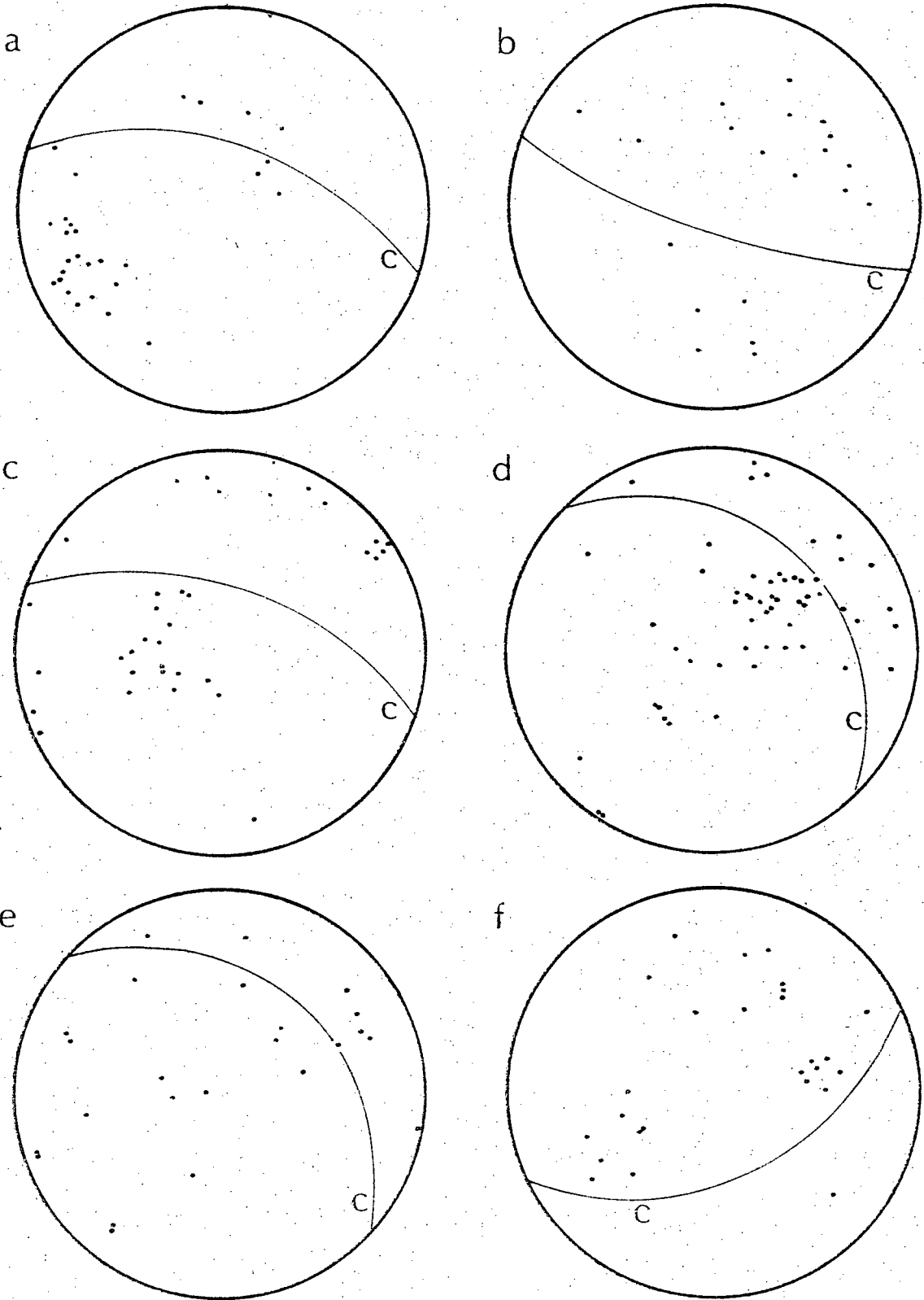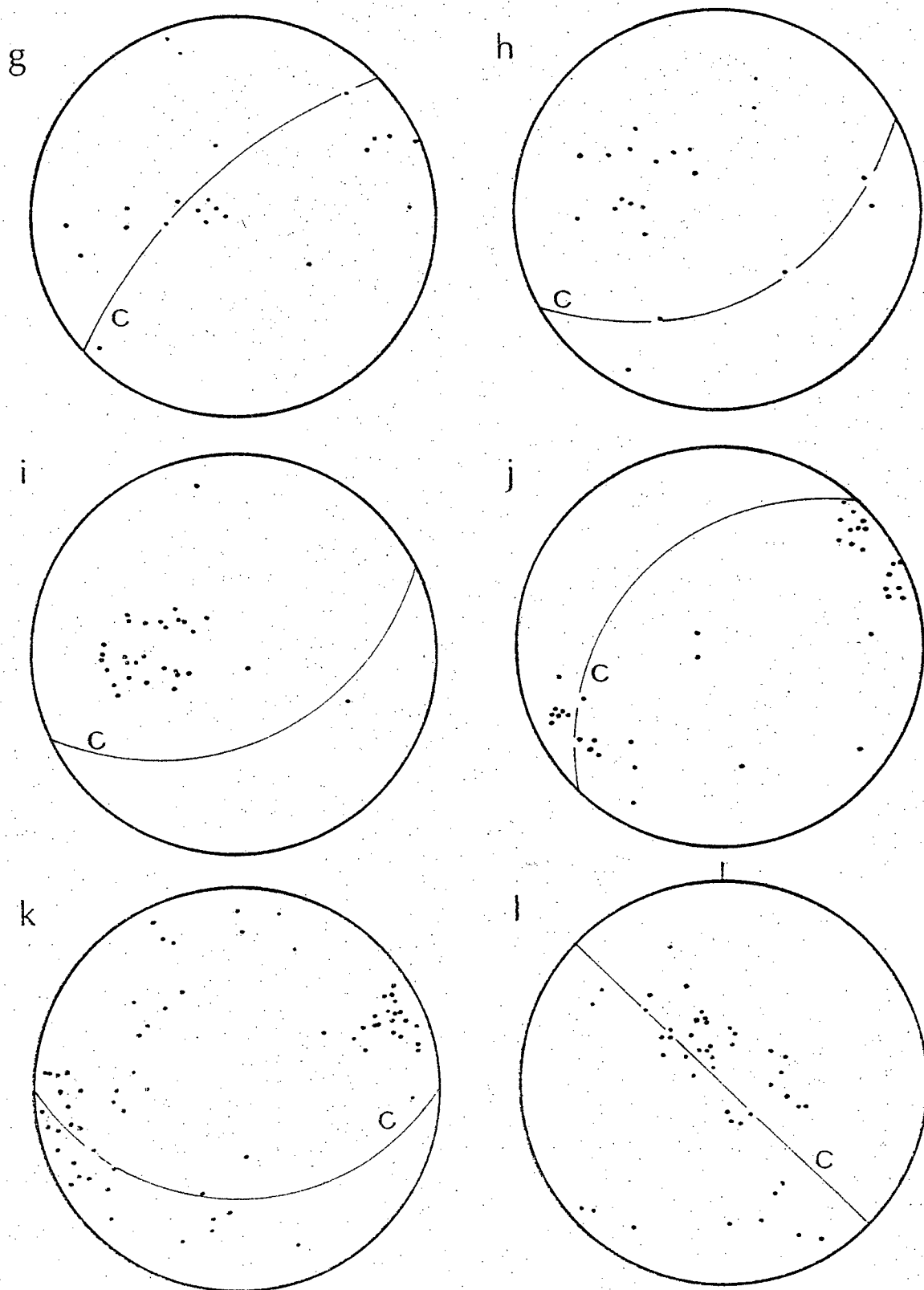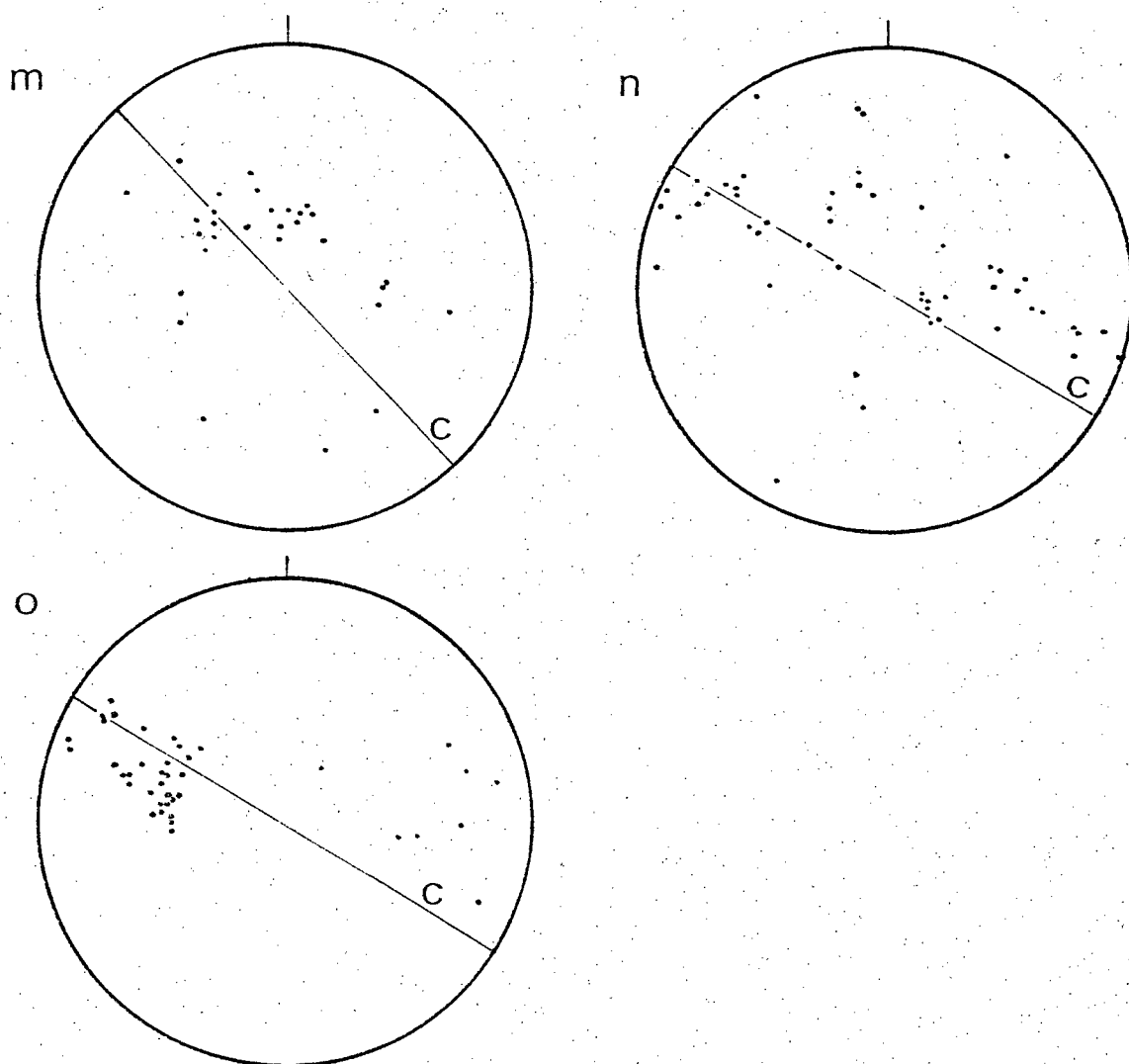
Figure 17.

Figure 17 (cont'd)

Figure 17.

(a)-(g) sections in upper ice layer;

(h)-(j) sections from 1.5 m depth;

(k)-(m) sections from 3.0 m depth;

(n),(o) sections from 4.5 m depth.

c = compositional layering

with smaller crystals than the bubble-poor ice, then ice containing small
bubbles, then pore ice. Lattice orientations provide additional evidence,
the lower ice containing crystals with c-axes parallel to the banding.
Such an increase in freezing rate could be produced by uplift of the lake
bottom and exposure to cold air temperatures.

(c) Tuktoyaktuk Pingo

This is lower and broader than Whitefish Summit Pingo, and appears
older, judging by the surrounding polygon pattern. It is one of a group
of three in the Tuktoyaktuk hamlet area. The pingo has been excavated to
expose the core which comprises segregated ice and pore ice. The stra-
tigraphy in the core was discussed by Rampton and Mackay (1971) and is
summarized here. Pond silt contains ice lenses and peat layers, and is
penetrated by ice wedges. Below the silt is sandy gravel which overlies
the pingo core. Nowhere do wedges penetrate the pingo ice, which comprises
alternating layers of ice and sandy ice. Rampton and Mackay (1971) refer
to normal faulting which occurred during uplift of the pingo - similar
faults have been reported in other pingos (Mackay and Stager 1966b). In
Tuktoyaktuk pingo the fault can be traced on each face of the cellar, and
the pingo core is upthrown relative to the gravel overburden, on a fault
plane dipping ca. 70°.

Ice Characteristics

The core contrasts greatly with that of Whitefish Summit Pingo.
Bubbles are very rare, and the compositional banding is determined by
sediment content (Fig. 18(a),(b)). Clay pellets up to 4 mm in diameter
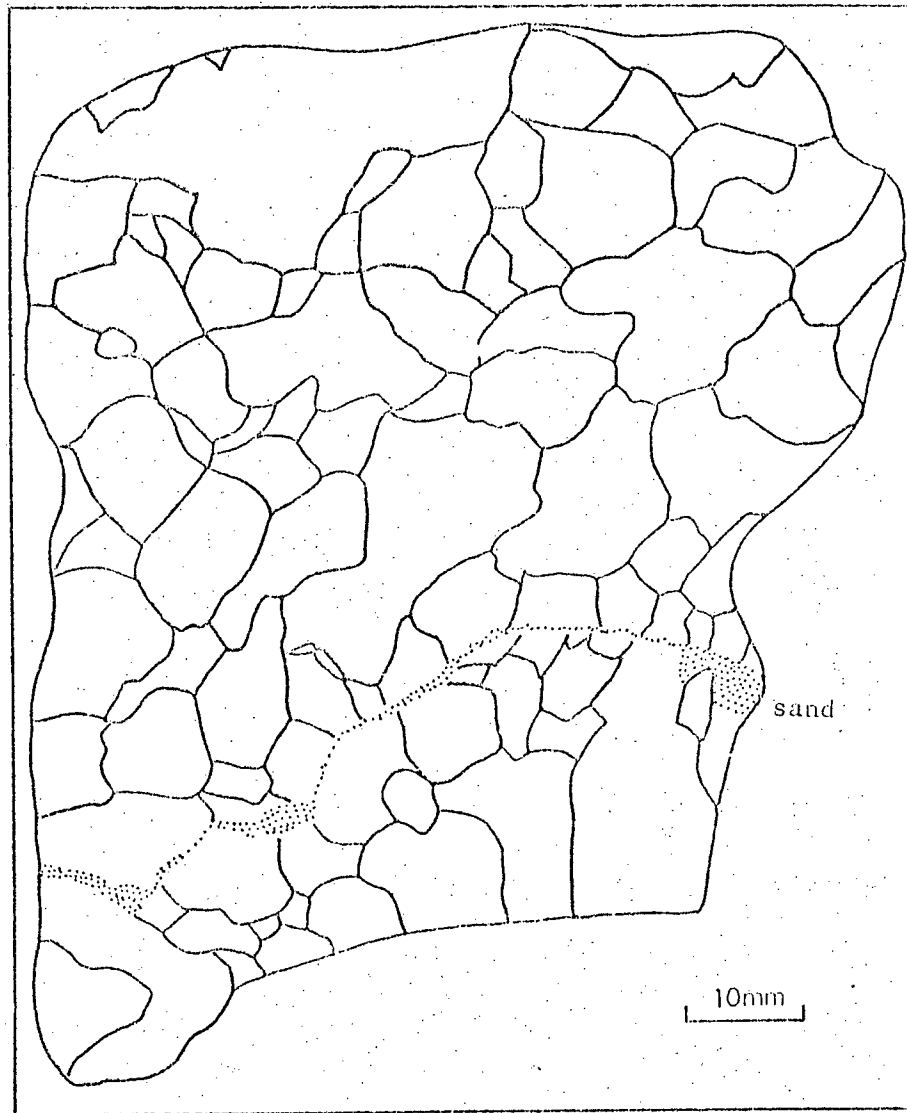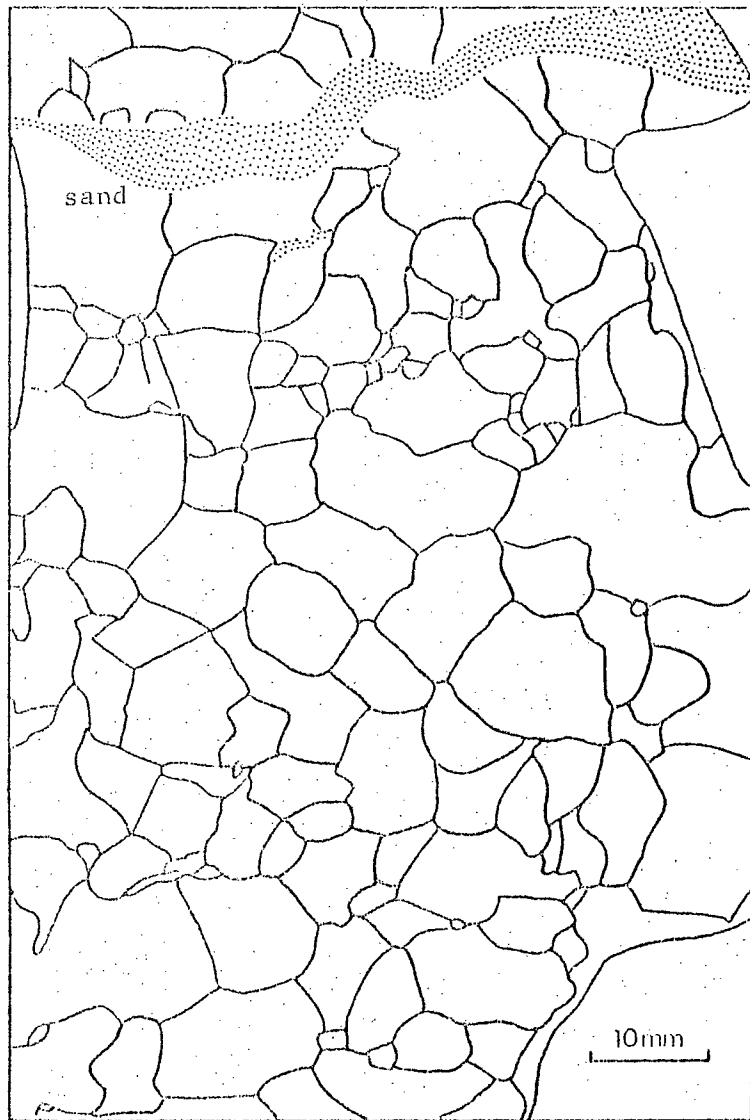
Figure 18.   Sediment and crystal characteristics, Tuktoyaktuk Pingo.

occur in discontinuous layers, more frequently sediment bands are of sand grade which continue laterally for many metres, indicating the regularity of the system. The bands are typically up to 10 mm thick, separated by 20-50 mm of sediment-poor ice. These layers are not planar but have local irregularities with vertical symmetry planes.

### Crystal Characteristics

Crystal shape characteristics were studied in vertical and horizontal sections, i.e. orthogonal and parallel to compositional layering, and were found to vary with crystal size and position relative to sediment bands.

Large crystals are anhedral with sinuous mutual contacts; boundaries with smaller crystals are strongly embayed, individual segments being slightly curved or straight. Mutual boundaries of small crystals are usually straight and give polygonal shapes. The small crystals have no pronounced substructure but embay large crystals along their sub-boundaries. Near sediment bands shapes of all grain sizes change such that boundaries approach the bands at right angles.

Crystal sizes are tabulated in Table 2, omitting crystals within sediment bands. Average sizes are fairly consistent throughout, for both section orientations, ranging from 47 $mm^2$ to 79 $mm^2$. However there exists a recognizable range in size within a given section, from $> 100$ $mm^2$ to $< 10$ $mm^2$. Size falls a further order of magnitude in sediment layers.

Substructure is confined to larger grains which have been embayed by small crystals lacking substructure. This suggests the substructure developed before formation of the small crystals. Petrofabric analysis shows that the small and large grains do not have markedly different lattice orientations, indicating that the small grains may have formed by polygonization of large strained grains.

Dimensional orientation diagrams do not exhibit single maxima (Fig. 19). Vertical thin sections contain vertical concentrations in crystals away from sediment bands and horizontal concentrations adjacent to sediment. Horizontal sections are dominated by long axes parallel to the strike of sediment bands. Thus sediment content plays a major role in determining dimensional orientation.

Optic axis orientations are shown in Figures 20, 21; Figure 20 represents sections parallel to the compositional layering and Figure 21 represents orthogonal sections. Figure 20(a) and (b) are from adjacent thin sections, (a) is 25 mm above (b); (a) shows a more diffuse pattern than (b), but there is a tendency toward a concentration approximately orthogonal to the layering. Component diagrams have been prepared on the basis of presence or absence of sub-boundaries (Fig. 20(c),(d)) and crystal size (Fig. 20(e),(f)). The diagrams are essentially similar, all are diffuse single maxima, but the crystals with sub-boundaries are slightly more concentrated than those without sub-boundaries and the large crystals are less scattered than the small. Sub-boundaries indicate basal plane slip and the small crystals represent break-up of larger grains.
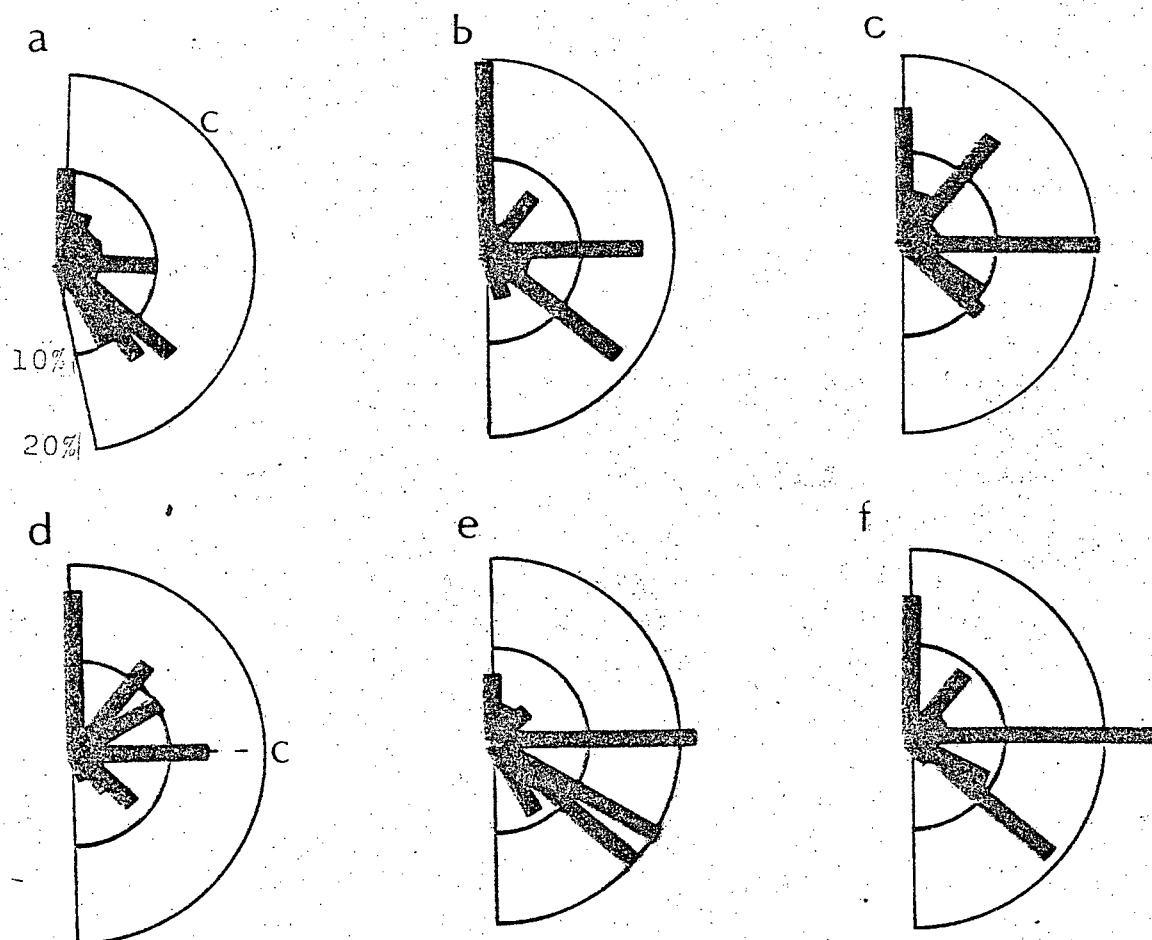
Figure 19.   Crystal dimensional orientation, Tuktoyaktuk Pingo.

(a)-(c) horizontal sections;
(d)-(f) vertical sections.

TABLE II
Crystal Size, Tuktoyaktuk Pingo

| Section Orientation | | Crystal Size, mm$^2$ |
|---|---|---|
| Horizontal | 100 crystals | 53 |
| | 119 crystals | 63 |
| | 114 crystals | 79 |
| Vertical | 97 crystals | 47 |
| | 105 crystals | 55 |
| | 114 crystals | 67 |

Figure 20.

Figure 20 (cont'd)



g

h

i

j

k

l

84
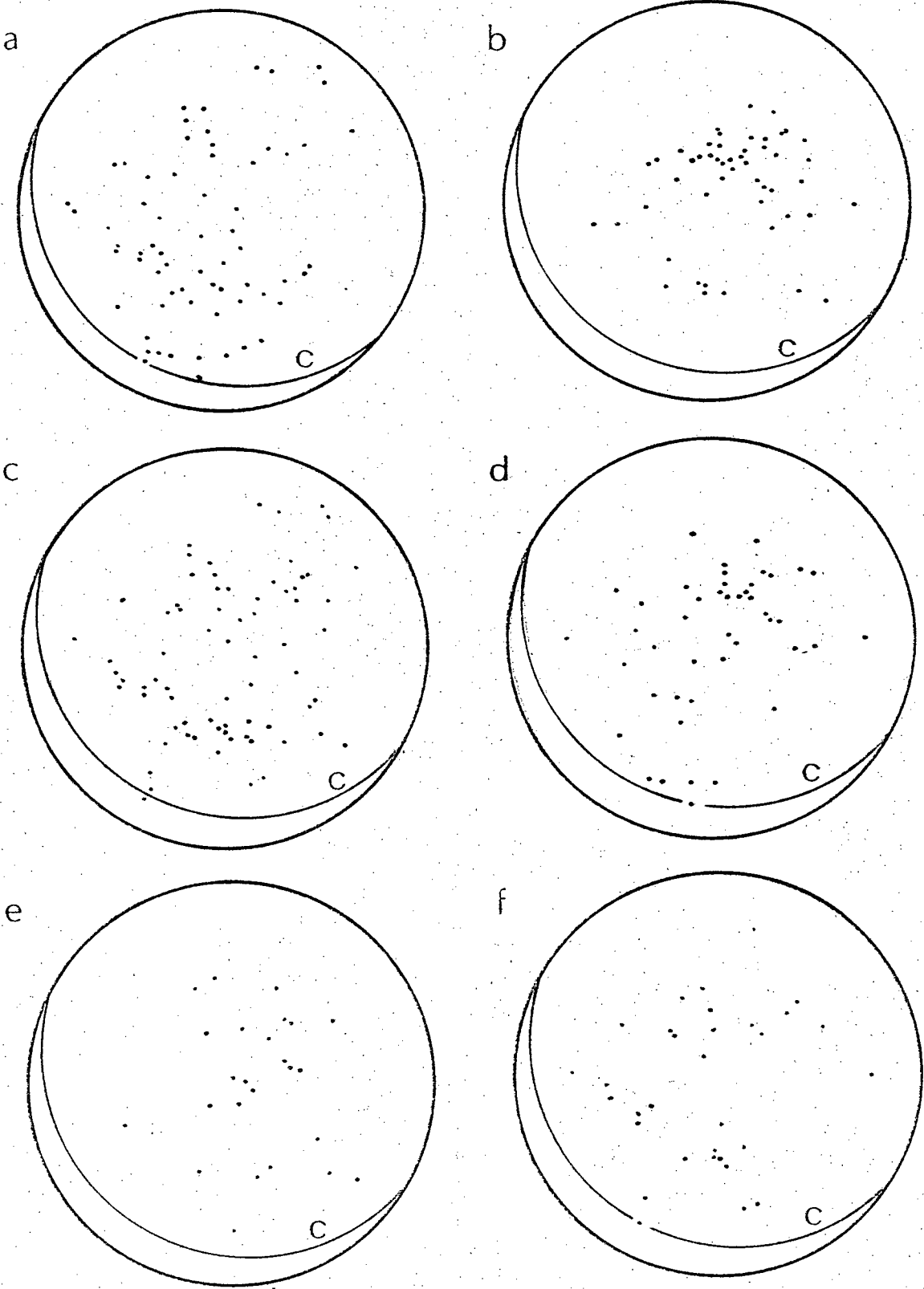


Figure 20. Tuktoyaktuk Pingo.

(a),(b) horizontal sections
(c)  crystals without sub-boundaries
(d)  crystals with sub-boundaries
(e)  large crystals
(f)  small crystals
(g)  horizontal section
(h)  small crystals
(i)  large crystals
(j)  crystals without sub-boundaries
(k)  crystals with sub-boundaries
(l)  crystals with dimensional orientation normal to layering
(m)  crystals with dimensional orientation at 45 to layering
(n)  crystals with dimensional orientation parallel to layering.

c = compositional layering

Figure 21.
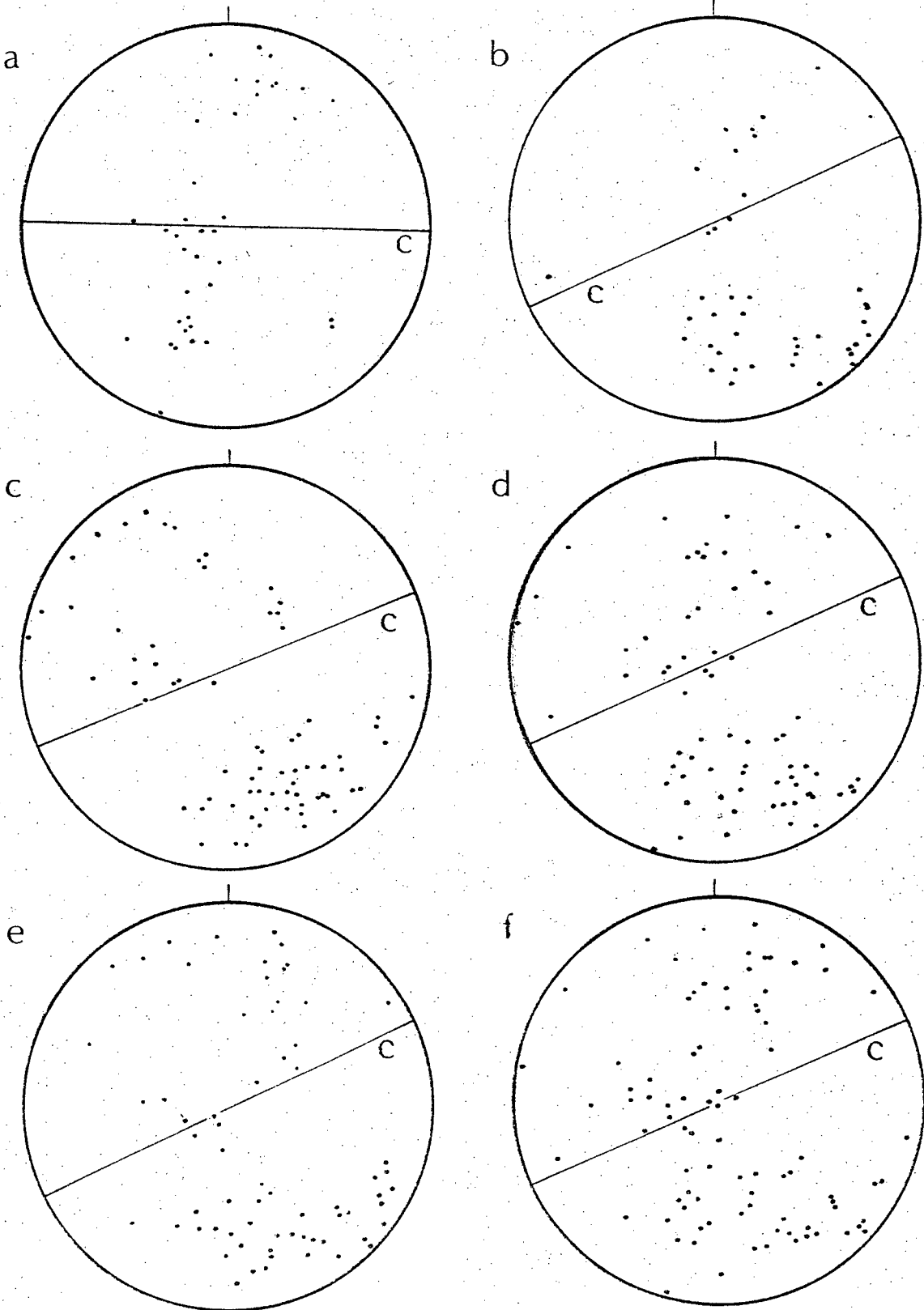
Figure 21 (cont'd)
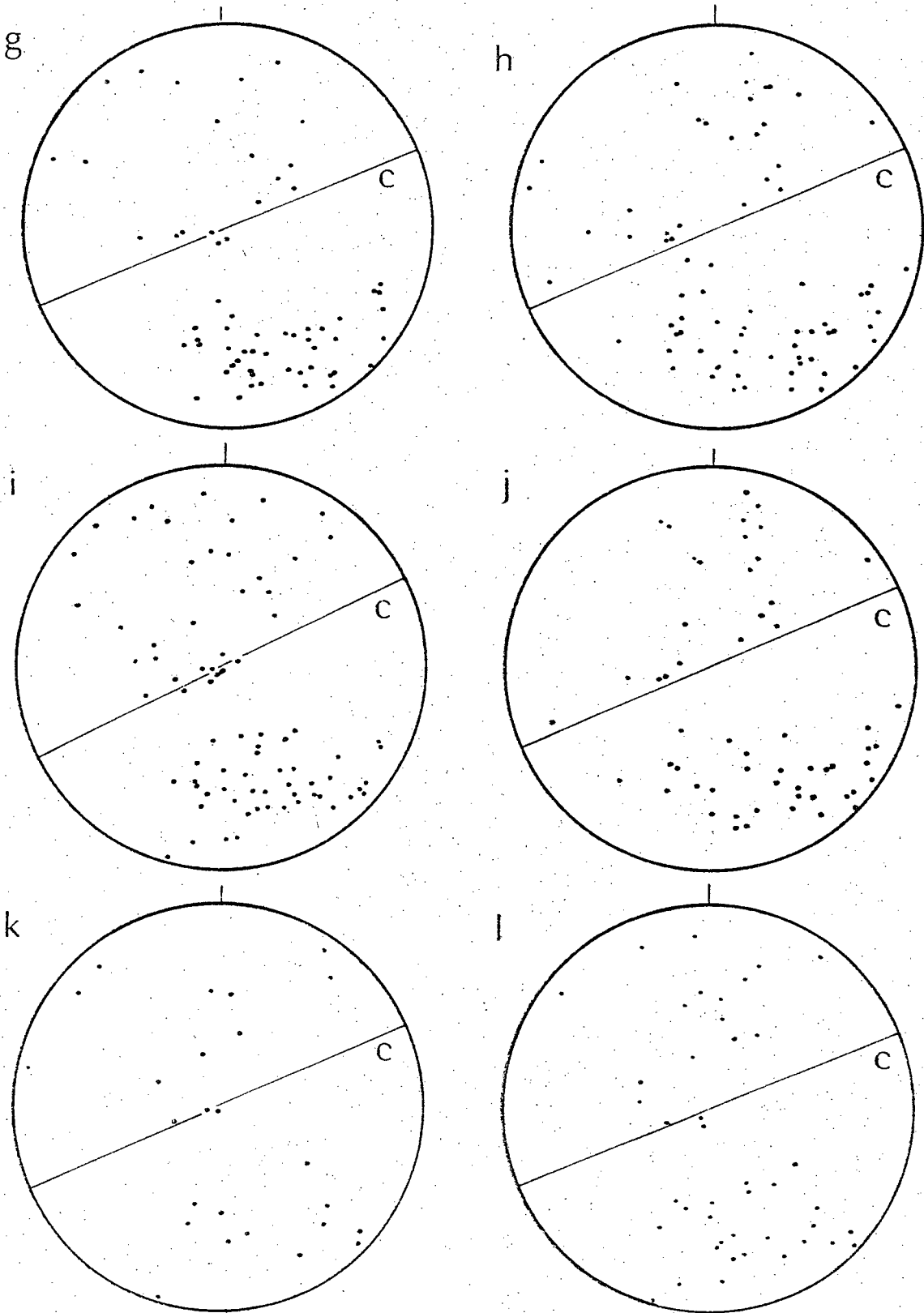
Figure 21 (cont'd)
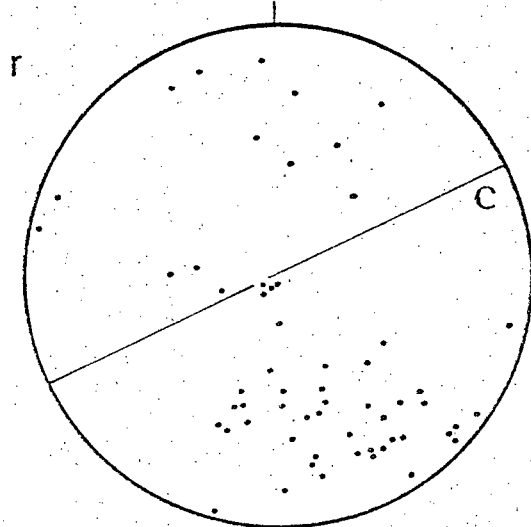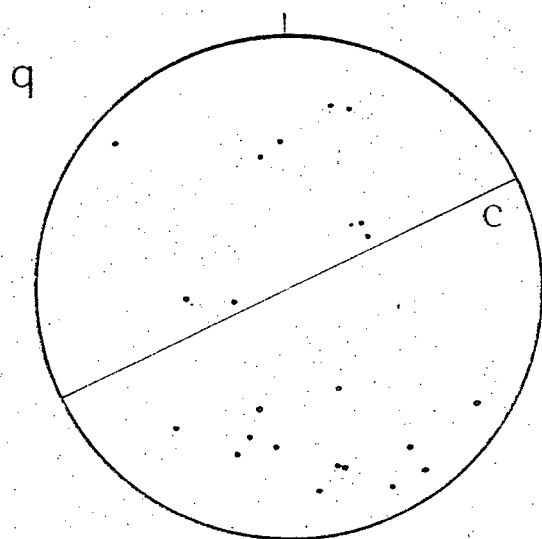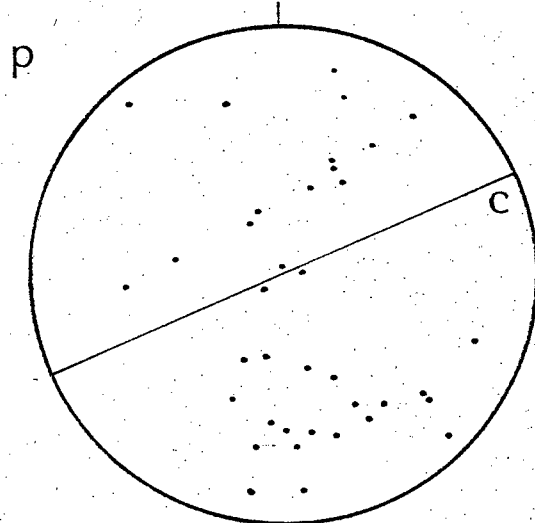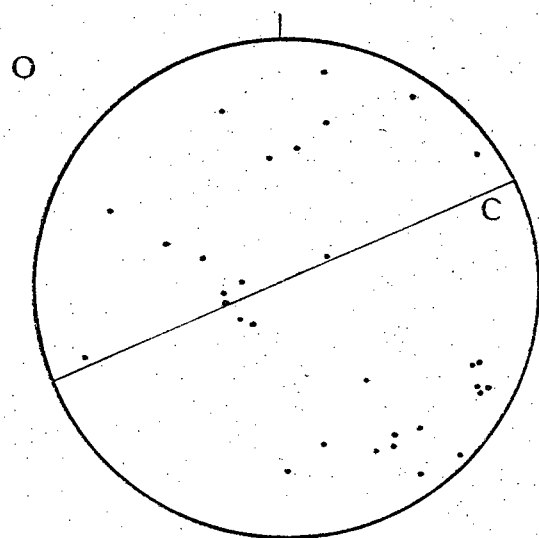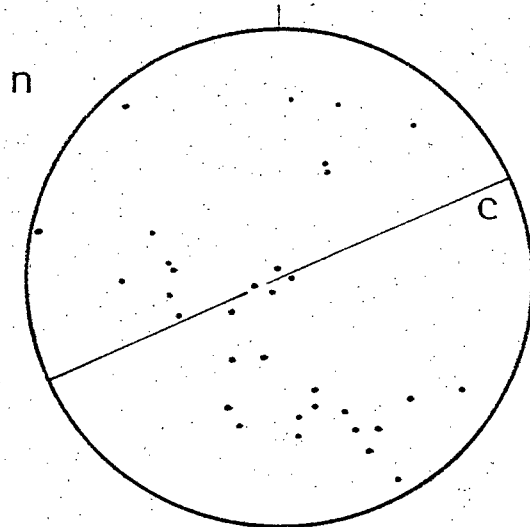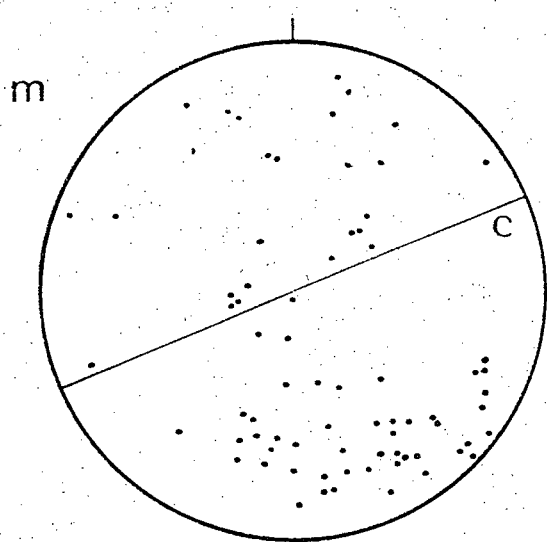
Figure 21.   Tuktoyaktuk Pingo Petrofabrics.

(a),(b),(c)  Vertical sections

(d)   73 crystals with at least one straight side

(e)   67 crystals with no straight sides

(f)   86 crystals away from sediment bands

(g)   64 crystals adjacent to sediment bands

(h)   73 crystals with sub-boundaries

(i)   78 crystals without sub-boundaries

(j)   58 crystals with long axes greater than 10 mm

(k)   25 crystals with long axes less than 6 mm

(l)   44 crystals with less than 6 sides

(m)   72 crystals with more than 6 sides

(n)   33 crystals with 6 sides

(o)   31 crystals with 40° dimensional orientation

(p)   37 crystals with 90° dimensional orientation

(q)   24 crystals with 0° dimensional orientation

(r)   59 crystals with other than 40°, 90°, 0° dimensional orientation

c = compositional layering

Figure 20(g) represents another section approximately parallel to the compositional layering (sketched in Fig. 18), and Figure 20(h)-(n) are component diagrams. Again there occurs a major c-axis concentration orthogonal to the layering, but with minor maxima also. In the component diagrams, Figure 20(k) indicates that crystals with sub-boundaries have a stronger concentration orthogonal to the layering than other crystals, which suggests these crystals are preferredly oriented for basal glide.

Figure 21(a)-(c) represent a vertical thin section, and component diagrams are shown in Figure 21(d)-(r). The general pattern is for a maximum at 60° to the layering, contained in a girdle orthogonal to the layering. The component diagrams show no major difference, although the concentration maximum is more pronounced in crystals with sediment in their grain boundaries (Fig. 21(g)) and the girdle pattern is better developed in other crystals (Fig. 21(f)). In terms of crystal shape, Figure 21(d) shows crystals with at least' one straight side; the pattern does not differ substantially from Figure 21(e) which represents crystals having all sides curved. The relationship between number of sides in crystals and their c-axis orientation was also investigated. The resulting diagrams for $n < 6$, $n > 6$ and $n = 6$, where $n =$ number of sides, are shown in Figure 21(o)-(r). Figure 22(a) and (b) represent crystals in a vertical section adjacent to that of Figure 21. The c-axis pattern differs substantially from Figure 21, many c-axes being close to the compositional layering. This is also evident in Figure 22(g) and (h) which represent vertical sections. Here the compositional layering is locally variable in thickness and orientation of which an approximation is shown in the

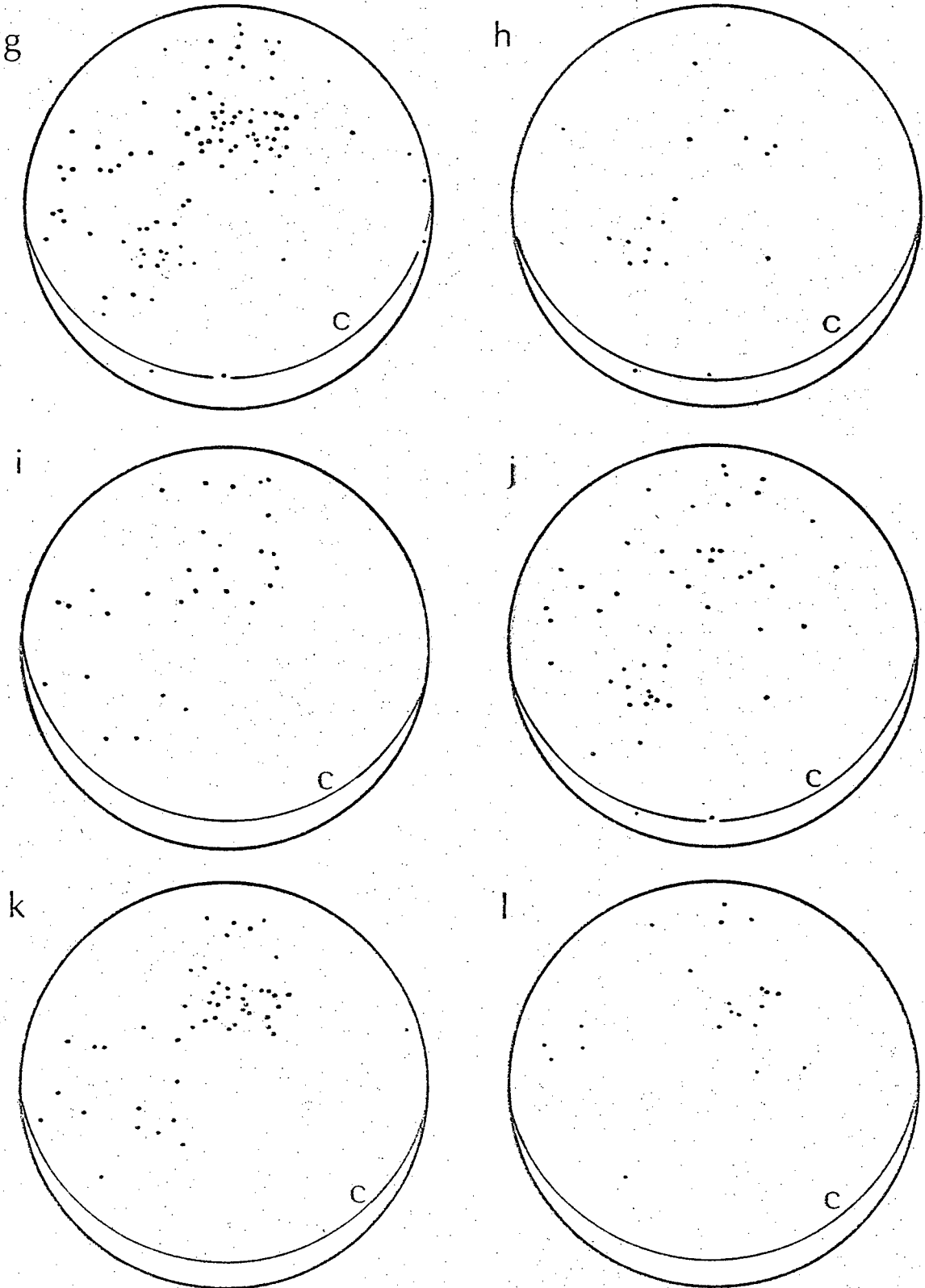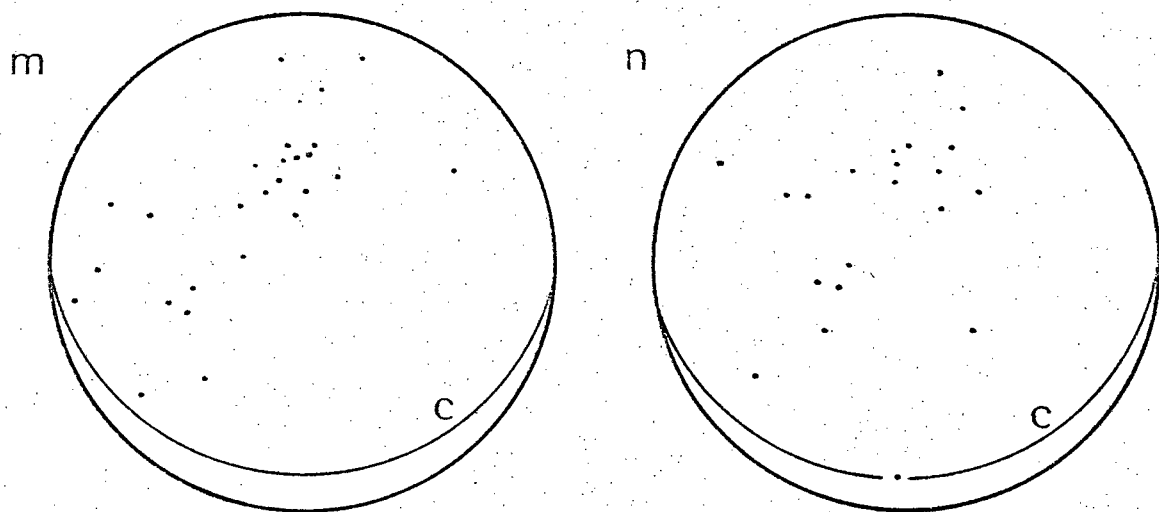Figure 22.
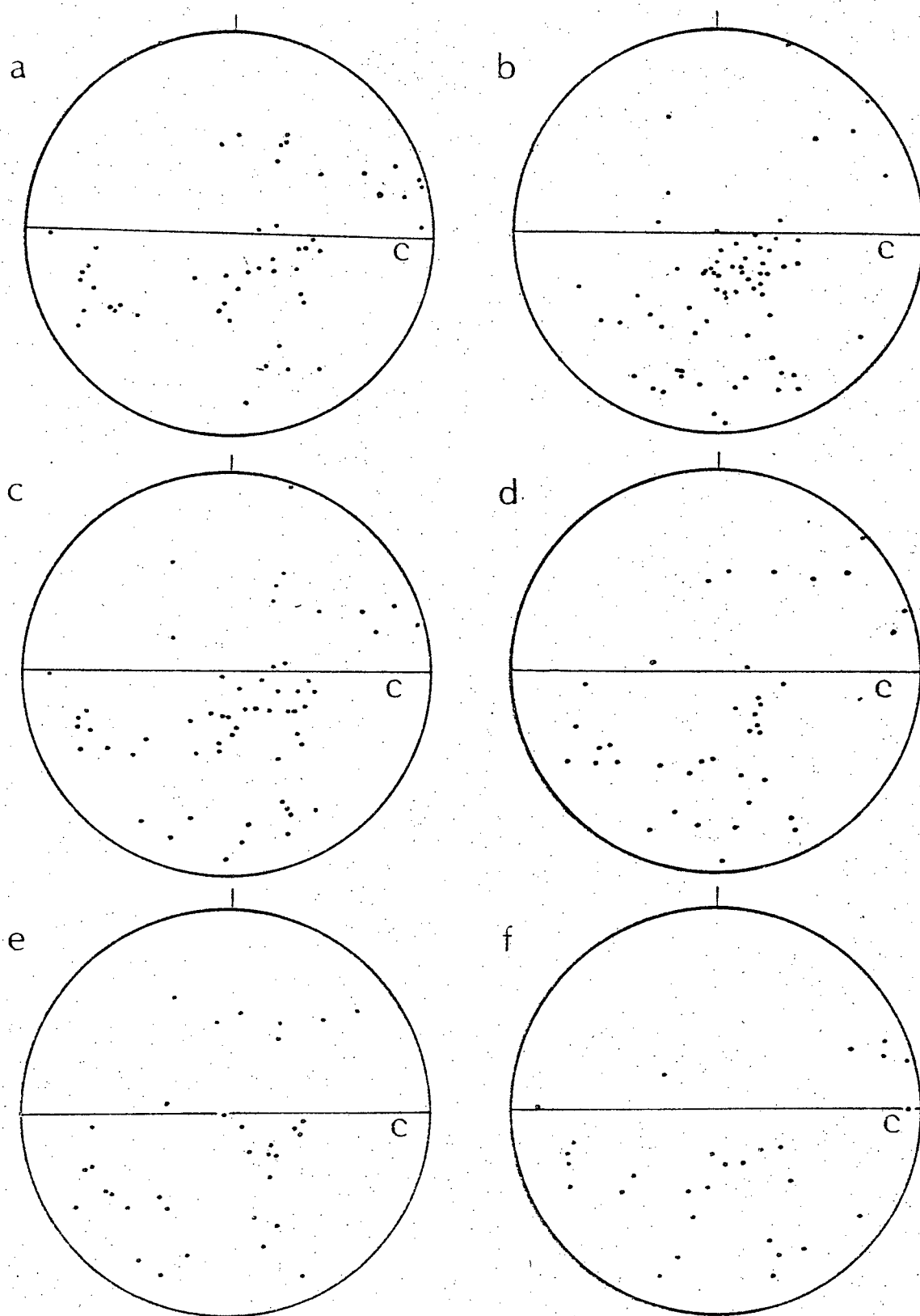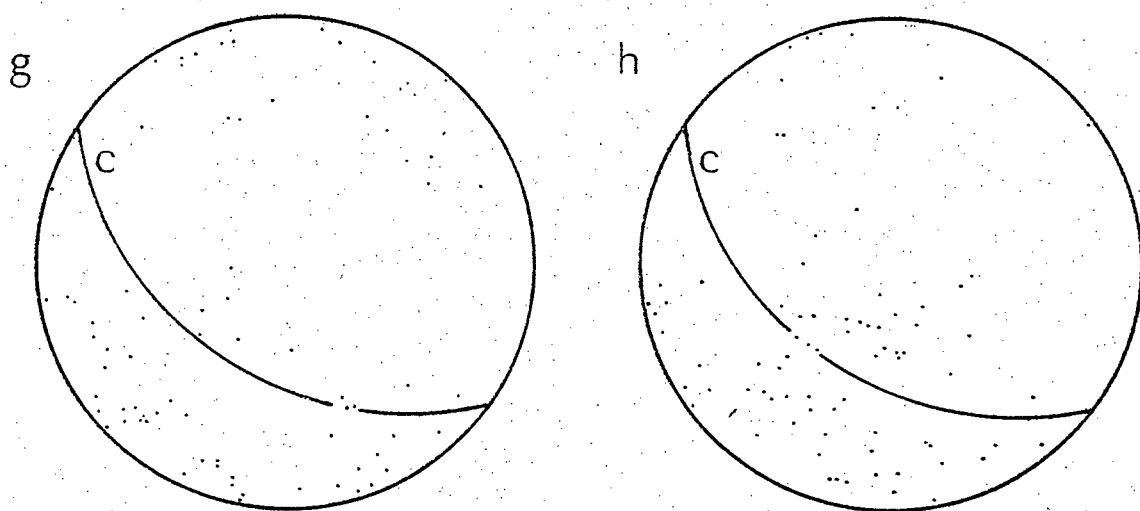
Figure 22.   Tuktoyaktuk Pingo.

   (a),(b)   vertical sections

   (c)   59 crystals with sub-boundaries

   (d)   39 crystals without sub-boundaries

   (e)   32 small crystals

   (f)   29 large crystals

   (g)   vertical section, 76 crystals

   (h)   vertical section, 78 crystals

   c = compositional layering

figures. Thus there is considerable variability of optic axis orientations in adjacent sections, and patterns cannot be related systematically to crenulations in compositional layerings.

### Interpretation

Tuktoyaktuk pingo core is characterized by alternating layers of pore ice and segregated ice; bubbles are almost completely absent. Thus growth conditions differed substantially from those of Whitefish Summit Pingo, and Tuktoyaktuk Pingo is a result of both segregated and pore ice growth. The layers of pore ice are up to 25 mm thick and the segregated ice layers reach 100 mm. Layers are traceable laterally for several meters, and are fairly constant in thickness.

Despite the overall symmetry of the mesoscopic features of the core, petrofabric diagrams show a range of patterns from single maxima orthogonal to the layering (Fig. 20(b)) to girdles parallel to the layering (Fig. 22 (g),(h)). These variations occur over short lateral and vertical distances; often the thin sections are from the same specimen, so there is no possibility of mistake in the orientation of the sections. Little heave has occurred compared with the involuted hill and there is no evidence of substantial flow in the body, although basal plane slip and deformation band development have occurred, indicating that any flow was concentrated in ice layers rather than in pore ice. However, this does not explain the local variability in petrofabrics. In terms of original growth conditions, the alternating segregated and pore ice layers indicate variations in water supply and pore water pressure.
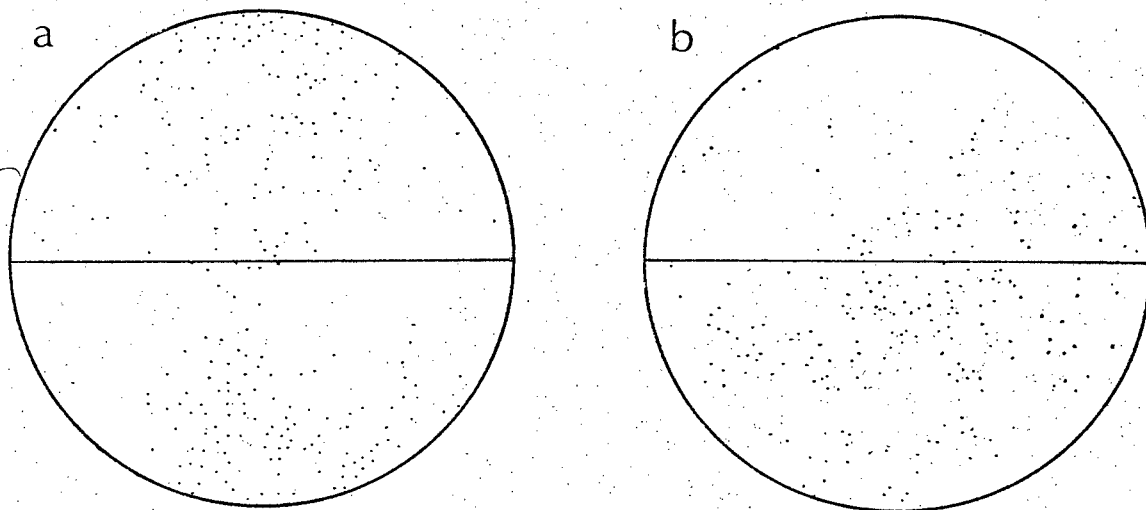
Figure 23. Summary petrofabric diagrams, Tuktoyaktuk Pingo.

(a) Summary diagram of Figures 20, 21.

(b) Summary diagram of Figure 22(a), (b), (g), (h).

## Conclusion

The three pingos discussed represent three different stages in
Mackay's (1973a) classification. Pingo No. 11 is indicative of a tempo-
rary, early growth stage in bulk water, and displays some similarity to an
icing mound. A change in growth conditions was recognized in Whitefish
Summit Pingo, related to uplift of the lake bottom, with growth of segre-
gated ice. In Tuktoyaktuk Pingo a further stage was shown by alternating
segregated and pore ice. In addition to differences in size, shape and
inclusion patterns in the three pingos, it was found that there were
related crystal characteristics, although not all petrofabric diagrams
could be explained.

## 4. Involuted Hill Ice

### Introduction

The term "involuted hill" was applied by Mackay (1963, p. 138) to
extensive ice-cored hills with flat tops. A notable feature is the pre-
sence of steep ridges which are frequently lateral, or cross the tops.
The hills are abundant near Tuktoyaktuk.

#### Field Characteristics

The surface form of the hills has been discussed by Mackay (1963,
1973b) and a gravity profile of one such hill was presented by Rampton
and Walcott (1974). The internal structure has been recorded from coastal
and inland slumps (Mackay 1973b; Rampton and Mackay 1971) and a Geological

Survey of Canada drilling project (Scott, personal communication 1974).

Characteristically 1-10 m of stoney clay containing a reticulate ice-vein

system overlies an ice core, with sand at depth. Observations of several

hills show that surface ridges are underlain by rises in the ice core.

Generally the reticulate ice veins are orthogonal and parallel to the

upper surface of the massive ice. Mackay (1974b) argues that the ice

veins formed in the clay during downward freezing, and the massive ice

core grew by a segregation process and that sand below the cores supplied

the water necessary for core growth. The cores may reach 25 m in thickness,

but drilling in a number of hills has shown thin discontinuous gravel,

sand and clay layers. In this study we discuss only one hill, 5 km south-

west of Tuktoyaktuk.

The presence of compositional layering in the core was pointed out

by Mackay (1963) to consist of alternating layers of clear and bubbly ice,

and occasional sediment-rich ice. The layering at the top is approximately

parallel to the upper ice surface, and becomes horizontal at depth. Ver-

tical fractures are present in the massive ice, and some ice wedges pene-

trate through the stoney clay overburden into the core.

Coastal erosion has removed a major section of the hill; total

retreat in the period since 1935 air photography has been> 240 m. This

retreat has produced steep ice cliffs, and has added to the creep process.

Sampling was carried out at sites where creep was minimal: (a) an

artificial pit on the landward side of the hill; (b) exposures away from

cliffs.

The presence of anticlinal folds in the layering of the ice core

has been pointed out; locally these folds are penetrated by ice wedges.

The sampling plan was as follows: (i) by coring from the exposed top of the massive ice, (ii) by coring from a pit, (iii) by sampling round a fold beneath a surface ridge, (iv) by sampling along the limb of an anticline adjacent to a wedge. The intention was to demonstrate (a) any changes in structure, petrofabrics and texture through the hill, indicative of growth mechanisms and subsequent deformation associated with heave and gravity creep, (b) the folding mechanism beneath "involutions" (c) the influence of wedge growth on the petrofabrics and texture in such a fold, (d) the characteristics of thermal contraction cracks in massive ice, and their mode of infil.

## (a)   Vertical ice cores

### Introduction

A SIPRE corer was used to obtain vertical cores (i) at the top of the hill, (ii) at sea-level. Thus the profiles obtained have a horizontal offset. The coring sites were chosen near exposed cliffs where little folding was observed, thus the core is thought to represent relatively undisturbed ice. Exposures on various parts of the hill display the reticulate vein ice system within the stoney clay overburden, the veins are approximately normal and parallel to the contact with the underlying ice. Those nearly orthogonal to the contact dominate.

### Ice Characteristics

A 3.8 m section of the upper core is shown schematically in Figure 24. The alternating bubbly/non-bubbly layering and sediment bands are apparent. Bubbles within a given band vary in size and shape, ranging up
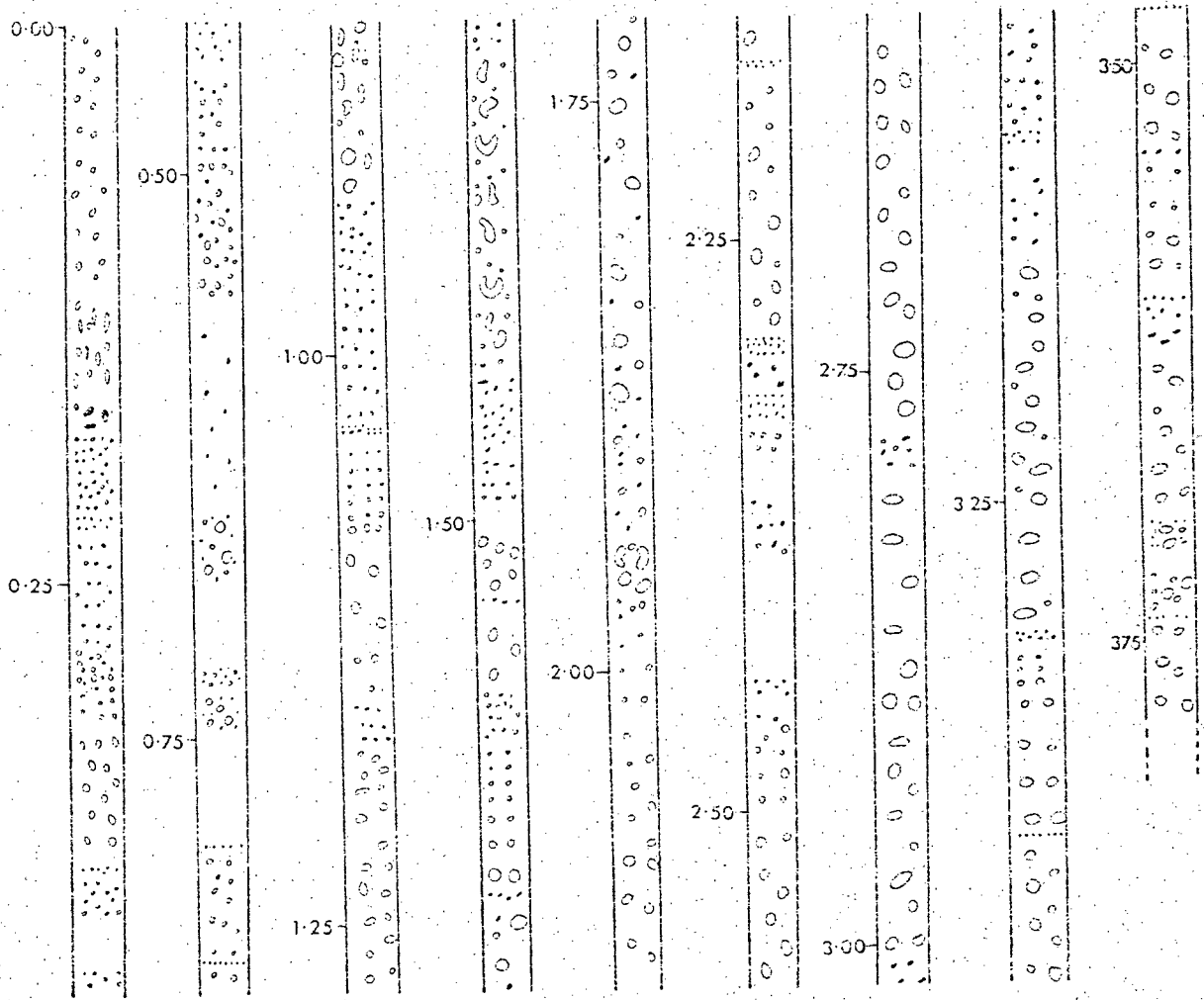
Figure 24. Stratigraphy of involuted hill ice core. Depths in metres.

bubbles    sediment
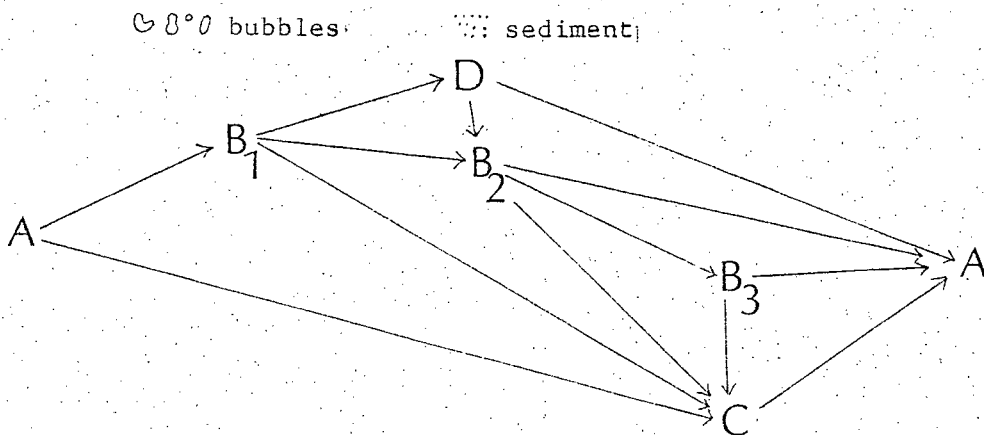


Figure 25. Probable downward transitions from one ice type to the next:
A = clear ice, $B_1$ = small bubbles, $B_2$ = medium bubbles,
$B_3$ = large bubbles, C = clay, D = sand.

to 10 mm long. The layers are shown as horizontal, although a slight

dip was present. It is evident that the upper ice has been subject to

considerable uplift, at least 15 m (the thickness of the ice core) and

locally differential uplift (folding). Additionally it is to be expected

that some creep under gravity has occurred, and varying thermal gradients

have been imposed. Thus some modification of the original growth forms

of the bubbles may have occurred. From Figure 24 we see that elongated

bubbles are orthogonal to the containing layers despite the dip of those

layers. Thus they have not been rotated parallel to the layering, or to

the fold axial surface.

Sediment occurs as clay pellets and thin sand layers; the two types

occur separately. These bands are much narrower and frequently less

extensive laterally (where exposed) than the bubble bands.

### Banding Pattern

The sequence of layering in terms of bubble and sediment content

is investigated by recording the frequency of transitions from one type

of layer to the next and preparing a downward transition probability

matrix. Probable transitions are shown in Figure 25, suggesting that

in some cases several possibilities are almost equally likely, e.g. from

medium bubbles to either clear ice or large bubbles or clay, whereas in

other cases one transition is more probable, e.g. clay to clear ice. Some

probable sequences are clear ice to clay to clear ice, clear ice to small

bubbles to clay to clear ice, etc. In terms of freezing conditions it

is apparent that there is no simple pattern in layerings and thus no

recognizable pattern in sediment or gas inclusion or rejection for the

given sample. Generally the inclusion of sediment indicates lower pore water pressure.

## Crystal Characteristics

The compositional layerings of clear ice, bubbly ice and sediment-rich ice each have related crystal sizes. The largest crystals occur in the clear ice, intermediate sizes in the bubbly ice, and the smallest in the icy sediment. Average sizes are given in Table 3 for several depths.

Table III

| Depth (m) | Crystal size ($mm^2$) | Ice type |
|-----------|------------------------|----------|
| 0 | 84 | Clear ice |
| 3 | 200 | Clear ice |
| 6 | 39 | Bubbly ice |
| 9 | 3 | Sediment-rich ice |
| 12 | 93 | Clear ice |

Crystal size in inclusion zones is controlled by the distance between inclusions (Fig. 26). This pattern is repeated throughout the thickness of the ice and indicates the influence of inclusions on grain boundary migration. Small inclusions are concentrated on grain boundaries, indicating that dragging of inclusions has occurred.
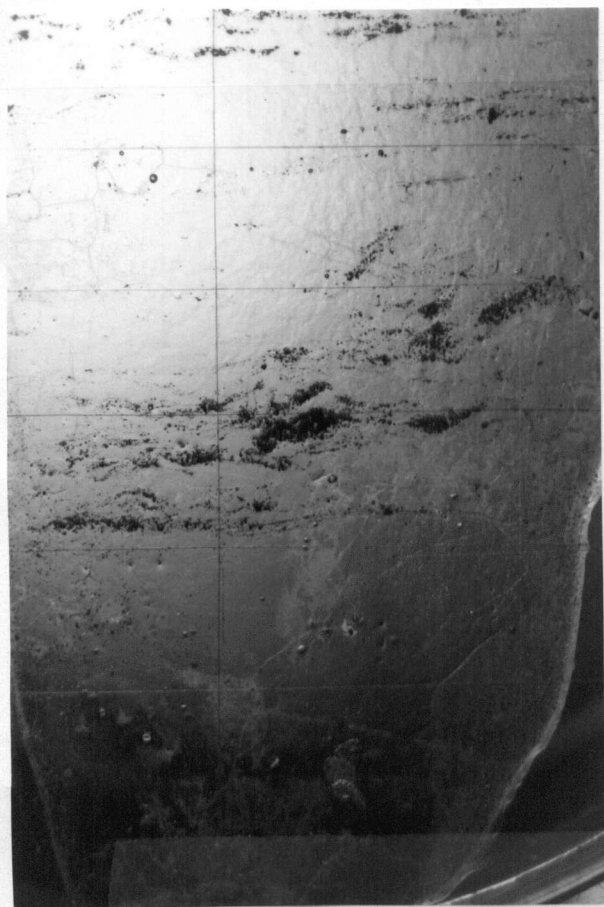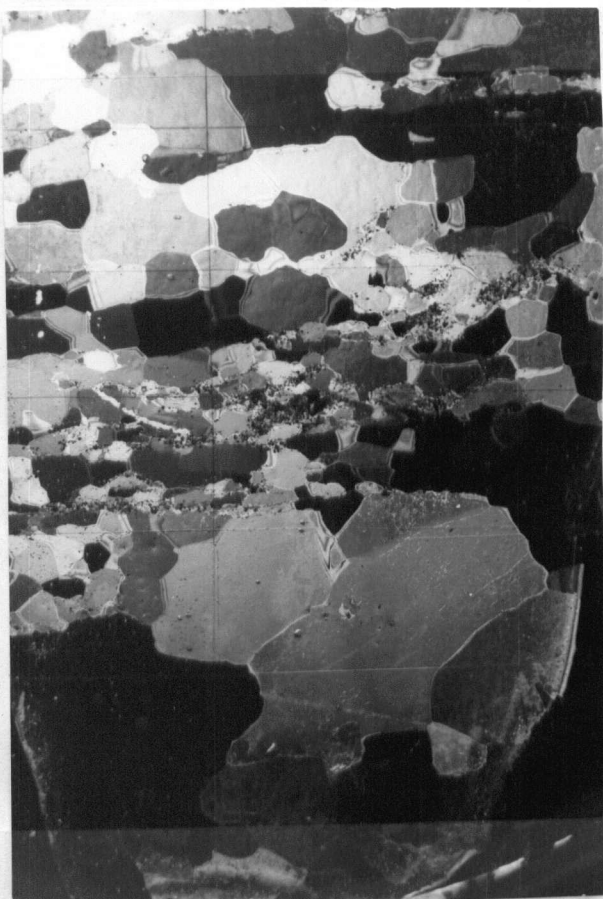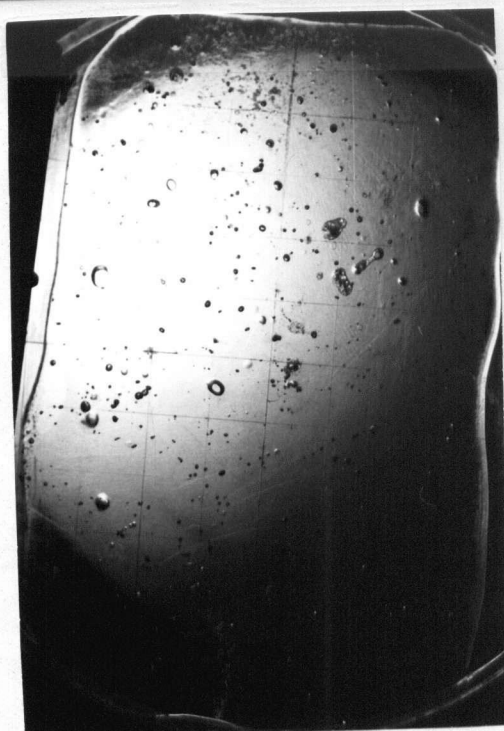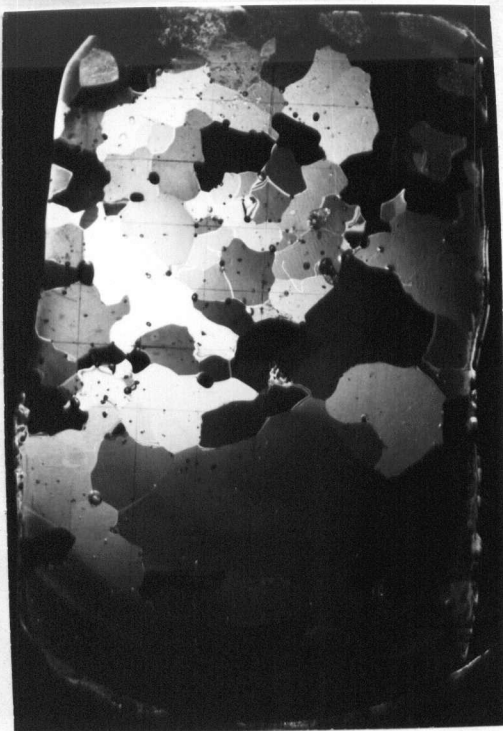
Figure 26.  Influence of inclusions on crystal size;
    (a),(b) influence of sediment (sand), vertical section,
    (c),(d) influence of bubbles, vertical section, 10 mm grid.

Crystal shape is related to inclusion type. In the case of clear ice there are no gross inclusions and no retardation of grain growth has occurred, thus crystals are large, anhedral and often interlocked. Serrations are rare at the boundaries of large crystals, rather the irregularities are on a centimetre scale. The smaller crystal size in bubbly ice is linked to a differing crystal shape; intergrowths are absent, boundaries are more gently curved except where influenced by bubbles, and in many cases are approximately straight. Similarly in sediment-rich ice the inclusions affect shapes; crystal size is smaller, boundaries are essentially straight from one inclusion to the next. Zones are not always separated by abrupt junctions, frequently one zone merges into the next. However, well defined sediment or bubble bands occur and the shape change is abrupt.

In addition to grain boundary migration and the influence of inclusions, there are other factors related to crystal size and shape. These are the presence of sub-boundaries, polygonized subgrains, and new grains formed during recrystallization. Sub-boundaries delimit zones of crystals with slightly differing lattice orientations and may thus intersect crystal boundaries.

In the lower section of the core the large crystals may have several sub-boundaries whereas they are absent from small grains. In the large crystals the sub-boundaries are orthogonal to the preferred dimensional orientation and are parallel to c-axes.

Crystal dimensional orientation is well developed parallel to the compositional layering in the upper part of the core. The pattern becomes

less pronounced with depth, but is locally strong where sediment bands influence the pattern. Frequency distribution diagrams of dimensional orientation for vertical sections parallel to the dip of the layering are shown in Figure 27(a)-(e).

The relationship of bubbles to texture also varies with depth. At the top bubbles are preferredly located on boundaries, although not necessarily at irregularities. The larger the bubble the greater the effect on texture. There appears to be a minimum size for a bubble to have control, and many small bubbles are contained within crystals. The larger the bubble the greater its effect on grain boundary migration. Boundaries may be temporarily retarded by, then break away from, or drag, small bubbles. Larger bubbles cause greater irregularities in boundary shape. Bubbles are less frequent on sub-boundaries, although in the larger crystals, the larger bubbles may be so situated. Bubbles tend to be absent from sediment bands, as is the case under growth conditions.

Sediment occurs as layers of clay pellets and icy sand. These layers are of lesser vertical and lateral extent than the clear and bubbly bands, but, depending on the sediment concentration, they have a marked effect on texture. The zones of higher sediment content provide distinct textural breaks; the overlying ice, whether clear or bubbly (Fig. 26), contains relatively large crystals which terminate at the sediment, with grain boundaries orthogonal to the layering. Crystals in the sediment bands were not readily observed by the thin section technique due to the difficulty of preparation of sections of dirty ice, but size is very limited. Where it is not concentrated in bands, sand tends to lie on grain boundaries, but not necessarily at irregularities in

Figure 27

j

k

l

10%

20%

m

n

o

p
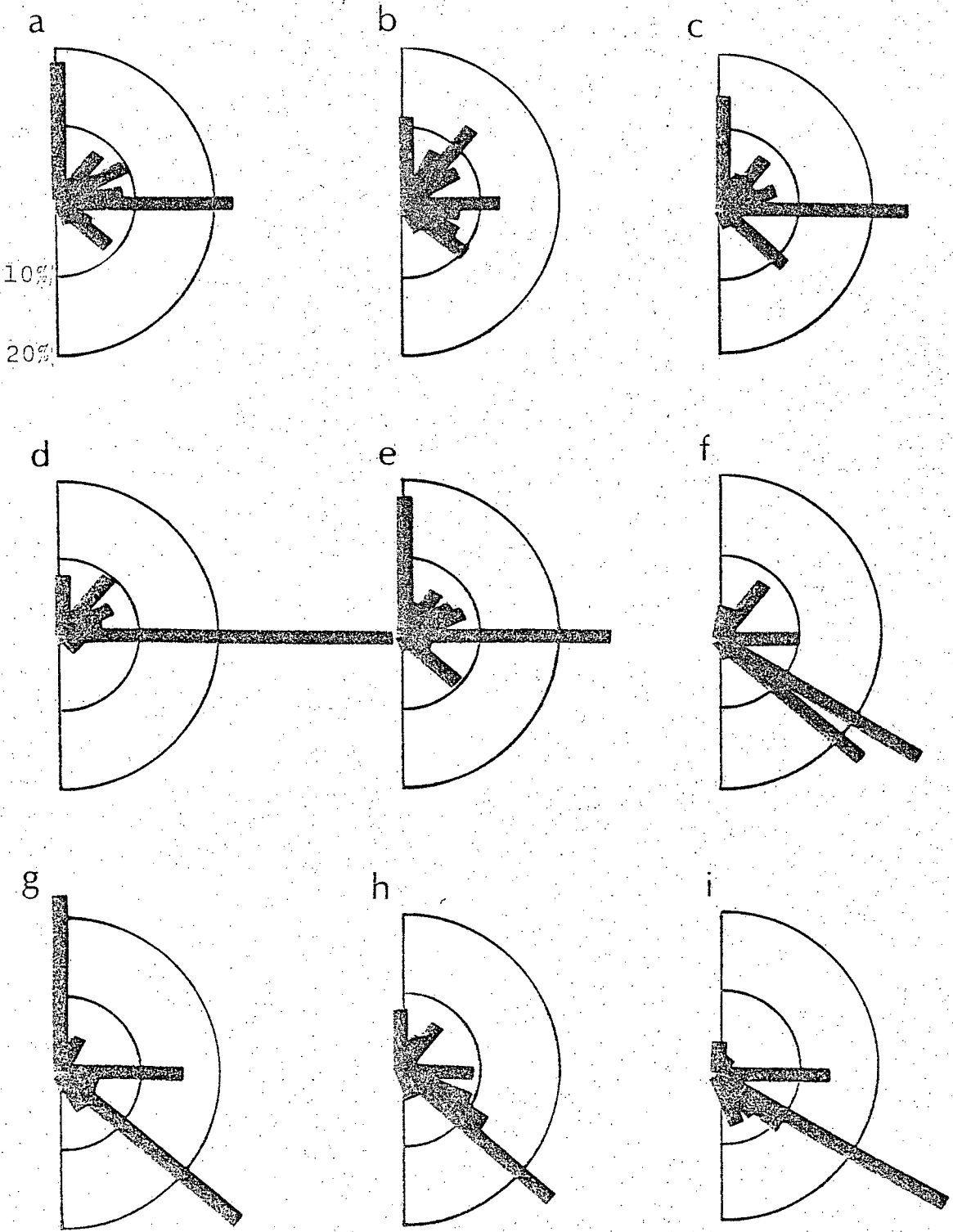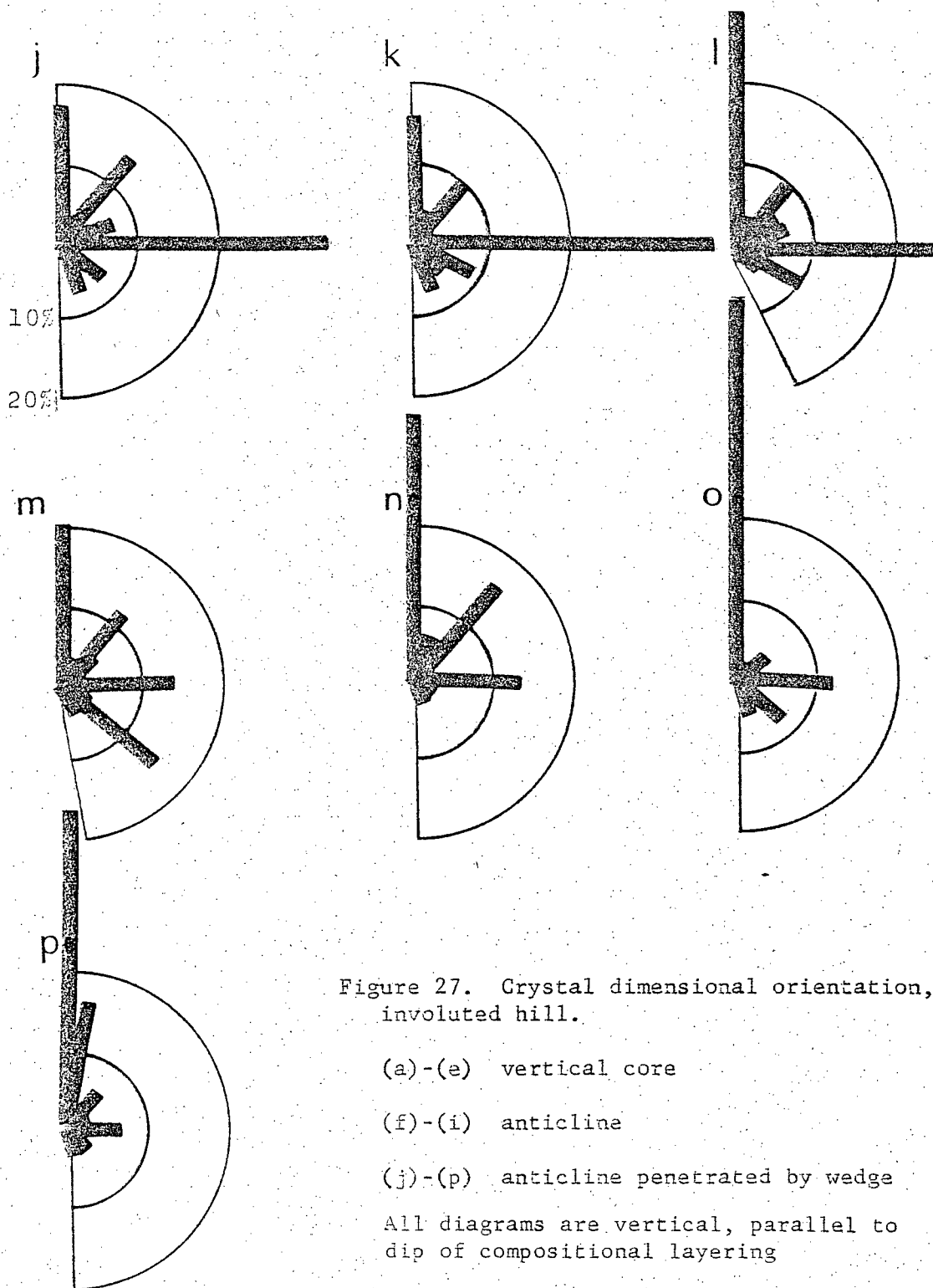
Figure 27.  Crystal dimensional orientation,
  involuted hill.

(a)-(e)  vertical core

(f)-(i)  anticline

(j)-(p)  anticline penetrated by wedge

All diagrams are vertical, parallel to
dip of compositional layering

those boundaries. Clay pellets are less texturally controlled, and often occur within crystals.

Where sediment bands are clear cut there are sharp changes in crystal size, from small in the sediment to very large in the inclusion free ice (Fig. 26).

The record of lattice orientations is incomplete as parts of the core were lost in transit. The available record is summarized in Figure 28. It is evident that strong concentrations occur at some depths; elsewhere the diagrams are more diffuse, but there is an overall tendency for c-axes to be orthogonal to the layering. Concentrations are greatest at the top of the core where some folding has occurred, and also in sections containing the strongest dimensional preferred orientations parallel to the layering. An example of the latter is where sediment bands occur, Figure 28(e); here flow has been concentrated in the ice with less sediment inclusions, with basal planes becoming parallel to the layering. Towards the base of the core the most recently grown ice has more diffuse distribution diagrams, but the major concentration is evident in addition to minor groupings and girdles. Figure 28(j) shows the characteristics of crystals outside the major concentration in Figure 28(i). In the upper part of the section such crystals are grouped rather than evenly distributed; in the lower part the crystals are smaller, separated and surrounded by larger crystals with c-axes in the major concentration. It is evident that some crystals with c-axes outside the maximum are large, but the majority are small and are probably being consumed by their neighbours.

Figure 23

g

h
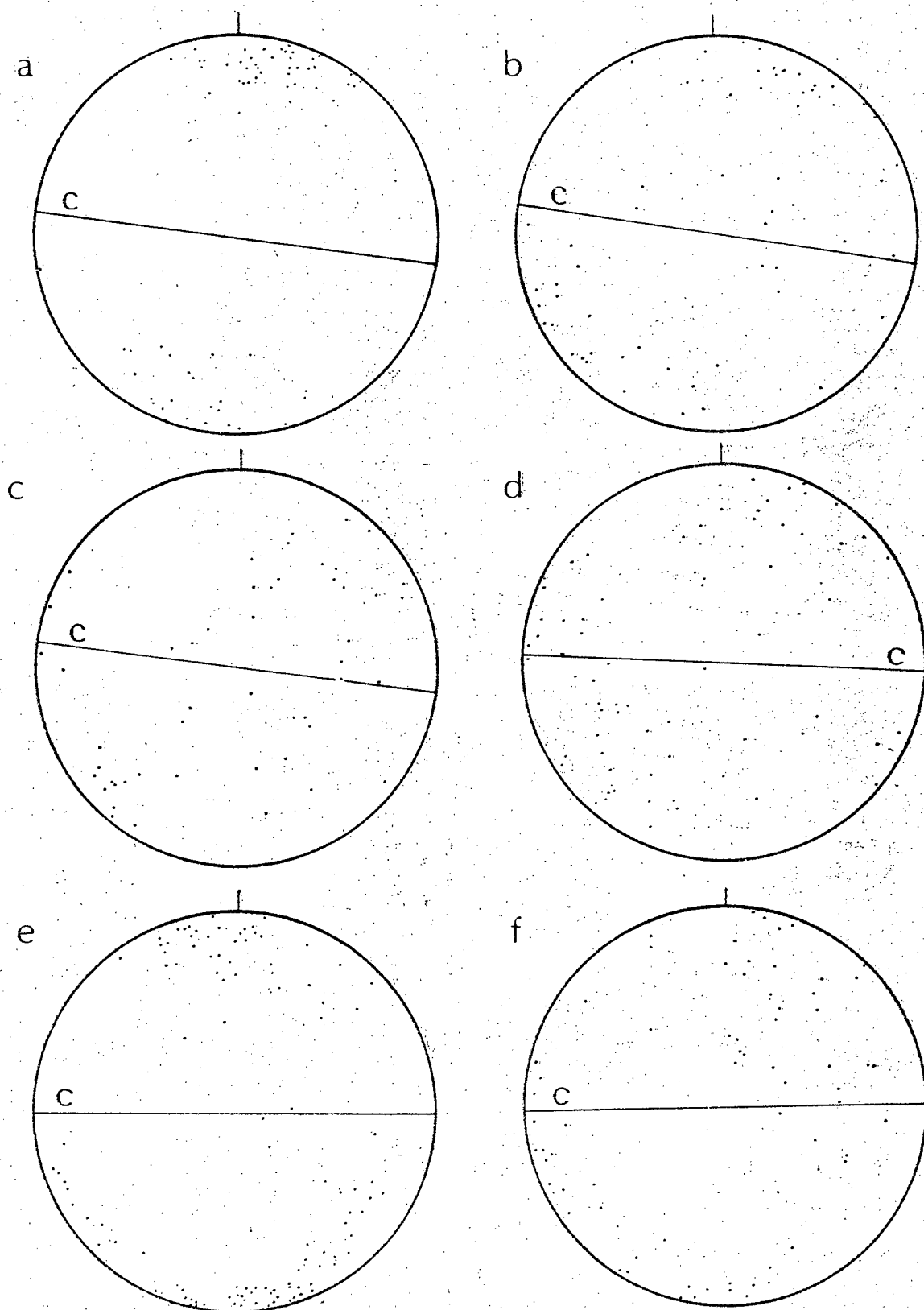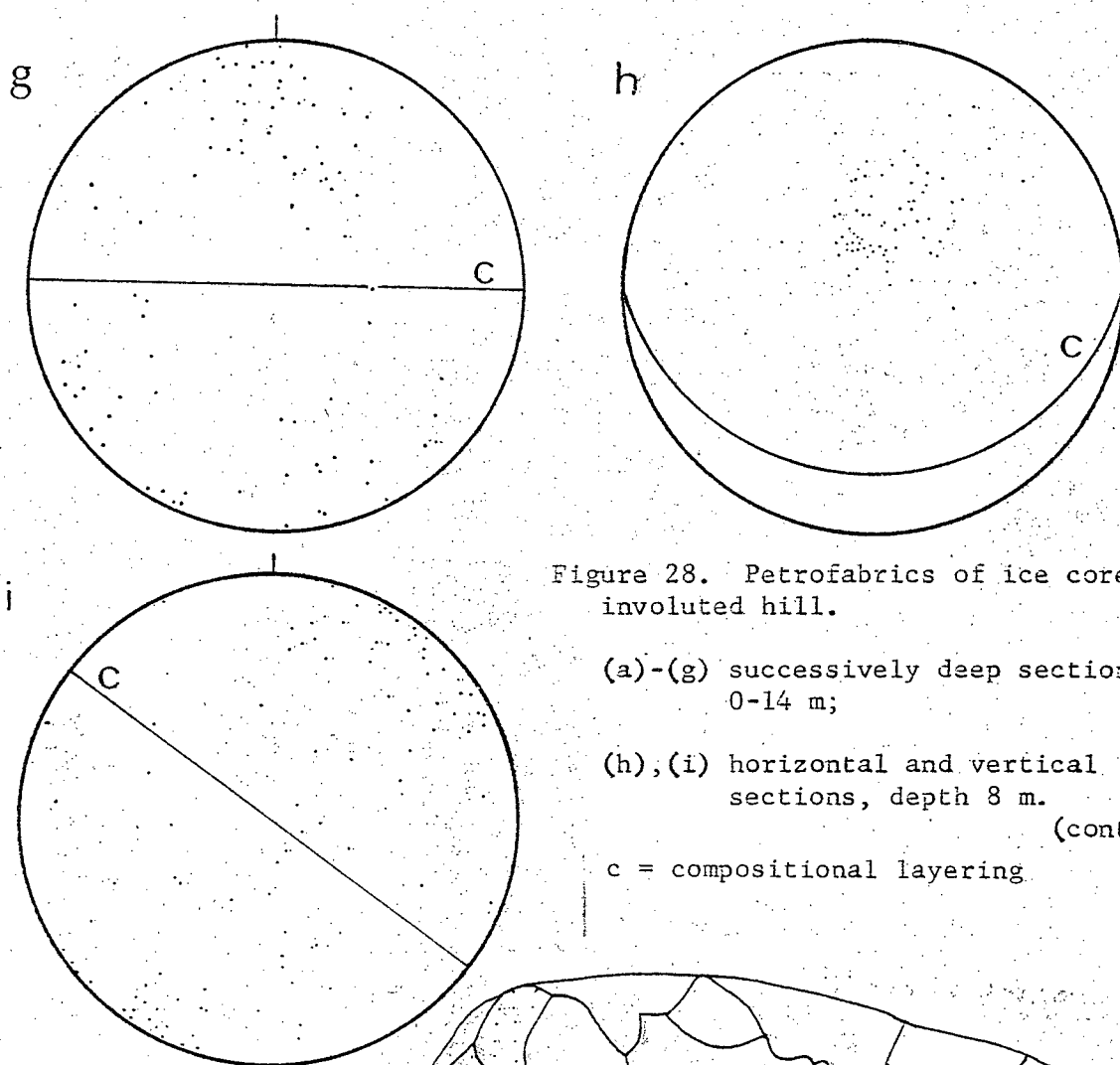
Figure 28. Petrofabrics of ice core, involuted hill.

  (a)-(g) successively deep sections, 0-14 m;

  (h),(i) horizontal and vertical sections, depth 8 m.

  (cont'd)

c = compositional layering

i

C

Figure 28 (cont'd)

  (j) vertical section indicating crystals outside the maximum.

  ... Crystals ... outside maximum.

j

10mm
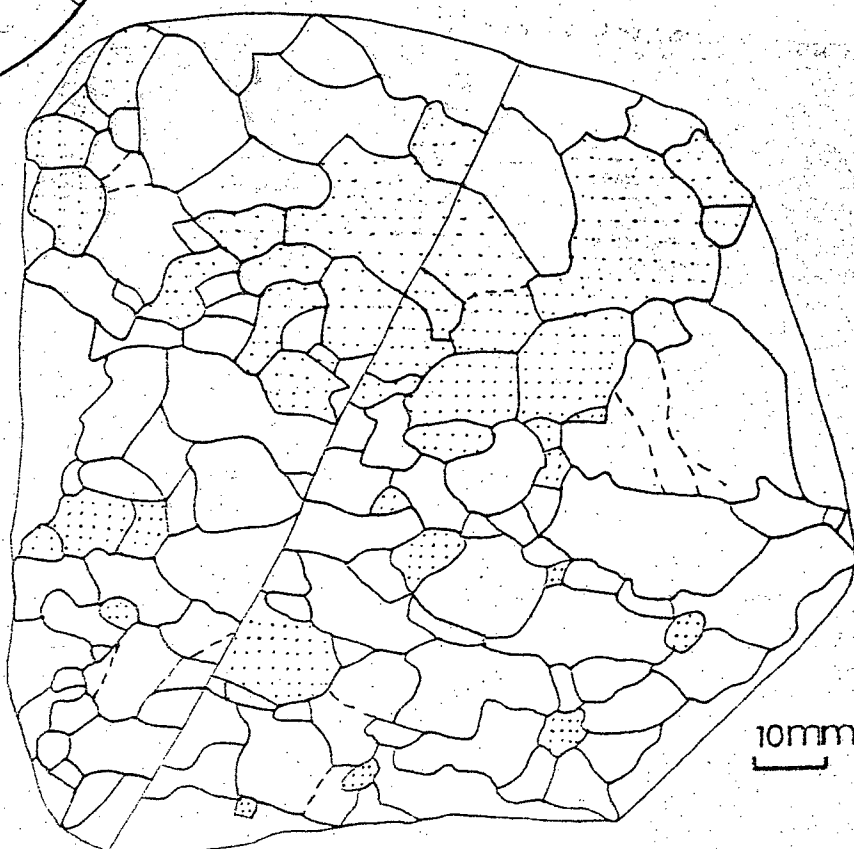
### Structural Features:  Fractures

Fractures occur throughout, and are typically approximately vertical, and pass through the layering sequence; rarely is there any offsetting.

### Microscopic Features of Fractures

In thin section fractures appear as narrow planar features marked by flattened gas inclusions, and sediment.  The gas inclusions occur on fracture surfaces passing through bubbly and bubble-free ice.  Bubbles adjacent to the fractures are not deformed more than others.  The paths of the fractures relative to texture are such that they are both intergranular and intragranular.  No local deviations occur; nor has there been any new crystal growth on the fracture surfaces.

### Interpretation

It is apparent that while there are contrasts in properties from layer to layer in the vertical ice core, there is no major change with depth of characteristics of a given layer type.  C-axis orientations are generally orthogonal to the layering throughout, although more dispersed patterns occur in bubble bands.  Weak c-axis maxima orthogonal to the layering are probably produced during the freezing process; this is true also of some pingos.  However it is evident that the ice has been uplifted by heaving, and that creep under the weight of ice and overburden has occurred.  The lattice preferred orientation has been accentuated especially in the inclusion free ice which now contains larger crystals. Dimensional orientation is parallel to the layering, whereas in the growth of ice in free water the orientation is parallel to the heat flow direction,

and thus orthogonal to any compositional layering. Also in the limited

work on textures in segregated ice, crystals tended to be columnar and

orthogonal to the plane of the lens (Penner 1961; Kaplar, personal com-

munication 1974). Thus the pattern observed here indicates flow parallel

to the layering. Differential flow may have occurred on layers of dif-

ferent inclusion content.

(b)   Anticlines beneath "Involutions"

### Introduction

Superimposed on the broad pattern of the topographic highs are

ridges which may be peripheral or may cross tops of hills. Coastal

exposures reveal the underlying structure to be anticlines in the ice,

the overburden being thinnest over fold crests, which undulate locally.

Some ridges contain ice wedges, with associated surface troughs, but

initially we consider a fold where wedges are absent, then proceed to

investigate the influence of wedge growth on such a fold. The charac-

teristic banding determined by bubble and sediment content continues into

the folds, with little variation in band thickness being observed over

folds. Thicknesses vary from 50 mm to 1 m, with occasional discontinuous

sediment layers 10 mm thick.

The sample sites (Fig. 30) for the fold comprised a vertical series

of samples through the axial plane, a series around the fold closure on

a bubble-free band, and samples of the contacts of the discontinuous

sediment bands with adjacent ice.

top

10mm

compositional
layering

axial plane

field position
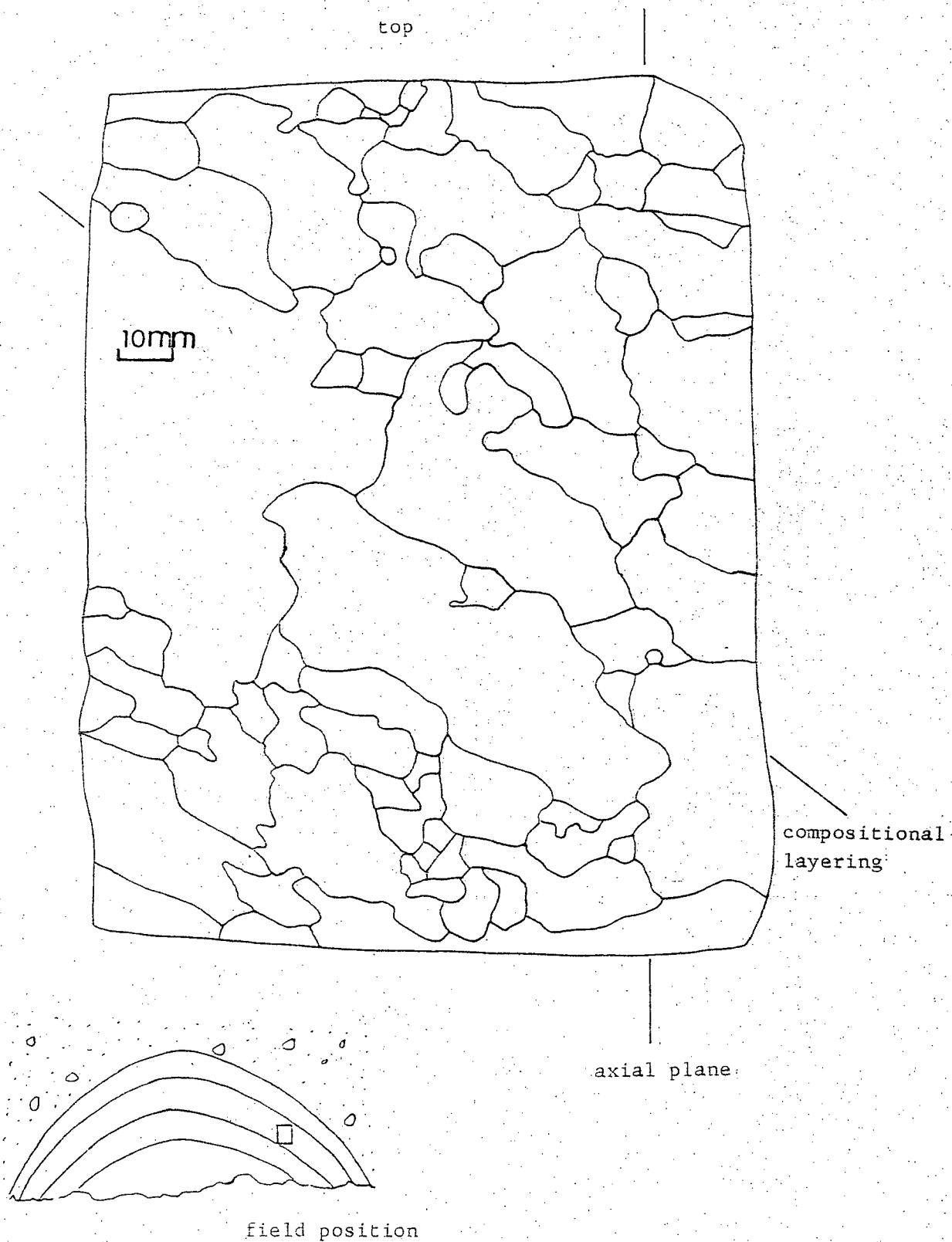
Figure 29. Crystal characteristics, anticline in involuted hill.

111



Figure 30. Anticline in involuted hill. c-axes

(a)-(e) Sections around fold.

c = compositional layering
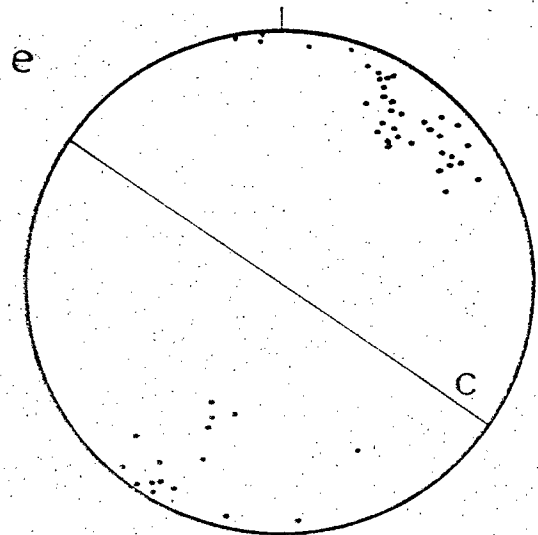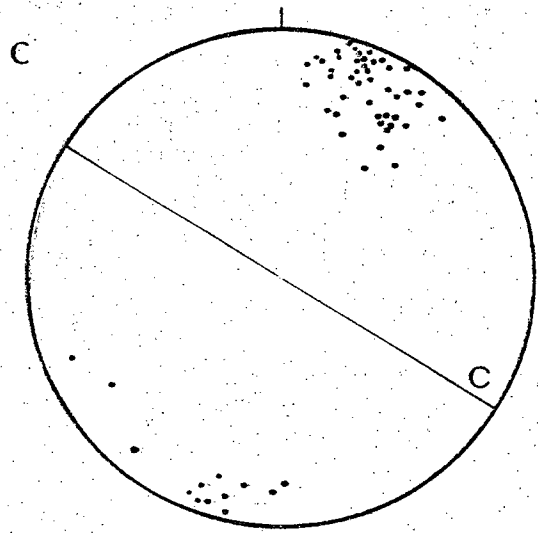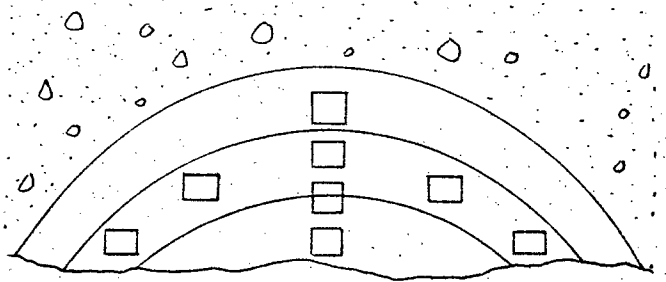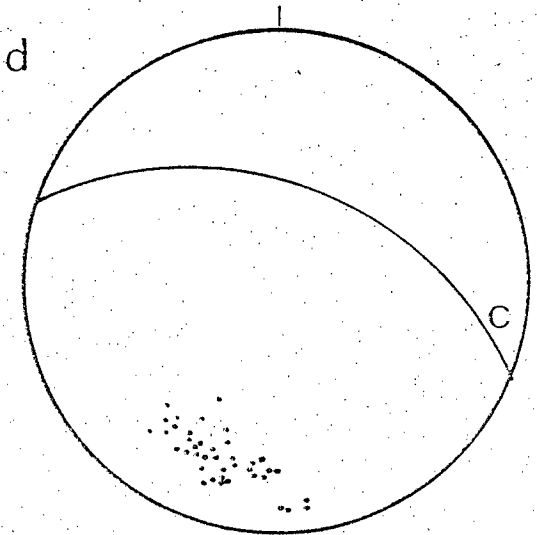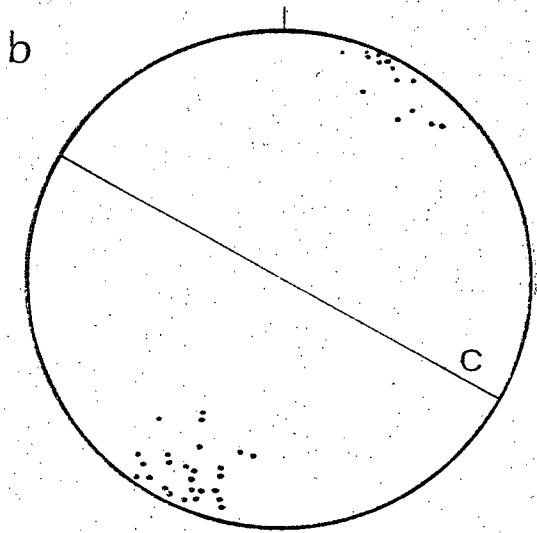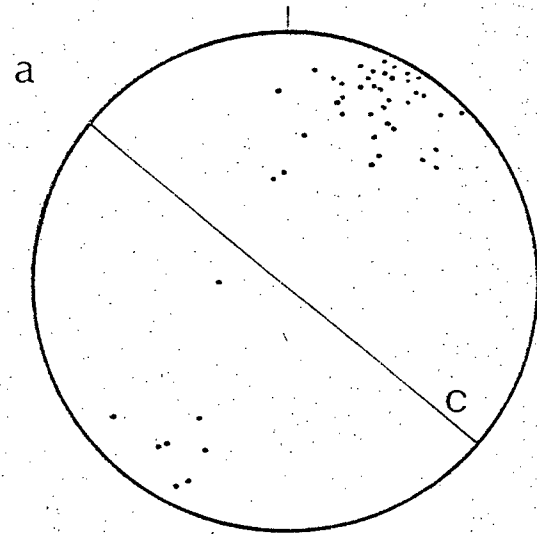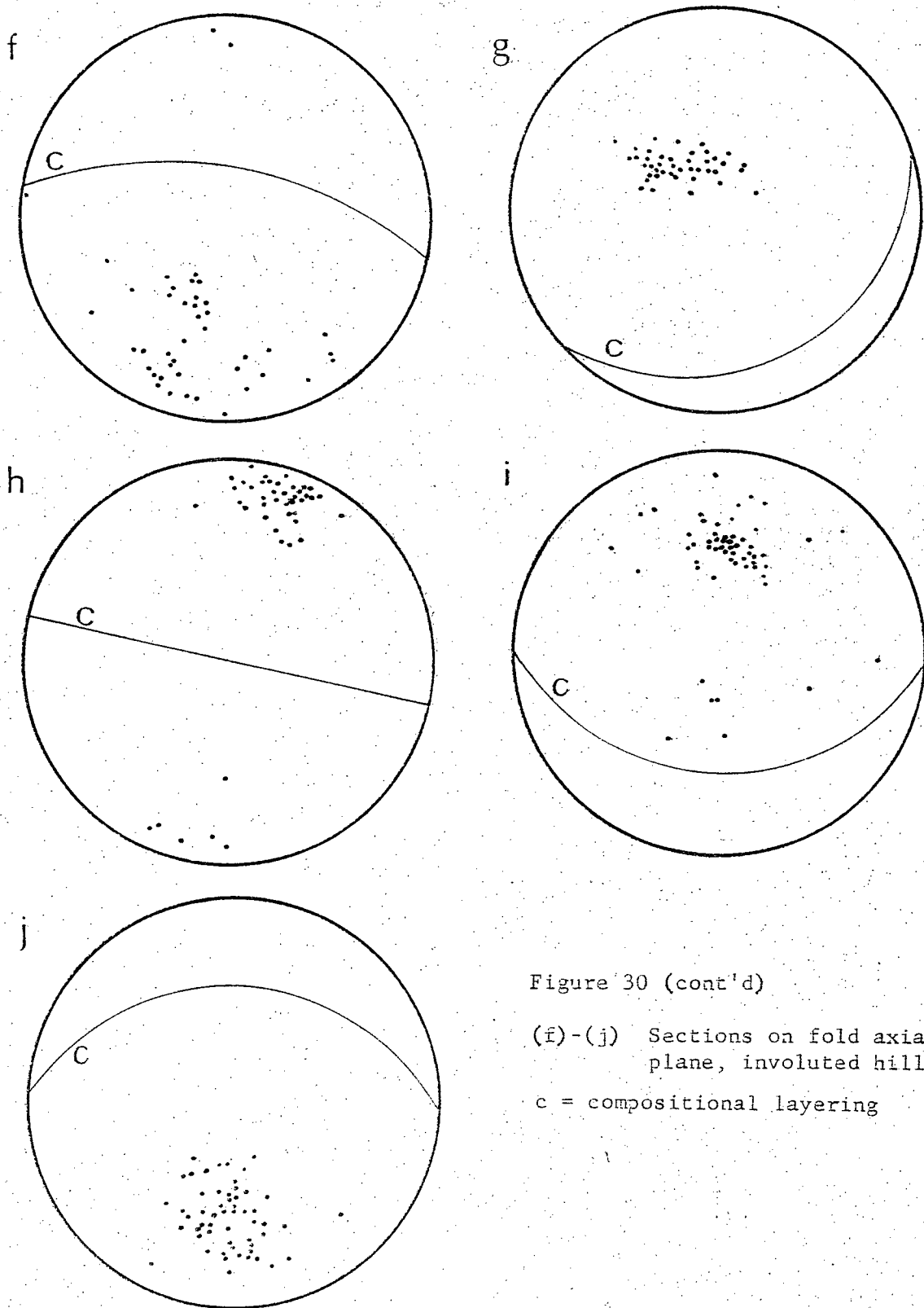
112



Figure 30 (cont'd)

(f)-(j)  Sections on fold axial
          plane, involuted hill.

c = compositional layering

## Ice Characteristics

The compositional layering is determined by bubble and sediment content. Within a given band bubble shape and size vary but with a general increase in size downwards. Ellipsoidal, flattened and irregular bubbles range up to 4 mm, with long axes paralleling the dip of the banding; spherical bubbles are smaller. Where sediment bands occur, bubbles are few, and there are no bubbles for 30 mm beneath the sediment.

### Crystal Characteristics (Fig. 29)

Bubbles usually occur on grain boundaries, the larger ones especially at sharp irregularities in the boundaries, or less frequently on sub-boundaries. Smaller bubbles are randomly scattered in relation to texture. Crystal size varies with position relative to sediment and bubble bands. In bands of high bubble content, crystal long axes average 10 mm, and range up to 25 mm. Inclusion-free zones contain crystals up to 50 mm long; within sediment rich bands, maximum dimensions are restricted to $< 5$ mm.

Crystal shape varies with crystal size (Fig. 29). Larger crystals are usually anhedral, irregular and inequigranular. Boundaries are curved to cuspate, strong embayments occur where grain boundaries and sub-boundaries intersect. Large crystals may be embayed by each other or small, strain-free crystals. Strong boundary curvatures other than embayments occur at bubbles, indicating an influence on grain boundary motion. Small crystals are anhedral but many mutual boundaries are straight. These are more regular and more nearly equigranular than large crystals.

Strain shadows occur rarely in small crystals, but frequently in larger crystals, and are parallel to the c-axis orientation and orthogonal to the sediment or bubble layering. Crystal dimensional orientation (Fig. 27) is generally parallel to the compositional layering, especially for large crystals; smaller crystals are more nearly equidimensional.

Sediment is generally of medium to find sand grade, occurring in discrete, discontinuous bands. Also some is dispersed in crystals and boundaries, with no preferred textural position. Clay pellets are observed scattered in layers, these are irregular in shape, and up to 3 mm diameter. Dense sediment bands cause textural changes - ice in such layers comprises small crystals. Zones of small crystals occur below such sediment bands. Where sediment grains are more separate, crystals from above the layer penetrate through, but with slight changes in dimensional orientation.

The c-axes of a series of vertical samples from clear and bubbly ice over a vertical distance of 4 m in the field, and samples from fold limbs were analyzed. From these were prepared component diagrams (Fig. 30), based on textural characteristics and relation to structures. All diagrams are essentially identical, in the form of axial symmetry, the axis being orthogonal to the compositional banding, around the fold.

### Interpretation

It is evident that anticlinal folds underlie zones of thinner overburden, but it is not clear how the thickness pattern arose. The stoney clay material is widespread in the area and overlies most massive ice

bodies drilled so far (Mackay 1973b). Rampton (1972b) has described

the material as a reworked till which has been subject to slumping and

mudflow activity, thus lateral variations in thickness are to be expected.

Additionally Mackay (personal communication 1975) points out that there is

increasing evidence for a several metre deep thaw in the area, which could

be responsible for removing material on hillsides. The reticulate vein

ice pattern over the massive ice shows little evidence of creep, but over-

lying material may have moved downslope. Whatever its origin, the varia-

tion in overburden thickness is related to the upfolds in the ice.

The original compositional layering has not been greatly affected

by the folding process; bed thickness in the upper layers is greatest over

the fold crest, but lower down the section bed thickness becomes more

uniform around the fold (Fig. 31).

In relatively undeformed ice, bubble elongation is parallel to the

temperature gradient during growth, whereas in this ice bubbles tend

toward parallelism with the dip of the layering. Assuming the bubbles

were originally orthogonal to the layering, differential flow occurred

during folding. Also flat bubbles are essentially parallel to the folia-

tion. These flat bubble surfaces are parallel to the basal plane of the

containing crystals. A further textural feature is the position of

bubbles relative to grain boundaries. Large crystals were strained and

polygonization has occurred. Additionally recrystallization has produced

a strong c-axis maximum fabric.
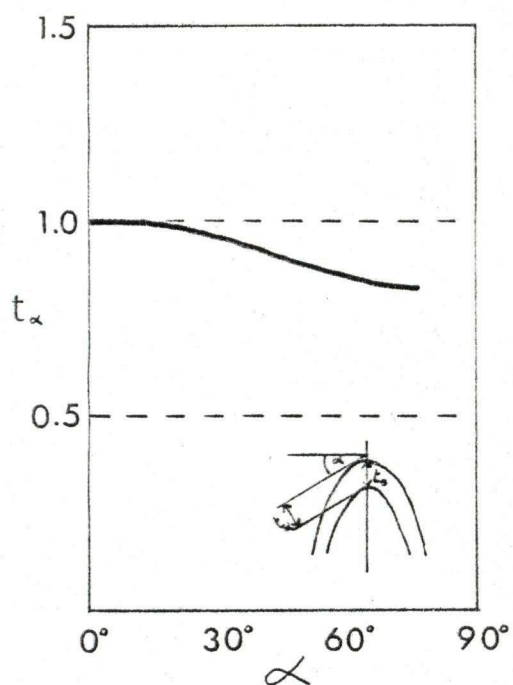
Figure 31. Bed thickness around fold in Figure 29.



Figure 32. Wedge penetrating anticline in involuted hill. Note upturning of banding of massive ice.

Table IV

Crystal size in involuted hill ice
adjacent to wedge

| Distance from wedge (m) | Crystal size ($mm^2$) |
|:---:|:---:|
| 5.0 | 785 |
| 3.0 | 563 |
| 2.0 | 361 |
| 1.0 | 303 |
| 0.25 | 68 |
| 0.1 | 26 |

(c)    Anticline Penetrated by Ice Wedge

### Introduction

Thus far we have considered relatively undisturbed core ice, and
ice folded by differential uplift; we now consider such a fold penetrated
by a wedge.  The wedge has grown where the clay overburden is thin (1.5 m).
The time of initial cracking is unknown, but from the size of the wedge
(approximately 3 m across) it has been growing for a few thousand years.
This is a rough estimate, as the probability of cracking varies with wedge
size (Mackay 1974a).  However, near this wedge there has been long-term
peat accumulation indicated by a wedge with at least 4 growth periods
(Mackay 1974a, Fig. 18).  This site was the depression between two invol-
ution ridges, and wedge growth occurred during peat accumulation.  Thus
conditions suitable for wedge growth have prevailed for the time taken to
accumulate at least 2 m of peat, namely about 5000 years.  Although both
wedges did not necessarily grow at the same time or rate, the larger wedge
on the ridge may well have grown first as it was on a ridge (otherwise the
smaller wedge would have penetrated massive ice), thus clear of snow, and
subject to rapid cooling which aids in the cracking process.  Recent frac-
turing was detected petrographically.

The compositional layering in the ice could be traced from its
relatively undeformed state up to the wedge contact, where it became
upturned and penetrated by cracks sub-parallel to the wedge.  As in
other exposures, the compositional layering was determined by bubble
and sediment content with large bubbles above but usually not immediately
below sediment bands.

The sampling plan for these structures was designed to trace any textural and fabric changes with distance from the wedge, characteristics of faults and joints, and any variations in wedge ice.

### Banding Characteristics

Bands of differing composition have different thicknesses, but all bands are essentially parallel and uniform in thickness on fold limbs. No major thickening occurs adjacent to the wedge, but attitude changes, the characteristic upturning being shown in Figure 32. A series of fractures occurs parallel to the wedge between which segregated ice can still be seen. Banding also occurs in the wedge, in the form of vertical to steeply dipping bubble foliations.

### Ice Characteristics

As was found elsewhere in the ice body, bubbles occur above sediment bands but very rarely immediately below. Various sizes and shapes of bubble occur within the bands: (a) Above sediment layers the bubbles are often flat, and in the basal plane of the containing crystal; (b) spherical bubbles up to 1 mm diameter are often surrounded by "satellite" bubbles 0.13 mm in diameter; (c) elongate bubbles 2-3 mm long; (d) irregular bubbles, especially where connected by threads along grain boundaries. In general, spherical bubbles occur in groups, but elongate and irregular bubbles show no zonation within a given band.

At 0.25 m from the wedge the compositional layering is disturbed by fractures associated with, and parallel to, the wedge. Fracture

separation decreases to 10-20 mm adjacent to the wedge and the fractures are up to 15 mm wide. The infils comprise bubbly ice, but segregated ice is still evident between them. Bubbles in the fracture zones are $< 0.5$ mm, generally spherical, and very numerous, giving the ice a cloudy appearance. Layering of bubbles parallel to the fracture walls is evident. Where the fractures offset sediment bands, elongate bubbles up to 10 mm long trend parallel to the fracture.

Despite the fracturing, the original layering is decipherable up to the wedge, and contrasts with the wedge ice. The wedge ice is characterized by steeply dipping bands containing bubbles and some fine grained sediment. The bubbles are (a) spherical, approximately 0.3 mm; (b) elongated, up to 4 mm, parallel to fractures; (c) irregular, 0.05 mm.

### Crystal Characteristics

Crystal size in the segregated ice changes systematically with distance from the wedge as shown in Table 4 and Figure 33. The reduction in grain size is considered to be due to flow and polygonization of larger grains and growth of new grains oriented favourably to accommodate the stress exerted by the growing wedge. A similar variation in crystal size was found by Corte (1962a). Additionally there is a variation in size related to sediment content; crystals within sediment bands are $< 0.5$ mm in diameter, while adjacent to such bands crystals are 5 mm and increase to 35 mm away from the sediment.

Crystal shape also varies with distance from the wedge, and with the presence of sediment. Three metres from the wedge, crystals are
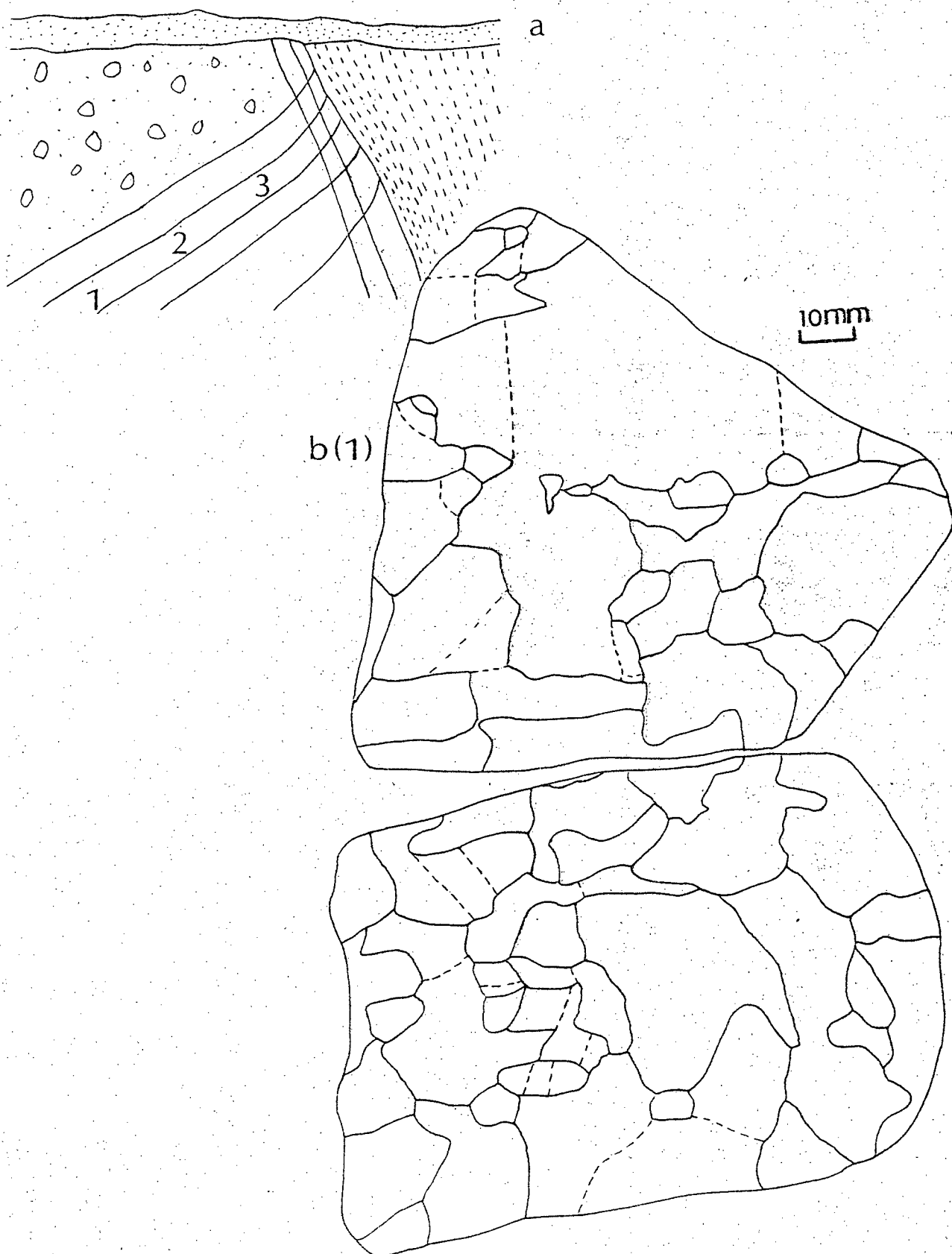
Figure 33.   Change in crystal size in massive ice adjacent to wedge.
Vertical sections orthogonal to wedge.  (a) sample sites,
(b) sample 3.0 m from wedge ... continued.

c(2)

10mm

d(3)

10mm
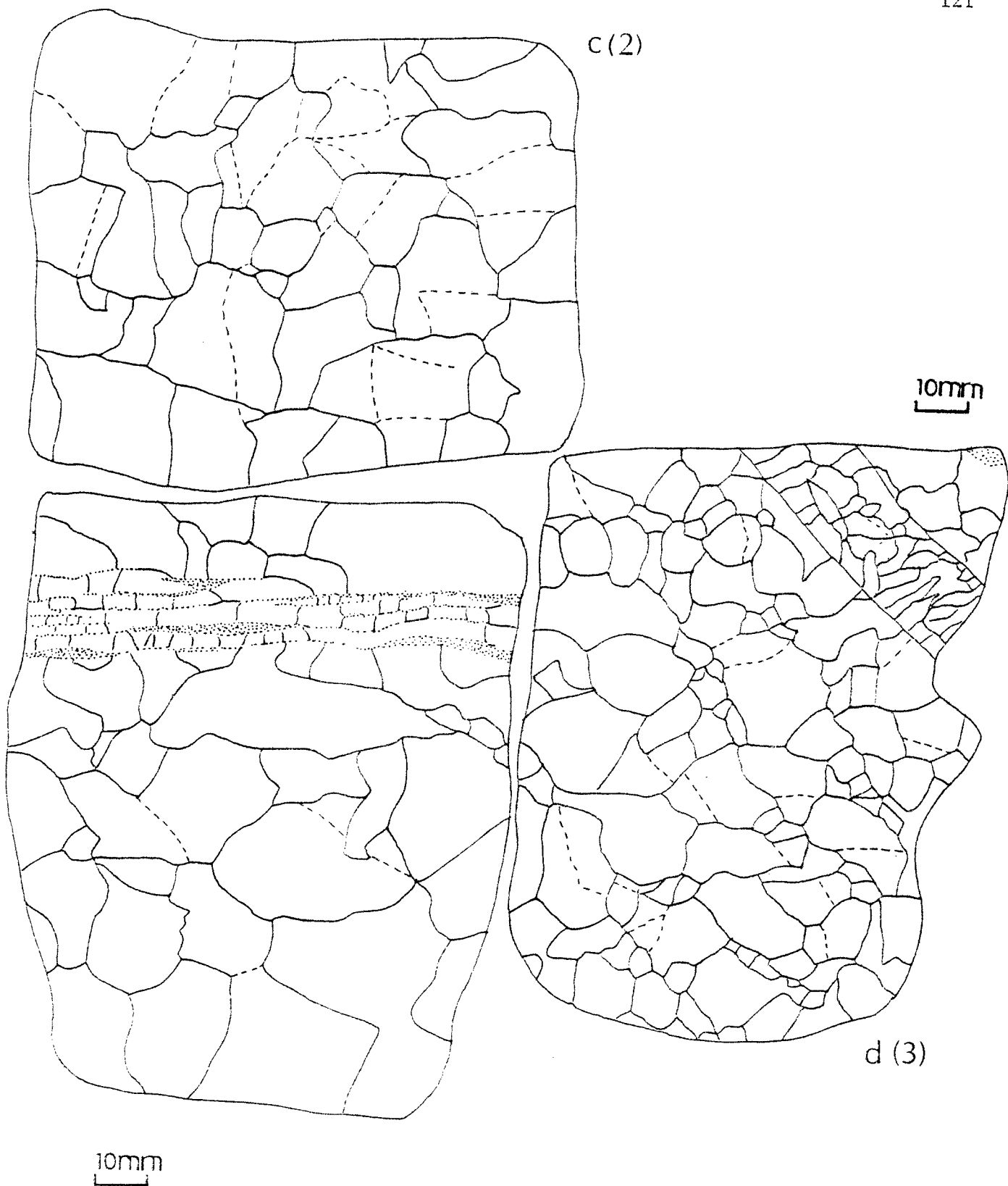
Figure 33 (continued).   (b) 2.0 m from wedge (note influence of sediment),
(c) 1.0 m from wedge (note old fracture at top right).

inequigranular and interlocking, with curved, serrated and sometimes
cuspate boundaries. The degree of irregularity decreases toward the
wedge; while some larger crystals retain some strongly curved sides, the
smaller crystals have straight mutual boundaries. This suggests polygon-
ization gave rise to a reduction in crystal size, and that new crystals
grew. Fractures cross this ice in an intergranular and intragranular
fashion and fracture infils contrast with the above pattern; small crys-
tals ($<$ 2 mm) form a competitive zone at the fracture boundary, from which
grow elongated crystals ($<$ 7 mm) orthogonal to the fracture, while in
the centre some crystals are parallel to the seam. Locally the generally
straight fracture sides show strong irregularities and it is apparent that
fracture crystals have invaded the surrounding segregated ice, by a grain
boundary migration mechanism.

Between fractures the segregated ice comprises straight-sided
crystals, $<$ 15 mm diameter. The segregated ice contains offsets on which
no new crystal growth has occurred; offsets up to 5 mm have been observed.
The adjacent wedge ice differs in that crystals are elongated parallel to
the bubble zones and reach 25 mm in length.

The relationship of bubbles to texture is such that spherical bubbles
lie on boundaries, on sub-boundaries and within crystals. Flat bubbles
occur only within crystals, indicating a lattice control; also, no bubbles
$<$ 1 mm were flat, so a minimum size is necessary. Some local irregu-
larities in boundaries are associated with bubbles. In the fracture zones
bubbles are $<$ 1 mm in diameter and spherical within boundaries of competi-
tive growth crystals; near the central seam bubbles are elongated parallel
to the seam, and cross grain boundaries.

Petrofabric diagrams were prepared for samples progressively near
to the wedge. At 5.0 m from the wedge a c-axis maximum occurs orthogonal
to the compositional layering, which is similar to that for the fold which
has suffered no wedge penetration (section (b)). At 3.0 m from the wedge,
a single maximum lies at approximately 60° to the layering (Fig. 34(a)),
and becomes rotated into the layering at 1.0 m from the wedge (Fig. 34(c)).
Thus the c-axis patterns become progressively more similar to those of the
wedge, indicating the influence of wedge growth. Although the composition-
al layering of the segregated ice remains, the petrofabrics are such that
the contained crystals respond to the growth stress of the wedge in a
similar manner to the outer wedge crystals.

Superimposed on this pattern are fractures in which the texture is
similar to that of fractures discussed in section (a), above. Similarly
the lattice orientations (Fig. 34(e)-(h)) compare with recent fracture
infils discussed elsewhere (p. 155 ff.), indicating that post-solidifica-
tion changes have been limited. In addition there occur older fractures
which have been deformed and the contained crystals have lattice orienta-
tions nearer to the wedge pattern.

Figure 35 gives grain type distributions, i.e. histograms of numbers
of sides to grains in thin sections from the core, folded ice and folded
ice with wedge. There is an obvious tendency for grains to have 5 to 6
sides in the core ice and folded ice. In the ice adjacent to the wedge
a change is evident - grains tend to be 6 to 7 sided, and there are more
grains with > 10 sides. This may be associated with the progressive
fabric change in that new crystal growth has occurred on old grain boundaries
and that a previously single boundary has become multiple.

Figure 34. Fold penetrated by wedge, involuted hill.

(a) Sample 3.0 m from wedge

(b) sample 2.0 m from wedge

(c) sample 1.0 m from wedge

(d) sample adjacent to wedge

(e) crystals in fracture near wedge

(f) crystals in fracture near wedge

(g) x 20 crystals in bubbly ice

. 20 crystals in clear ice

(h) 25 crystals at edge of fracture

(i) 50 elongated crystals in recent fracture

(j) 18 crystals in old fracture

(k) x 10 small crystals in fracture

. 40 crystals in clear ice

(l) x 23 crystals adjacent to sediment

. 37 crystals away from sediment

(m) 50 small crystals

(n) x 50 small crystals

. 50 large crystals

(o) 47 crystals between two fractures

(p) 96 crystals in fractures

(q) 109 crystals away from fracture.


c = compositional layering
f = fracture
w.b. = wedge boundary

Sample positions
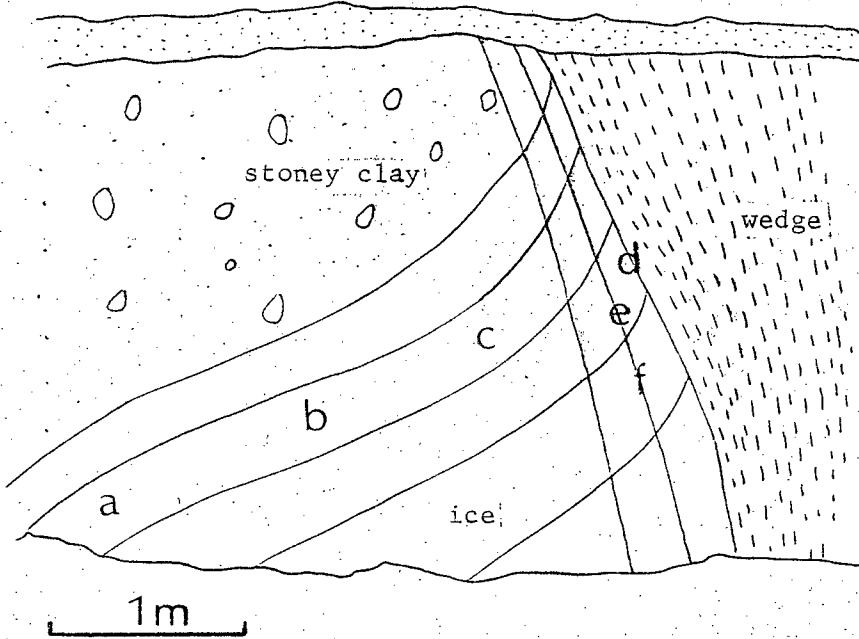
Figure 34.
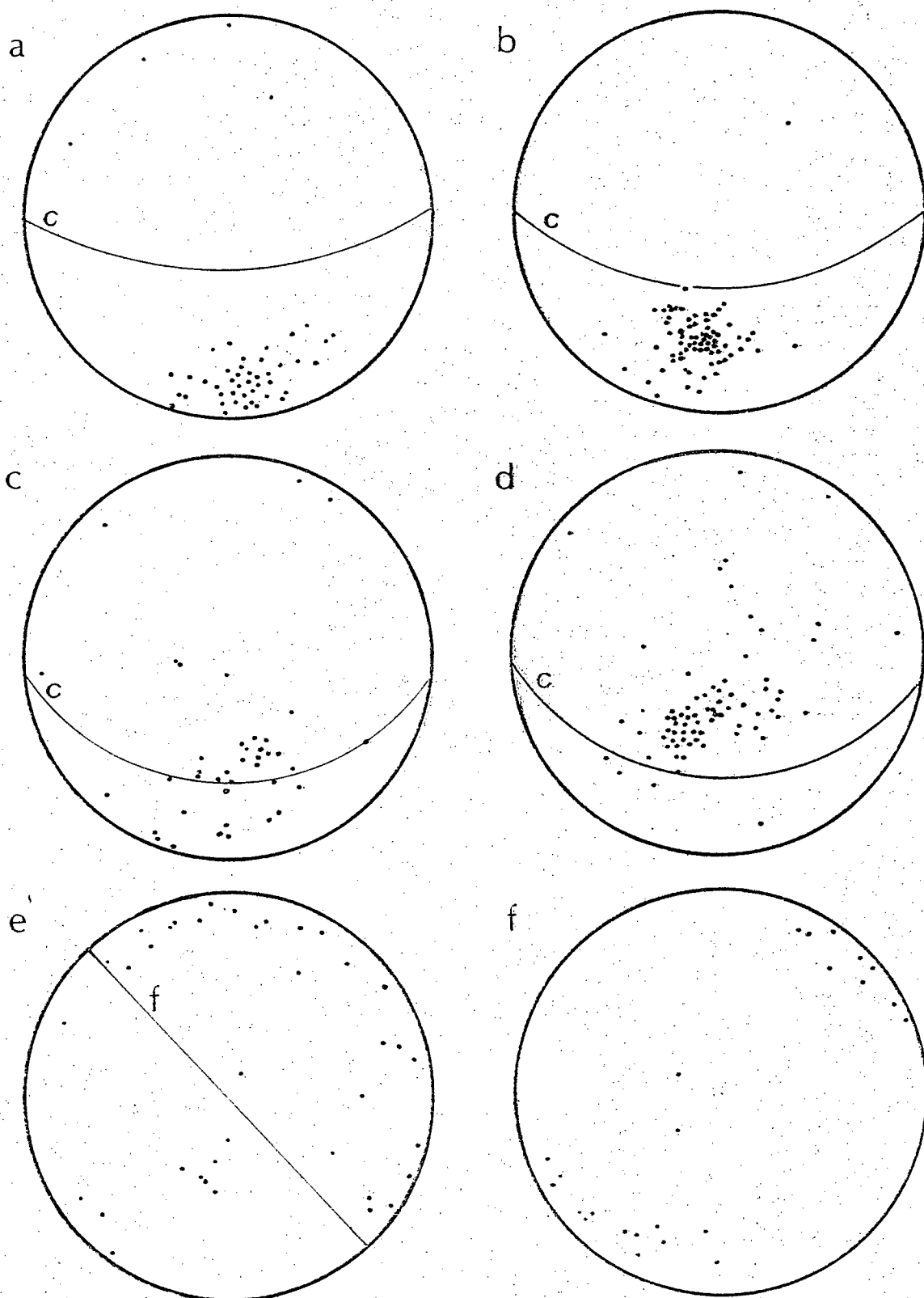
Figure 34 (cont'd)
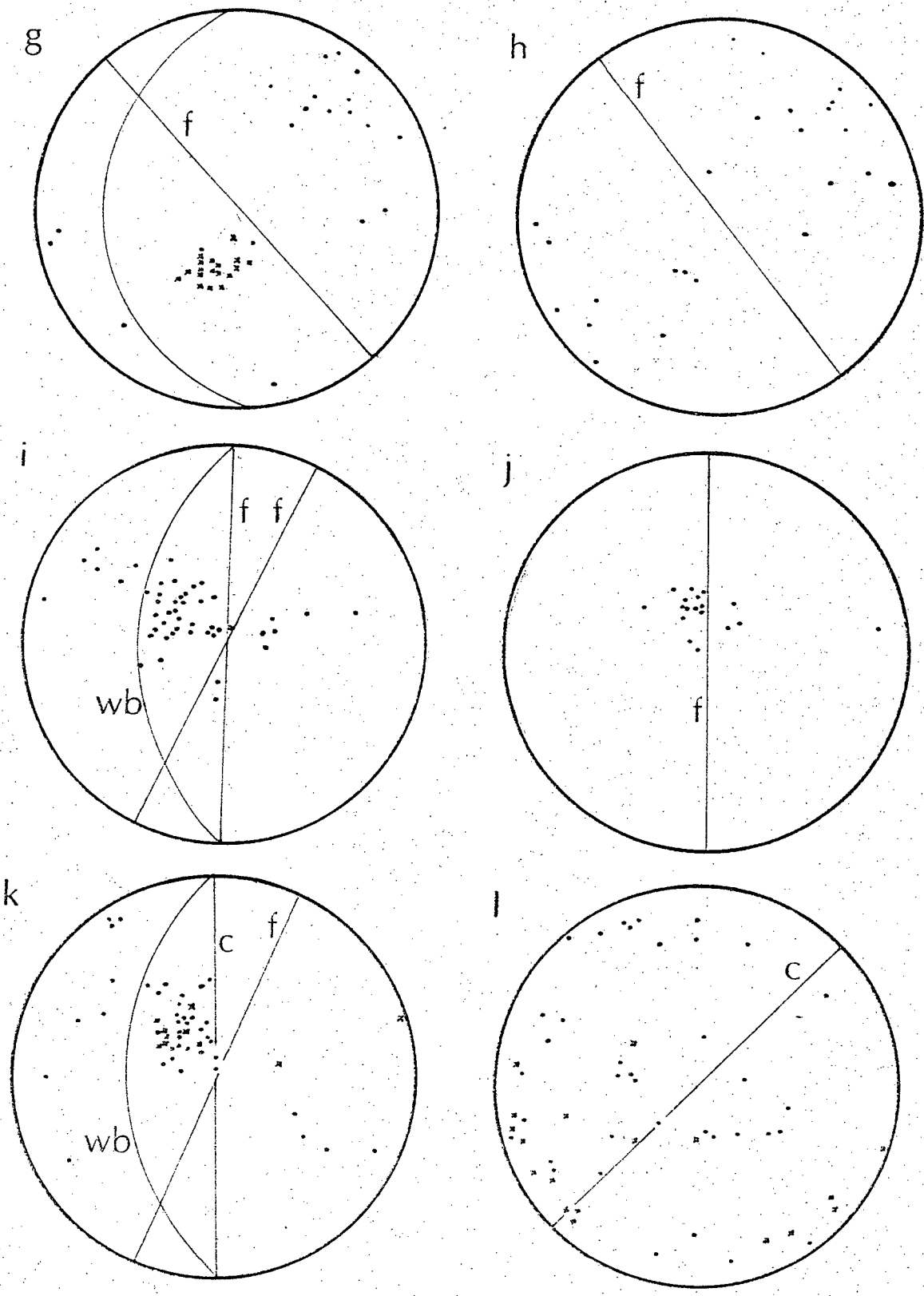
Figure 34 (cont'd)
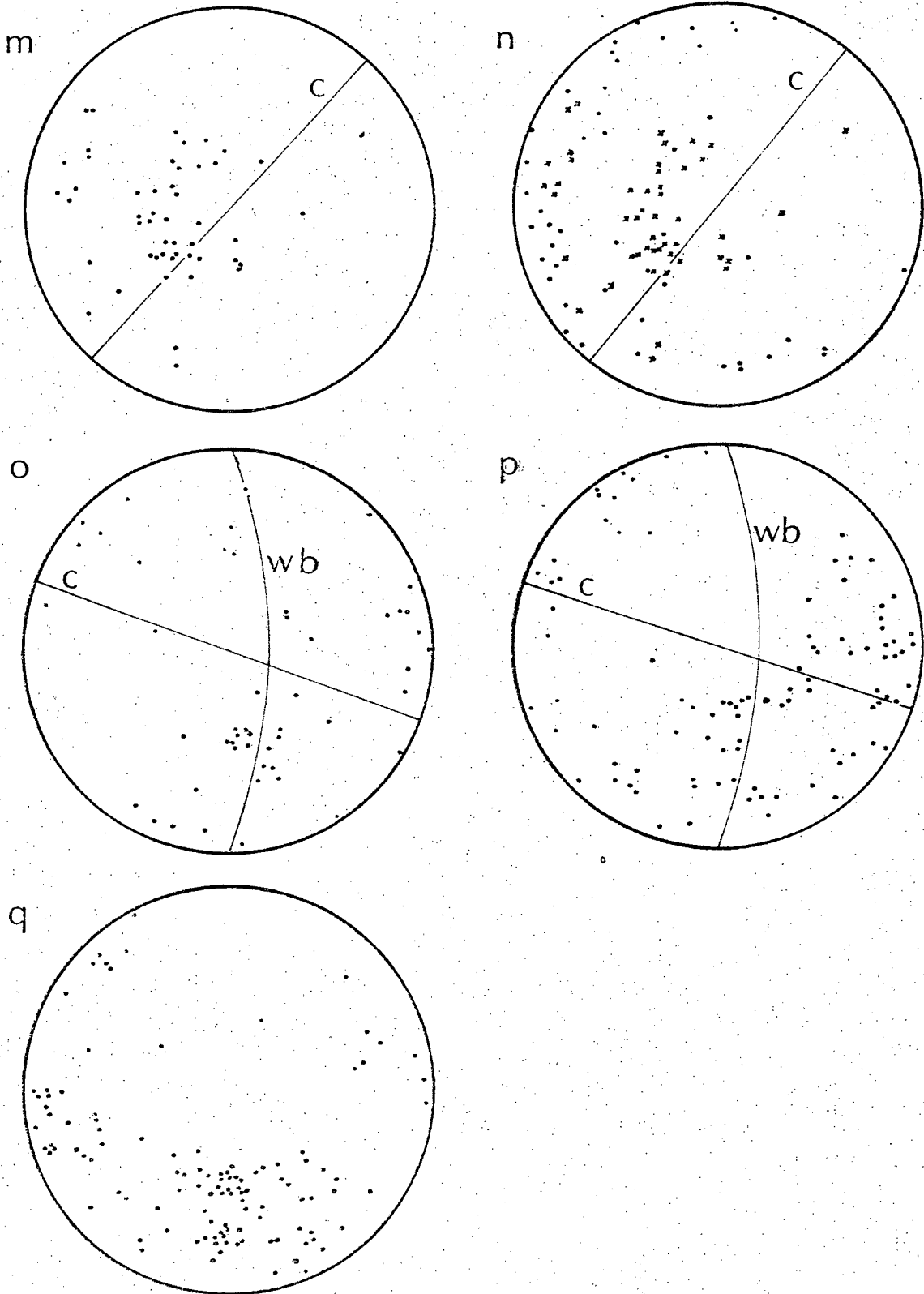
Figure 35
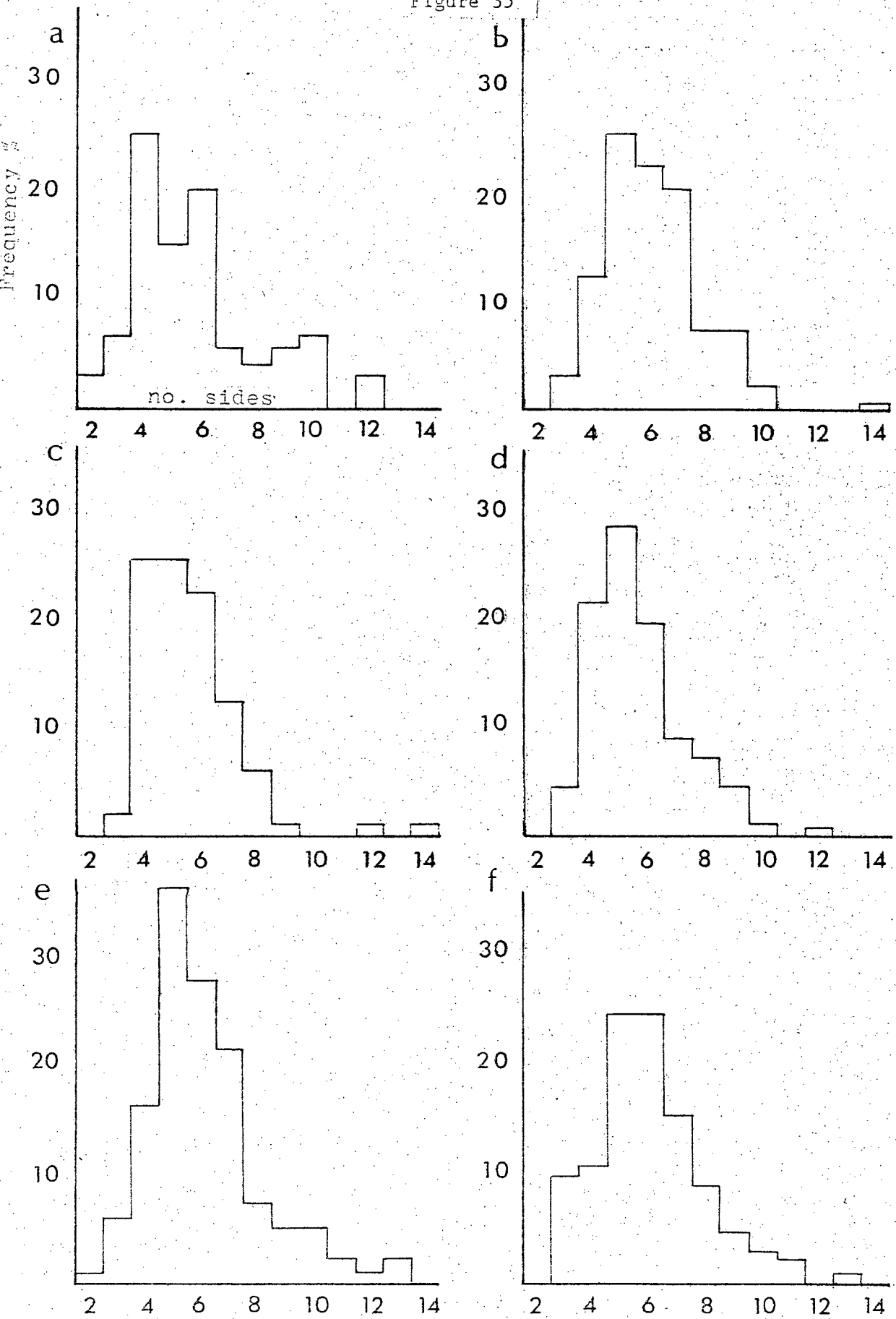
Figure 35 (cont'd)
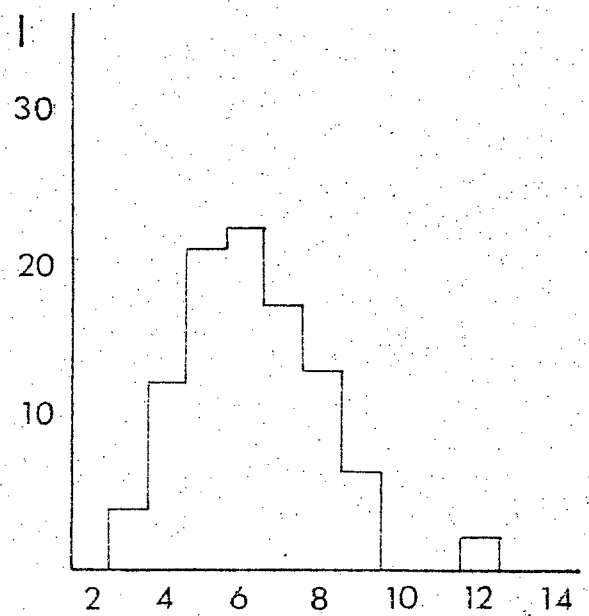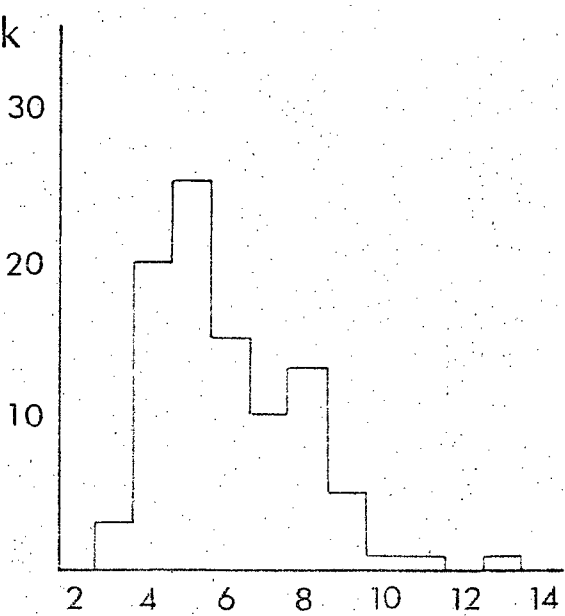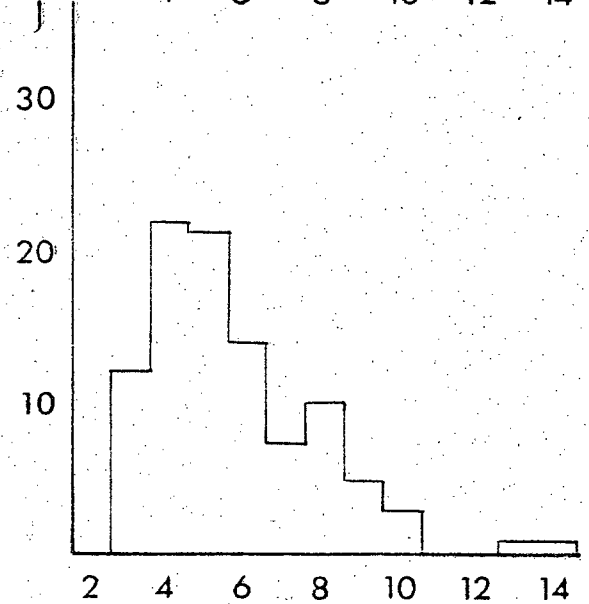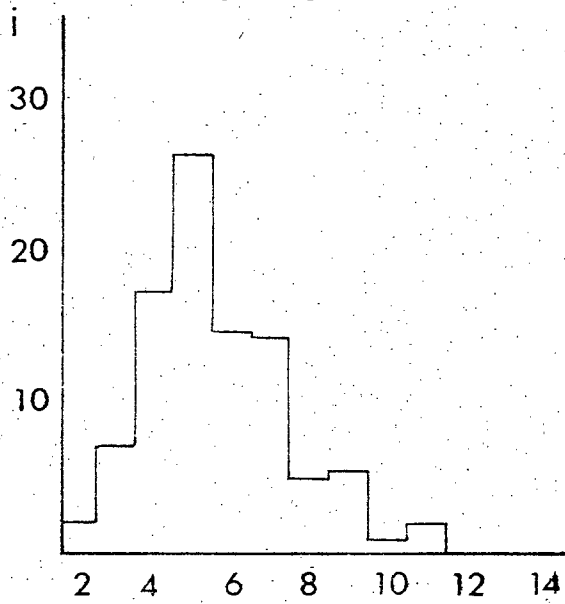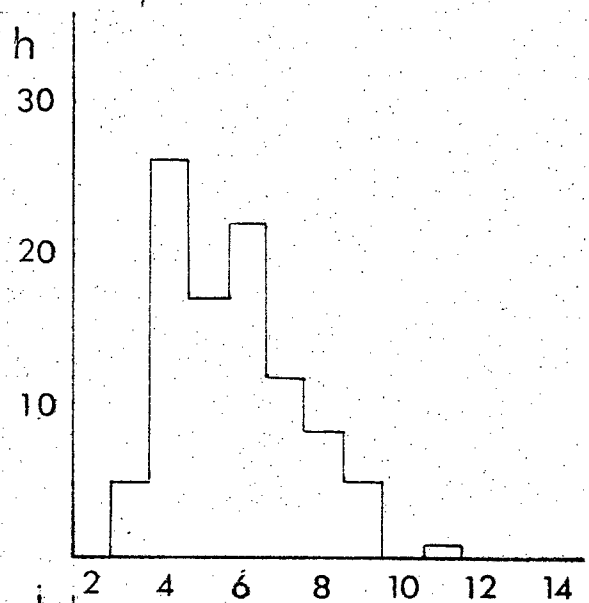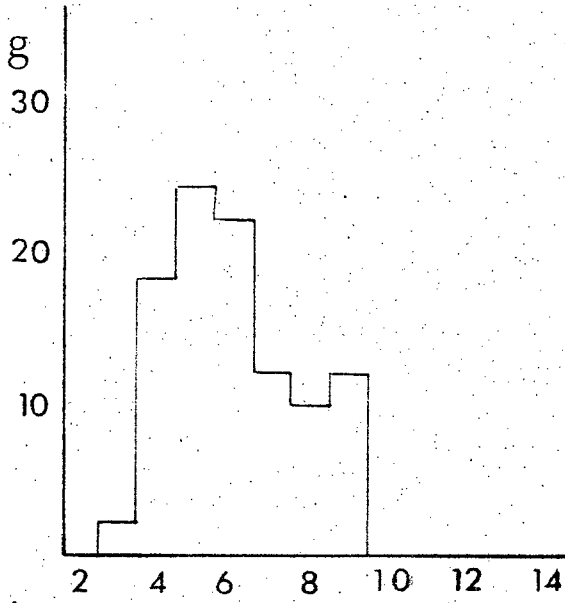
Figure 35 (cont'd)
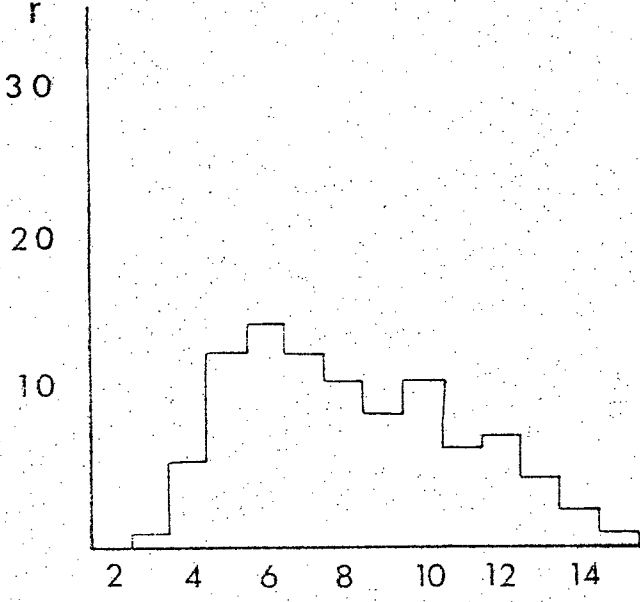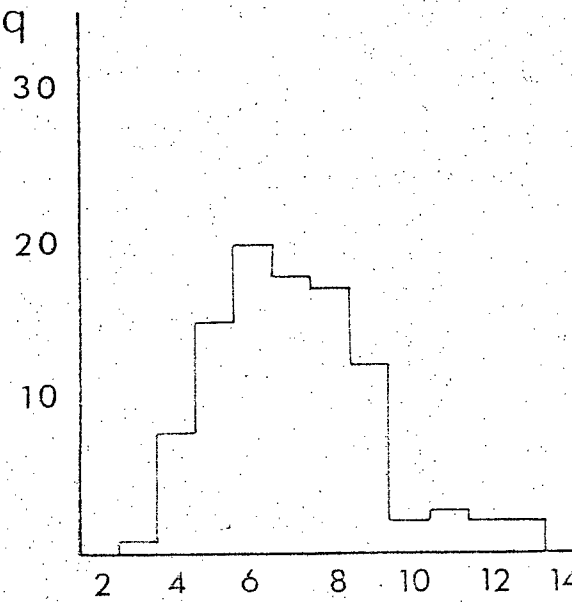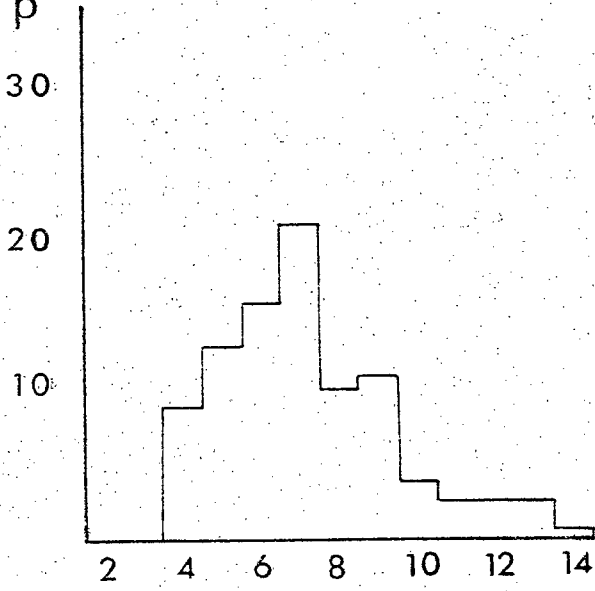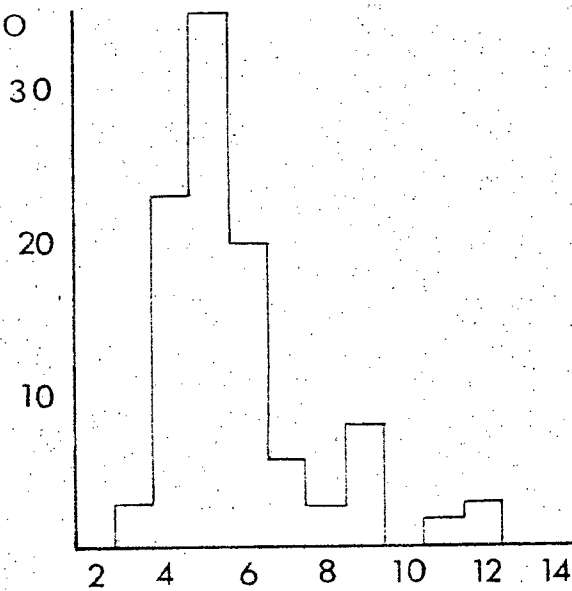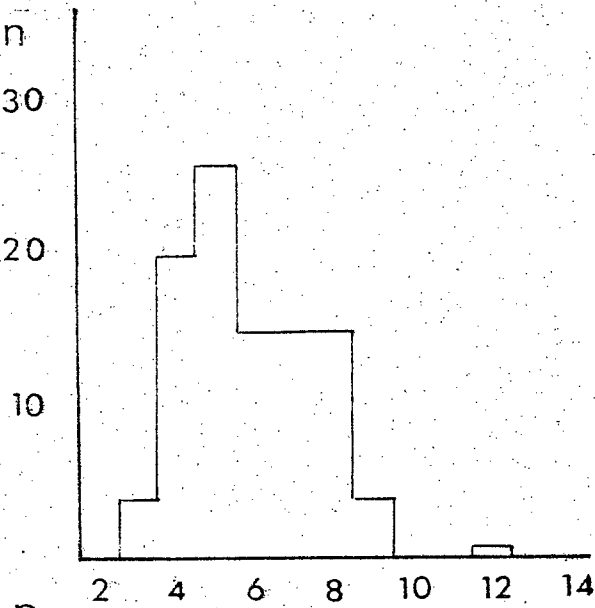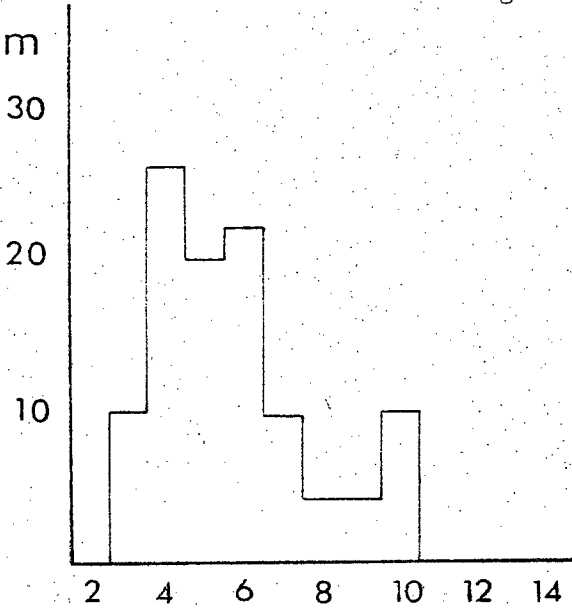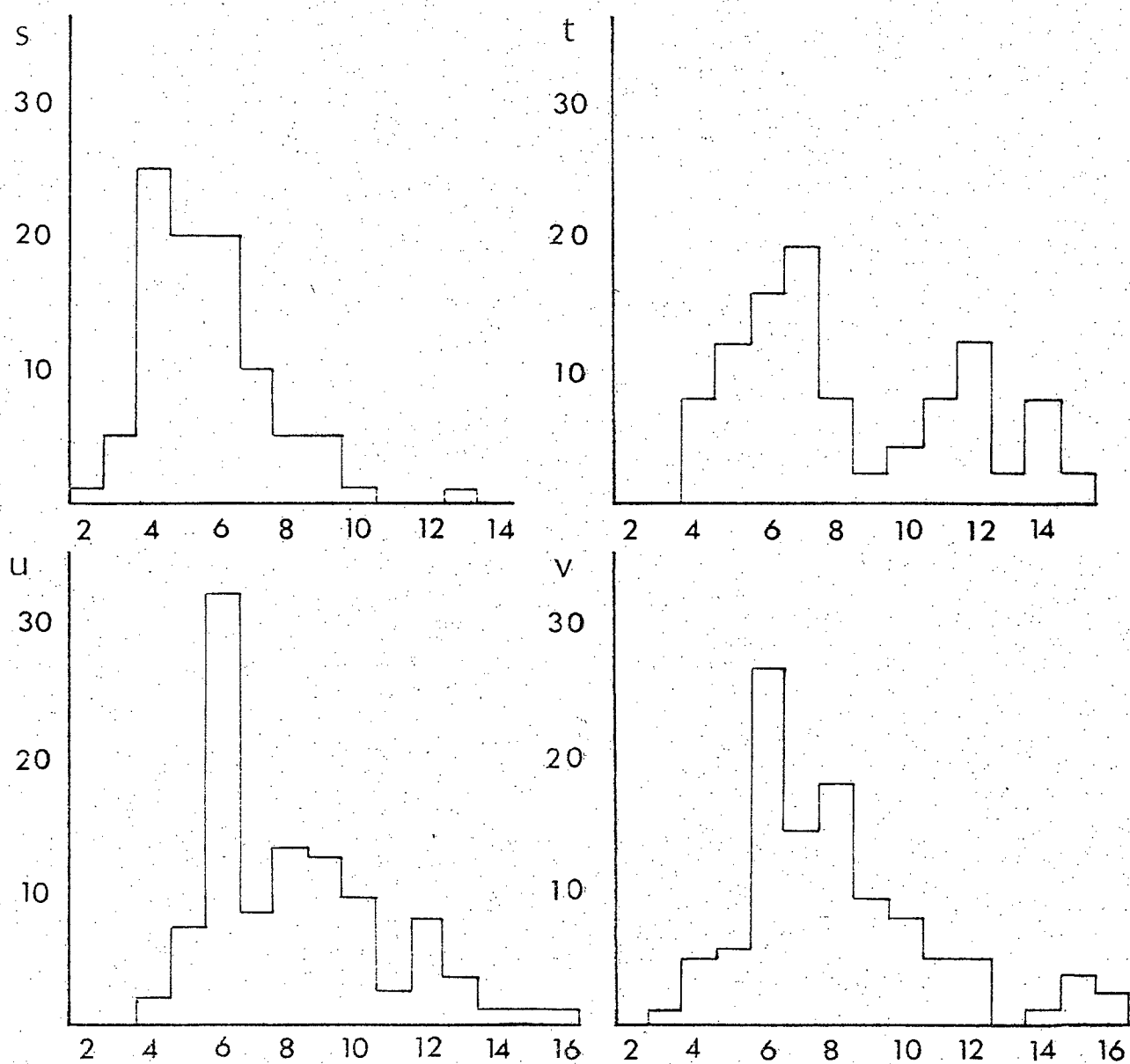
Figure 35. Grain type distributions for thin sections from core ice, folded ice and folded ice penetrated by wedge, involuted hill.

(a)-(f)  core ice, successively deep samples

(g)-(l)  anticline

(m)-(v)  limb of anticline, samples progressively near wedge.

Crystal dimensional orientations are shown in Figure 27. The maximum moves from parallelism with the compositional layering at 5.0 m from the wedge (Fig. 27(j)) to approximate parallelism with the wedge contact at that contact (Fig. 27(n)-(p)). In the latter case a secondary maximum occurs orthogonal to the first (Fig. 27(n), (o)), representing the columnar crystals in recent fractures. Early dimensional orientations associated with growth conditions in the segregated ice have become obliterated.

### Interpretation

Progressive changes in textural and petrofabric characteristics with distance from the wedge are recognized. Comparisons among the undeformed banded ice (a), folded banded ice (b), and the present samples indicate the influence of the wedge. Many crystal features are symmetrically related to the wedge.

Lattice orientations in the banded ice change from patterns typical of the folded ice without a wedge into patterns similar to wedge ice, along a distance of 5.0 m. The sequence of fractures indicates the transformation of growth fabrics due to wedge growth.

Adjacent to the wedge, crystal dimensional orientation changes from parallelism with the compositional layering of the segregated ice to parallelism with the wedge.

Crystal size decreases towards the wedge, due to polygonization of larger grains, and growth of new grains.

Comparison of the results of sections (b) and (c) indicate the influence of wedge growth on the ice. We know that the wedge is growing actively as recent cracks have been recognized petrographically. Thus. the characteristic grain sizes and shapes and preferred orientations have been produced primarily by syntectonic plastic deformation in the form of dislocation glide, polygonization by dislocation climb, and recrystallization. It is evident that recrystallization has occurred, as marked changes in crystallographic orientation have occurred. These could not be produced solely by polygonization of early grains, as subgrains would have their orientations close to those of the original. However, dislocation glide and climb are also occurring. The decrease in crystal size toward the wedge is indicative of polygonization causing reduction of the primary grains, and also the growth of new crystals, i.e. recrystallization, to give preferred dimensional orientations related to the wedge.

It is evident that wedge growth has led to the establishment of horizontal compression in the frozen ground. Lachenbruch (1962) discussed the zone of stress relief around a thermal contraction crack after fracture. The horizontal stress component normal to the crack wall vanishes at the crack walls, but increases asymptotically to the precracking value at large horizontal distance from the crack.

In the present study we are also concerned with compression caused by expansion of permafrost in summer. This was not treated by Lachenbruch, but it is to be expected that maximum stress will occur adjacent to the wedge, and stress will fall with distance from the wedge.

The only previous mention of the influence of a wedge on adjacent ice was by Corte (1962a) who found that the change in fabric in the surrounding ice was confined to 30 cm from a small ( 1 m wide) wedge. In the present study modification of fabric was recorded up to 3 m from a large (3 m wide) wedge. Corte did not comment on any upturning adjacent to the wedge, but Péwé (1962) reported the effect up to 3 m from wedges. In addition to the effect on the surrounding material, ice in a wedge is itself deformed. Black (1953) argued that horizontal compression produced shear planes adjacent and parallel to wedge sides. Thus it is difficult to specify the stress field adjacent to the wedge. If we assume uniaxial compression, the theory of Kamb (1959) predicts a c-axis maximum around the unique stress axis, although in experimental work Kamb (1972) found an incomplete small-circle girdle around the compression axis, in ice at $0°C$. Kamb (1972) also deformed ice in simple shear (-5° to 0°C), which recrystallized to give a two maximum fabric, one maximum at the pole of the shear plane and the other at 20° from the shear direction. When a compressive stress was superimposed across the shear plane the two maxima combined in a small-circle girdle around the compression axis. In the present study the fabrics were single maxima but not centred on the stress axis (assuming compression normal to the wedge axial plane). But the maximum is parallel to the maximum in the wedge ice, and thus parallel to the pole to the wedge boundary and compositional layering in the wedge. Thus it may be that shear has occurred parallel to the wedge boundary.

5.  Tension Crack Ice

Introduction

Tension crack ice grows in cracks resulting from mechanical rupture of the ground associated with the growth of segregated or intrusive ice (Mackay 1972b, p. 8) and is best observed on pingos. Exposure to depth of the cracks is rare, but probing shows some of them to be several metres deep. Open cracks have been observed frequently in winter and spring when there is no surface water flow, and it has been argued that infil is from surface water. Thus there is no evidence for syntectonic crystal growth as may occur in rock veins (Raybould 1975). However, tension cracks may open year-round and in summer infil might be more rapid, if water is available. Crack patterns are usually dominated by a master crack, with other cracks radiating from the pingo. The cracks are usually vertical, and planar. Tension crack ice was collected from two sites: (a) Pingo Number 9 (Mackay 1973a, Fig. 15), (b) Peninsula Point Pingo, near Tuktoyaktuk (Fig. 1).

The aims of the present investigation were:

(i) to study one season's growth of tension crack ice;

(ii) to compare new growth with older ice; to show changes over time;

(iii) to compare tension crack ice with wedge ice.

(a)     Pingo Number 9 Tension Crack

Field Characteristics

This pingo is growing in a lake which drained shortly before 1950,
and its growth has been monitored since 1970. Tension cracks are evident
across the pingo (Mackay 1973a, Fig. 15). Bench marks on each side of the
crack were surveyed in June 1973 and again in June 1974 and the mean annual
growth of tension crack ice was 100 mm (Mackay, personal communication).
There was no observable movement in a direction parallel to the crack. Ice
samples were removed from within the previous season's active layer, before
thaw-down in July 1974, thus the maximum age of the ice is known. Cracking
occurred after complete freeze back of the active layer during winter
1973-74. A crack may open year round (Mackay, personal communication
1975), thus it may have occurred any time after freeze back of the active
layer and before spring melt. Water has not been known to move up the
tension crack from depth, so the source is thought to be surface snow melt.
The ice grew immediately below the ground surface, on a fracture surface
in frozen soil. Thus nucleation was not on crystals in the fracture wall,
although such may have occurred at greater depth, where the crack probably
propagated through earlier tension crack ice.

The lateral contacts between the ice and adjacent active layer are
abrupt, but locally irregular. Also some small pockets of ice occur in
the active layer, parallel to the crack. A prominent banding occurs in
the ice, determined by bubble content (Fig. 36). These bands are parallel
to one another and to the plane of the crack, but with lesser irregularities
than the ice-soil contact. The crack was closed for most of its length, but
displayed local open zones which could be probed to 1 metre.

Figure 36.

Tension Crack Ice
Pingo No. 11
Bubble bands.
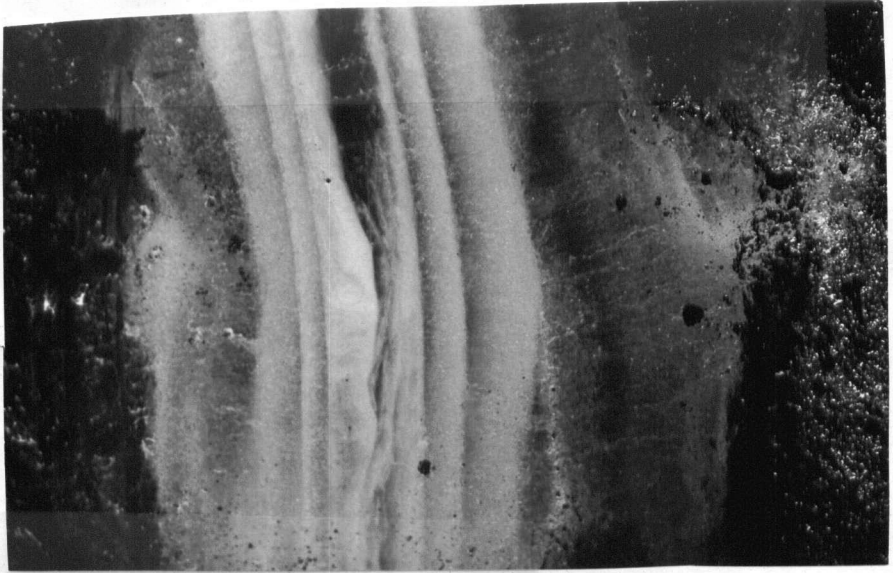


Figure 37.

Central curved
crystals
10 mm grid.



a

b

c
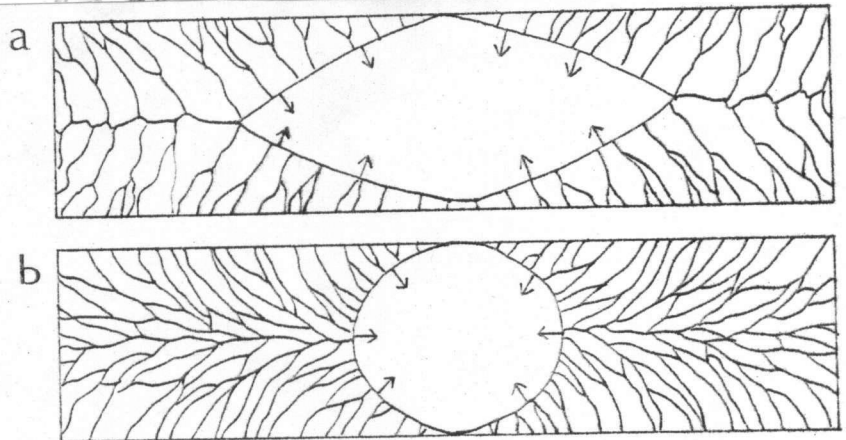
Figure 38.

(a) Rhombic interface

(b) elliptical interface

Schematic (vertical
scale exaggerated).

(c) curved crystal fibres in syntaxial
growth, after Durney and Ramsay
(1973).

incremental
dilation
across vein

new
fibre
growth
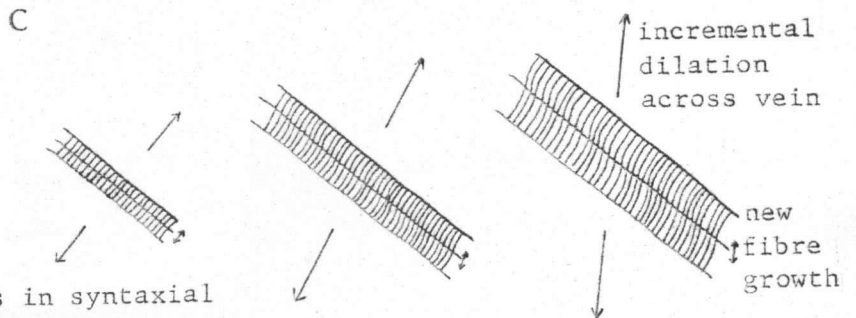
## Ice Characteristics

Banding was determined solely by gas content; the lack of soil inclusions suggests the active layer was still frozen during melt-water flow. Band type and thickness were approximately symmetrical about the crack centre. On each side of the crack occurred a 10-20 mm thick zone of mainly clear ice in contact with the soil. Adjacent to these were 1-2 mm bands of small spherical bubbles, the bands being planar and continuous laterally and vertically, but slightly offset at rare sediment inclusions. Next in sequence came 20-30 mm bands of bubbly ice, bubbles being < 1 mm and decreasing in concentration towards the centre of the crack. Next there occurred abrupt changes to very high bubble content, again decreasing toward the crack centre across bands 10-15 mm thick. Narrow bands (4-5 mm) repeated the concentration pattern, followed by clear ice to the centre of the crack. In this body, growth occurred at a vertical interface, yet it is evident that many bubbles have been retained in the ice, and did not float up under buoyancy. This may be because the ice grew rapidly and surrounded bubbles while they were still too small to free themselves from the interfacial tension, or because growth was not taking place into a "pool" of water, but in a thin film on the surface.

It is interesting to compare bubbles in this ice with those in the Tuktoyaktuk icing mound, which grew at approximately the same time. In the icing mound a steady water supply was available and freezing rate gradually fell, thus large bubbles grew, elongated in the freezing direction whereas in the tension crack ice water supply was probably intermittent, and freezing was rapid so that only small bubbles grew.

## Crystal Characteristics

Crystal size varied across the crack. Adjacent to the soil occurred a zone of small crystals, less than 0.1 $mm^2$, from which grew a zone of larger crystals elongated orthogonal to the banding. Some reached 5 mm x 2 mm and extended into the first bubbly band, while most crystals terminated at the band contact, and gave way to new crystal growth ($\leqslant 0.1$ $mm^2$) with larger crystals extending from the competitive zone. Further crystals grew from this zone, reaching $\leqslant 10$ mm x 3 mm; some were truncated, but others widened at that surface. In addition to the widening of pre-existing crystals new crystals grew, this being the bubbly zone discussed above. Crystals became more elongated as bubble concentration decreased, a pattern which was repeated toward the crack centre, the central clear zone comprising large crystals, $\leqslant 7$ mm long by 5 mm wide.

Crystal shape varied with size. In competitive growth zones, shapes were generally anhedral, but some straight compromise boundaries occurred. Elongated crystals tended to be gently curved rather than serrated. In many cases the outer boundary of elongate crystals was straight in horizontal and vertical sections, thus parallel to the crack. This reflects variations in supply of melt water. A temporary cessation of water supply was followed by slight melting on resumption of flow. Rapid cooling would give copious nucleation at the interface, although locally growth would occur in lattice continuity with pre-existing crystals. At the centre of the ice body, there were departures from the trend of dimensional orientation orthogonal to the plane of the crack. Local zones of curved crystals are shown in Figure 37. These indicate multi-directional crystal growth into enclosed space, rather than curved growth due to incremental dilation

of the fracture. In the latter circumstance curvature would be as shown in Figure 38(c), i.e. no converging pattern is evident. Also such curvature requires displacement non-normal to the fracture walls. There is no evidence for this from detailed bench mark surveys.

It is interesting to consider the form of the ice-water interface during the latter part of freezing, its effect on crystal characteristics, and on susceptibility to later cracking. From the above it is apparent that due to slight lateral variations in crack width some parts impinged before others. Where a pool of liquid was left it is argued that the interface advanced as in Figure 38(a), rather than as the more rounded form shown in Figure 38(b). In this instance (Fig. 38(a)) there is an almost invariant direction of maximum thermal gradient at all points; thus any grain favourably oriented for growth is able to grow at optimum speed and "wedge out" less favourably oriented grains. In contrast, in the case of a more-rounded interface (Fig. 38(b)), the direction of maximum thermal gradient changes continually and thus no one grain is favourably oriented for a long period, and more grains survive to the centre. Similar results have been found in metals (Savage and Aronson 1966). Once freezing is complete, there is a general decrease in temperature of the body, and we must consider the response to contraction of each part. During the infil of the tension crack, crystals grow from each side and reject solute which piles up between the two interfaces. After impingement of the grains these segregates may persist as grain boundary films below 0°C. Thus contraction stresses may rise to high levels while the grain boundary contact area is small. Also, the larger the solidifying grain size, the smaller the area of grain-boundary contact for a given liquid content (Smith 1953). Thus

142

coarser grained sections are more susceptible to contraction cracking, and especially where there is a steep angle of grain abutment (Fig. 38(a)). It is also noted that in cast metals it has been observed (Lees 1946) that fine-grained materials are far more resistant to cracking than coarser materials, due to their greater ability to accommodate the contraction strains. Thus from the description of crystal features it is clear why certain areas of the infilled fracture may open before others.

Optic axis orientations are shown in Figure 39(a). The overall pattern is a girdle preferred orientation in a plane parallel to the banding. Thus basal planes are orthogonal to banding. Component diagrams indicate that small crystals in competitive zones show diffuse girdle patterns (Fig. 39(b)); elongate crystals show stronger girdle concentrations (Fig. 39(c)), thus a stronger preferred orientation developed as growth proceeded. It is noted that in comparison, c-axes of crystals in veins indicate growth in optical continuity with wall crystals, although c-axes parallel to long axes are frequently found.

### Interpretation

The pingo in which the tension crack occurs is actively growing and has been under observation for several years (Mackay 1973a). Tension cracks are recognizable on air photographs. As part of a study of pingo growth, bench marks have been installed on the pingo, including one on each side of the crack at the top. Detailed surveys show that a separation of 100 mm occurred between June 1973 and 1974. No relative vertical or lateral displacement of the benchmarks was recorded. The time of fracture is unknown, but was after complete freeze-back of the active layer.
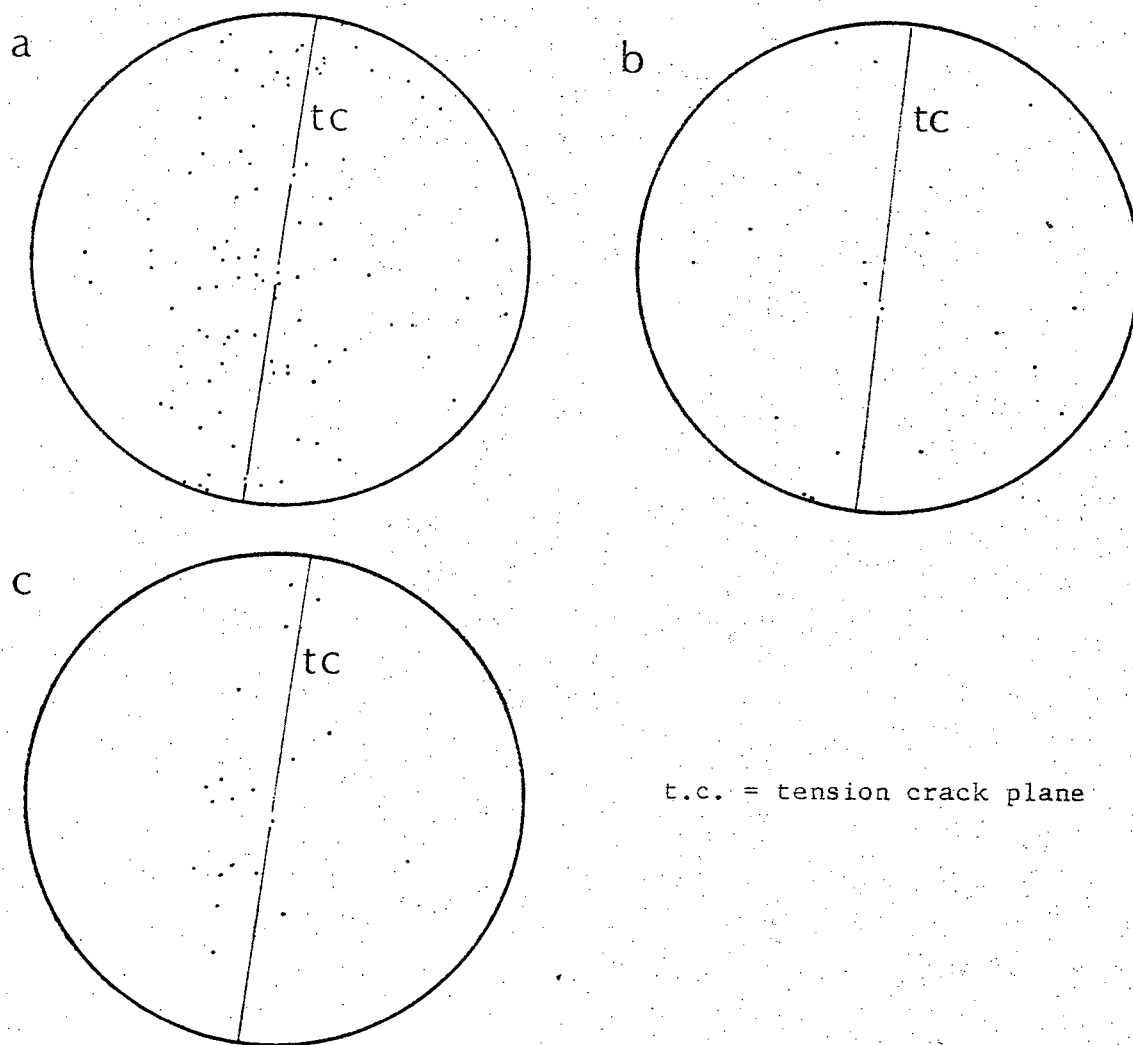
Figure 39. Tension Crack, Pingo No. 11.

      (a) Vertical section, orthogonal to crack, 100 crystals

      (b) 20 crystals adjacent to organic soil

      (c) 20 columnar crystals at crack centre.

It is not known whether the crack opened 100 mm in one event, or whether gradual opening occurred after the initial fracture. Neither field not petrologic data provide suitable indicators. The ice studied grew in the active layer; surface water, probably from snow melt, drained into the crack and froze with copious nucleation on the crack wall. Crystals with c-axis preferred orientations in a girdle parallel to the plane of the crack grew from the chill zone. These crystals also had a strong dimensional orientation orthogonal to the crack wall. Thus crystal growth occurred in the basal plane. By comparison with the icing mound ice, which also grew by a basal plane mechanism, the tension crack crystals are more numerous, and smaller. Also in the tension crack there are more layers of new growth. This indicates variations in supply of water. Supply of surface water to the crack may have been interrupted frequently. If flow ceased temporarily, then recommenced, crystal growth could occur (a) in lattice continuity with previously existing crystals, (b) by new nucleation, (c) by growth on vapour crystals. Evidence for (a) occurs in the discussion of textural criteria; (b) and (c) cannot be distinguished. Where the crystals growing from each side of the crack meet, a central seam occurs, with local openings. Textural criteria may be used to distinguish between openings which never closed, and new "fractures". Locally there were found lens-shaped zones in which crystals had dimensional orientations orthogonal to that opening, all around the edge. In some cases crystals could be almost parallel to the crack, whereas if there had been closure and a new opening occurred, such curved crystals would not necessarily occur.

(b)    Peninsula Point Pingo Tension Crack

### Field Characteristics

This is a pingo near Tuktoyaktuk (Fig. 1) which has been subject to coastal erosion; only half the pingo remained in 1935 air photographs but little further erosion has occurred since then. It is thought unlikely that the pingo has been growing recently, thus the pingo core and tension crack ice are old compared with Pingo No. 9 and this therefore provides an opportunity to look for modification of growth features in the ice.

No major ice core has been observed during the period of exposure of the section, although 2 m thick ice layers have been reported occasionally. In July 1973 slumping exposed tension crack ice (Fig. 40) half way up the pingo in sands; a contact of tension crack ice and core ice was not exposed. The surrounding sands are fine to medium grained; sedimentary structures have not been greatly disturbed during freezing; plane beds contain some organic matter, and ripple marks also occur. These beds are not disturbed adjacent to the ice, which indicates a tension crack origin without sub-stantial lateral stress caused by growth and summer expansion as occurs in ice wedges. A mineral stained layer 75 mm wide occurs adjacent to the ice on one side.

### Ice Characteristics

The ice body was approximately 160 mm wide with an abrupt contact with the surrounding sand. The compositional layering was determined by gas content; sediment content was low. The layering (Fig. 41) was quite different from that of Pingo No. 9. There was no symmetry to the banding,

Figure 40.

Peninsula Point Tension Crack

Note absence of deformation
of bedding adjacent to ice.
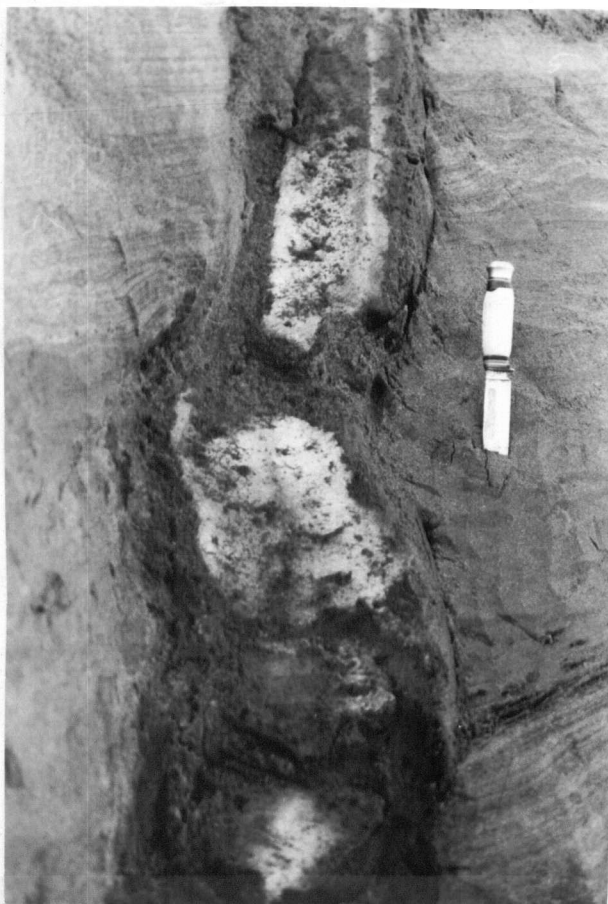


Figure 41.  Bubble banding in tension crack.  Note irregular shapes
in centre, small bubbles and some sediment on right.
Sample 110 mm across.


146

there being three bands of differing widths and contained bubble types

parallel to the plane of the ice body.


## Bubble Characteristics

(a) A 50 mm wide zone of ellipsoidal, elongate and irregular bubbles

with a horizontal lineation, approximately orthogonal to the crack, and

2-5 mm long. They are not volumes of revolution and have thus suffered

post-solidification modification. Many curve upwards 20°- 30° adjacent

to zone (b);

(b) The central zone comprises 45 mm of very elongate bubbles with

a sharp bend (40°) near the junction with zone (a) and pointed at the other

end. These bubbles are up to 18 mm long and are separated by more clear

ice than those in zone (a), but with a few small (2 mm) spherical bubbles

in trains, suggesting break-up of larger bubbles (Kheisin and Cherepanov

1969);

(c) The junction between (b) and (c) is abrupt and contains a dusting

of sand. Zone (c) is whitish due to the high concentration of small

bubbles, and some larger, up to 3 mm. At the outer ice-sand contact are

some irregular, elongated (4 mm) bubbles orthogonal to the contact.


## Crystal Characteristics

Crystal size varies throughout the ice body (Fig. 43) but shape is

less variable; zones are considered with reference to bubble zones:

(a) Crystals are 20 mm x 10 mm and anhedral, irregular in shape.

Elongate bubbles are parallel to crystal long axes and usually in grain

boundaries.

148
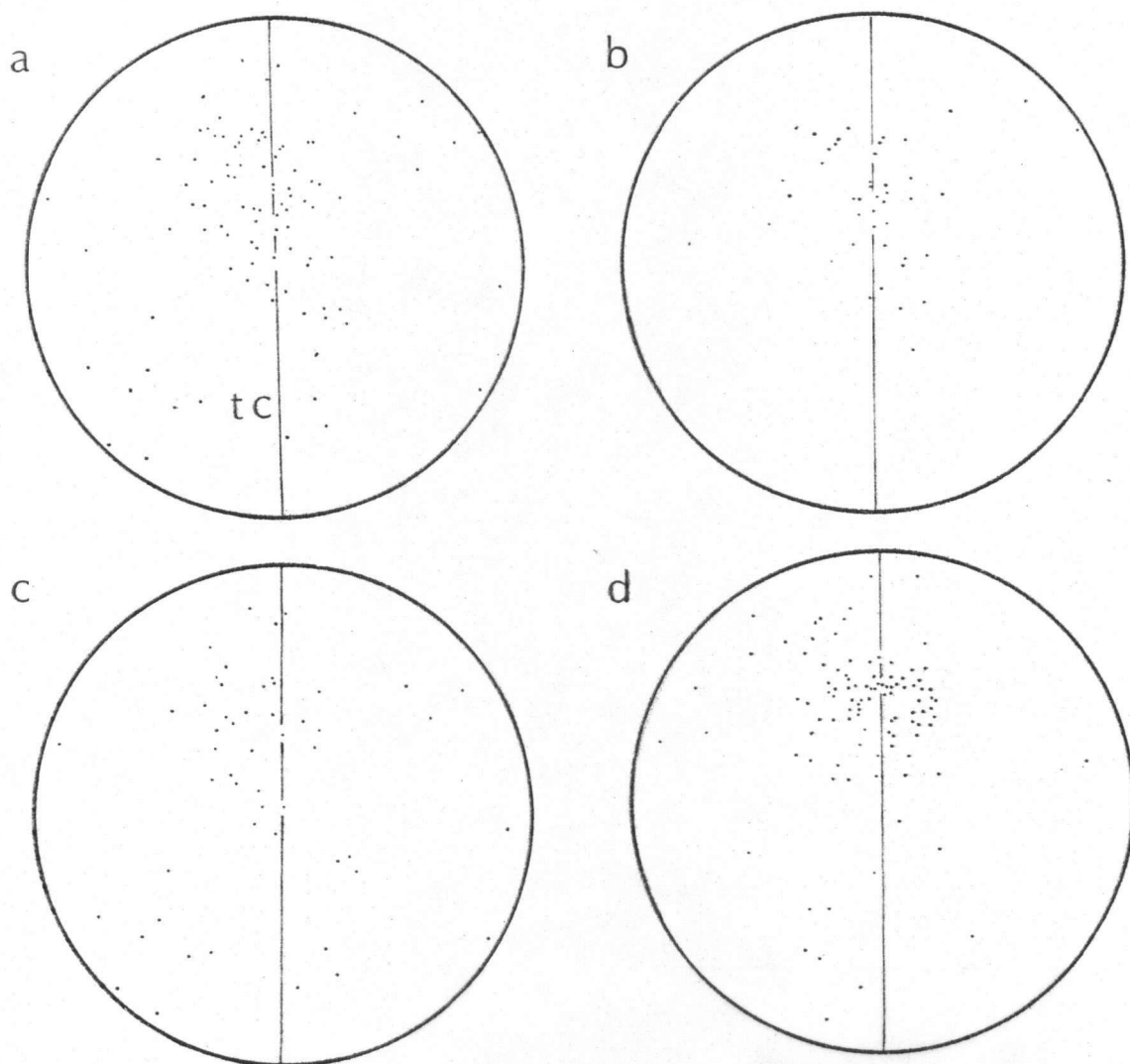


Figure 42.  Peninsula Point Pingo
            Tension Crack.

(a) Vertical section orthogonal
    to crack plane, 96 crystals.

(b) Right side of (a),
    44 crystals.

(c) Left side of (a),
    52 crystals.

(d) Vertical section orthogonal
    to crack plane, 100 crystals.
    t.c. = tension crack plane
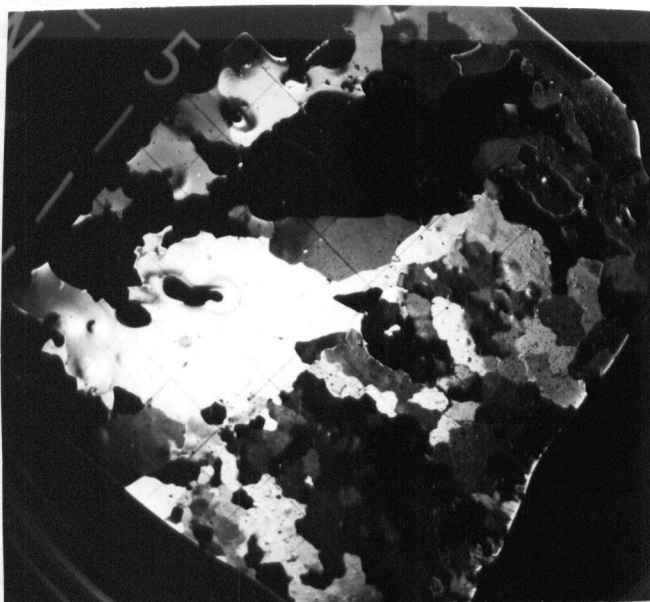
Figure 43.  Crystal characteristics,
    (compare with bubble and sediment in Figure 41).   Vertical section
    orthogonal to crack.   10 mm grid.

(b) Crystals are 20 mm x 10 mm and elongated parallel to the bubbles, i.e. at 30° to the horizontal. Shapes are anhedral and irregular. Many elongate bubbles lie in grain boundaries, others cross boundaries and change shape at the boundary. Tapering bubbles always lie on grain boundaries; conversely small spherical bubbles are intragranular.

(c) Crystal size is smaller than zones (a) and (b), generally 15 mm x 5 mm, with some 3 mm x 2 mm. Orientation is horizontal, and shapes are very irregular and serrated. Sub-boundaries occur with strain extinction. Larger bubbles tend to occur at grain boundaries.

Thus there is a strong relationship between crystal characteristics and bubbles in all ice zones. Additionally zone (c) contains small amounts of sediment which again are concentrated on grain boundaries.

In comparing the crystal and inclusion characteristics of this ice with those of the previously discussed tension crack it is evident that the primary growth features have been modified; competitive growth zones have disappeared, crystal shapes are considerably modified and bubbles have moved relative to grain boundaries.

Petrofabric diagrams are given in Figure 42(a)-(d), for vertical thin sections orthogonal to the plane of the crack. The pattern comprises a broad maximum in the plane of the ice body and at about 45° to the horizontal superimposed on a minor girdle. Some crystals in the eastern side of the body have more dispersed c-axis orientations but these crystals have no apparent differences from the others in thin section. It is recalled that in the tension crack on Pingo No. 9 optic axes gave a vertical girdle which became more narrow with distance from the ice-soil interface

and represented growth conditions where basal planes were parallel to the freezing direction.

## Interpretation

The tension crack ice discussed here is of considerably greater age than that in Pingo No. 9 and the pingo in which it is located has suffered long term coastal erosion. The sampling site has been subject to varying temperature gradients and stress systems as unloading occurred during erosion. It is evident from crystal and bubble characteristics that original sizes and shapes have been modified considerably. Bubble and crystal characteristics would have been related symmetrically to the freezing direction during initial growth, as has been observed in several recently grown ice bodies (e.g. Tension Crack Ice, Pingo No. 9; Icing Mound Ice); bubbles would be volumes of revolution elongated in the freezing direction and columnar crystals would be parallel to that direction. In the Peninsula Point Pingo, bubbles have irregular shapes, the irregularities being related frequently to crystal grain boundaries; also bubbles have broken up into strings or groups. Such features are readily explained in terms of changing thermal conditions, but the optic axis distribution diagrams, which are homogeneous for all parts of the body, are unusual. The influence of sediment on crystal size is evident from Figure 43; trapping of sediment on grain boundaries has retarded grain boundary migration in the right hand side of the figure relative to the left hand side.

6. Thermal Contraction Cracks and Wedge Ice

## Introduction

Ice wedge ice, formed by the infilling of thermal contraction cracks, is widespread in the Tuktoyaktuk and Pelly Island areas, as in other arctic regions. Mackay (1974a) has discussed cracking of wedge ice on Garry Island, but there is no published work on ice wedge petrology in the area. Elsewhere Black (1953, 1954, 1963) and Corte (1962a) have reported on the form and crystal characteristics of ice wedges in Alaska and Greenland, respectively. In the Soviet Union, similar work has been carried out by Shumskii (1964). Cracking in Antarctica has been studied by Black (1973).

## Wedge Growth Mechanism

Ice wedges grow from winter thermal contraction cracks which become infilled by hoar frost, snow and surface water. In his theoretical work Lachenbruch (1962) argued that a rapid temperature drop superimposed on generally low temperatures is responsible for cracking. However, Grechish-chev (1970) considered Lachenbruch's work as only a first approximation, as it was based on a linear dependence of thermal expansion and contraction on temperature. Further, Grechishchev pointed out that the moisture content in the soil has a considerable effect on thermal characteristics. He argued that the water content of the active layer decreases downward and so the thermal conductivity varies. Thus in the first half of the cold period tension occurs in the lower one-third of the active layer while the top is in compression.

In the present study, no measurements were made of temperatures, stresses, crack frequency or depth, as such would require a much longer period of study. The Pelly Island site, discussed below, is near Garry Island where Mackay (1974a) has made a long term study of ground temperatures and cracking patterns in low and high centred polygon wedges.

Once fracture has occurred, some infilling proceeds by hoar crystal growth and snow melt before warming of the ground closes the cracks; it is likely that only a minority of closure is due to infil by crystal growth (Black 1953). Expansion of the ground in summer causes horizontal stress on the whole ice wedge. No quantitative estimate of the stresses involved has been found in the literature, although Black (1953, p. 72) states that horizontal stresses are produced "... well above the limits of ... shear of ice." Also a rough estimate of horizontal compression can be obtained from Lachenbruch (1962, p. 23) as summer expansion approximates winter contraction. Thus stresses of several bars are operative, and temperatures are high, causing modification of growth features.

It is the purpose in this section to discuss petrologic aspects of the mode of fracture in ground ice, fracture infil, the relationship of succeeding fractures to earlier ones, the prograde fabric of a growing wedge, and the influence of a growing wedge where it penetrates massive ice.

(a)    Fracture propagation in relation to permafrost features

Single fractures in sediment are difficult to find, and thin section preparation poses many problems, thus individual thermally induced fractures in massive ground ice only are considered. The ice body is an

involuted hill near Tuktoyaktuk, the core of which has been exposed by coastal erosion. Some knowledge of inclusion and crystal characteristics of the massive ice is necessary in order to understand fracture propagation. A detailed discussion is given elsewhere (pp. 95-151) but a summary is included here. The massive ice has a characteristically large grain size, ranging from 15 $mm^2$ in bubbly layers to $\leqslant 600$ $mm^2$ in bubble-free zones. Bubbles in the massive ice occur in wide bands, range up to 3 mm in diameter and are located both on grain boundaries and within crystals. As such they represent major defects in the structure and might be expected to influence fracturing. Bubbles control crystal size in the massive ice, smaller crystals occurring in bubbly zones. Thus there exists a greater grain boundary area, also grain boundaries by definition separate material of differing lattice orientations. These grain boundaries are zones of atomic disorder, and frequently contain sediment and segregated solutes. All these factors tend to alter the response of the ice body to stress.

The c-axes of the massive ice crystals are approximately vertical and in the fracture plane, thus the basal planes are orthogonal to the fracture surface. Thus, prior to fracture, the massive ground ice has markedly different crystal characteristics and bubble pattern from ice samples used in laboratory experiments on fracture.

Typical fractures are shown in Figure 44. It is evident that cracks have propagated through coarse-grained ice and tended to be transgranular rather than intergranular. No major changes in fracture orientation occur at grain boundaries, thus slight changes in lattice orientation exert no

Figure 44.

Infilled fractures, large crystals are "massive ice," which have been cut by fractures.

10 mm grid.

Crossed polarizers
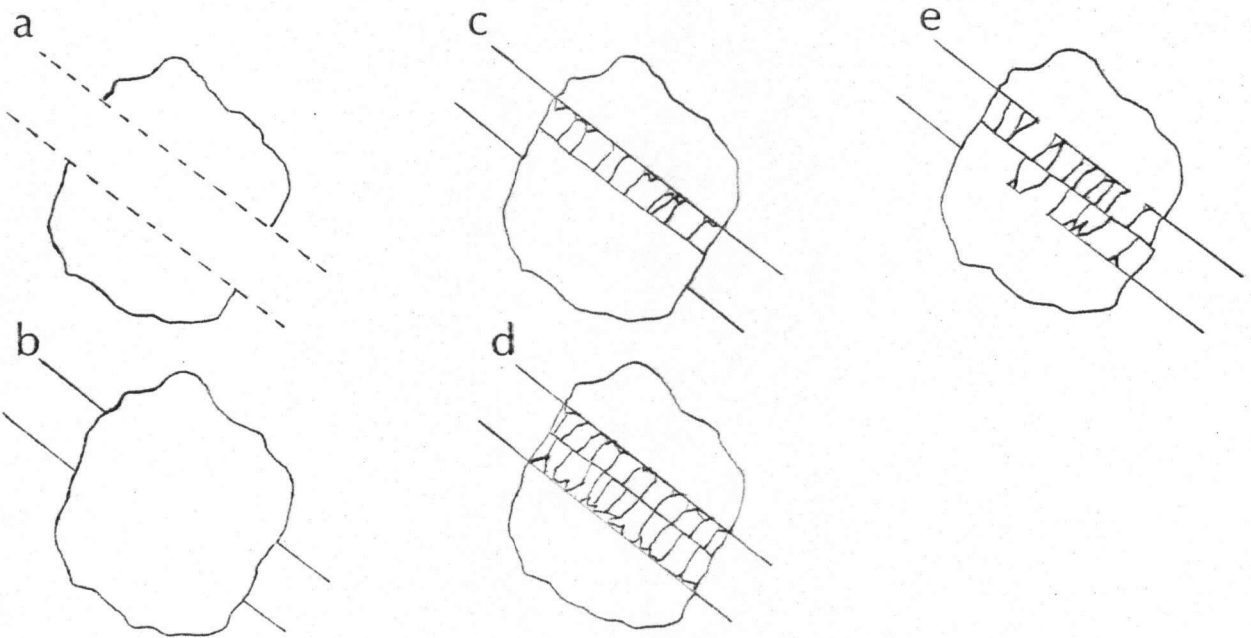




Figure 45. Types of fracture infil. (a) open fracture, (b) no new crystal growth, (c) new growth on one side, (d) new crystal growth on both sides, (e) new growth on parts of both sides.

major control, in contrast to the results of Gold (1961) on thermal shock. However, bands of differing lattice orientation in crystals are approximately vertical and thus may have aided the fracture process.

The transgranular cracks contrast with those of Anderson and Weeks (1958) for a sea-ice beam which failed in tension by fracture along the basal planes of crystals. However, in sea ice the basal planes are also the sites of brine pockets which act as stress concentrators. Such gross liquid inclusions have not been observed in ground ice but gas bubbles occur; these are not generally located parallel to basal planes. The influence of bubbles is not clear, as any bubbles in the fracture path are obliterated during later infil of cracks.

The speed of fracture propagation is unknown, but from the petrologic evidence it appears that fracture has been rapid, such that texture has exerted little influence.

(b)  Infil of fracture

The exact widths of fractures are unknown, as some contraction of the cracks may occur before infil (Black 1953) and some flow has occurred prior to sampling. However, an estimate can be obtained from bubble zones parallel to the fracture seam, and from boundaries between original fractured grains and the infil crystals. These zones are up to 3 mm wide. As is evident from Figure 44, in some cases the "massive" ice crystals have grown across to the fracture seam; in other cases, a group of new crystals grew. The question arises of why both these cases occur. Petrofabric diagrams of fractured crystals show that there is no significant difference

between crystals in the two cases. An individual crystal which is fractured (Fig. 45(a)) may be subject to one of several growth patterns: in (b) new growth occurs on neither side; in (c) new growth occurs on one side; in (d) new growth occurs on both sides; in (e) new growth occurs on parts of both sides. Whatever the growth type, the seam is central, so nucleation and growth rates in all cases are approximately equal; otherwise offsets would occur in the seam.

The fractures are oriented such that "massive ice" crystal basal planes are approximately orthogonal to the crack surface. The basal plane is the plane of most rapid growth of ice (Hillig 1958), thus nucleation and growth of new crystals is rapid. Also the infil crystals have a wider range of c-axis orientations, which has had little effect on the infil process (Fig. 46). Figure 46(a) represents a vertical section orthogonal to a fracture showing c-axes of massive ice crystals to be vertical in the fracture plane, while infil crystals form a vertical girdle normal to the fracture. Figure 46(b),(c) show c-axes of massive ice crystals in a horizontal section, and Fig. 46(d) indicates that infil crystals give a vertical girdle. A further vertical section is represented in Fig. 46(e) and infil crystals give a similar pattern to Fig. 46(a). The petrofabric pattern for these fracture infil crystals thus differs markedly from that of the recent tension crack (Fig. 39) where a broad vertical girdle parallel to the crack was found. However, it is noted that in the tension crack copious nucleation occurred on the soil, rather than on fracture ice or hoar, and such crystals had a much less preferred orientation than the columnar crystals which developed from the chill zone. In the case of the thermal fracture a much smaller space for crystal growth is available, and a well developed columnar zone has not developed. The influence of hoar
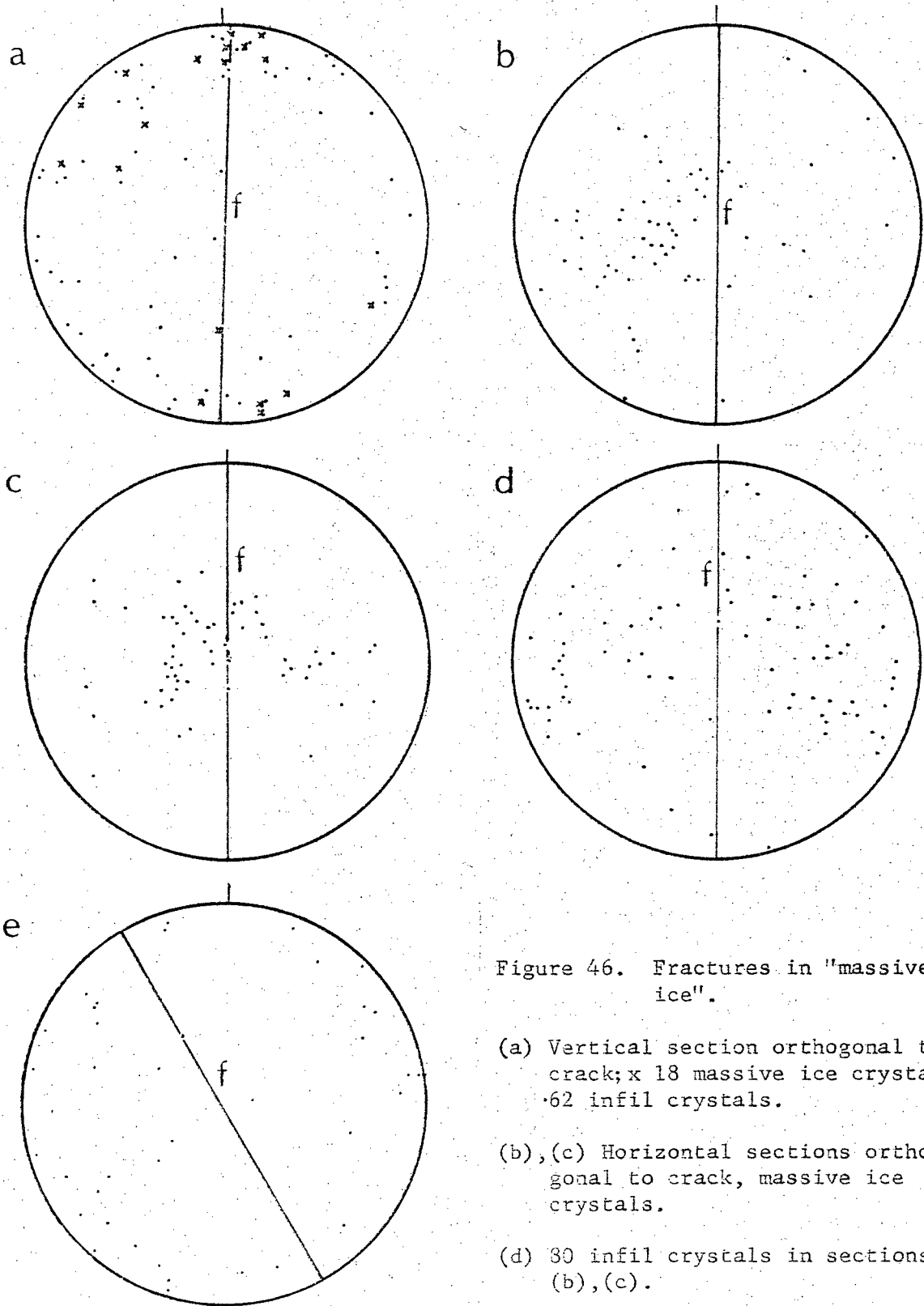
Figure 46. Fractures in "massive ice".

(a) Vertical section orthogonal to crack; x 18 massive ice crystals; ·62 infil crystals.

(b),(c) Horizontal sections orthogonal to crack, massive ice crystals.

(d) 30 infil crystals in sections (b),(c).

(e) Vertical section orthogonal to locally dipping fracture. 40 infil crystals.

f = fracture

crystal growth on infil crystals is not known. It is interesting to note that both tension crack and thermal fracture infils differ from rock vein infils where c-axes tend to be normal to the vein.

The infil texture differs markedly from the "massive ice." Crystal size is obviously limited by the space available for growth, and crystal shape tends toward columnar, parallel to the growth direction, and orthogonal to the fracture surface. No well developed zone of competitive growth occurs. Mutual boundaries are straight or gently curved, locally with small gas bubbles. No intergrowths occur at the central seam in the initial growth period. Sub-boundaries were not observed in the newly grown infil crystals. Subsequent changes in this overall pattern are discussed later. A small amount of ice growth occurs on the surface of the fractured massive ice before bubbles form. This indicates a build up of dissolved gas at the solid-liquid interface in the initial freezing. The bubbles occur on both sides of the fracture over large areas thus indicating a widespread event.

Black (1953) discussed the response of fracture infils to compressive stress. Cracks with air bubbles and hoar infils became shear planes whereas cracks with clear ice were stronger and shear took place adjacent to them. Similarly, tensile stresses would be expected to produce differing responses on different fracture infils. It must be remembered that at different depths the ground is subject to different stress systems at the same time. Thus fractures which are initiated in a zone of tensile stress may propagate into compressed zones (Lachenbruch 1962).

Where a "stratigraphy" of fractures was observed, it was seen that small crystals in older fractures had embayed the "massive ice" crystals.

Thus the original fracture surface was no longer approximately planar, representing the adjustment of crystals to the stress system.

## (c)   Subsequent Fractures

It is evident from the above discussion that an infilled fracture presents markedly different texture and petrofabrics from the original massive ice. The smaller infil crystals have a greater specific grain boundary area, partially in a vertical seam on which are abundant gas bubbles. Also a greater range of c-axis orientations occurs, including some crystals with vertical basal planes. However, it is apparent from Figure 47 that where refracturing has occurred the cracks do not follow the same plane. Series of fractures are observed (between which massive ice may still be recognized); some cross, and in other cases a crack may trend into a previous one. In general there is no apparent control by earlier fractures, i.e. the texture and presence of central seams of fractures containing bubbles had little effect on subsequent fractures. This may be due to the factor, pointed out in the discussion of Tension Crack Ice, that finer grained materials are more resistant to cracking than coarse grained due to their greater ability to accommodate contraction strains.

## (d)   The Prograde Fabric of Wedges

A site on Pelly Island (Fig. 1) with large-scale wedges was studied in order to investigate changes in texture and petrofabrics across wedges, and the intersection of two wedges.
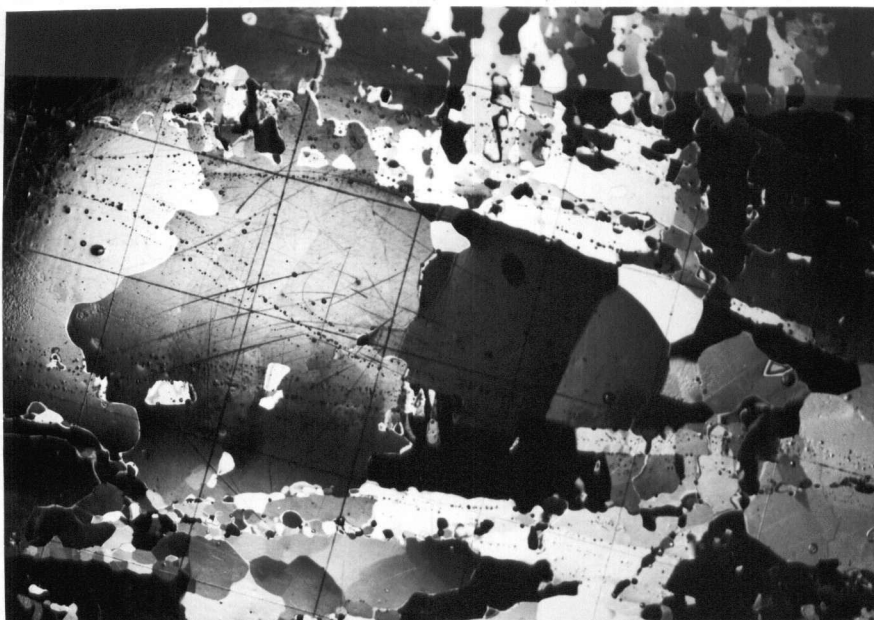
Figure 47. Parallel and converging thermal
contraction cracks in massive ice. Horizontal
section. 10 mm grid.

Crossed polarizers

Field Characteristics

The Northwest coast of Pelly Island has a low-lying area of polygon flats in lacustrine clays, presently under active coastal recession. Wedges are readily observed on a low cliff, and polygon troughs and ridges are well developed. Many wedges are greater than 2 m across and some are over 3 m. The upper surfaces of most coastal wedges and surrounding peat and clay have been subject to melt down and periods of freeze-back. Thermokarst and thermal erosion was greatest over and adjacent to wedges, the hollows having been infilled subsequently by peat, clay and pond ice. In one case this left a large wedge in an inactive state and led to new wedge growth adjacent and approximately parallel to the first.

The wedges have the characteristic fan-shaped foliation (Black 1953) determined by bubble and sediment content, with a general decrease in bubbles from the centre outwards. Large clay inclusions are found at the contact with surrounding material. In addition to the fan-shaped foliations, oblique fractures cross the wedges (Fig. 48).

Samples were taken from a large wedge, 3.3 m wide with an overburden of peat and clay 0.4-0.5 m deep. Melt-down had occurred below the present active layer (Fig. 49) as indicated by a chemically stained layer in the clay which adjoins the lower shoulder of the wedge. This is not a two-tier wedge, but greatest melting occurred at the boundary of the wedge, above which occurs a body of pond ice which froze omnidirectionally. The upper wedge surface has a relief of 0.1 m. Exposure of ice was limited to a depth of 1 to 1.5 m below the wedge top due to slumping, thus no samples could be removed from greater depths. Four samples were taken across the wedge from the centre to the boundary.
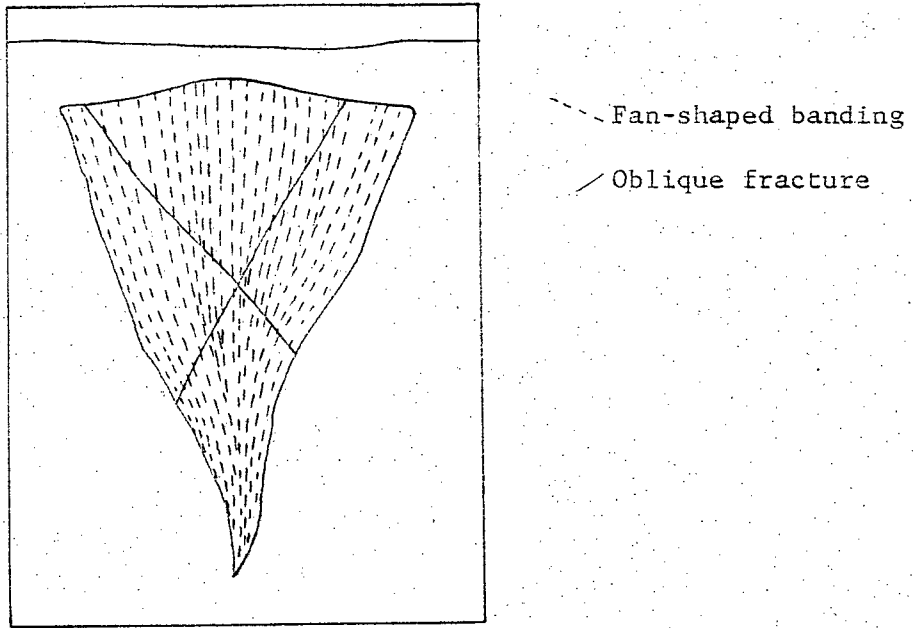
Figure 48. Bubble bands and oblique fractures in wedge.
(schematic)
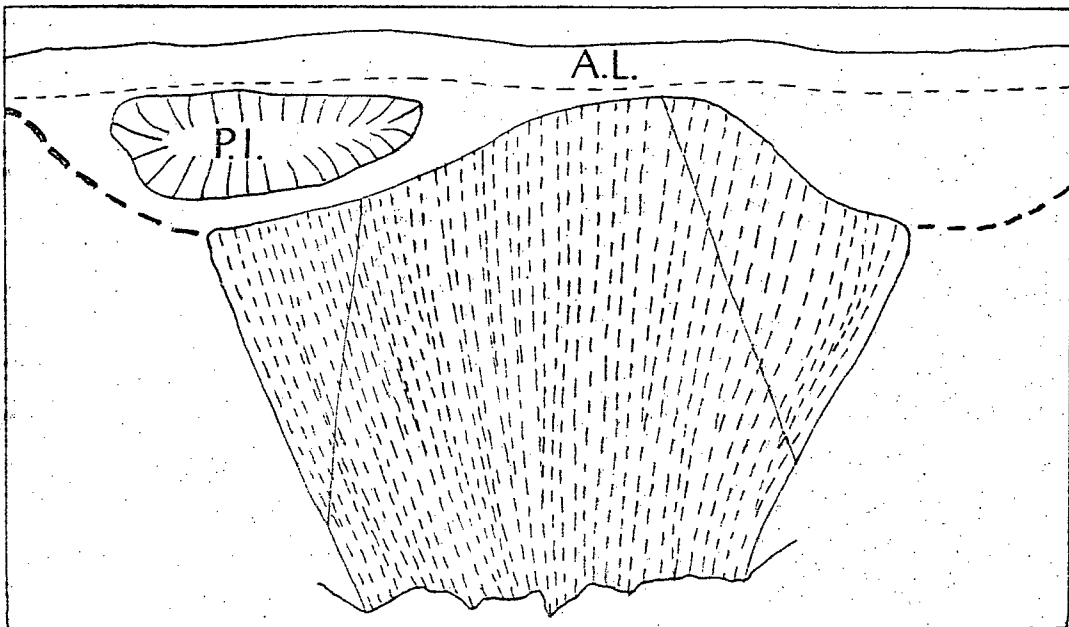


Figure 49. Melt-down adjacent to large wedge.
A.L. = present active layer;
P.I. = "pond ice";
— — = base of thawed zone.

### Ice Characteristics, wedge centre

The bubble foliation of the central portion of the wedge presents a complex pattern. It is evident that cracking does not always occur centrally, as later oblique cracks offset earlier foliations (by a few mm). Bubbles, usually elongated vertically, average 10 mm in length and <1 mm diameter; some spherical bubbles (<1 mm) are interspersed with irregular ones. Within a given foliation, bubble shape is fairly constant, these foliations are <3 mm wide and separated by clearer ice. Peat and sediment inclusions are scattered along the traces of old fractures; larger inclusions may have been broken up and offset by subsequent oblique fractures. More recent fractures have larger, sub-planar concentrations. Inclusions thus occur as: (a) individual fragments of 1-2 mm; (b) planar zones continuous laterally for 80 mm; (c) pods extending 2-3 mm out from the fracture surfaces. These inclusions provide no information concerning crack widths, as particle migration, and flow of ice have occurred since the fractures were infilled. Within a given fracture there is no apparent relationship between sediment or organic matter and bubble inclusions, i.e. the bubble contents above and below organic matter are similar.

### Ice Characteristics, wedge boundary

The ice at the wedge boundary differs from that described above. The fracture pattern is less complex, the bubble foliations and the intervening "clear bands" are wider, reaching up to 20 mm. Bubbles are mainly vertically elongated, 10 mm long, with fewer spherical bubbles than in the centre of the wedge. Thus, while the foliations have become rotated the bubbles remain essentially vertical. The fractures sub-parallel to the

wedge boundary have clay inclusions up to 3 mm wide and are more continuous than those in the centre of the wedge. Usually the fractures with high clay content have few bubbles. Later fractures are oblique to the earlier fractures and to the wedge boundary, and have low sediment content.

### Wedge Centre

Bubble Characteristics.- Maximum information was obtained from vertical sections orthogonal to the trend of the wedge. Bubbles occur in markedly different densities within individual bands, which range in dip from $40°$ to vertical, but not all bands strike parallel to the wedge. Bubble shapes are (a) elongate, (b) spherical, (c) irregular.

(a) Elongate bubbles are oriented approximately vertically, whether the containing foliation is vertical or oblique. Individual bubbles are $\leqslant 8$ mm long and $\leqslant 0.5$ mm diameter, some having slight curvature, but most are regular cylinders.

(b) Spherical bubbles are $\leqslant 1$ mm in diameter and occur individually, in groups, or within bands of mainly elongate bubbles.

(c) Irregularly shaped bubbles are similar in distribution to the spherical, but may reach 3 mm in length.

Organic matter occurs mainly in small pockets in discontinuous trains approximately parallel to bubble bands.

Crystal Characteristics.- Crystal size varies markedly throughout the section (Fig. 50), the average size being 4 mm x 3 mm and the range from $<1$ mm x $<1$ mm to 42 mm x 8 mm, the latter being vertically elongated. Crystals are anhedral with straight or slightly curved boundaries. Some

Figure 50. Vertical section, orthogonal to wedge axis, centre of wedge.

10 mm grid. ⊢—⊣

Crossed polarizers
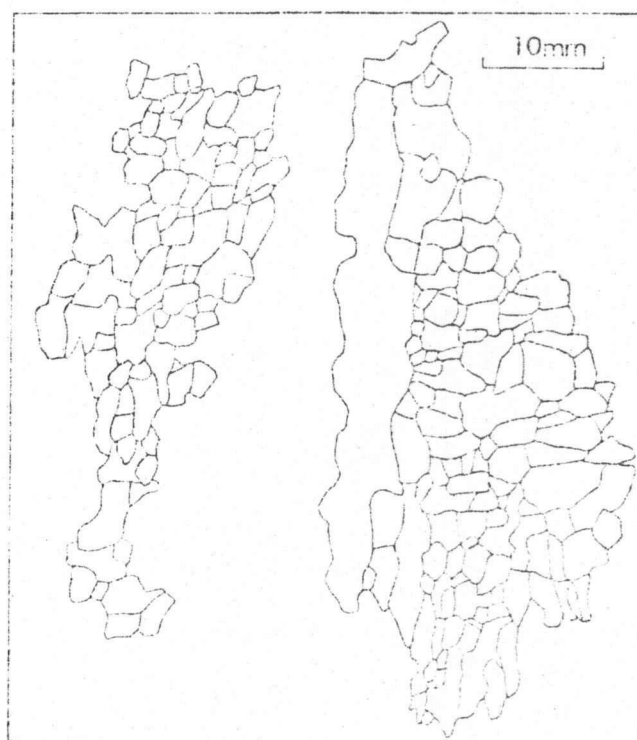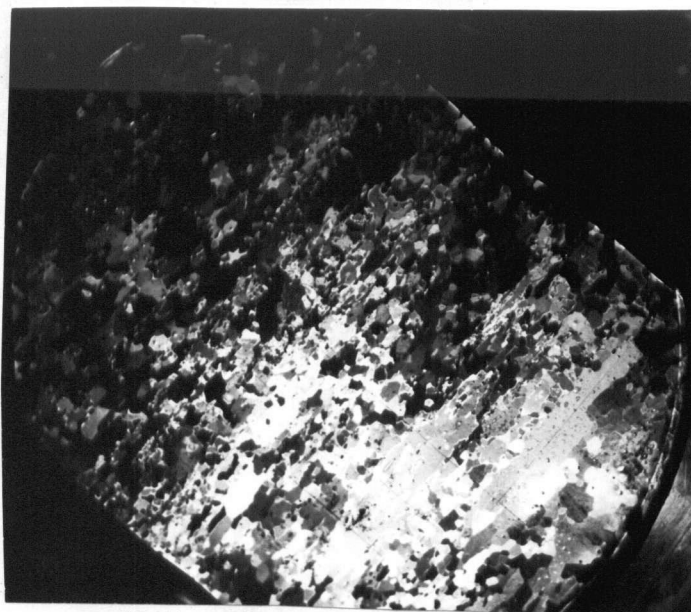


Figure 51. Sketch of grains in Figure 50 for petrofabric analysis, shown in Figure 52.

of the larger crystals have more irregular boundaries due to the presence

of small crystals along their margins. There are differing textural zones,

areas where grains are equigranular with no complex intergrowths contrast-

ing with areas where grains are markedly dissimilar in shape, size and

substructure. Dimensional orientation (Fig. 55(a)) is predominantly ver-

tical throughout, but locally more strongly developed, and some recent

fracture infil crystals have horizontal axes. Spherical bubbles tend to

be on or near crystal boundaries rather than in the centres of crystals.

No major change in shape of bubbles occurs at grain boundaries. Elongated

bubbles rarely occur within a single crystal, most cross boundaries or

terminate upwards at boundaries. The latter suggests that migration is

controlled by the grain boundary. Most inclusions of organic matter are

at grain boundaries. A photograph of one thin section is given in Fig. 50,

and a sketch of grains for petrofabric analysis in Fig. 51. The general

petrofabric pattern for the sample is a broad subhorizontal girdle (Fig.

52(a),(b)), but local concentrations exist, indicating the complex influence

of multiple fractures. Crystal growth in fractures is expected to be

initially productive of a vertical girdle normal to the crack, unless

crystals grow as extensions of cracked crystals, where a horizontal girdle

pattern would be expected. Subsequent periods of thermally induced stress

cause flow and reorientation. Later fractures may also interrupt the

pattern. Component petrofabric diagrams (Fig. 52(c)-(1)) have been prepared

on the basis of crystal size, number of sides per crystal and bubble

content. There are no significantly different patterns for each set of

diagrams. Thus the broad horizontal girdle is homogeneous throughout the

section.
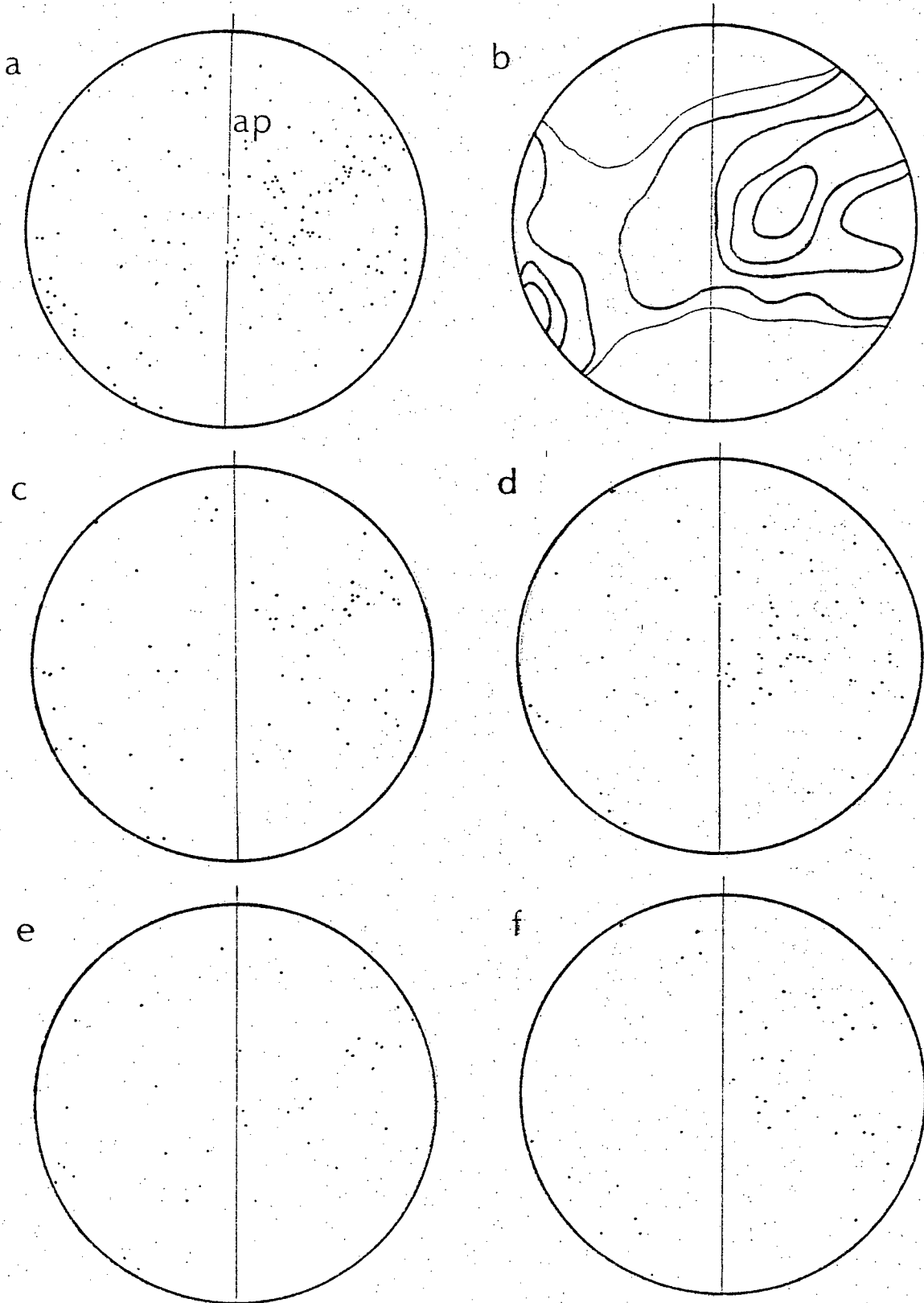
Figure 52.   (a),(b) 140 crystals, vertical section orthogonal to wedge axis,
at wedge centre, (c) 57 crystals with vertical dimensional
orientation, (d) 83 other crystals, (e) 40 crystals with $>6$
sides, (f) 40 crystals with 6 sides, ... continued.

Diagrams in plane of sections    a.p. = axial plane of wedge
Contours at intervals  1, 2, 4, 6, 8 $\sigma$
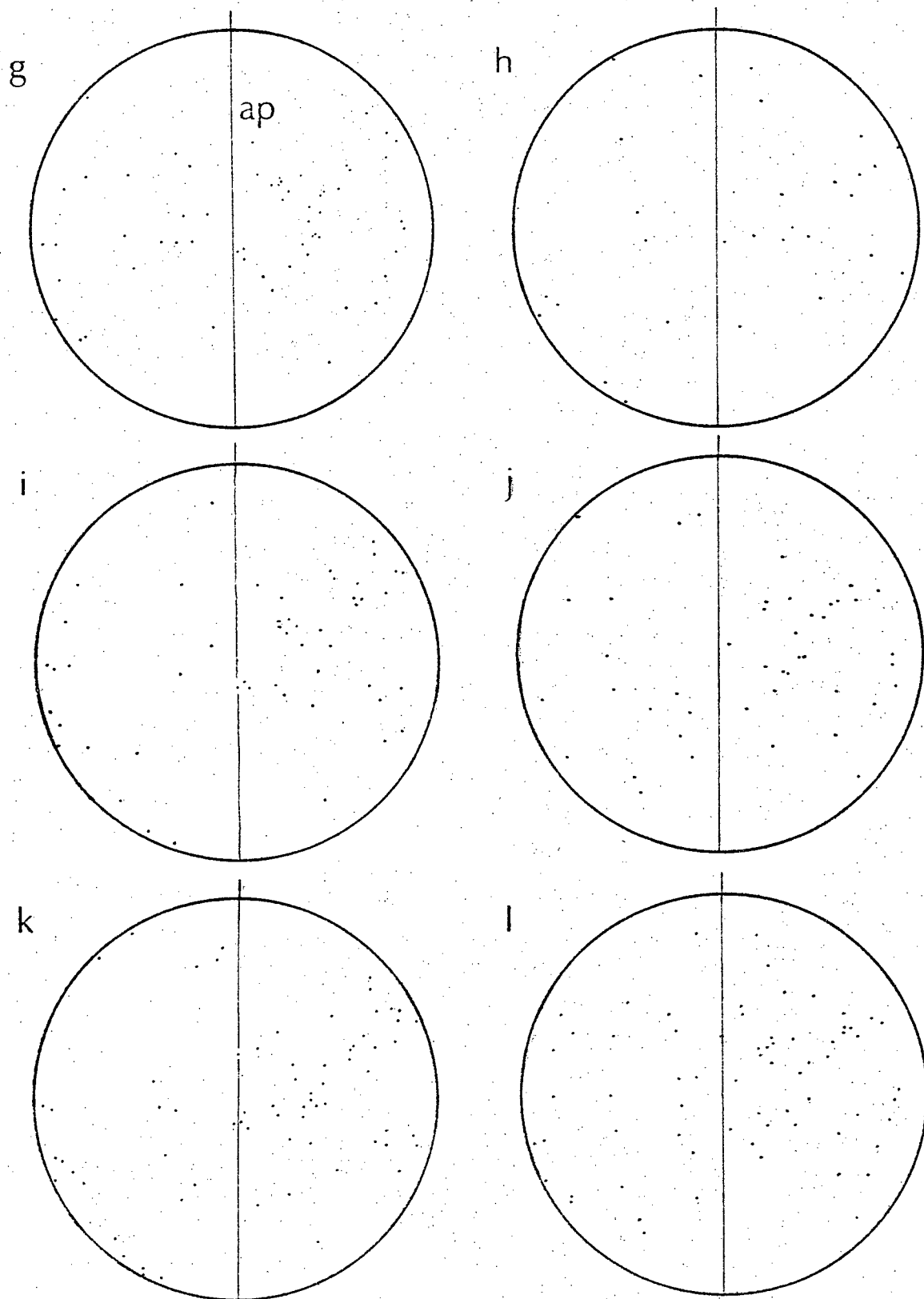
Figure 52. (Cont'd) (g) 60 crystals with < 6 sides, (h) 24 crystals, >5 mm long axes, (i) 52 crystals 3-4 mm axes, (j) 58 crystals <2 mm axes (k) 69 crystals containing bubbles (l) 71 crystals without bubbles.

Diagrams in plane of sections a.p. = axial plane of wedge

## Wedge Boundary

The contact of the wedge with the surrounding clay is irregular and clay blocks are contained within the ice. These blocks have rounded edges and are dissimilar to clay in a lens ice-clay system. The fracture pattern is simpler than at the wedge centre; most fractures trend parallel to the side of the wedge and are often traceable continuously through the section, although some are slightly offset by later, oblique fractures (Fig. 53). Many earlier fractures have 2-5 mm thick sediment inclusion layers, while others are less continuous. These early fractures have fewer bubbles but more sediment than later fractures.

Bubble Characteristics.- Bubbles in the older fractures have been subject to more thermomigration and fracturing. As the younger fractures tend to occur in the central portion, bubbles are better preserved there than at the sides. Owing to these changes, the characteristic wedge "foliation" is less easily traceable near the wedge boundary, especially where clay inclusions, and less commonly organic matter, are present. Where bubbles occur at the sides, they are more irregular than in the wedge centre. Spherical bubbles are less abundant than at the wedge centre, 0.5 mm in diameter, and tend to surround elongate bubble zones. These probably represent the interaction of bubbles during wedge growth. Usually the greatest irregularity appears on the side of the bubble nearest the wedge boundary. The later "foliations" are bubble-bands 3 to 5 mm wide containing more regular vertically elongated bubbles, whatever the orientation of the band.

Crystal Characteristics.- Crystal size varies throughout the section, but is generally larger at the wedge boundary than in the wedge centre,

Figure 53. Junction of
wedge with clay. Note
bubble trains parallel to
junction, and the oblique
fracture.
10 mm grid. Vertical section
perpendicular to axis of wedge.
Plane polarized light.
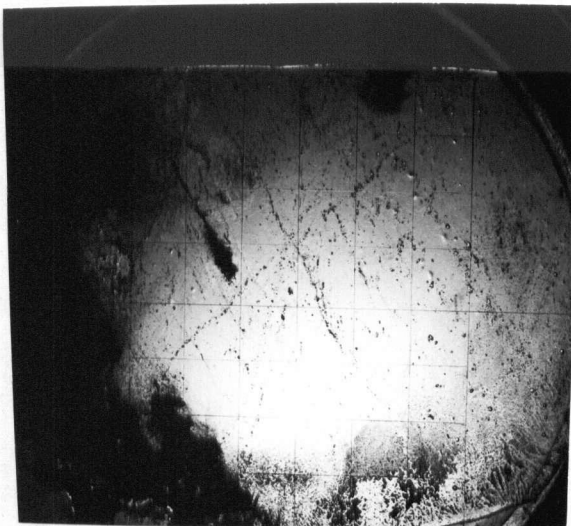


Figure 54. Vertical section,
wedge boundary, orthogonal
to wedge axis.
10 mm grid.

Crossed polarizers
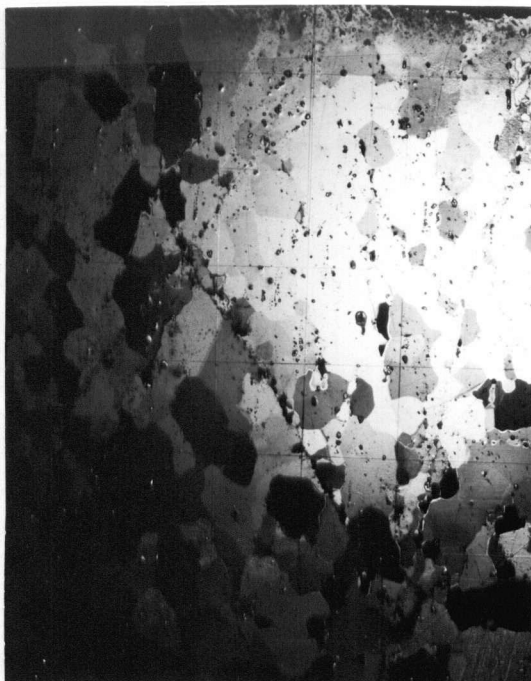
average size being 7 x 3 mm. Away from the edge of the wedge, crystals reach 15 x 10 mm, but small crystal zones also occur (Fig. 54; also compare Fig. 50).

Crystal shape is anhedral but with the smaller crystals tending to have some straight sides. The most pronounced grain boundary irregularities are vertically upward indentations at the base of crystals, associated with bubbles. Upward migration is unlikely as migration would tend to be downward for most of the year to the warmer region. Grain boundary migration can occur in any direction, thus it is more likely that bubbles have locally retarded that process. Some of the larger grains ($> 10$ x $> 6$ mm) are cut by later foliations, thus an increase in crystal size occurred before the latest fractures. Some bubble irregularities occurred after the latest fractures, but the time of fracturing is unknown.

Dimensional orientations (Fig. 55(b)) are generally vertical or parallel to the local fracture, the older fractures dominating, but this pattern is complicated where new fractures occur. Substructure occurs, mainly in the larger grains, as slightly differing extinction across crystals, not as distinct bands.

There is thus an overall relationship of texture and foliation. In the zone of older fractures, small crystals are effectively bounded by fractures. Later fractures cross these older grains. In comparison with sections from the wedge centre, a higher proportion of bubbles occurs within crystals, thus while bubble migration and grain boundary adjustment have occurred, bubbles have not all been trapped on boundaries.
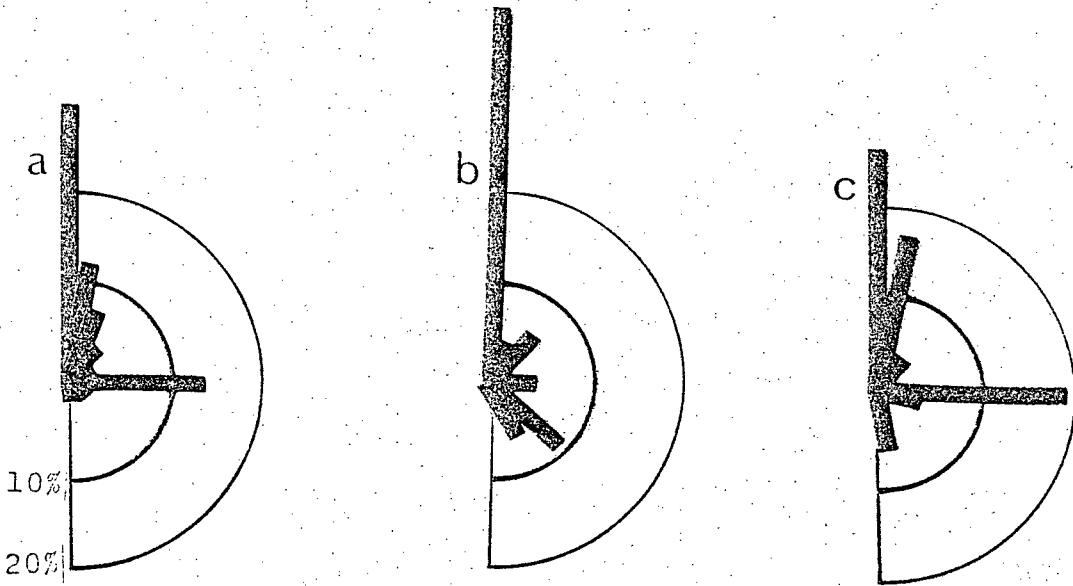
Figure 55.   Dimensional orientation, vertical sections.

   (a) Centre of wedge, section orthogonal to wedge axis;
   (b) Boundary of wedge, section orthogonal to wedge axis;
   (c) Junction of two wedges.
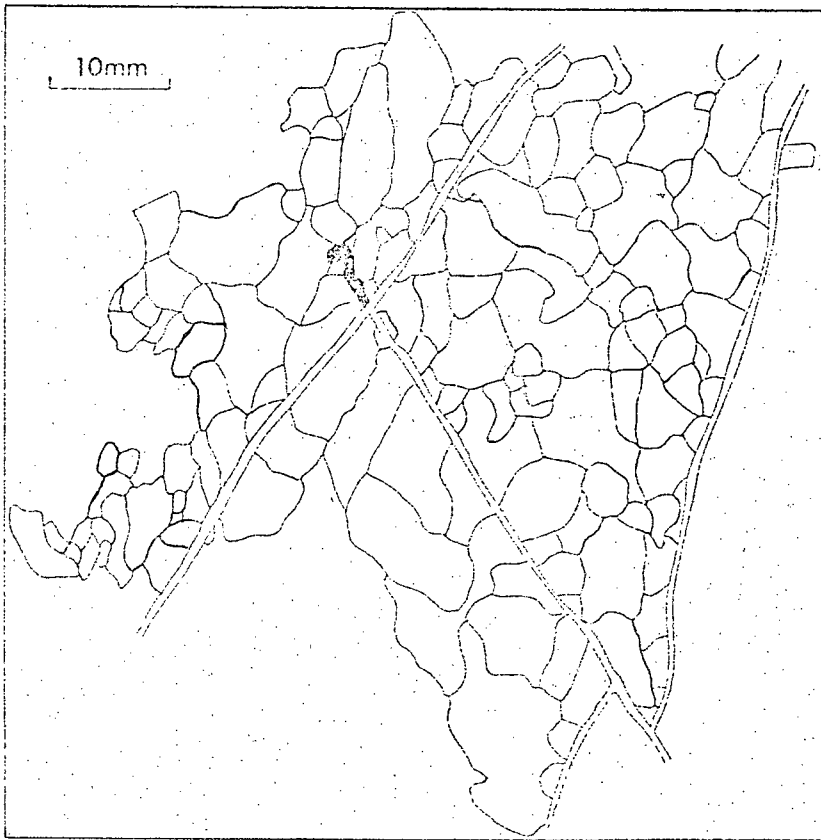


Figure 56.   Sketch of grains for petrofabric analysis, shown in Fig. 57.
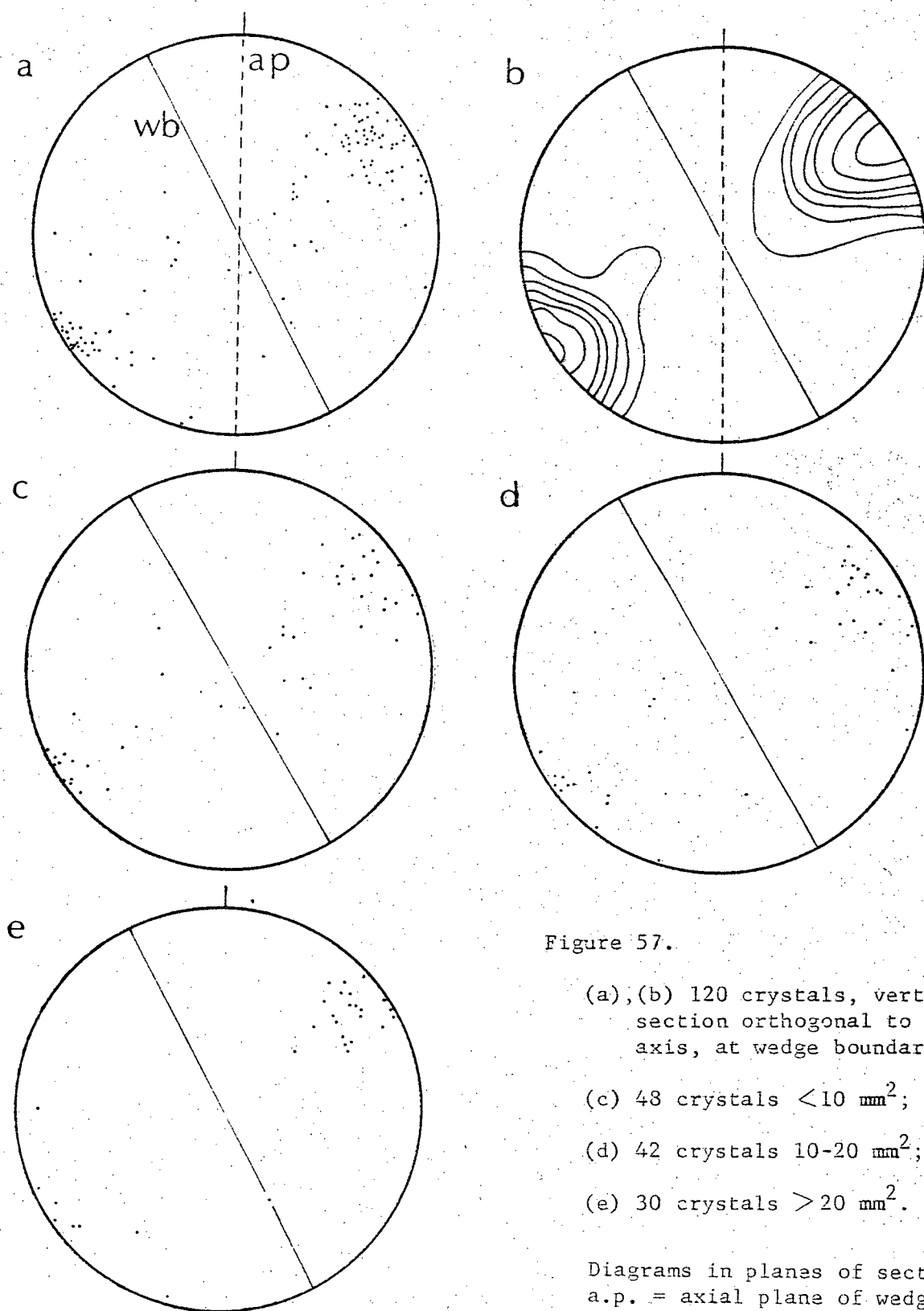
Figure 57.

(a),(b) 120 crystals, vertical
section orthogonal to wedge
axis, at wedge boundary;

(c) 48 crystals $<10$ mm$^2$;

(d) 42 crystals $10-20$ mm$^2$;

(e) 30 crystals $>20$ mm$^2$.

Diagrams in planes of sections
a.p. = axial plane of wedge
w.b. = wedge boundary
contour intervals 2, 4, 6, 8,
10, 12, 14 $\sigma$

Petrofabric diagrams are given in Fig. 57, for the section sketched in Fig. 56. The pattern is seen immediately to be more concentrated than the previous case, displaying a strong point concentration orthogonal to the plane of the major foliation, with a minor girdle orthogonal to the compositional layering. The fabric has thus become reoriented into higher symmetry than that of the wedge centre. Component diagrams were prepared on the basis of crystal size, position relative to fractures, and dimensional orientation. The three diagrams (Fig. 57(c)-(e)) differentiating crystal size show that crystals $<10$ mm$^2$ tend toward a girdle pattern which was characteristic of the wedge centre, while the larger the grains, the nearer the pattern approaches a point concentration. There is no significant difference among diagrams based on dimensional orientation.

## Horizontal Sections

As a check on textural variation across the section, horizontal thin sections were compared. The fracture pattern is more pronounced in the wedge centre, most fractures are parallel to the wedge trend, but some intersect. Bubble inclusions are most strongly concentrated in younger fractures which separate zones of clearer ice and of randomly scattered bubbles; few discrete bands occur near the wedge edge. Organic matter is much less common than bubbles in the central section -- inclusions are restricted to small parts of a few fractures, occurring in the form of streaks and blobs. At the wedge boundary, organic matter is in the form of linear inclusions only. Average crystal size varies from 3 x 2 mm in the wedge centre to 6 x 5 mm in the outer section. Crystal shape in the centre is generally subhedral, curved faces being on the side away from

recent fractures. Most complex shapes are found near those fractures in crystals which have dimensional orientations orthogonal to the cracks, whereas those further away are more nearly equidimensional. In the section near the wedge boundary, shapes are mostly anhedral but with no complex intergrowths or serrations. Major boundary irregularities are associated with bubbles, indicating relative bubble-boundary migration. Substructure is not well developed in any section; it occurs in larger crystals in the wedge centre and more frequently at the wedge boundary. The only pre-ferred dimensional orientation is orthogonal to recent fractures, indicating space infilling; later periods of strain modify such a pattern. In the central section bubbles and texture are related in two ways: (a) recent fractures are marked by continuous lines of bubbles in their centres, crystals from each side of the wedge meeting at the seam, and (b) away from recent fractures, bubbles tend to be in grain boundaries, probably resulting from trapping during recrystallization. Near the wedge boundary, bubble bands are less distinct, and the larger grains have grown past the old bands, bubbles occurring within crystals and at boundaries. Organic matter always occurs at boundaries.

### Junction of Two Wedges

In addition to the fabrics of single wedges, a junction of two orthogonally intersecting wedges was studied. No major differences from single wedges were found. Crystal size ranged from 2 mm x 1 mm to 22 mm x 8 mm, averaging 7 mm x 5 mm. No prominent banding was distinguished on the basis of grain size, except where a recent fracture was indicated by a small crystal zone. Shape is generally anhedral, although some crystals have one or more straight sides, and dimensional orientation is vertical,

parallel to bubble foliation, and more pronounced than in single wedges. The petrofabric diagram (Fig. 58) shows a broad horizontal girdle which is broader and weaker than the pattern in single wedges, but contains two orthogonal maxima, normal to the two wedges. From the limited work done here it is not possible to suggest relationships of individual maxima to each wedge.

### Discussion of Wedge Ice

The number of samples described here is limited compared with the work of Black (1953), but within a given wedge systematic changes were recognized. In a single wedge grain size increased outward from the centre and crystals became dimensionally oriented parallel to the compositional layering. Towards the sides of the wedge optic axis orientations form a strong point maximum orthogonal to the layering due to recrystallization. The lower symmetry of the fabric diagrams of the wedge centre is due to the presence of multiple oblique fractures and associated new crystal growth. With increasing distance from the centre there is less disturbance and fabrics adjust to the imposed stress system, producing a strong point maximum. While the major stress is horizontal, wedges retain a wedge shape and basal planes of crystals are parallel to the bubble layering. Towards the wedge boundary the layers increase in dip, but non-spherical bubbles within the layers retain vertical orientations, due in part to the stress system and partially to the vertical temperature gradient. The sample from the junction of two wedges shows the influence of both wedges.
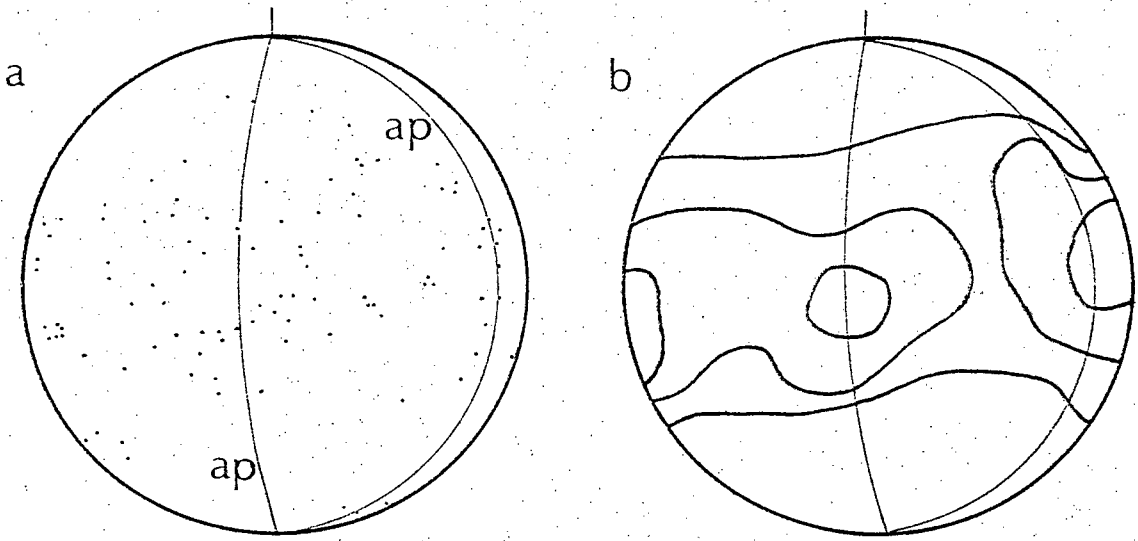
Figure 58.   (a),(b) 100 crystals at junction of two
             orthogonal ice wedges.

             Vertical section
             a.p. = axial planes of wedges
             contour intervals 2, 4, 6 $\sigma$

In comparison with Black's (1953) results, the fabrics found here are fairly simple. C-axis maxima are generally orthogonal to compositional layerings whereas Black found this pattern plus a range of others. However Black studied many more wedges which included wedges in various states of activity, including buried wedges. Buried wedges had equigranular crystals (Black 1953, p. 65) which is evidence of grain growth.

In the theoretical work of Lachenbruch (1962) and Grechishchev (1970) the wedges were considered to be fairly uniform. In the present study the variability in compositional and crystal characteristics has been recognized. Compositional layers differ in orientation throughout the wedge and the contained ices respond in different manners. The layers are defined by bubbles and other gross defects which act as stress concentrators. Thus theoretical models of cracking are not rigorously applicable. Additionally the presence of grain boundaries, which are zones of atomic disorder, may influence crack propagation. The general increase in grain size toward the edge of the wedge and associated change in optic axis lineations toward a point concentration orthogonal to the local foliation is due to basal slip and grain growth occurs in suitably oriented crystals, while other crystals are consumed in the boundary migration mechanism. Inclusions may affect the boundary adjustments, and bubbles are subject to horizontal stresses and a vertical temperature gradient which produces their vertical elongation.

Shumskii (1964, p. 202) reported that at the upper end of wedges

> ... crystals are columnar. The stratification becomes quite
> indistinct ... and the number of mineral inclusions decreases
> considerably.

This suggests that the upper ice was pool ice, frozen in the wedge trough. Such misinterpretations are readily made in light of the fact that thermal erosion of ice wedges may occur, as discussed by Mackay (1974d). Refrozen infils of such channels have been observed, and subsequent fractures cross these infils (Mackay, personal communication 1975).

(e)    The Influence of Wedge Growth on Massive Ice

In addition to sites such as Pelly Island, where wedge systems have developed in sediments and organic matter, wedges have also grown in segregated ice bodies. The latter type is less frequent and characterized by larger polygons. As recent fractures were identified petrographically, the wedge appears to be growing, and thus actively stressing the surrounding ice. The compositional layering of the massive ice is deformed adjacent to the wedge, shown in Figure 32. Petrologic analysis shows a decrease in grain size toward the wedge, and a change in petrofabrics from that typical of folded massive ice toward that of a wedge. In addition recent fractures showed their characteristic features. By comparison with folded ice which did not contain a wedge, the influence of the wedge is apparent.

(f)    Comparison of Tension Crack Ice and Wedge Ice

Wedge ice is a result of the infil of fractures produced by thermal contraction of the ground, whereas tension crack ice infils fractures produced by mechanical rupture of the ground associated with the growth of excess ice at depth, as in the case of pingos. However, tension crack ice is also subject to thermally-induced strains.

Wedges characteristically form a polygonal pattern (although there may be no surface expression on slopes, due to soil creep) whereas tension cracks are best observed on pingos, but may extend on to adjacent lake flats, and have been traced for 2 km (Mackay 1973a, p. 992, Fig. 18). Thus the two ice types may be distinguished frequently by surface expression. Where exposure to depth occurs the relationship of the ice body to surrounding material differs; no upturning occurs at the tension crack boundary (Fig. 40), whereas sediment and ice banding are deformed adjacent to wedges (Fig. 32).

Where such rare sections are not available, the petrologic characteristics of the ice are useful; however, no tension crack ice from the lake flats was studied. In comparison with wedge ice, one season's growth of tension crack ice may be much greater (in this study 100 mm) and has multiple bubble bands and crystal layers containing larger crystals than wedge ice. Also lattice preferred orientations are more concentrated in the girdle pattern. In the case of the old tension crack ice there are again major dissimilarities from wedge ice in terms of banding, bubbles, crystal size, shape and orientation.

7.  <u>Reticulate Vein Ice</u>

<u>Introduction</u>

Fine-grained sediments, such as glacial tills, lake and marine clays and mudflow deposits are of widespread distribution in the field area. Within such sediments, reticulate ice veins have been recognized forming a three-dimensional pattern (Mackay 1974b). The veins tend to occur in the upper 10 m of exposures and are frequently underlain by massive segregated ice. The primary veins may be either vertical or horizontal (Mackay 1975c) and range up to 5 m in length and 0.3 m in width. Ice within the veins is often inclusion free.

Several theories of vein growth have been proposed (Popov 1967; Danilov 1969; Katasonov 1967; Mackay 1974b, 1975c; McRoberts and Nixon 1975). The theories of Popov, Danilov and Katasonov have been discounted by Mackay (1974b) who presented a theory which explains the near surface position of the vein systems and the lack of excess water on thaw; the vertical and horizontal orientations are due to shrinkage cracks and the water is derived from the adjacent "frozen" clay blocks, after downward penetration of the freezing front.

McRoberts and Nixon (1975) gave a discussion of Mackay's (1974b) paper in terms of hydraulic fracturing. In reply Mackay (1975c) pointed out that horizontal hydraulic fracturing was unlikely, and that vertical veins formed by such a mechanism could probably be distinguished by further study of ice vein patterns, ice petrofabrics and water chemistry.

In this study reticulate vein ice was obtained from above the massive segregated core of an involuted hill. Emphasis is given to considerations of ice petrofabrics as an aid in understanding growth and post-solidification features.

## Field Characteristics

The site chosen for sampling is an upper, active slump face in a coastal exposure where several periods of slumping have occurred. A variable thickness of stoney clay (1-10 m) overlies a massive segregated ice core. At this site the reticulate vein ice pattern is dominated by vertical veins (Fig. 59) which reach 0.25 m in thickness but are usually 10 to 100 mm thick, and widen downwards. They are traceable vertically for several metres, to the top of the present slump, and terminate downwards in massive segregated ice; frequently they become thinner just above the ice core. Horizontal veins also occur but are less continuous; the enclosed clay blocks are up to 1 m x 0.3 m x 0.3 m. The topography of the hill and the upper surface of the underlying massive segregated ice is undulating. The veins are perpendicular and parallel to the upper massive ice surface, except where slight downslope creep has occurred. Thus the system has been subject to heaving during later massive ice growth.

## Ice Characteristics

The contact of the vein ice and surrounding clay is irregular, but abrupt, and a mineral film is observed between ice and clay. Inclusions occur in the form of bubbles and small clay blocks; no structures are apparent. Samples were taken from both vertical and horizontal veins, and thin sections parallel to and orthogonal to the vein trends are discussed.

Figure 59.  Reticulate ice vein system.  Vertical veins dominate.  Massive ice below.
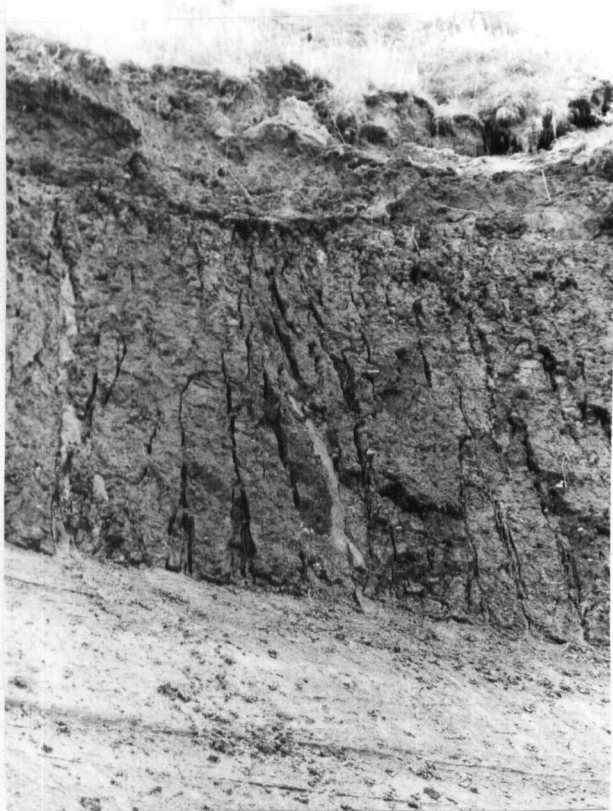


Figure 60.  Vertical section, parallel to vein plane.  Grid 10 mm. └───┘ Crossed polarizers



Figure 61.  Vertical section, parallel to vein plane. Grid 10 mm. └───┘ Crossed polarizers
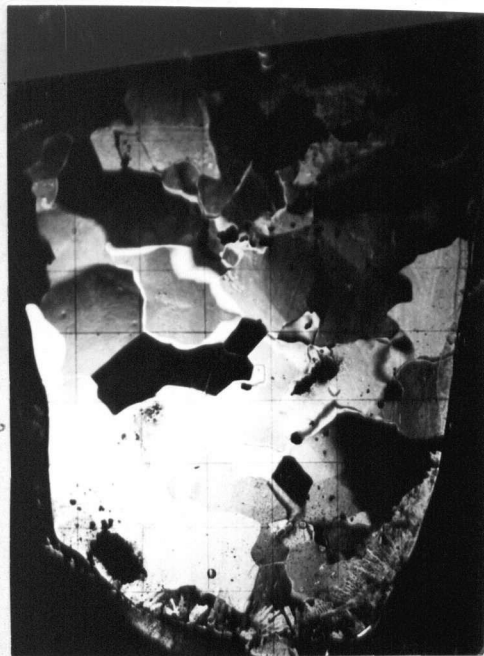
(i)    Narrow Vertical Veins

Inclusion Characteristics

Bubbles are few, spherical and small (<1 mm diameter) or ellipsoidal
(3-4 mm long).  Positions are apparently not related to the vein boundary
or to clay inclusions.

The clay blocks are irregular with conchoidal faces similar to those
reported for horizontal lenses by Penner (1961), and range in size up to
30 mm on a side.  No pattern of the blocks relative to the vein orienta-
tion was recognized.

Crystal Characteristics

Crystal size is large (Fig. 60) ranging from 4 x 5 mm to 20 x 30 mm,
and shapes are anhedral, inequigranular.  Boundaries vary widely; in a
given crystal, 2 or 3 sides may be essentially straight while the others
are very highly curved and interlocking, especially along embayments.
These embayments develop along sub-boundaries, which are well developed
in many grains.  While many sub-boundaries are parallel in a given crystal,
others radiate from a point, often an inclusion.  There is no well developed
dimensional orientation.

Sediment inclusions have an obvious control on texture.  Most parti-
cles are:  (a) on boundaries where they help to pin boundary migration;
(b) on sub-boundaries which result from dislocation production at the
inclusion; or (c) at the junction of sub-boundaries and boundaries where
embayment has been arrested.  Locally very complex boundaries are associated
with a group of inclusions.  The few bubbles are generally on grain boundar-
ies.

Figure 61 shows a thin section vertically below that previously discussed. This shows the local variability in crystal size. In some cases it is apparent that one crystal has been subdivided by straight sub-boundaries, by a polygonization mechanism. These sub-crystals have close extinction positions.

## (ii) Wide Vertical Veins

### Inclusion Characteristics

Generally the wider veins differ in inclusion characteristics from the narrow veins. Bubbles occur in the central zone, but not near the contact with the clay. Usually the bubbles are very fine, spherical, and occur in groups and networks. The absence of bubbles in the outer zone suggests slow freezing, and rejection of solute, as is also seen in the mineral films on the clay blocks.

Clay occurs as finely dispersed particles, and irregular blocks 10 mm across, all away from the contact.

### Crystal Characteristics

Crystal size and shape determine two zones; close to the vein edge crystals are elongate, $>10$ mm x 6 mm, and in the centre of the vein are large crystals $> 30$ mm x $>20$ mm (Fig. 62). The elongate crystals are anhedral with curved to serrated boundaries with serrations normal to the dimensional orientation which is orthogonal to the clay contact. The larger central crystals are anhedral, boundaries are curved or have small serrations. These crystals are more nearly equigranular and more interlocking

Figure 62. Vertical section
normal to vein plane. Note
horizontal columnar crystals
on left-hand side, adjacent
to clay.
Grid 10 mm. Crossed polarizers



10mm
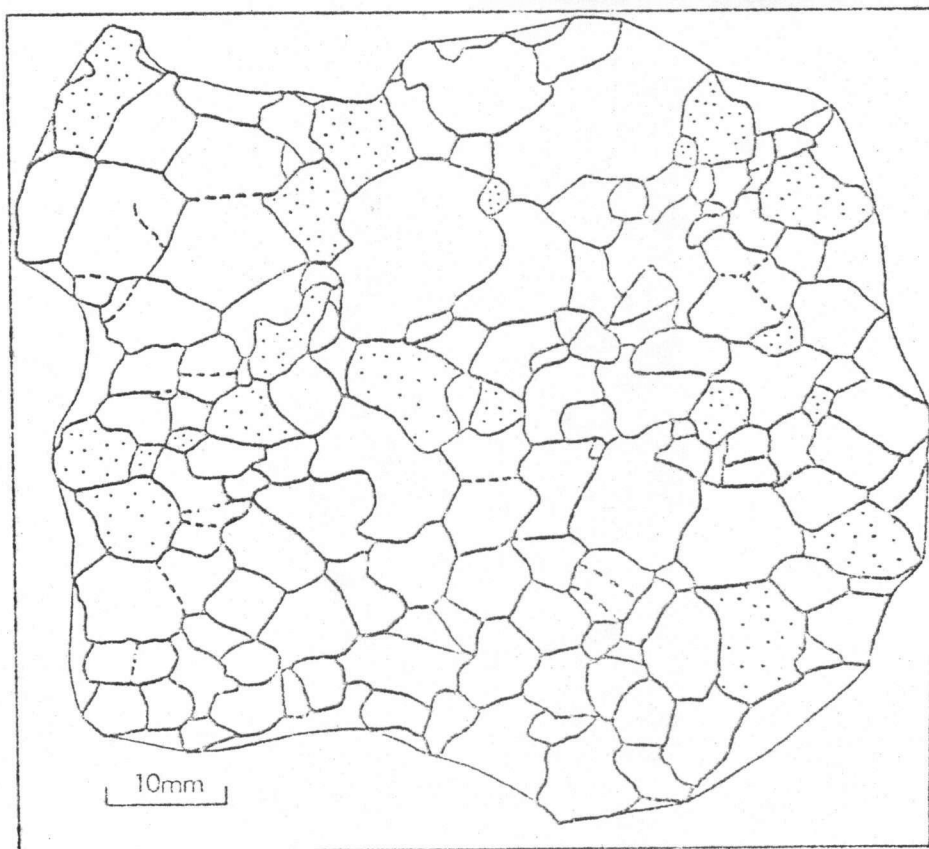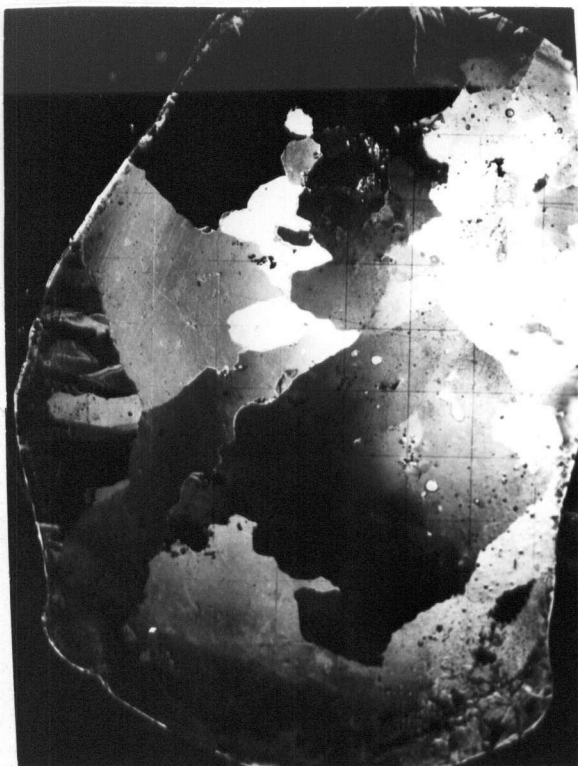
Figure 64. Sketch of grains for petrofabric analysis, Figure 63(b).
Shaded grains have c-axes outside the maximum. Vertical section,
parallel to vein plane.

in nature. Substructure occurs in the central crystals but is rare in the marginal, elongated crystals.

Also the relationship of crystals and inclusions differs in the two zones. Most of the sediment is intracrystalline in the centre of the vein, but intercrystalline in the zone of elongated crystals. The networks of bubbles are not everywhere related to present grain boundaries; the bubbles generally lie vertically below the boundaries, suggesting relative downward motion of bubbles.

Petrofabric diagrams are shown in Figure 63(a)-(f) for samples parallel and orthogonal to lens trends. Figure 63(a),(b) represent the c-axes of crystals in thin sections parallel to vertical veins (Fig. 60, 61, 64). Here the optic axis pattern tends toward a maximum orthogonal to the plane of the vein, as found by Mackay (1974b, p. 231). Crystals outside the maximum are shown by shading in Figure 64; they do not differ in textural characteristics, but often occur in groups.

Figures 63(c)-(f) are for crystals in sections orthogonal to the vein trend, (Fig. 65(a),(b)). From the previous diagrams, a horizontal point concentration orthogonal to the vein would be expected. This is not the case, and is partially explained by the fact that the previous sections were from the vein centre, whereas the later sections include crystals at the edge of the vein. Figure 63(d) shows the relative patterns for central and marginal crystals of Figure 63(c). The central crystals tend toward a horizontal girdle and the marginal crystals a vertical girdle. However, this is based on a small number of samples, and is not repeated in the other samples, especially the wide veins, in fact in Figure 63(e) the marginal crystals are on a horizontal girdle. Figure 63(f) comprises only
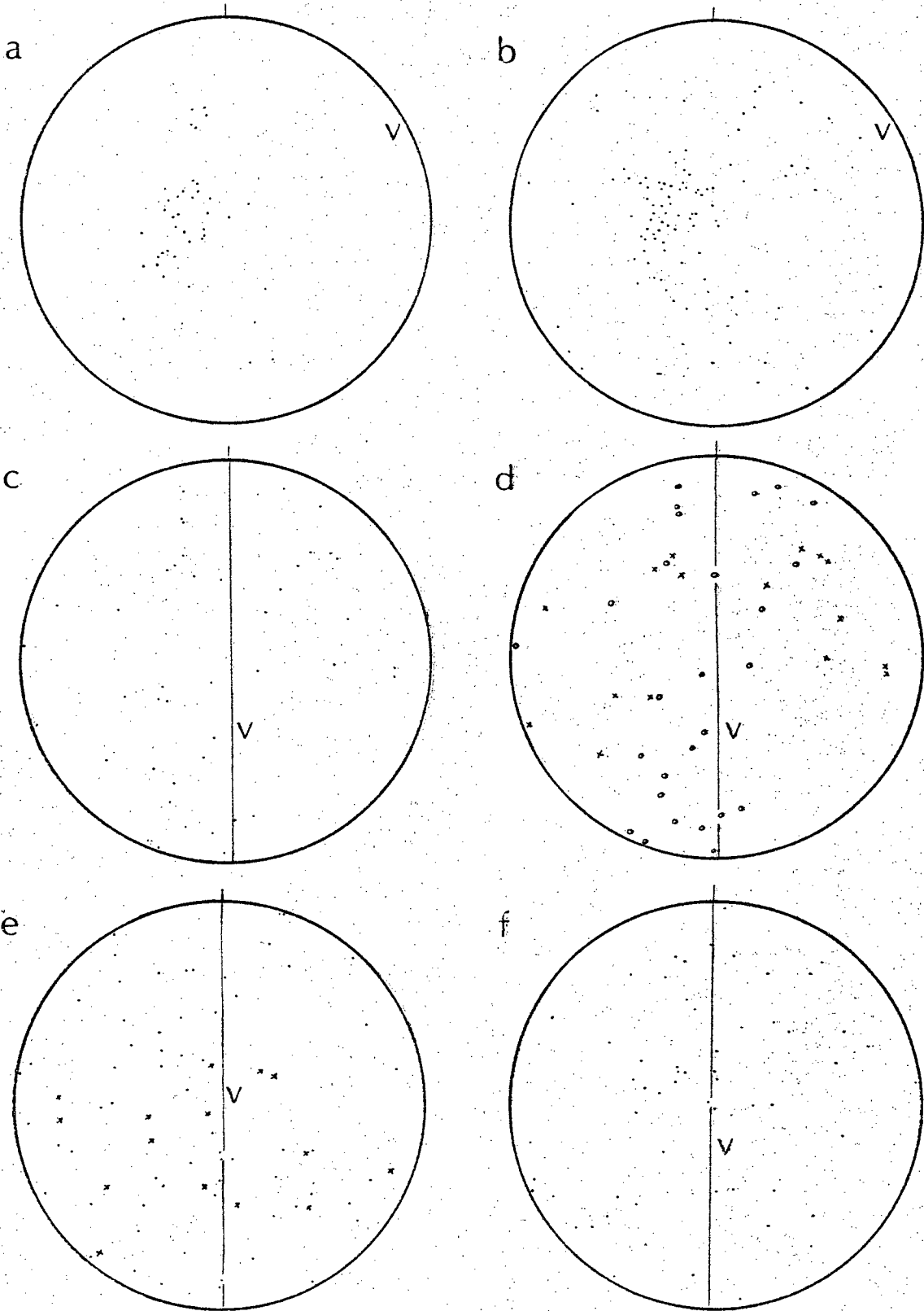
Figure 63. (a),(b) vertical sections, parallel plane of reticulate vein
(40, 100 crystals),
(c) vertical section, normal to vein plane (42 crystals),
(d) x 16 crystals in vein centre, o 26 crystals adjacent to clay,
(e),(f) vertical section normal to vein, x crystals on boundary.

v = vein plane

a

10mm

clay

b

clay

10mm
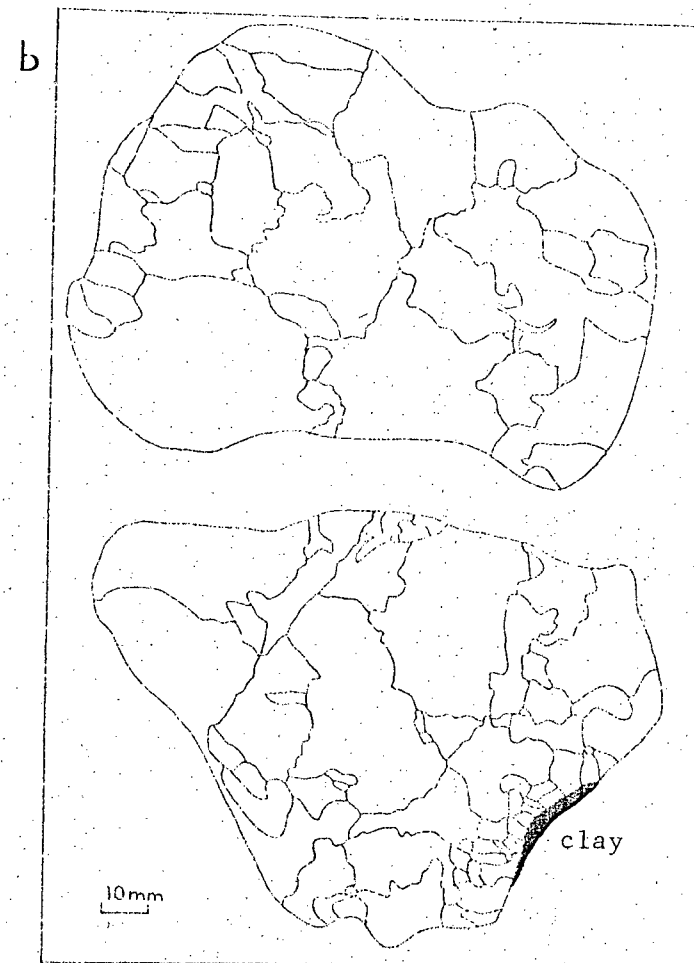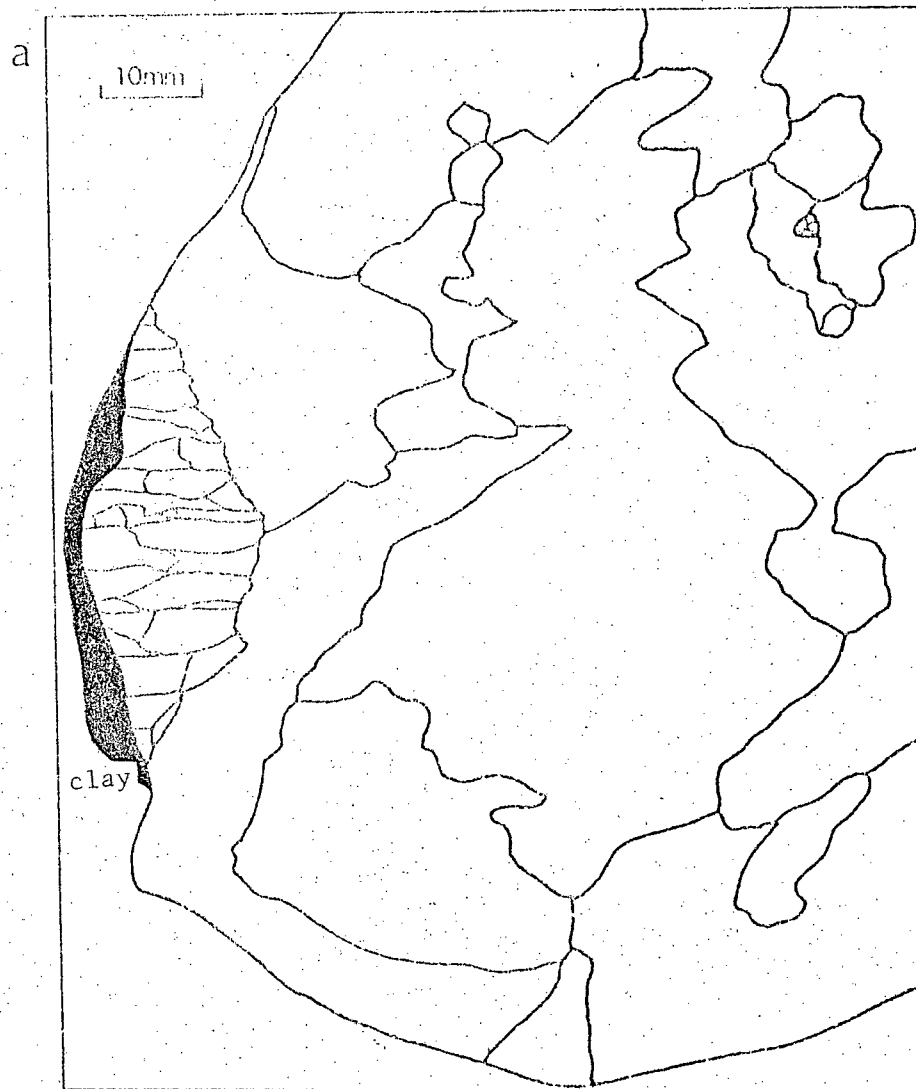
Figure 65(a),(b). Vertical sections normal
to plane of wide veins. Note textural
change on sides adjacent to clay

marginal crystals (those in Fig. 66) and tends to a vertical girdle pattern. This complexity of fabric diagrams is related to several factors; directions of heat flow and water supply in the initial and later growth periods, and adjustments during heave caused by the growth of the underlying massive segregated ice.

## Interpretation

Lens ice in clays has been discussed by Penner (1961); the crystals were large and extended across the lens. This has also been observed by the present author in small lenses in clay above Tuktoyaktuk pingo core. In these cases the ice bodies were perpendicular to the heat flow directions, i.e. normal lens growth, in contrast to reticulate vein growth where veins occur parallel and perpendicular to the "freezing front." Also in the reticulate pattern, lenses are more widely separated and the enclosed clay contains no smaller lenses and is over-consolidated. It is considered (Mackay 1974b, p. 235) that veins continue to grow on their outer surfaces by water migration from the adjacent clay blocks, well above the lower permafrost surface. Considering the narrow veins, central crystals have their c-axes orthogonal to the vein trend, and are similar to crystals in lenses, whereas marginal crystals have their basal planes orthogonal to the vein. Thus the central crystals are typical of lens growth; the marginal crystals differ in crystal size, shape, dimensional and lattice orientations, and relationship to inclusions and may represent distinct growth conditions. They may thus represent the later stage of growth from water migrating from the adjacent clay, as described by Mackay (1974b). However, in the case of the wider veins crystal characteristics differ again. The central crystals have the features of ice growth in bulk water while the marginal crystals are similar to those in the narrow veins.
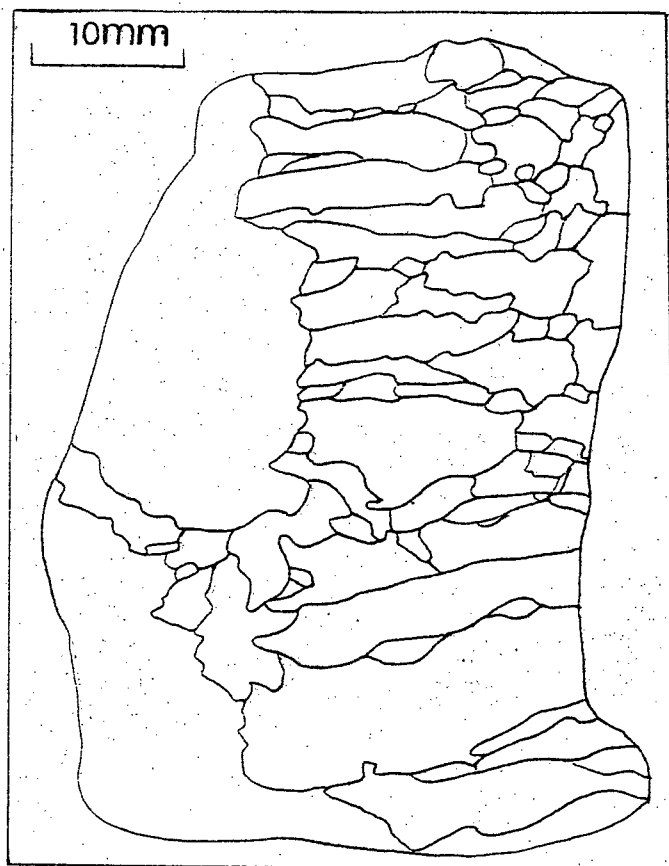
Figure 66.  Columnar marginal crystals in vertical
section normal to plane of wide vein.

Active Layer Ice

## Introduction

The active layer is the zone of material above permafrost which thaws and freezes annually. While the thawing occurs unidirectionally, downwards, there is evidence that freeze-back may occur both downwards from the surface, and upwards from the top of permafrost. Detailed temperature measurements by Lachenbruch et al. (1962) indicate the complexity of the thermal regime of the active layer and the multi-directional nature of freezeback. In any given area the active layer thickness may vary considerably with soil and vegetation type, as discussed by Mackay (1975d). Further, changes in active layer characteristics can occur due to change in climatic parameters, surface cover, or by sedimentation. Where sedimentation, say, takes place, the base of the active layer, and any included ice, becomes incorporated into permafrost as the permafrost table aggrades during re-establishment of thermal equilibrium.

It is the intention in this section to examine the characteristics of ice grown in the previous season's thawed layer as an aid to understanding the thermal regime of active layers, and to enumerate some features of ices so formed as a basis for discussion of aggradational ice.

Ice in the active layer is discussed from two sites, an area of tundra polygons subject to coastal retreat, and a second site in high centred polygons near Tuktoyaktuk.

(a)    Ice in the Active Layer Adjacent to Wedges

### Introduction

Extensive marine undercutting of the polygon area led to block collapse along ice wedge boundaries which exposed small ice bodies in the active layer of the adjacent organic-rich soil (Fig. 67). This ice had apparently grown since the previous summer.

### Field Characteristics

The ice bodies were 0.1 m thick on the exposures nearest to the wedge, and tapered away from the wedge, under an overburden of 0.25 m of organic soil; the bodies extended for up to several metres parallel to the trend of the wedge. Alternating 1-2 mm bubbly and non-bubbly layers were visible in the field, local irregularities occurred in the layers, but elongate bubbles were generally orthogonal to the layering.

### Section Parallel to Wedge Trend

Bubble Characteristics.- The contact of the ice with adjacent organic matter is abrupt and few vegetational inclusions occur; bubbles comprise the major inclusion type. In a vertical thin section parallel to the wedge the bubbles occur generally in sub-horizontal layers within which size and shape are consistent, but there also occur shorter (10-20 mm) narrow (3-4 mm) curved (convex upward) layers of peat particles and bubbles. Probably the local accumulations of fine peat fragments at the interface caused variations in rates of ice growth and bubble nucleation and growth. Elsewhere there occur elongate bubbles orthogonal to the layers, and also

Figure 67. Block slump on coast exposing ice in the active layer adjacent to wedges.
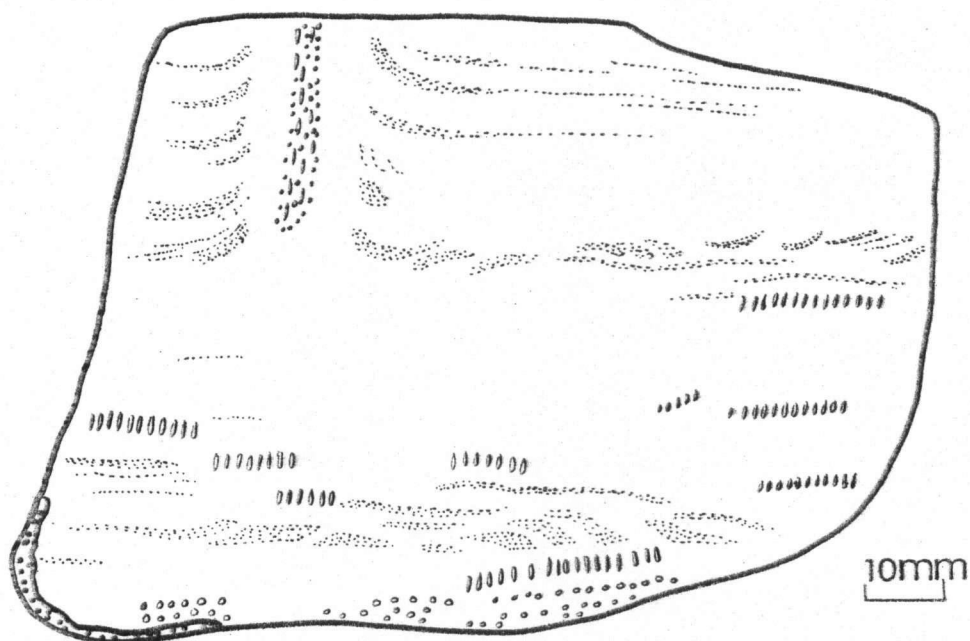


Figure 68. Peat and bubble pattern, vertical section parallel to wedge.



Figure 69. Petrofabrics of vertical section, parallel to ice wedge, active layer ice. 34 crystals.

c = compositional layering
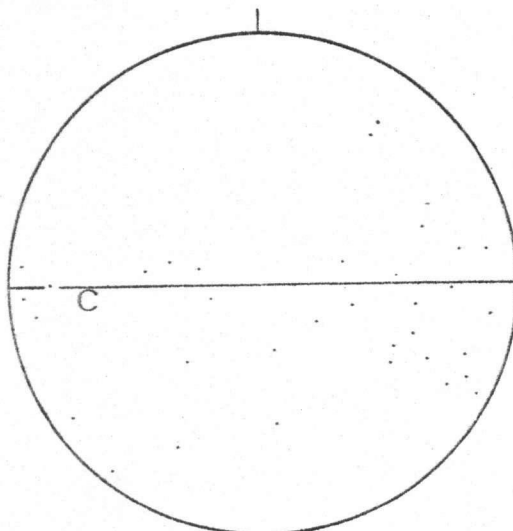
larger bubbles at the lower part of the body, adjacent to the organic matter. The above pattern is disrupted as shown in Fig. 68. A separation of 15 mm occurs in the upper layers which are upturned locally. The vertical 30 mm long disruption zone comprises clear ice surrounding a central core of elongate, and spherical bubbles, the zone does not penetrate to the base of the ice but terminates centrally. This pattern suggests fracture due to pressure associated with multi-directional freezing in the active layer.

Crystal Characteristics.- Crystal size and shape, and dimensional and lattice orientations vary throughout the body. At the upper and lower boundaries of the ice occur zones of small crystals, which widen away from those boundaries and give rise to vertically elongate, dendritic crystals >50 mm long x 5 mm wide. These crystals display horizontal offsets at bubble and peat layers, but no termination occurs. No pronounced substructure was observed. These crystal characteristics are disturbed at the disruption zone, crystals are shorter and wider, but maintain a dendritic shape.

Lattice orientations for 34 crystals are shown in Fig. 69 for crystals in the main mass, and disruption zone. C-axes tend to be contained in a broad horizontal girdle which suggests extension in the basal plane.

A second vertical section parallel to the wedge, but adjacent to the soil, was analysed.

Crystal Characteristics.- Crystals differ in size and shape from those in the previous section. Although most have vertical dimensional

orientations, horizontal boundaries are frequent (Fig. 70) and often coincide with bubble layers. Sub-boundaries are well developed, and exemplified in the large upper crystal. Here the sub-boundaries are associated with bubble bands. Above sub-boundaries, bubbles are elongate up to 6 mm, while in the sub-boundaries, bubbles are smaller and sub-spherical or slightly elongate in the sub-boundary. Many elongate bubbles have slightly bulbous and flat ends. The flat end is often oblique to the bubble axis, but parallel to the basal plane in a given crystal.

The presence of the crystals with horizontal dimensional orientations remains to be explained. The latter section was adjacent to the soil whereas the previous section was not; thus the influence of crystal growth at the soil ice interface was investigated in a section orthogonal to that interface.

### Sample Adjacent to Soil, Orthogonal to Soil-Ice Interface

Bubble Characteristics: In this sample the outer contact of ice with organic matter is included, and the associated bubble pattern (Fig. 71a) differs from that in the previous samples. Bubble trains orthogonal to the soil curve upwards into horizontality. Most bubbles are elongate parallel to the trains, and range downwards in size from 4 mm x 0.5 mm adjacent to the soil.

Crystal Characteristics: Crystal shape is related to bubble trends in that dimensional orientation is parallel to the trains (Fig. 71b). Crystal size is variable - small crystals occur adjacent to the soil and size increases away from the soil. There is no tendency for bubbles to

Figure 70. Vertical section, normal and adjacent to soil, active layer ice. Note horizontally elongated crystals, compare Fig. 71b for influence of growth normal to soil.

subgrain boundaries
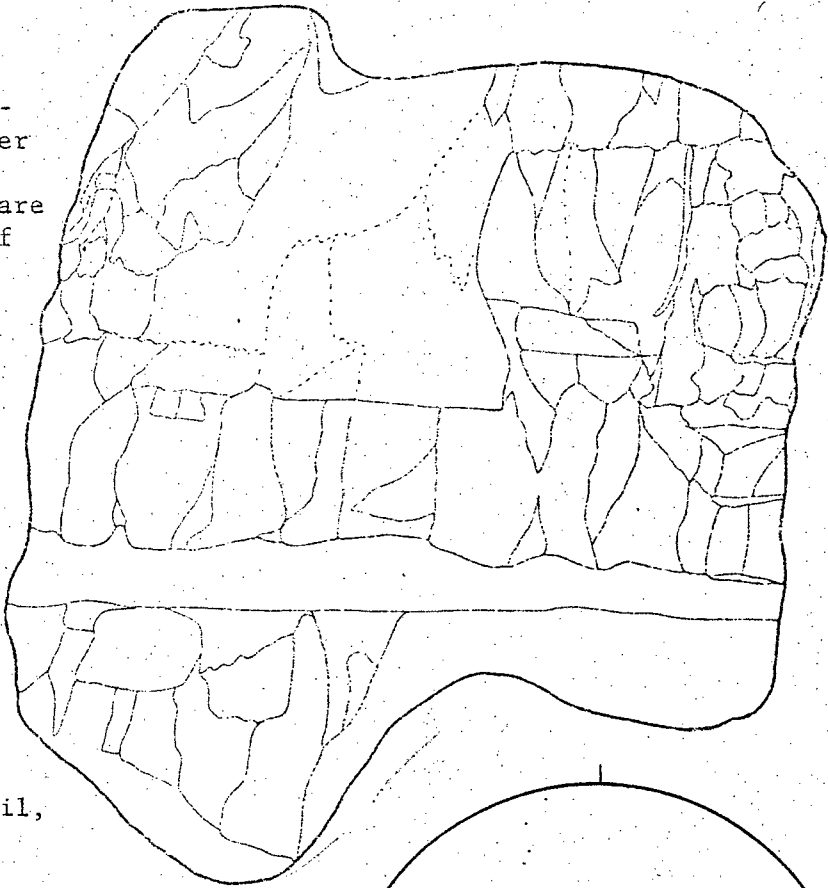
Figure 71. Vertical section orthogonal to soil, active layer ice.
  (a) Bubble pattern,
  (b) Crystal pattern.

a

b
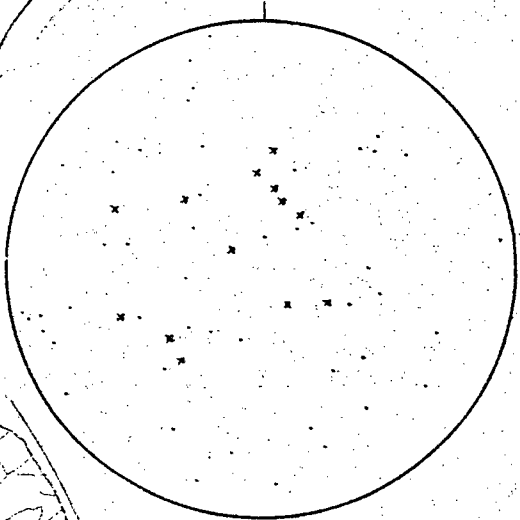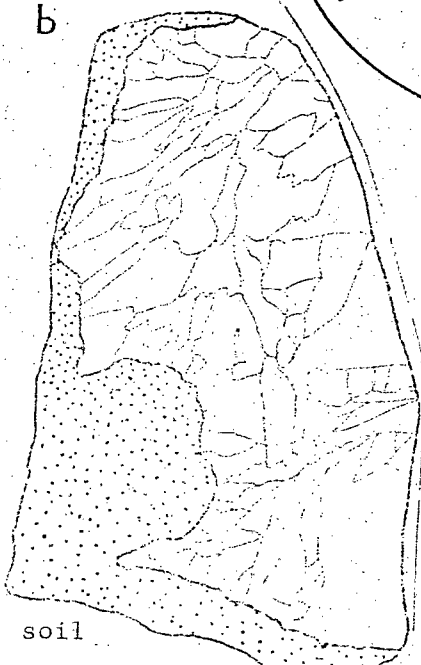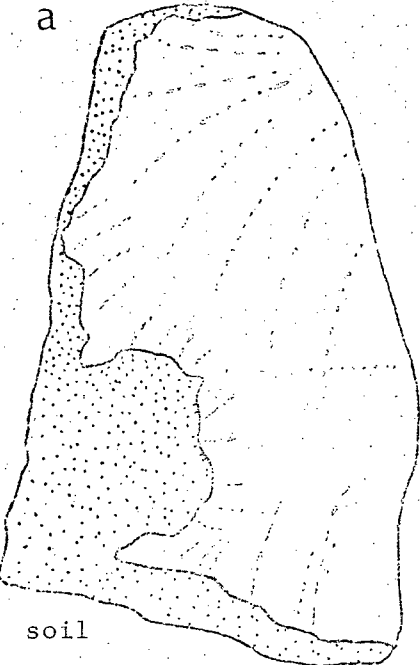
Figure 72. Petrofabrics, crystals in Fig. 71b. x crystals adjacent to soil.

soil

soil

occur preferentially on crystal boundaries; some horizontal offsets of upward growing crystals occur at bubble layers in the lower ice. C-axis orientations for 63 crystals are shown in Figure 72. The sample was limited by the small size of the specimen; the pattern is a broad concentration, with crystals adjacent to peat being centrally situated. Thus the crystals with horizontal dimensional orientation in Figure 70 are extensions of crystals which grew orthogonal to the soil.

### Samples with Fractures

Introduction: In addition to the previous samples there are some which contain fractures. Here we investigate the influence of bubble and crystal characteristics on fracturing.

The fractures were observed in the field, prior to sampling, and thus are not due to sampling, or thermal shock during handling. The fractures were open, and thus occurred under "dry" conditions.

Bubble Characteristics: In common with other active layer bodies, there are alternating layers of high and low bubble contents, which are horizontal and parallel away from the influence of the soil. The contained bubbles are spherical, or elongated normal to the layers.

Crystal Characteristics: A range of crystal shapes occurs, and the influence of bubble bands on shape is found as before; many crystals terminate abruptly at horizontal bubble bands. Figure 73 demonstrates the influence of several bands. C-axis orientations are given in Figure 74(a), (b); the overall pattern is an incomplete horizontal girdle and a minor vertical point concentration. A further section (Fig. 74(c)) shows a broad

Figure 73. Active layer ice, vertical section, showing the influence of bubbles on crystal growth. Growth direction is down from the top.

a



b



c
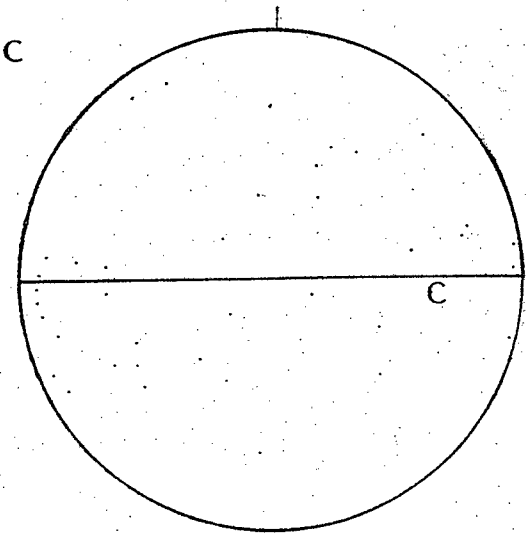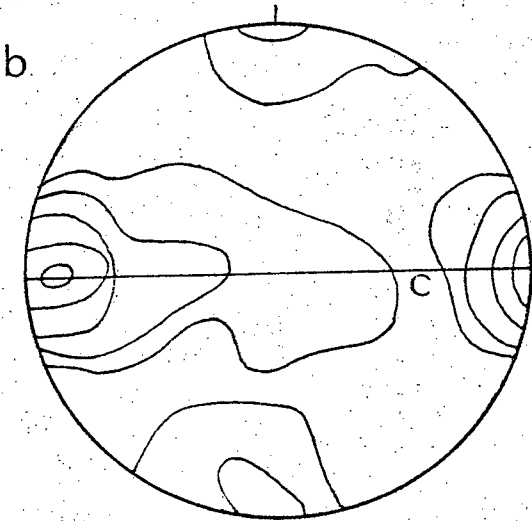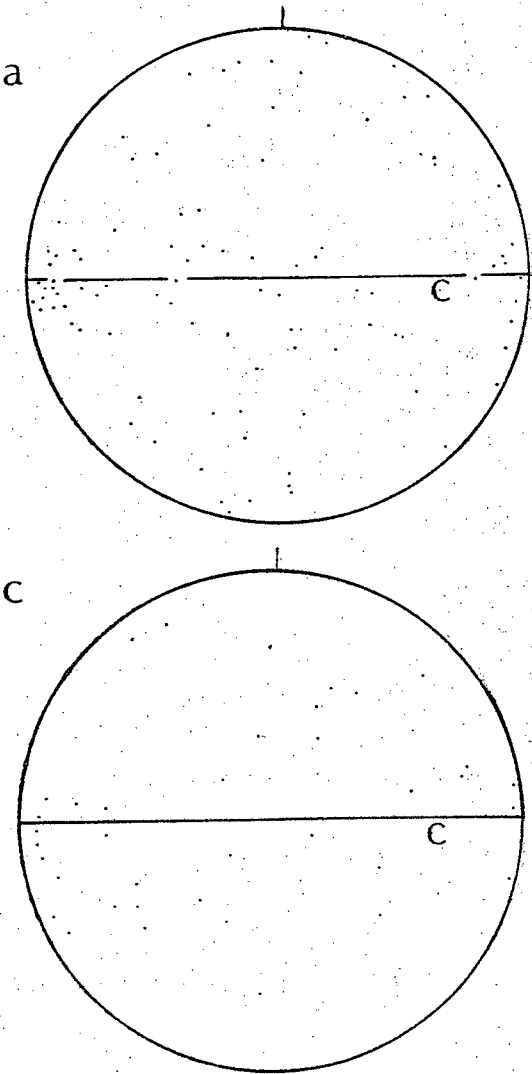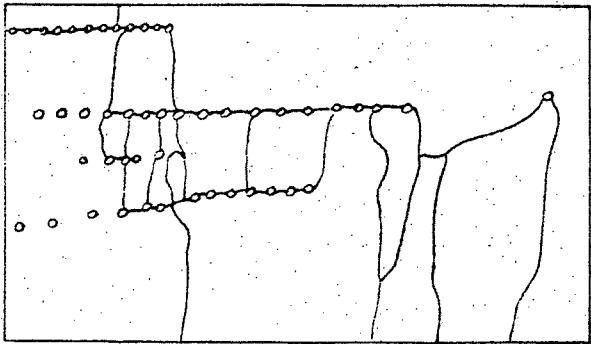


Figure 74. Petrofabrics of active layer ice.
(a),(b) vertical section, 95 crystals;
(c) vertical section, 40 crystals.

contour interval 2, 4, 6, 8, 10$\sigma$

Figure 75. Vertical section showing influence of bubble layers on fracture propagation.
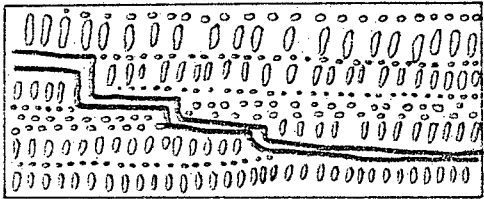
horizontal girdle also, this suggests basal plane growth in a plentiful water supply.

Fractures: The above pattern of crystal growth is disturbed by fractures, of which the surfaces of separation are parallel to bubble layers, but stepped locally (Fig. 75). Due to the close association of bubble bands and crystal boundaries it is likely that the fractures have propagated along the weak zones.

### Interpretation

The ice bodies grew in the previous season's active layer, and therefore represent one winter's growth; any post-solidification modification has had limited time for development. The overall inclusion pattern is horizontal bubble bands and vertically elongate bubbles, respectively parallel and orthogonal to the freezing front, but also locally curved trains orthogonal to soil. Crystal dimensional orientation is essentially vertical, although controlled locally by horizontal bubble bands. Lattice orientations are such that basal planes are vertical, parallel to the growth direction, although some are horizontal, in crystals which have horizontal dimensional orientations and occur at bubble bands, indicating lateral growth from the soil. Post-solidification features are the fractures which are concentrated on bubble bands. The stress system responsible for the fractures is not clear, the fractures are horizontal, in contrast to vertical thermal contraction cracks. The coastal block slumping occurred in early June 1973, thus fracture may have been due to sudden exposure to warm air temperatures, but this is speculative. There may also have been an influence of the collapsing blocks.

(b)    Tuktoyaktuk Site

### Field Characteristics

An area of high centred polygons lies above flats surrounding a creek south of Tuktoyaktuk. During early June 1974 small excavations were made in the polygon area during a study of wedges and polygons. Small ice bodies were found at a depth of 0.3 m, and reported to the author. There was an abrupt contact between the ice and the organic soil above and below, which was virtually ice-free.

### Ice Characteristics

The ice bodies generally extended laterally up to 120 mm and vertically for 80 mm. No structures, e.g. fractures, were apparent; few organic material inclusions occurred, but bubbles were abundant. The included soil was largely close to the ice-soil contact, while bubbles formed curved, converging trains.

### Bubble Characteristics

The curved bubble trains begin adjacent and orthogonal to the ice-soil contacts, which indicates multiple freezing directions. In addition, in some cases a zone of small spherical bubbles lies parallel to the soil, from which the trains originate (Fig. 76(a)). Also a few spherical bubbles are incorporated into the zone of bubble trains. The spherical bubbles are $\leqslant 2$ mm in diameter, and elongate bubbles are $\leqslant 3$ mm long and $\leqslant 1$ mm in diameter.

a
b

soil

soil
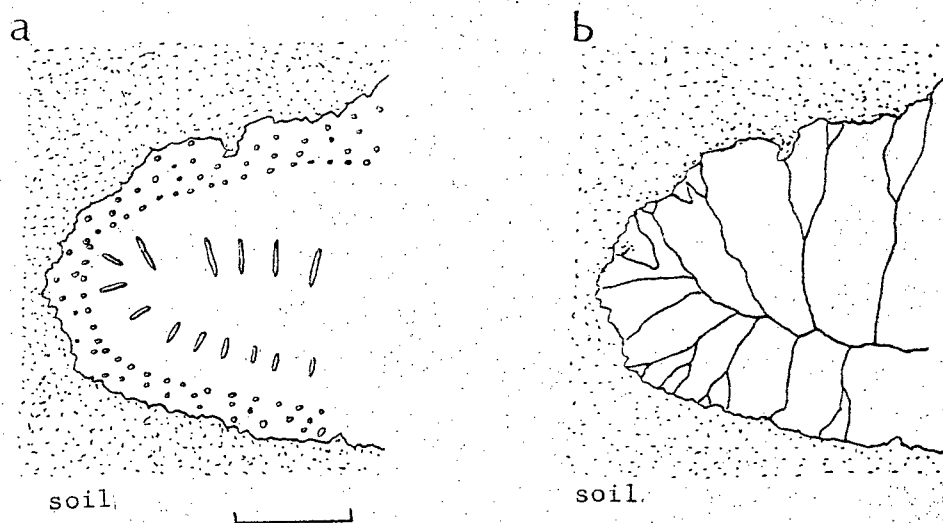
Figure 76.   Active layer ice, Tuktoyaktuk, (a) bubble pattern,
             (b) crystal pattern.

             vertical section
             scale   10 mm

## Crystal Characteristics

Crystal size varies, ranging from 2 mm x 3 mm in irregular crystals adjacent to the peat, to 10 mm x 6 mm in elongate crystals. The latter crystals have simply shaped compromise boundaries, with occasional serrations. The preferred dimensional orientation of the elongated crystals is orthogonal to the soil. The relationship of bubbles to texture is such that bubble trains and crystal dimensional orientations are parallel and layers of spherical bubbles are confined to grain boundaries.

## Interpretation

The active layer position and lack of ice in the surrounding soil suggest that water was confined during downward freezing from the ground surface and upward freezing from the top of permafrost. The two freezing fronts met and confined the water body which froze omnidirectionally. The bubble trains and dimensional orientation of elongate crystals indicate the change in freezing direction during progressive solidification into enclosed water. It is likely that at the time of solidification a steeper temperature gradient existed in the upper part of the active layer than below, as air temperatures were lower than those in the soil below. Evidence for this is that downward growing crystals have cut off the growth of other crystals, as has been found in metal castings where different temperature gradients have been maintained on different faces of a solidifying body. Additionally bubble patterns differ slightly in the two zones.

## Ice Bodies with Multiple Freezing Histories

### Introduction

In the ice bodies discussed so far it is evident that one major growth period has been responsible for the features observed (except in wedge and tension crack ice). However, it is known that the crests of pingos may rupture and expose the ice core to meltdown. Ice wedge ice in troughs may be subject to melting and thermokarst development; also a thickening of the active layer, by natural or artificial means, may lead to thaw of ice bodies. If, at a later date, lower mean annual temperatures prevail it is to be expected that refreezing may occur, with associated growth of ice bodies with different features from the previous. Sedimentation, soil creep or peat growth may produce similar results. Thaw unconformities and subsequent refreezing have been recognized at several sites in the field area. Such conditions are discussed for two sites: (a) Tuktoyaktuk Coast, (b) Pelly Island.

### (a) Tuktoyaktuk Coast

#### Introduction

This is a generally flat-lying area about 2 m above present sea level with a complex pattern of high-centred ice-wedge polygons. It is not known whether the wedges are presently active. In addition to wedges there is abundant ice in the form of horizontal and dipping layers outcropping in coastal exposures, causing rapid coastal retreat. It is this retreat which led to lake drainage and the growth of pingos shown in Mackay (1973a, Fig.15).

The polygon patterns but not the layers of ice are apparent from such aerial photographs.

These layers are of varying size, shape and orientation, ranging from thin seams to 1 m thick tabular blocks 3 m in extent. The origin of these bodies is not immediately discernible on the basis of previous discussions.

## Field Characteristics

In June 1973 a storm caused rapid coastal retreat and exposure of many ice bodies by collapse of large blocks of organic soil and ice wedges (Fig. 67).

Most ice bodies were at least 0.3 m below the present active layer, the local soil having high organic and ice contents including aggradational ice. Ice body size and shape varied from small lenses through bodies 0.5 m by 0.2 m, to laterally extensive sheets over 3 m long. Inclusions were mainly bubbles and soil fragments, both in horizontal layers and vertical to curving trains. Some bodies appeared to have frozen omnidirectionally, some had truncated bubble bands which suggested later melting and subsequent refreezing. In addition some near surface bodies occurred at the base of the previous season's active layer. These three major types of body were sampled for thin section analysis.

### (i)   Ice Bodies with Omnidirectional Bubble Trains

#### Introduction

Such features suggest that a pool of water froze inwardly from all directions. Thus a series of samples was taken to include ice-soil contacts and bubble trains from all parts of the body.

Body No. 1

Bubble Characteristics. This ice typically has a high content of bubbles in layers and groups, 1 mm diameter bubbles occupying up to 40% by volume. Fractures disturb this general pattern. For example a sample containing alternating clear and bubbly layers of spherical 1 mm and elongate 2.5 mm bubbles contained a fracture surface with voids or gas inclusions. Although the bubble layers may dip at up to 40°, bubbles are elongate, vertically, suggesting modification of bubble orientation by thermomigration in a vertical temperature gradient. In comparison, bubbles in trains in active layer ice are parallel to the trains (Fig. 71(a)).

Crystal Characteristics. In a horizontal section (Fig. 77) at the top of the body, large crystals (long axes $\leqslant 50$ mm) occur throughout the section, but in the fracture zone, crystals are smaller ($< 2$ mm). The large crystals are anhedral and strongly serrated (3-4 mm amplitude) but not deeply intergrown, whereas crystals in the fracture are anhedral, approximately equigranular, with singly curved or straight boundaries and no serrations. Lineage substructure occurs in the larger grains, but not within fracture crystals. No pronounced dimensional orientation occurs in this plane. Lattice orientations are shown in Fig. 78 for crystals in the layered ice and fracture. C-axes in the layered ice are near the plane of the bubble layers, and in a point concentration. Crystals in the fracture have grown with a less preferred orientation, at 20 to 65° to the fracture plane.

A series of sections was prepared from a vertical face displaying bubble trains converging toward the centre of the body, indicating freezing from the peat on all sides. Again bubbles are vertical in trains of all

207
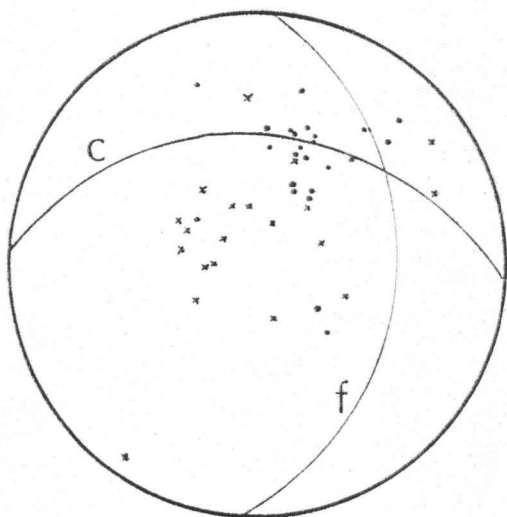


Figure 78. Petrofabrics of ice in Fig. 77. x = fracture crystal.
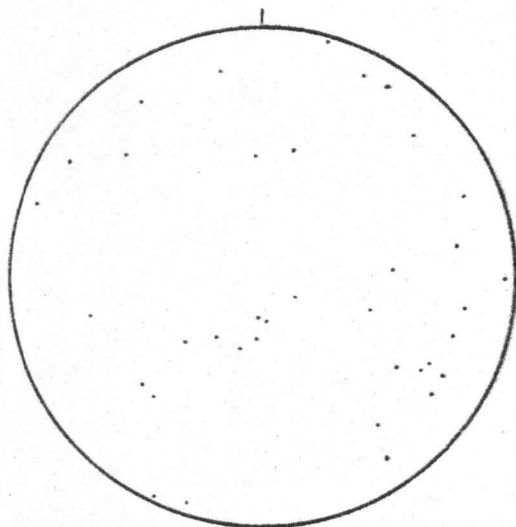


Figure 80. Petrofabrics of ice in Fig. 79.
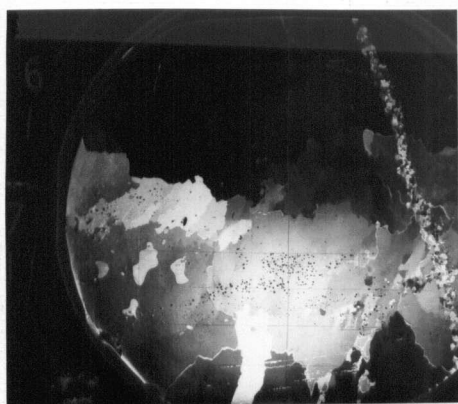


Figure 77. Horizontal section, containing vertical fracture, right hand side. 10 mm grid. Crossed polarizers
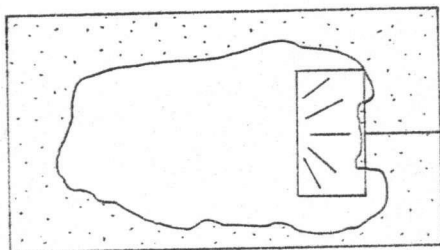


Figure 79. Vertical section adjacent to soil. Multi-directional crystal orientations. Scale 10 mm.
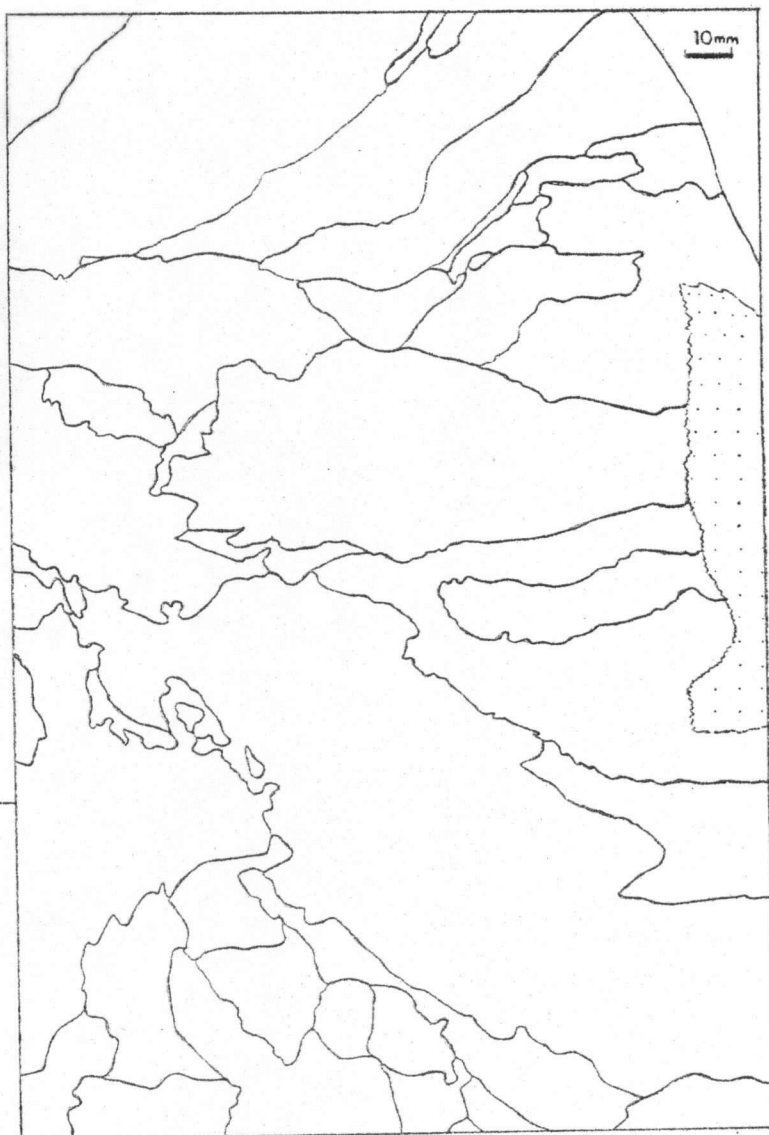
orientations, due to later temperature gradient effects. Peat forms another inclusion type, trending inwards from the surrounding peat mass, and in separate inclusions.

Crystal Characteristics. Crystals are large and elongate, parallel to the bubble trains, thus dimensional orientation varies systematically around the ice body, being everywhere orthogonal to the ice-peat contact and curving to the centre of the body (Fig. 79). Grain boundary serrations are orthogonal to long axes, indicating dendritic growth, and crystals became narrower as they converged in the growth direction. Substructure occurs in bands parallel to the elongation; these often trend from peat inclusions, in the growth direction, suggesting a slight lattice offset where the crystal has grown round the peat. Where multiple bands occur radially from inclusions, a form of polygonization (Knight 1962b) has occurred due to growth stresses. Bubbles occur in groups near crystal boundaries, and as single bubbles on boundaries. No major changes occur in boundaries at the bubbles, despite other evidence of thermomigration. In the central zone, crystals become more equiaxed, and smaller. Fewer peat inclusions occur and bubbles are close to grain boundary irregularities. Lattice orientations for 37 crystals are shown in Fig. 80. In the outer zone, c-axes are parallel to the elongation direction.

### Interpretation

These ice bodies occur in a low-lying area of large tundra polygons and abundant organic matter. Presently some thermokarst activity is occurring adjacent to the larger wedges.

From the orientation of bubble trains and the dimensional orientation of elongate crystals it is evident that the ice body grew omnidirectionally. Thus the surrounding material was in a frozen state; it is thus argued that the body is a frozen melt pond. The crystals in the horizontal section from the top of the body have horizontal c-axes which frequently occurs in the freezing of bulk water whereas at the curved margin of the body crystals have c-axes orthogonal to the boundary which indicates growth normal to the basal plane, which is less frequently observed, although reported by Michel and Ramseier (1971) in lake ice. There is no chill zone of competitive growth evident in the vertical sections, so the crystals grew in lattice continuity with crystals in the peat. Toward the centre of the body lattice orientation tends toward that characteristic of basal plane growth. Some post-solidification modification has occurred in that bubbles are not elongate, parallel to bubble trains, but in a vertical direction, indicating thermomigration in a vertical temperature gradient. The lineage substructure is present only in pre-fracture grains and is thus due to freezing conditions, probably the incorporation of inclusions, but it may have been exaggerated by stresses produced by freezing of confined water.

The crystal characteristics of this ice body are quite distinct from those of lens ice where growth is unidirectional. In lenses bubble and crystal dimensional orientation are not multi-directional.

From the air or ground surface the area appears typical of ice-wedge polygon flats. There is no surface expression of the thermokarst-type ice.

Body No. 2

A second ice body has similar gross characteristics, indicative of freezing in a cavity within frozen peaty material. However, the inclusion content differs from the previous case and influences crystal characteristics.

Inclusion Characteristics.  There occurs a reduction in peat concentration from dense in the top left hand corner through a zone of dispersed particles and occasional streaks, to clear at the base; this corresponds to the sequence: - elongated and spherical bubbles, spherical bubbles, bubble-free.

Crystal Characteristics.  Texture is again related to inclusion content. Grain size in the peaty zone averages 12 $mm^2$, compared with 544 $mm^2$ in the peat-free zone (Fig. 81). The former grains are anhedral, approximately equigranular and lack serrations and substructure; the latter grains are anhedral with multiple curved or serrated boundaries, and are elongate with well developed substructure. Variation of dimensional orientation indicates progression of the freezing interface. In the upper inclusion zone, peat is generally confined to grain boundaries or dispersed pockets in crystals, whereas in the lower peaty zone the peat inclusions are concentrated on parallel lines in individual crystals, apparently the basal planes. The freezing interface advanced downwards from the top and impurities were rejected except at grain boundaries, whereas in growth from the base, crystals extended in the basal plane, and inclusions were trapped.

In the absence of detailed thermal data it is difficult to compare downward and upward freezing. However, it is to be expected that a steeper

Figure 81. Vertical section normal to soil contact. Converging crystal pattern. Small crystals in upper left are within peat. Scale 10 mm.
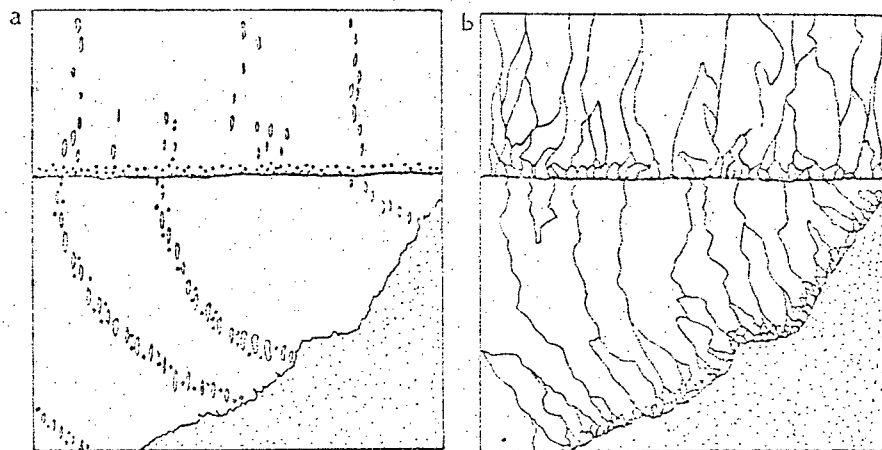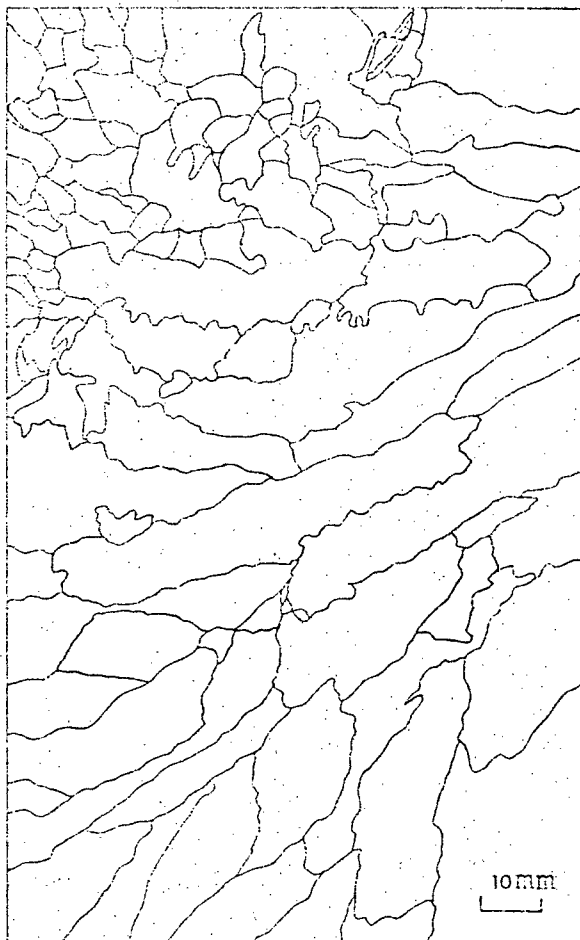


Figure 83. Schematic diagram of multiple growth periods.
  (a) Bubble pattern. Note vertical bubbles in lower, curving trains, and horizontal truncation.

  (b) Crystal pattern. Note competitive growth zone at ice-soil contact and above truncation zone. Note also curved, elongate crystals, parallel to lower bubble trains.

thermal gradient would exist in the overlying material, and thus influence freezing rate and the incorporation of inclusions. This is true especially in the case of buoyant inclusions which would be trapped at the top of the cavity.

Lattice orientations for the crystals in Figure 81 are shown in Figure 82. A change in lattice orientation with depth is recognized. A broad horizontal maximum (a) becomes more dispersed with depth (b),(c). A second sample shows a change in lattice orientation from a broad horizontal girdle (d) to a 45° girdle (e) to a partial vertical girdle (f).

### (ii)   Truncated Bubble Patterns

#### Introduction

The above discussion described bodies which had not been subject to great post-solidification changes. Nearby occurs an ice body with different mesoscopic features. The curved, radiating bubble trains occur at the lower edges of the body, but in the top centre the pattern is disturbed.

#### Inclusion Characteristics

At the base of the ice, bubble trains are normal to the contact with the peat and include some peat fragments, then curve upwards at 45° to the horizontal (Fig. 83(a)). Bubbles are approximately spherical or ellipsoidal, elongate vertically within the trains which cross individual crystals, while dispersed bubbles are contained mainly within crystals. Above, this pattern includes groups $10/100 \ mm^2$ of bubbles 1-2 mm in diameter. A surface of truncation can be traced laterally and is seen to cut across original bubble trains of several orientations. The surface contains peat
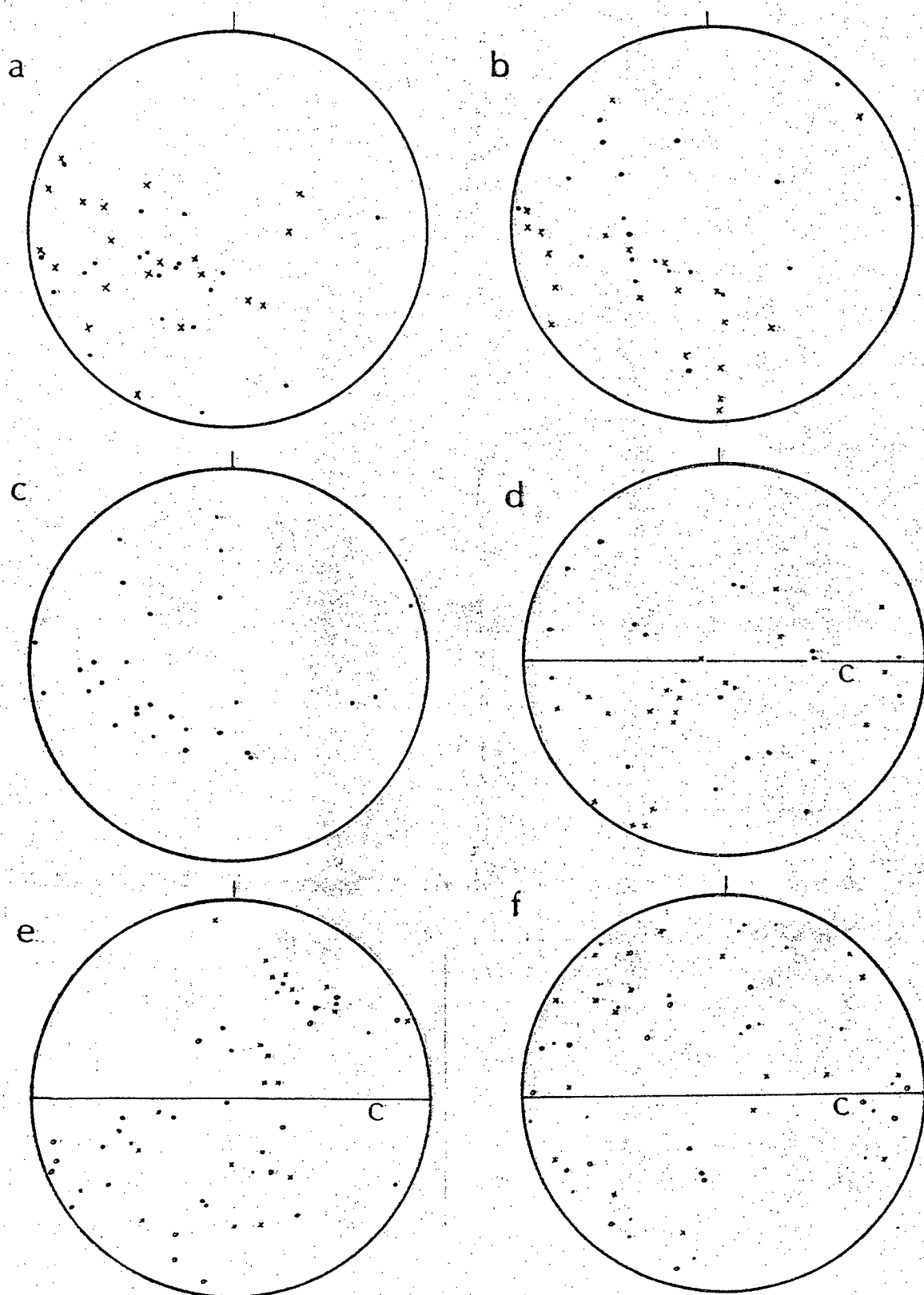
Figure 82. Petrofabrics for crystals in vertical sections.
(a),(b),(c) represent Fig. 81, succeedingly deep zones;
(d),(e),(f) second sample, similar to Fig. 81.

fragments, above which is a laterally extensive layer of small spherical bubbles, in marked contrast to the underlying ice. Above, groups and contained elongated bubbles are oriented differently from those in the ice beneath the truncation zone, but orthogonal to that zone, indicating upward ice growth.

### Crystal Characteristics

We consider firstly crystals below the apparent "truncation zone", then the effect of that zone, followed by crystals above that zone. In the lower ice, crystals increase in size upwards, reaching > 600 $mm^2$ at the cut-off. Crystal shape is anhedral with strongly serrated boundaries. Dimensional orientation is parallel to the bubble trains, and serrations are orthogonal to crystal long axes, as in the previously discussed ice bodies (a).

Crystal characteristics change at the truncation zone (Fig. 83(b)). Crystal size is 6 $mm^2$, increasing upwards to 45 $mm^2$. Crystal shape in this competitive growth zone is less complex than in the underlying ice, many straight compromise boundaries occur, and curved boundaries have single curvature, which is typical of competitive crystal growth. Upwards a dimensional orientation develops parallel to bubble elongation.

The relationship of bubbles to crystal characteristics varies with position. In the lower ice, bubbles occur in groups within crystals rather than on boundaries, as was found in lake ice by Swinzow (1966). A small amount of ice growth occurred above the truncation zone before bubble nucleation; bubbles were at first essentially randomly distributed, as found in competitive growth zones elsewhere (icing mound ice, tension crack ice) then became preferredly sited in layers.

Lattice orientations are shown for the lower ice and upper ice in Figure 84(a)-(d). Figure 84(a) includes crystals from the base of the lower ice up to the truncation zone; an upward increase in c-axis preferred orientation occurs in association with an increase in crystal size. Figure 84(b)-(d) similarly shows the change in c-axis distribution upwards from the truncation zone.

## Interpretation

From the bubble patterns, crystal size, shape, dimensional and lattice orientations, it is evident that initially growth of ice occurred in a hollow within frozen peat, as in the previously discussed bodies. Later some melt-down occurred, as is seen from the truncation of bubble trains and the horizontal layer of organic matter and gas inclusions. Also a major change in crystal characteristics occurs where new upward crystal growth took place. The truncation zone is not a temporary standstill in growth of the body, as it truncates bubble trains of several orientations and may be traced laterally into the adjacent organic matter. From field relationships it appears that several melt-down and regrowth events occurred in the area.

A second such body occurs nearby, displaying similar features. The early growth has been subject to melt-down; large crystals terminate abruptly upwards at a laterally extensive bubble layer containing vegetational debris. Copious crystal nucleation occurred at this layer, followed by upward growth. Thus the previous more detailed description is not of a rare occurrence, field characteristics suggest the growth history applies to many bodies along the coast. However the presence of such ice can not be readily inferred from surface expression.
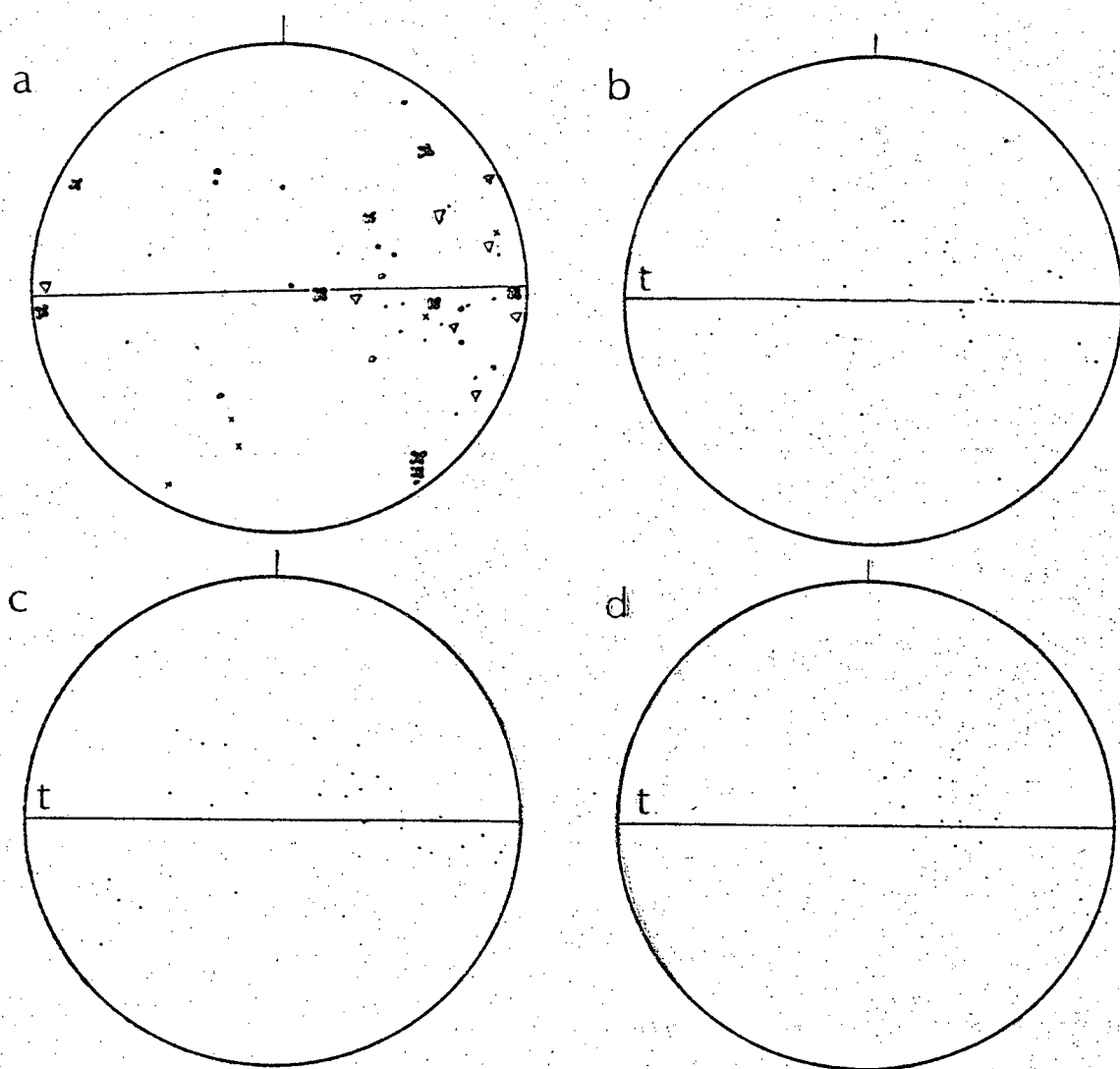
Figure 84.   Petrofabrics; crystals below and above truncation zone.

   (a) crystals below truncation zone; symbols in sequence indicate
       distance from soil-ice contact;

   (b),(c),(d) crystal zones progressively upward from truncation zone.

   Diagrams parallel to sections.
   t = truncation zone

(iii) <u>Ice at the Base of the Active Layer</u>

## Introduction

The ice bodies discussed in sections (a) and (b) were overlain by several metres of organic soil, but there also occur ice layers immediately at the base of the active layer. These are of particular interest as slight variations in active layer thickness occur from year to year and thus the upper part of such ice would be expected to reflect these variations.

## Field Characteristics

The ice body to be discussed lies near those in (a) and (b), above. It was exposed in June 1973 and sampled before active layer thaw reached the top of the ice. Measurements in August 1973 showed that local active layer depth was greater than overburden thickness.

The ice was lensoid in shape, 0 to 0.5 m in thickness, with a flat lower surface and convex upper surface, overlain by 0.3 m of organic soil (Fig. 85). Similar material underlay the ice, but with a higher ice content than the overlying soil.

## Ice Characteristics

The upper contact was less abrupt than the lower, and vegetational fragments, including roots, were observed near the top, as well as cylindrical bubbles (Fig. 86). Bubbles at the top of the body are cylindrical and trend normal to the upper surface. These extend 8 mm into the sample, below which is a 5 mm thick bubble-free band, above a surface containing peat and roots. These roots lie on the surface, but below are orthogonal

Figure 85. Lensoid ice body
exposed by block collapse.
Overburden thickness 0.3 m.
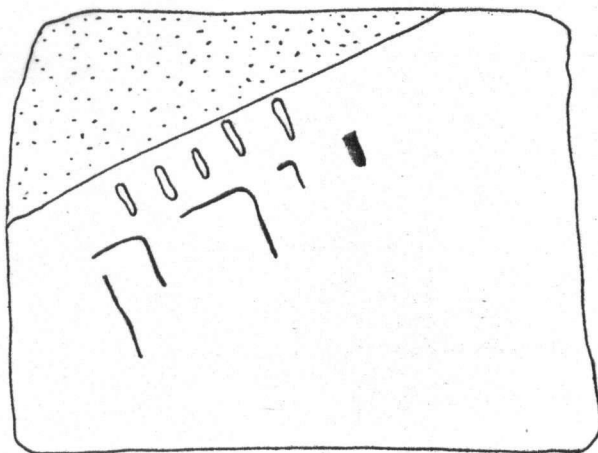


Figure 86. Schematic diagram of
top of Fig. 85. Root shapes,
infilled bubbles and bubbles.
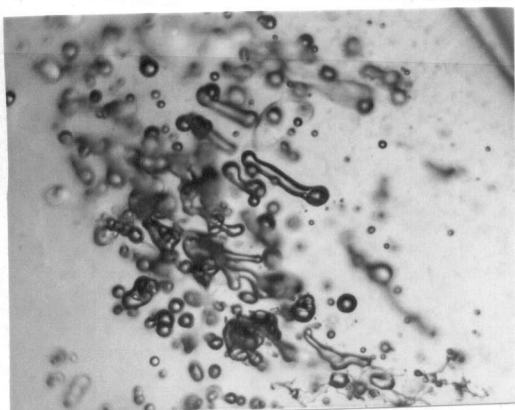


Figure 87. Detail of
bubble shapes in ice of
Fig. 85. Long side is
8 mm.
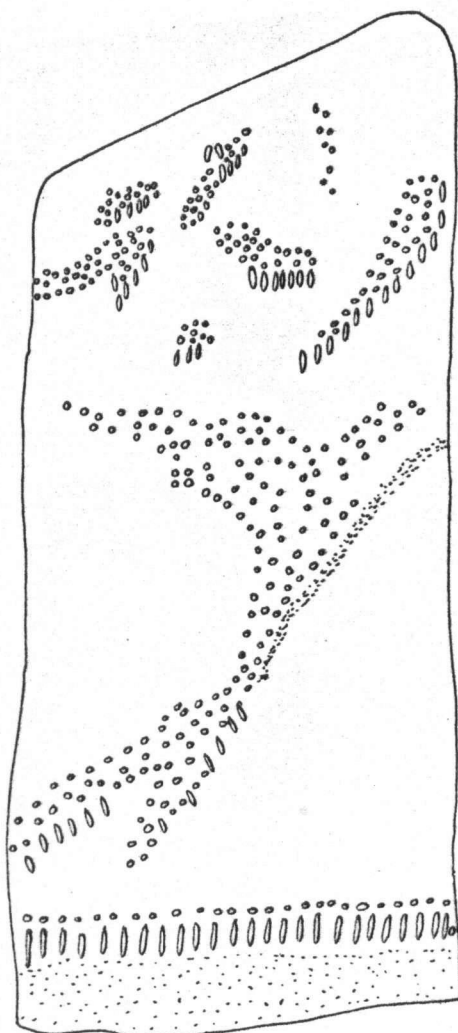


Figure 88. Bubble pattern
throughout lensoid body (Fig.
85). Note zones of elongate
and spherical bubbles at
base, above peat.

to the surface. These features are interpreted as indicating melt-down of the ice body to the peaty surface, followed by upward refreezing. The roots were originally orthogonal to the ground surface, and parallel to the freezing direction; thus orientation is maintained below the melt-down surface.

## Bubble Characteristics

Below the melt surface the only inclusions are bubbles, in groups containing 2-3 mm long individuals, 1 mm in diameter, and some dispersed spherical bubbles, $\leq 1$ mm diameter. Elongate bubble orientation varies from orthogonal to the ground surface at the top, towards vertical at 100 mm depth. The detailed shapes of bubbles are complex, elongate bubbles have bulbous ends and local promontories (Fig. 87). Narrow or wide points on individual bubbles do not correlate with one another indicating varying freezing conditions or post-solidification changes. The former presence of bubbles at the peaty surface is seen by infilled cylindrical pockets of peaty material (Fig. 86).

Further down the ice body, bubbles are confined to a curving zone (Fig. 88). Also at the contact of the ice and underlying organic-rich soil is a 10-20 mm horizontal band of vertically oriented ($\leq 5$ mm) bubbles with bulbous ends above which is a zone of spherical bubbles ($\leq 1.5$ mm), (Fig. 88).

## Crystal Characteristics

Crystals display a range of sizes, shapes and dimensional orientations throughout the body. In the thin section parallel to the upper surface, crystal size is locally difficult to estimate due to the highly developed

sub-boundaries. The original growth boundaries are taken to be serrated compared with sub-boundaries; also the latter are the sites of embayment at their contacts with boundaries. On this basis, grain size is 20 to 30 mm long by 5 to 10 mm wide. Within these are elongate subgrains, usually parallel to the crystal long axes, but locally sub-boundaries converge. Crystal shapes are highly serrated, with serration amplitudes of 1-2 mm; some are superimposed on straight sides. The bubbles show no preferred positions on boundaries, nor are sub-boundaries generally related to bubbles. Where bubbles are in boundaries there are distinct changes of curvature of boundaries and flattening of bubbles; away from such boundaries bubbles are approximately spherical. Bubble size ranges from 0.1 mm to 0.5 mm. The sub-boundaries are well developed; not all are straight, but curve to maintain approximately 120° intersections with boundaries. Crystal characteristics in the vertical sections vary with depth. In the central ice, crystal size is very large, $\leqslant$ 90 mm x $\leqslant$ 30 mm, elongate vertically, with small crystals $<$ 5 mm across at grain boundaries of large crystals, thus in vertical trains; a further train crosses from the left hand side of Figure 89a, dipping at 40°. Lower this pattern changes, large (80 mm) crystals have long axes at 45° to those above, again with small ($<$ 5 mm) crystals in their boundaries (Fig. 89(b)). These boundaries are highly indented, and internal strain bands intersect the boundaries at indentations. These bands are 2-3 mm wide and mostly continuous across the crystal. In a horizontal section the influence of these bands is evident; grain boundaries parallel to the bands are approximately straight while boundaries trending normal are highly indented. The small crystals tend to be equidimensional with straight to gently curved boundaries and no substructure. Bubbles are not present in the small crystal zone, elsewhere positions are apparently random relative to grain boundaries.

Figure 89.  Vertical sections, lensoid body (Fig. 85).
  (a) Large, vertical grains with sub-boundaries, crossed by and
      separated by zones of small crystals.  10 mm grid.
  (b) Below Fig. 89(a).  Note horizontally elongated crystals in basal
      peaty zone.  10 mm grid.⌐⌐
      Crossed polarizers

a

b
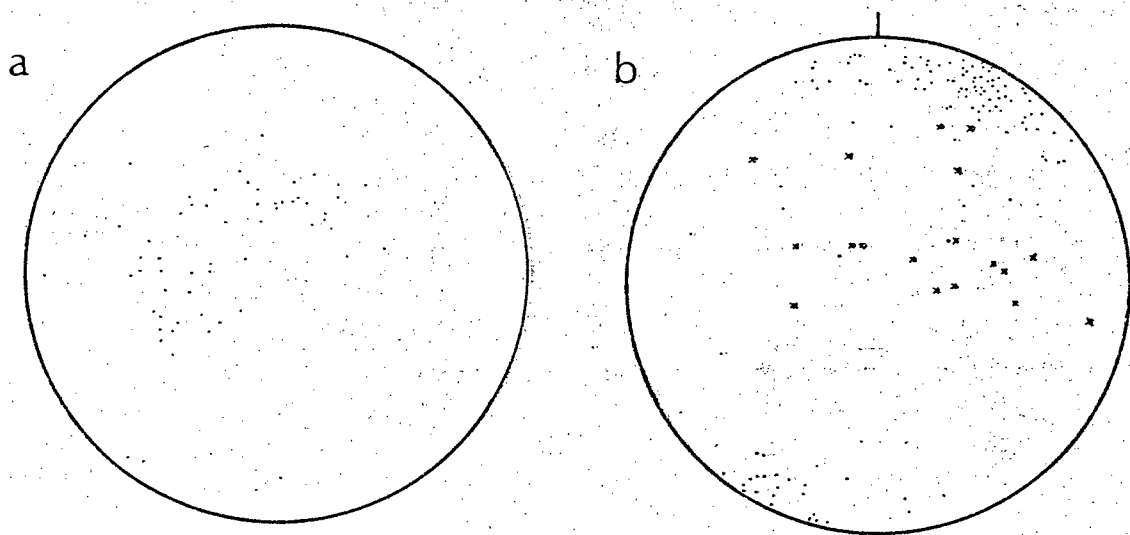


Figure 90.  Petrofabrics of ice in Fig. 85.

  (a) Horizontal section, top of sample, 60 crystals.
  (b) Vertical sections, 120 crystals, including bands of small
      crystals.
      x 18 horizontally elongated crystals at base.

      Diagrams parallel to sections

At the base of the ice body lies a zone of markedly different texture (Fig. 89(b)). The crystals are very elongated horizontally up to 80 mm, and boundaries are difficult to define due to peat content.

Petrofabric diagrams are given in Figure 90(a),(b). Figure 90(a) represents the crystals in a section parallel to the upper surface, which give a point concentration. Figure 90(b) represents vertical sections in which all crystals are contained in a point concentration, except for the lower zone of horizontally elongated crystals which are contained in a minor horizontal girdle.

### Interpretation

The field, bubble and crystal characteristics of the body indicate a fairly complex history. Unfortunately the lateral features of the body are not known, thus the origin of the lower zone of horizontally elongate crystals is not clear, although an abrupt change from the overlying ice is evident, in terms of shape and lattice orientation. The geomorphic position of the body, namely in an area of ice wedge polygons subject to thermokarst activity (see (a) and (b), above) and coastal recession means that thermokarst and thermal erosion (seaward water flow through wedge troughs) processes have operated. Also Mackay (1972d) has shown that ice lensing occurs in ridges adjacent to wedges. Thus a complex thaw and freeze history may have taken place. The upper root pattern is evidence of a recent melt-down and refreezing cycle, but this does not explain the major part of the body. There is no small crystal zone typical of chill type growth, as discussed in the cases of tension crack, icing mound and thermokarst depression infil ices. Had upward growth occurred from above the zone of horizontally elongated crystals, a zone of competitive growth

or growth in lattice continuity would be expected, but neither are found.

Nor is there an upper chill zone. It appears that such a chill zone

occurred at the top and was removed by downmelting to the inclusion zone,

then upward freezing in lattice continuity occurred. However, if the body

grew essentially by downward freezing, for example water being drawn up

progressively into the polygon rim from the adjacent deep wedge trough,

the contact with the lower zone of horizontally elongated crystals must be

explained. In the absence of knowledge of the lateral extent of the body,

but knowing the pattern of wedges it is suggested that the body tapered

off laterally, and the growth direction was offset from the vertical at

depth as indicated by the bubble orientation (Fig. 88). This conclusion

must be considered speculative, but the complexity of the history is recog-

nized.

(b)  Pelly Island

### Field Characteristics

On the northwest coast of Pelly Island is a low lying area of polygon

flats comprising lacustrine clays with a well developed ice-wedge system.

Many wedges are over 2 m across and some greater than 3 m. Polygons have

diameters of up to 10 m with rims reaching 1 m high and deep troughs.

These troughs have been subject to thermal erosion. Coastal exposures

indicate that several periods of melt-down and freeze-back have occurred,

and several wedges have irregular upper surfaces. Thaw zones may be traced

into the adjacent sediments, indicated by surfaces of iron staining, and

differing lens structures in the clays. Within the refrozen peat and clays

over the wedge margins are "pond ice" bodies (Fig. 91) characterized on

Figure 91.  Field position of
    "pond" ice over wedges,
    Pelly Island.



Figure 92.  "Pond" ice body.  Wedge
    ice below.



Figure 93.  Inclusion
    pattern, "pond" ice,
    vertical section normal
    to side.
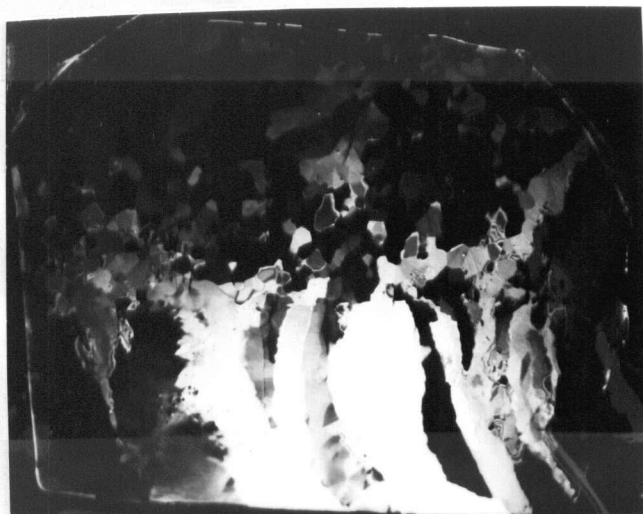
Figure 94.  Crystal pattern
    vertical sections normal
    to side.  10 mm grid.
    Crossed polarizers

melting surfaces by etched out crystal boundaries and bubble trains. These patterns indicate multiple freezing directions; the ice type is thus readily distinguishable in the field from lens ice or wedge ice. In some cases an individual "pond ice" body has been subject apparently to later melting and upward refreezing. Both peat and clay appear as inclusions within the ice. A sample of this ice was taken from the area shown in Figure 92 and hand specimen characteristics are given in terms of sediment and bubble content.

### Ice Characteristics

Firstly the features normal to a side of the pond are given, then those in a vertical plane parallel to the side.

### (i) Features Normal to the Side

The nature of the freezing process is best understood from study of a vertical sample orthogonal to the side of the body. No fractures were observed in hand-specimen; inclusions are discussed in terms of peat, sediment, and bubbles. Peat and sediment content is confined to a small dusting of particles in the top 20 to 30 mm, the zone of spherical bubbles.

### Bubble Characteristics

The bubble pattern comprises seven distinct zones:

(a) at the top of the sample is a 10-20 mm deep zone of small ( $<$ 1 mm diameter) spherical to ellipsoidal bubbles in a generally random pattern with some locally higher concentrations;

(b) a narrow essentially bubble-free zone;

(c) a 40 mm deep band crosses the sample sub-horizontally, containing vertically elongated bubbles 10 mm long and $\leq 1$ mm in diameter. Some have variable thickness, including bulbous ends. These elongate bubbles may occur in local groups or interspersed with small ($\leq 1$ mm) spherical bubbles;

(d) the next lower band comprises trains of elongate and spherical bubbles curving down from band (c) and away from the side of the pond, and into a lower narrow band of small spherical bubbles (Fig. 93);

(e) below occurs a series of trains trending upwards in the mirror image of band (d). The trains are curved but contained elongate bubbles (5 mm) are more nearly vertically oriented, and interspersed with small (1 mm) spherical and ellipsoidal bubbles. Trains are 30-50 mm long, separated by 20-50 mm of clear ice, and become narrower upwards;

(f) beneath the trains is a thin band of bubble-poor ice, then a horizontal discontinuous band of slightly elongated (3-5 mm) vertical bubbles, interspersed with some spherical and irregularly shaped bubbles, indicative of melt;

(g) below is a zone of low bubble content, containing patches of spherical and irregular bubbles in a trend similar to that in zone (d) but formed during a separate freezing period. Sediment occurs as pods and streaks above zone (f), and parallel to trains in zone (e) and become narrower upwards.

### Crystal Characteristics

Crystal size is discussed with reference to bubble zones (Fig. 94).

(a), (b) and (c) contain crystals averaging 3 mm x 2 mm, and ranging up to 12 mm x 10 mm;

(d) at the base of the zone of elongated bubbles begins a zone of narrow elongated crystals > 30 mm x 6 mm, which curve round into horizontality in zone (e);

(e) crystals are slightly larger than in zone (d) and the dimensional orientation is a mirror image to that of zone (d) thus corresponding to the bubble pattern.

(f),(g) and (h) contain larger crystals, up to 50 mm long, < 10 mm wide in a pattern shown in Figure 94.

Crystal shape variations correlate with bubble zones. Zones (a), (b) and (c) contain anhedral equigranular crystals with no strong intergrowths or serrations. In zone (d), shape changes to anhedral, serrated, elongated crystals with a curved dimensional orientation. Wedging out of crystals has occurred during downward growth. Zones (e), (f) and (g) contain anhedral, serrated elongate crystals with a radial variation in dimensional orientation, shown in Figure 94(b),(c).

Substructure is confined to larger crystals. In zones (a), (b) and (c) some large crystals are embayed by smaller crystals, the boundary segments at embayments are straight. In the lower zones elongate crystals contain complex sub-boundaries, in patterns parallel and normal to long axes.

The broad relationship between bubble pattern and texture is evident from the above discussion and Figures 93, 94.

Petrofabric diagrams for this series of samples are shown in Figure 95. Crystals in the upper zones (Fig. 95(a)) have c-axes in a zone parallel to the top of the body. An interesting distribution of c-axes exists in the lower zones, shown in Figure 95(b). The initial freezing pattern was from all sides towards a central point, thus as the freezing interface changed, so the crystal dimensional orientations changed. But the crystals were large and growth continued in lattice continuity rather than requiring further nucleation. After a period of melt-down, refreezing occurred, again from all sides. Upward growth occurred on the already existing lattice sites, thus the lattice orientations are maintained. Downward growth occurred as an extension of the chill zone, in the form of a columnar zone. Where the two zones approached, dimensional orientation changed to remain orthogonal to the freezing interface, but lattice continuity was maintained, even in horizontal crystals. Thus the girdle of c-axes is explained. Substructures observed in the larger crystals are due to internal strain. The enclosed freezing discussed above, and later temperature fluctuations which would lead to expansion and contraction, gave rise to the small-angle boundaries.

(ii)  <u>Sections Parallel to Side of Ice Body</u>

Sediment bands are not continuous throughout the body, but taper inwards from the contact with the surrounding clay, of which they are composed. Slight curvatures of the bands result from variations in the shape of the freezing interface. Within the bands, sediment occurs as small ($< 5$ mm) "pods" and as parallel streaks, probably on crystal basal planes. Characteristically a band has one diffuse and one abrupt boundary, the former being the first to freeze, indicating laterally uniform freezing conditions.
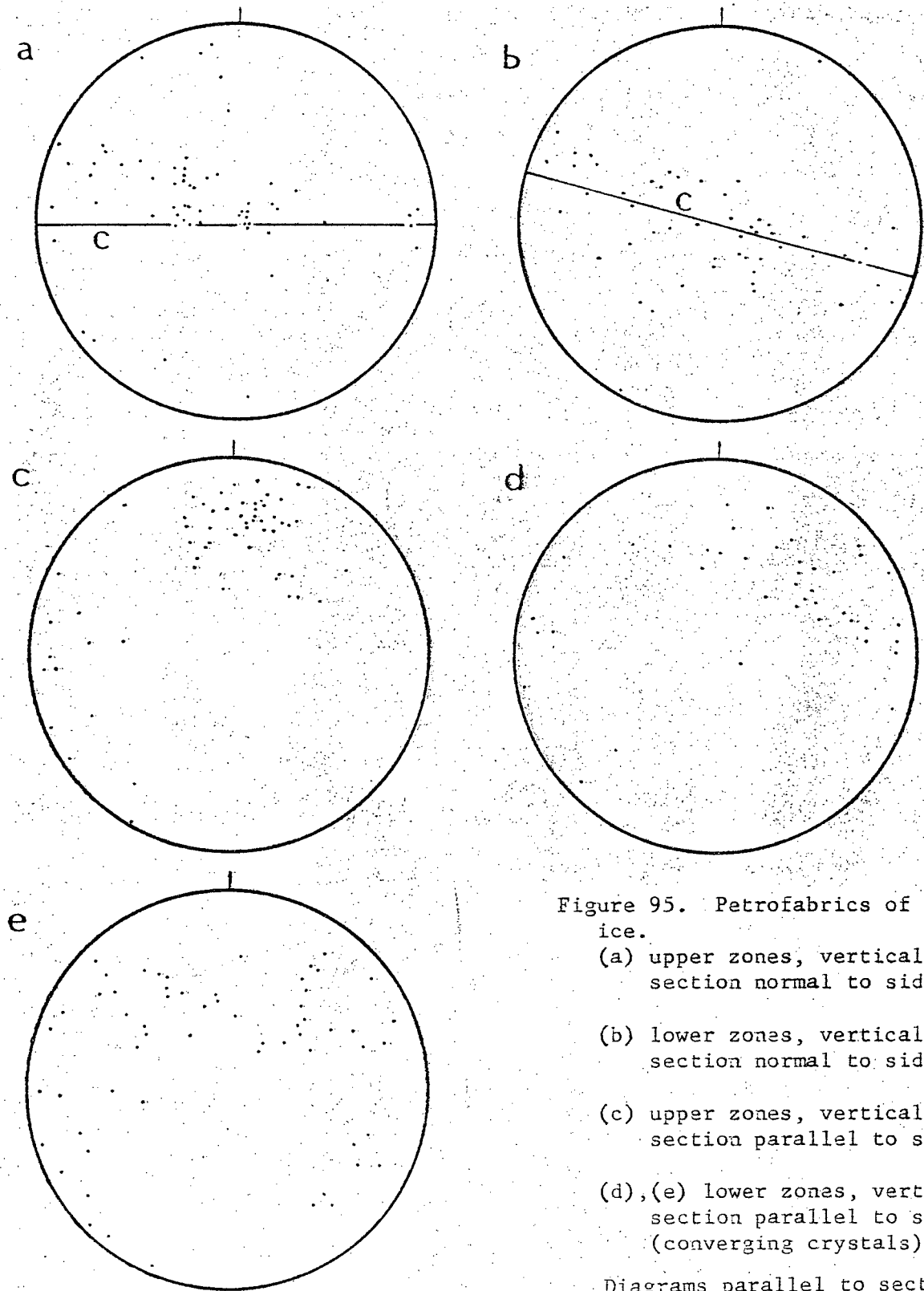
Figure 95. Petrofabrics of "pond" ice.

(a) upper zones, vertical section normal to side;

(b) lower zones, vertical section normal to side;

(c) upper zones, vertical section parallel to side;

(d),(e) lower zones, vertical section parallel to side (converging crystals).

Diagrams parallel to sections
c = compositional layering

## Bubble Characteristics

Bubble content is variable (Fig. 96):

(a)  A high concentration of bubbles occurs in the ice above the top sediment band, comprising two types:  (1) spherical, $\leqslant 1$ mm diameter, randomly positioned with respect to elongate bubbles and sediment, (2) elongate $\leqslant 1$ mm diameter, up to 13 mm long, with bulbous ends, oriented orthogonal to the sediment banding, and arranged in groups;

(b)  in the top sediment band is a much lower bubble concentration than in zone (a), spherical and elongate bubbles occur where the sediment content is lower;

(c)  below the sediment band is a bubble-poor zone grading into more bubbly ice comprising (1) elongate bubbles which occur singly or within patches of spherical and mainly close to the sediment band, (2) spherical bubbles $< 1$ mm diameter in a 20-30 mm thick zone immediately above the sediment, (3) curved trains, 70 mm long and 10 mm in diameter which contain spherical and ellipsoidal bubbles, trend upward from the second sediment band, (4) bubble groups occur midway between sediment bands and not associated with a train;

(d)  in the upper part of second sediment band occur both spherical and elongate bubbles, but none were observed in the lower part;

(e) between the second and third sediment bands are few bubbles, there being occasional spherical and elongate bubbles above the sediment;

(f)  the lower sediment band is bubble-free.

Figure 96.   Bubble and clay
   inclusion zones, vertical face
   parallel to side of "pond" ice.
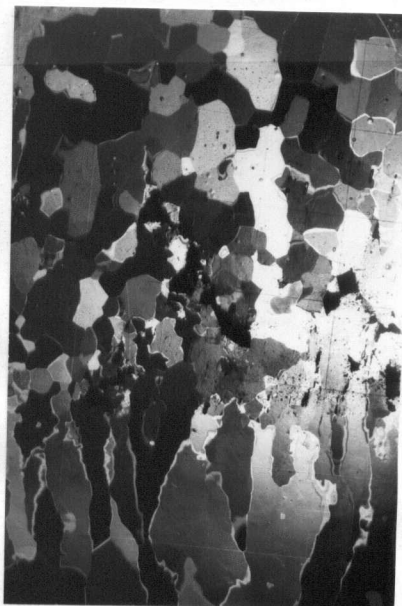


Figure 97.   Vertical section, top
   of Fig. 96.   Textural change
   at clay inclusion zone.

   10 mm grid ⌐———⌐
   Crossed polarizers

### Crystal Characterisitcs

Textures are discussed in relation to sediment and bubble bands. Within the upper bubble and sediment band are crystals averaging 5 mm x 4 mm, and ranging from 2 mm x 1 mm to 15 mm x 8 mm. Below this sediment band are larger vertically elongate crystals averaging > 30 mm x 10 mm, and ranging from 6 mm x 4 mm to > 40 mm x 20 mm (Fig. 97). Lower there occur much larger crystals, up to 48 mm x 30 mm but occasionally around 7 mm x 2 mm. There is a further change in grain size to more equigranular below the lower sediment band. Grain shape varies with grain size. In the small crystal zone crystals are anhedral, boundaries are straight or have simple curvature. There is a slight dimensional preferred orientation parallel to bubble elongation. The elongate crystals are anhedral with well developed serrations and embayments; again the dimensional orientation is orthogonal to the sediment band. In the lower part of the sample elongation is more complex.

Substructure is only poorly developed in the upper small crystal zone but is strong in several of the elongate crystals, frequently parallel to the dimensional orientation; a second rectangular substructure occurs lower down.

There is no strong relationship between bubbles and texture, other than parallel dimensional orientation. In the case of elongate bubbles, some pass across crystal boundaries, others terminate at boundaries, while spherical bubbles are scattered randomly with respect to boundaries. An exception to the above pattern occurs where a bubble train within otherwise clear ice is contained within one large elongate crystal. The relationship between sediment and texture is two-fold:

(a) "pods" of sediment are not contained within crystals;

(b) "streaks" of sediment tend to be vertical or locally orthogonal to the trend of the band, but not related to crystal structure or grain boundaries, as individual lines cross more than one crystal.

It is not clear whether the sediment pattern is a function of a complex interface shape during freezing, or later thermomigration.

C-axis orientations for the sample are given in Figure 95. Small crystals in the zones (a), (b) and (c) give an approximately vertical maximum which may occur during initial downward freezing (Michel and Ramseier 1971) and a minor vertical girdle (Fig. 95(c)). The crystals in the girdle do not differ in other characteristics from the surrounding crystals, although some deviate from the vertical dimensional orientation. Crystals in the zone of elongate crystals are shown in Figure 97 and their c-axes plotted in Figure 95(d). The maximum deviates from that in Figure 95(c). Below, the pattern is more complex (Fig. 95(e)) due to the change in freezing direction and dimensional orientation, but from comparison with diagrams for the orthogonal series of sections it is seen that c-axes are orthogonal to the local freezing direction, and thus the pattern is effectively an extension of the c-axis horizontal pattern rotated for the local freezing interface.

Interpretation

From the field relations and inclusion, petrofabric and crystal characteristics the history of the ice body can be described. After considerable development of the wedge system a greater depth of thaw, indicated by the surface of iron staining traceable laterally from wedges

into the adjacent sediment, occurred and differing lens structure in the
clays. Additionally thermokarst and thermal erosion processes have opera-
ted over the wedges. Refreezing occurred from above and below, and above
the wedge pools of water froze to give the pattern shown in zones (g)-(h)
(Fig. 96). A subsequent melt-down removed the upper part of this ice and
caused changes in bubble shape and the introduction of sediment (above zone
(f)). Refreezing again occurred simultaneously from above and below giving
rise to the equigranular chill zone crystals in zone (a) to (c) and the
curving, converging bubble trains and curved, elongate crystals of zones
(d) and (e), those in (e) being extensions of crystals in zone(f). The
zone of competitive growth above zone (f) from the previous freezing was
removed by melt-down. Bubbles within the trains in zones (d) and (e) are
now elongate vertically having been subject to thermomigration in a vertical
temperature gradient.

Crystal c-axis orientations change from vertical at the top to more
nearly horizontal then change pattern due to the freezing direction change.

### Relationship of Ice Type to Surface Form

Aerial photographs of the area show the well-developed pattern of
ice wedge polygons with associated ridges. Field examination of the area
disclosed the presence of very deep troughs over some wedges which obviously
did not freeze each winter. Also it is evident that some thermal erosion
is occurring laterally at the top of some troughs, and considerable over-
hangs of organic soil are developing (Fig. 91). However, these latter
features are not always obvious from air photographs. Nor is the presence
of the ice bodies discussed above immediately evident from air photographs

or surface field examination; their characteristics and distribution were well displayed only on coastal sections. Thus, in summary, the ice type had no specific surface expression, but is an excellent indicator of the complex thermal history of the area. Similar processes of melt-down adjacent to wedges are now occurring nearby. A further, more minor, point to be extracted from the discussion is the importance of preparing thin sections of several orientations.

## 10. Aggradational Ice

### Introduction

Aggradational ice is ice which grew at the base of an active layer and became incorporated into permafrost as the permafrost table rose. This rise in the permafrost table may be due to thinning of the active layer in a climatic change or sedimentation on the ground surface. A subsequent change in surface conditions could destroy such ice. As surface conditions vary considerably in space and time it is to be anticipated that aggradational ice characteristics will be variable laterally.

We discuss aggradational ice from two sites: (1) an involuted hill near Tuktoyaktuk, (2) a construction site at Tuktoyaktuk.

### (a) Involuted Hill Site

#### Introduction

In a previous section (Involuted hill ice - folded ice penetrated by wedge) we discussed a site where peat had accumulated and an ice wedge had

grown in a multiple fashion (Mackay 1974a, p. 1379, Fig. 18). This is evidence of a rise in the permafrost table, and we now discuss ice in the adjacent soil.

### Field Characteristics

The involuted hill on the coast near Tuktoyaktuk is typical of all such hills in the area, in terms of surficial form, and coastal recession has exposed some of its internal features. It is evident that several metres of peat has accumulated in inter-ridge depressions (Fig. 98), and that some minor thawing activity has occurred adjacent to some of the larger ice wedges. Here we discuss ice which is, by definition, aggradational, and which has not been disturbed by large scale thermokarst activity.

Most of the ice is in a dispersed, particulate form and unsuited for thin section preparation, but at what was probably a depression in a onetime permafrost table, there occurs a lensoid ice body which is suitable for analysis.

### Ice Characteristics

The lower surface of the body is undulating and there is no abrupt boundary with the soil, rather there is a gradation from peat through icy peat to peaty ice to ice. Within the ice body proper are bubble trains of varying orientation; these are truncated and new trains occur above (Fig. 99(a)). The upper ice-soil contact is again not abrupt.

### Bubble Characteristics

The bubble pattern comprises the following zones:
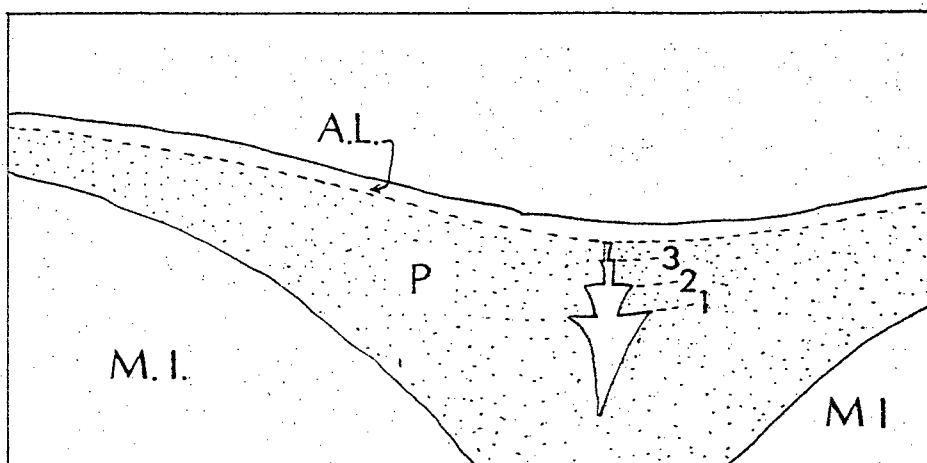
Figure 98. Schematic diagram, peat accumulation and wedge
ice growth, involuted hill. A.L. = active layer. 1,2,3
indicate old active layers. P = peat, M.I. = massive ice.



Figure 99a. Schematic diagram,
peat and bubble pattern,
aggradational ice.
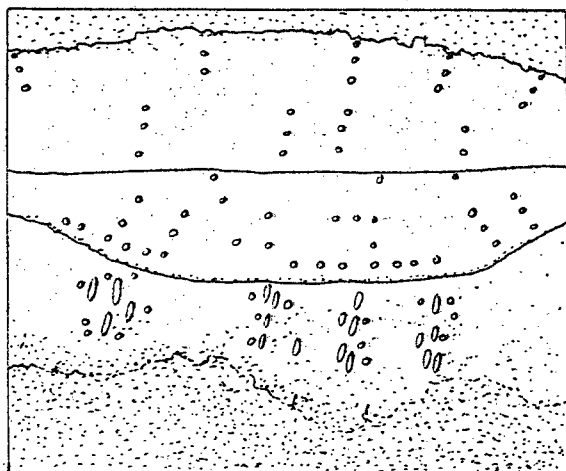


Figure 99b. Schematic diagram,
crystal pattern, aggradational
ice.
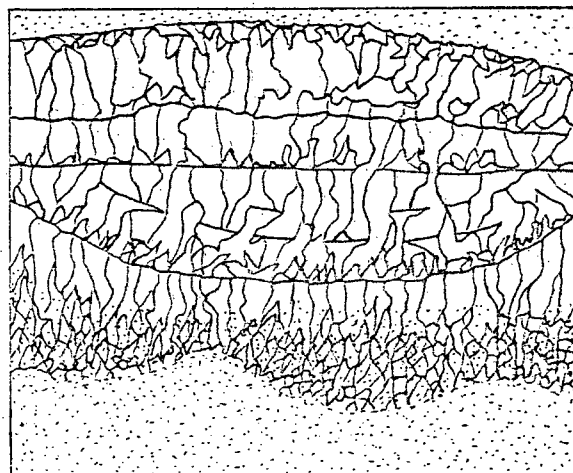
(i)   Lower zone:  This zone comprises vertically elongate and some

spherical bubbles which are $<1$ mm diameter, and lengths are $< 4$ mm.

There is no overall regular pattern in the form of layers of a given

bubble size or shape, rather there are groups of locally higher concen-

tration, surrounded by spherical bubbles.  This zone has a high peat

concentration in particulate form which may have controlled bubble growth,

but if any pattern of bubbles existed immediately after solidification, it

has since been modified.

(ii)  Central zone:  The pattern in zone (i) is abruptly truncated in a

curved surface, which is not a growth feature.  Within zone (ii) is a

series of discontinuous 1-2 mm layers containing bubbles trending away

from the contact between zones (i) and (ii).  Above, the ice becomes

clearer and is truncated approximately horizontally.

(iii) Upper zone:  Above the truncation of zone (ii) is a pattern of

elongate bubbles trending orthogonal to the truncation zone and upper

surface, which is typical of omnidirectional freezing as discussed else-

where.   The contacts are abrupt, and bubble shape is thin, $<1$ mm diameter

and elongate, 3 mm.

### Crystal Characteristics

The crystal size and shape characteristics are closely associated

with bubble zone features, and are discussed in terms of those zones

(Fig. 99(b)).

(i)   Lower zone:  This zone has a high inclusion content in the form of

peat and bubbles, and crystal size is generally 1-2 mm for equant crystals,

with some elongated crystals up to 5 mm.  Grain boundaries are usually

straight from one inclusion to the next, but some larger crystals are very
irregular.

(ii) Central zone. At the lower edge a mass of small crystals grows up
from the truncation of zone (i). The discontinuous bubble layers have a
marked effect on crystal form - crystals terminate at these zones and new
growth occurs on the other side. Where no such bubble layers occur elonga-
ted crystals reach 30 mm long and 3 mm wide.

(iii) Upper zone. Crystal shape corresponds to the bubble pattern, crystals
have grown orthogonal to both the upper surface of zone (ii) and the top of
the ice body. In some cases the lower crystals are in lattice continuity with
those in zone (ii) but in general new growth has occurred. Competitive growth
zones on all sides of the body give rise to elongate crystals up to 20 mm long
which trend toward the centre of the body. Crystals in the upper part are
longer.

Lattice orientations are shown in Figure 100; slightly differing c-axis
patterns correspond to the several bubble and crystal zones. In the lower
zone the pattern lacks preferred orientation (Fig. 100(a)) from which develops
a slight concentration in zone (ii) (Fig. 100(b)). A transition occurs in
the upper zone, where a random orientation for crystals around the edges
(Fig. 100(c)) becomes a weak girdle orthogonal to the dimensional orientation
(Fig. 100(d)) in the elongate crystals. The samples are too small for rig-
orous discussion, but Fig. 100(d) corresponds to elongate crystals.

### Interpretation

The growth sequence of layers is zone (i), zone (ii), zone (iii).
Zone (i) represents a locally higher water content in the peat which gave
rise to the transition from peat with a high interstitial ice content to
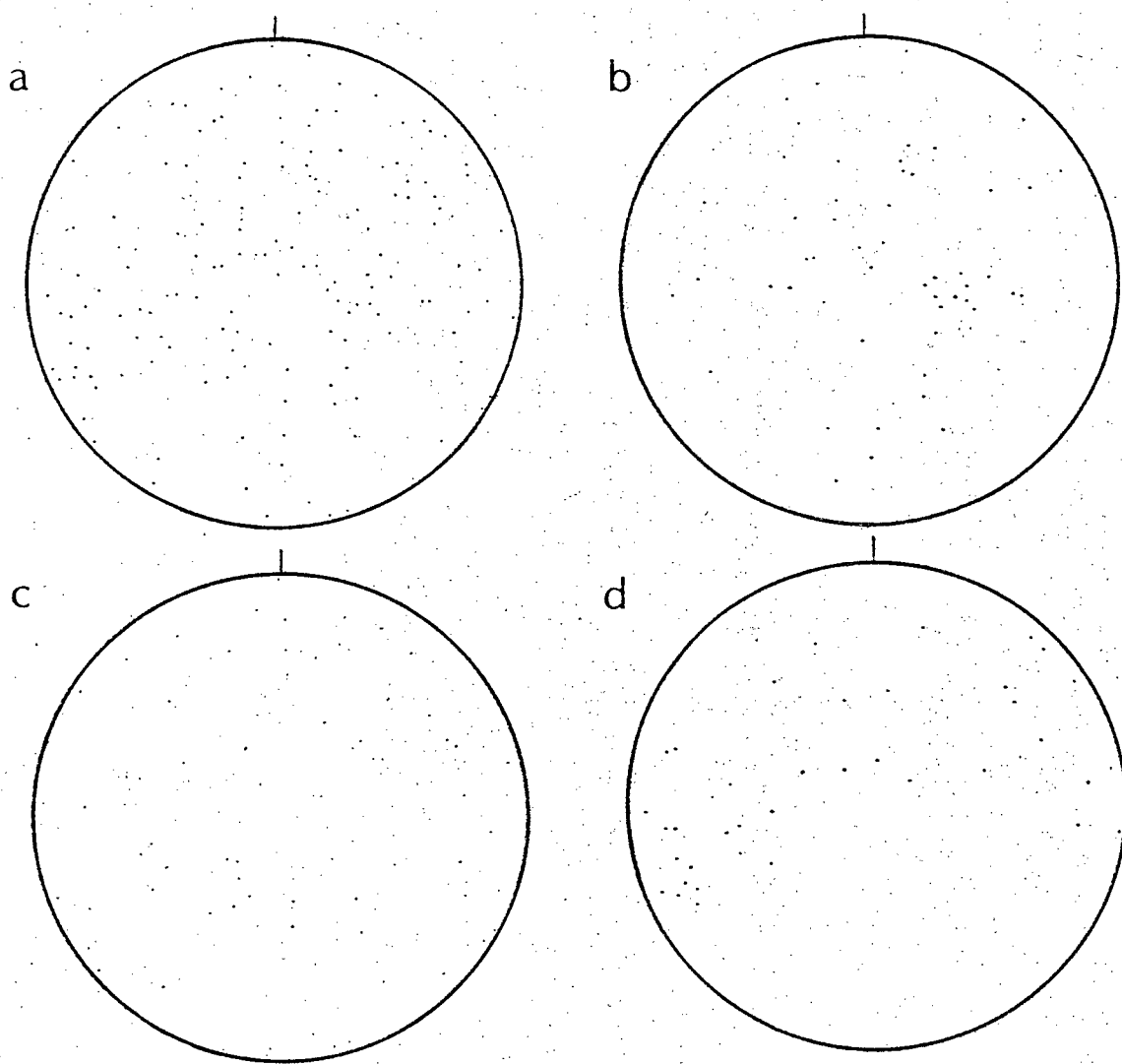
Figure 100. Petrofabrics for aggradational ice.

    (a) lower zone

    (b) second zone

    (c) edge crystals, upper zone

    (d) elongate crystals, upper zone.

peaty ice. The peat and bubbles (which, in addition to dissolved air, may incorporate gases from reactions in the peat) may have encouraged copious nucleation, and have a strong control on crystal size and shape. This ice body was later subject to melt-down from above as is evident from the irregular upper surface of zone (i) and the abrupt truncation of crystal features. Zone (ii) represents a new growth period as seen by the transition in crystal and bubble dimensional orientation - growth is everywhere orthogonal to the irregular upper surface of zone (i). This zone is in turn truncated but the lower part of the zone became incorporated into permafrost. A further type of growth occurred in zone (iii). Here the bubble pattern and crystal dimensional and lattice orientations indicate simultaneous growth vertically from above and below, and laterally. This latter zone is at the base of the present active layer and may be quite recent. It is thus in a position where disturbance is likely with a slight change in surface conditions. In the case of such an event zone (iii) might be melted down and display the features typical of zones (i) and (ii).

(b)    Tuktoyaktuk Site

    Introduction

The Polar Continental Shelf Project has a base in Tuktoyaktuk, which was built in 1966. This entailed the laying of a gravel pad on the existing active layer, on which buildings were sited. Gradually permafrost aggraded through the old active layer until equilibrium was re-established.

In June 1973, the Metallurgy Division of the Department of Energy, Mines and Resources dug small excavation pits into the gravel pad, for the purpose of erecting a test compound. During these excavations ice was

encountered in several forms:- particulate, and in small bodies; samples
of the latter ice type were supplied to the author.

### Field Characteristics

The material of the "gravel pad" comprised a mixture of gravel, sand
and organic matter (bulldozed from the nearby tundra). Ice samples were
removed from beneath 0.9 m of overburden, at which depth the ice formed
discontinuous layers, <75 mm thick and <300 mm diameter.

### Ice Characteristics

No structures were evident in the ice (some small fractures were
probably a result of the digging). Inclusions occurred in solid and gaseous
form; bubbles displayed a slight tendency to banding locally, parallel to
the ground surface and orthogonal to bubble dimensional orientation, while
sediment appeared to be randomly positioned. Bubbles were generally cylin-
drical in shape, <1 mm in diameter, <15 mm long and vertically oriented.
Sand grains and fragments of organic material were <0.1 mm.

### Crystal Characteristics

Crystal size and shape vary with inclusion content. Small crystals,
2-3 mm in diameter, were found near the top of the specimen, where a higher
sediment content occurred, and size increased to 5-25 mm below. Most
crystal boundaries were straight or only slightly curved, an individual
crystal generally had 6 sides, both convex and concave boundaries; these
characteristics are complicated by the presence of solid and gaseous inclu-
sions. Grain shape becomes more complex in zones of high inclusion content,
with irregular boundaries, also sub-boundary development is closely
associated with inclusions.

Lattice orientations are given in Figure 101, which shows a high degree of preferred orientation, with a single maximum parallel to the direction of bubble elongation.

## Interpretation

The equidimensional crystals are close to an equilibrium configuration. Grain boundaries are mutually adjusted, probably sub-boundaries have become boundaries, except where interfered with by inclusions owing to the high content of vertically elongated bubbles. C-axis orientations are parallel to inferred heat flow directions, thus crystals extended parallel to the c-axis as found in the experimental work of Kaplar (personal communication, 1974). The ice is aggradational, in the sense that the permafrost table has risen due to artificial sedimentation.
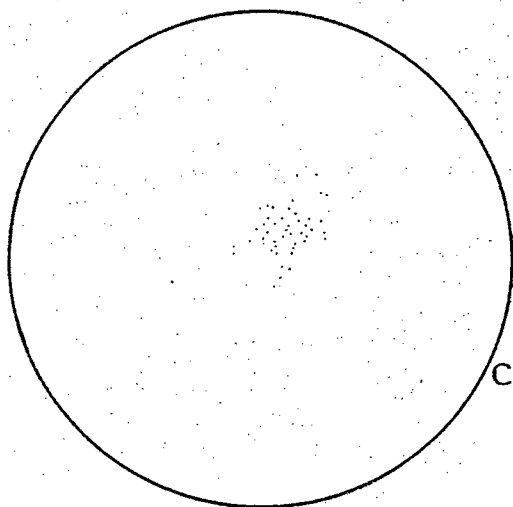
Figure 101.   Petrofabrics, aggradational ice, Tuktoyaktuk.
              Plane of diagram horizontal, parallel to section

Chapter 5

SUMMARY AND CONCLUSIONS

The widespread distribution of ground ice along the Arctic Coast and Mackenzie Valley had been recognized previously, and a classification of ice types had been established in terms of water supply, transfer mechanisms and associated ground ice forms. This was based on long-term observations and precise surveys of a range of growing ices, but little petrofabric study. In the present study a field area was chosen near Tuktoyaktuk in order to undertake both detailed field study of ice in good exposures and in bodies of known history, and petrofabric analysis of those ices. Thus it was possible to compare ice of known age ( $<$ 1 year) with older bodies and thus to elucidate both growth features and post-solidification changes.

Crystal and inclusion characteristics typical of growth of ice in bulk water, as reported in lake ice and laboratory studies, were found to apply to some ice bodies. Although previous field and laboratory work on petrologic aspects of segregated ice and pore ice growth has been limited, the results here are in agreement with earlier reports.

Modification of growth fabrics was recognized in several ice types, for example in ice wedges where progressive changes in crystal features occurred from the centre (recent growth) to the wedge margin; also the fabric of segregated ice adjacent to a wedge changed due to the growth of that wedge.

Thus each ice type has a particular texture related to its history, and petrologic criteria are added to a modified version of Mackay's (1972b) ice classification given in Appendix 1.

A brief summary of each ice type is given below:

1. Lake ice comprised an upper zone of small crystals from which grew vertically elongate crystals, parallel to the heat flow direction, with optic axes in a horizontal girdle.

2. Icing mound ice comprised an upper chill zone of small crystals, adjacent to the soil, from which grew elongate crystals normal to the upper surface, with optic axes normal to the long axes. Bubble bands were parallel to the upper ice surface and contained elongate bubbles normal to the bands. A later fracture infil comprised ice with different crystal and inclusion characteristics related to the local thermal gradient.

3. Ice from three pingos was studied and found to differ in all three. A small pingo of known age displayed crystal features typical of ice growth in bulk water and is interpreted as freezing of a residual pond, as freezing was unidirectional, rather than injection ice which would give evidence of multidirectional freezing.

   A second pingo exhibited a clear ice and bubbly ice core overlying pore ice. An increase in freezing rate during growth was indicated by a change in inclusion content and crystal lattice orientation (optic axes normal to freezing direction). This is attributed to uplift of the lake bottom and exposure to cold air temperatures.

In the case of Tuktoyaktuk pingo there is a pattern of alternating
layers of segregated ice and pore ice, in marked contrast to the
previous cores. A general tendency exists for optic axes to be normal
to the compositional layering, but markedly different patterns exist.
Some flow has occurred since cessation of growth.

4. Involuted hill ice represents an extension of segregated ice growth,
   with considerable upward movement of the ice. An increase in c-axis
   concentration orthogonal to the compositional layering and in dimensional
   orientation parallel to the layering occurred in anticlines in the ice.
   Where an ice wedge penetrated such a fold the petrofabric pattern
   changed adjacent to the wedge, and crystal size decreased toward the
   wedge, due to the stress system associated with wedge growth.

5. Tension crack ice from two sites was studied. Crack ice which grew
   in the 1973-74 season had fresh growth features markedly different from
   one season's wedge ice growth. Older tension crack ice, which had been
   subject to coastal recession, and thus unknown stress and temperature
   gradients, displayed features due to post-solidification modification.

6. Thermal contraction crack and wedge ice from several sites was studied.
   Individual thermally-induced cracks in segregated (involuted hill) ice
   were investigated; little relationship to the fabric of the massive
   ice was found, nor were subsequent fractures influenced greatly by
   earlier ones. Large wedges on Pelly Island showed the prograde fabric
   of growing wedges. Progressive increases in crystal size, degree of
   preferred dimensional orientation (parallel to compositional layering)
   with distance from the wedge centre were recognized. The influence of

a growing wedge on surrounding involuted hill ice was pointed out
above (conclusion No. 5).

7. Reticulate vein ice was examined at one site only, where vertical
veins dominated. Inclusion and crystal characteristics varied in each
sample. Narrow veins contained medium sized crystals with c-axes
normal to the vein. In large veins, central crystals were larger,
without a strong preferred c-axis orientation, and surrounded by
elongate crystals, normal to the vein.

8. Active layer ice indicated multiple freezing directions.

9. Ice with multiple freezing histories was discussed from two sites.
Omnidirectional growth within frozen soil was observed in coastal
areas of ice-wedge polygons. Crystals and bubble trains trend orthog-
onally from surrounding soil, while contained bubbles are vertical in
response to a later vertical temperature gradient. In some cases later
melting and refreezing was evident. The position of such bodies sug-
gests that they originate from omnidirectional freezing of pools or
channels produced by coastward flow of water.

10. Aggradational ice grew between two ridges of an involuted hill, and
in association with the upward growth of permafrost under a gravel
pad. In the former case upward growth followed by melt-down and sub-
sequent upward growth was recognized.

    It is emphasized that any one criterion is insufficient for inter-
pretation of the history of a given ice body. For example the orientation
of bubble long axes in the icing mound ice (Fig. 5) was parallel to the

growth direction as indicated by crystal zonation, crystal dimensional orientation, crystal c-axis orientation and the form of the mound. In contrast, in older, near-surface ices which have been subject to melt-down and strong temperature gradients (not measured) the bubbles have developed vertical dimensional orientations (Fig. 83(a)) despite the dip of the bubble train. However, the bubble trains, crystal zonation and dimensional orientations and shape of the ice-soil interface indicate the freezing direction, and the bubble orientation is interpreted as a result of thermomigration in a vertical temperature gradient. Also, in the case of folded involuted hill ice, bubbles were modified from their original form, but some understanding of the history of an individual body may be gained from consideration of all petrofabric properties. This is true especially where only limited samples are available, from a core, for example. In the present study samples were obtained from well exposed ice bodies, or from areas of which the geomorphic history was well known. Elsewhere, exposure may be lacking or topographic expression may not reflect subsurface ice form. In such instances the petrofabric features summarized here may be used as aids in classifying an ice sample, but all available sedimentary and other data should be employed.

Knowledge of crystal c-axis orientations is important in the interpretation of results of geophysical investigations on ground ice. For example, seismic wave velocity parallel to the c-axis is 200 $m.s^{-1}$ faster than elsewhere, thus prediction of fabrics would be helpful.

Suggestions for further work

The aim of the present study has been an understanding of petrological aspects of the growth and deformation of ice bodies in permafrost. The results summarized above indicate that some progress has been made in that a foundation has been established on which to base further field and laboratory study. In particular, petrologic analysis of ice in lenses grown under known conditions of heat-flow and water supply should be attempted. Those pingos and other ice bodies of which the recent growth histories are well known would provide excellent field comparisons. In terms of deformation, much could be gained from a knowledge of stress distributions around wedges, and creep rates of the larger ice masses. Detailed thermal data for the upper layers of permafrost are available and it is apparent that contained ice bodies have complex, cyclic, thermal strain histories which merit further study. Our understanding of the influence of inclusions on the flow of ice is limited and more experimental work is necessary to aid in field studies.

LITERATURE CITED

AD HOC STUDY GROUP ON PERMAFROST 1974. Priorities for basic research on
      permafrost. Committee on Polar Research, National Research Council.
      Nat. Acad. Sci., Washington, D.C., 54 p.

ANDERSON, D.L., and WEEKS, W.F. 1958. A theoretical analysis of sea ice
      strength. Trans. A.G.U., v. 39, no. 4, pp. 632-640.

BARI, S.A., and HALLETT, J. 1974. Nucleation and growth of bubbles at an
      ice-water interface. J. Glac., v. 13, no. 69, pp. 489-520.

BESKOW, G. 1935. Soil freezing and frost heaving with special application
      to roads and railroads (in Swedish). Swedish Geol. Soc. Ser. C,
      26th Yearb., No. 3 (Transl. by J.O. Osterberg, Northwestern Univer-
      sity, Evanston, Ill., 1947, 145 p.).

BLACK, R.F. 1952. Growth of ice-wedge polygons in permafrost near Barrow,
      Alaska, (Abstract). Geol. Soc. Am. Bull., v. 63, no. 12, pp. 1235-
      1236.

_____ 1953. Fabrics of ice wedges. Johns Hopkins University, Ph.D.
      dissertation (unpubl.), 87 p.

_____ 1954. Ice wedges and permafrost of the arctic coastal plain of
      Alaska. Unpubl. MS., 2 vol., 788 p. (Results of work under the
      auspices of the U.S.G.S.).

_____ 1963. Les coins de glace et le gel permanent dans le nord de
      l'Alaska. Ann. Geogr. v. 72, pp. 257-271.

_____ 1973. Growth of patterned ground in Victoria Land, Antarctica.
      pp. 193-202, in Permafrost: The North American contribution to tne
      Second International Conference. Nat. Acad. Sci., Washington, D.C.,
      783 p.

BOLLING, G.F., and TILLER, W.A. 1960. Growth from the melt. I. Influence
      of surface intersections in pure metals. J. Appl. Phys., v. 31,
      no. 8, pp. 1345-1350.

BROWN, R.J.E., and PEWE, T.L. 1973. Distribution of permafrost in North
      America and its relationship to the environment: A review. pp. 71-100,
      in Permafrost: The North American Contribution to the Second Interna-
      tional Conference. Nat. Acad. Sci., Washington, D.C., 783 p.

CAREY, K.L. 1973. Icings developed from surface water and ground water.
      U.S. Army CRREL Monogr. III-D3, 67 p.

CARTE, A.E. 1961a. Air bubbles in ice. Proc. Phys. Soc. (London), v. 77,
      pp. 757-768.

_____ 1961b. Grain growth in ice. Bull. de l'observatoire du Puy de Dôme,
      no. 3, pp. 129-136.

CHALMERS, B. 1959. How water freezes. Sci. Am., v. 200, no. 2, pp. 114-121.

COLBECK, S.C., and EVANS, R.J. 1973. A flow law for temperate glacier ice. J. Glac., v. 12, no. 64, pp. 71-86.

CORTE, A.E. 1962a. Relationship between four ground patterns, structure of the active layer and type and distribution of ice in the permafrost. U.S. Army CRREL, Research Report 88, 82 p.

_____ 1962b. Vertical migration of particles in front of a moving freezing plane. U.S. Army CRREL, Research Report 105, 8 p.

DANILOV, I.D. 1969. The permafrost-facies structure of the watershed relief forming deposits of the lower Enisei (in Russian). pp. 93-105, in Problems of Cryolithology, v. 1, ed. by A.I. Popov, Moscow Univ. Press, U.S.S.R., 176 p.

DURNEY, D.W., and RAMSAY, J.G. 1973. Incremental strains measured by syntectonic crystal growths. pp. 67-96, in "Gravity and tectonics", ed. by K.A. de Jong and R. Scholten, J. Wiley, N.Y. 502 p.

FIRST INTERNATIONAL CONFERENCE ON PERMAFROST, PROCEEDINGS 1966. Nat. Acad. Sci., N.R.C. Publ. 1287, Washington, D.C., 563 p.

FRENCH, H. 1971. Ice cored mounds and patterned ground, Southern Banks Island, Western Canadian Arctic. Geog. Annal., v. 53A, pp. 32-38.

GLEITER, H., and CHALMERS, B. 1968. Grain boundary migration. pp. 127-178, in Progress in Materials Science, v. 16, ed. by B. Chalmers, J.W. Christian and T.B. Marsalski, Pergamon Press, 195 p.

GLEN, J.W. 1974. The physics of ice. U.S. Army CRREL, Monogr. II-C2a, 80 p.

GOLD, L.W. 1957. A possible force mechanism associated with the freezing of water in porous materials, Highway Res. Board Bull. 168, pp. 65-73.

_____ 1961. Formation of cracks in ice plates by thermal shock. Nature, v. 192, no. 4798, pp. 130-131.

_____ 1963. Deformation mechanisms in ice. pp. 8-27, in "Ice and Snow", ed. W.D. Kingery, M.I.T. Press, Camb., Mass., 684 p.

_____ 1972. The failure process in columnar-grained ice. Nat. Res. Counc. Canada, Div. Bldg. Res., Technical Paper no. 369, 108 p.

GOUGHNOUR, R.R., and ANDERSLAND, O.B. Mechanical properties of a sand-ice system, J. Soil Mech. and Foundat. Div., Proc. A.S.C.E., v. 94, no. 4, pp. 923-950.

GRECHISHCHEV, S.S. 1970. On the basic methods of forecasting temperature tensions and deformations in frozen ground (in Russian). Moscow, Ministry of Geology of the U.S.S.R., 53 p.

HARRISON, J.D. 1965. Measurement of brine droplet migration in ice. J. Appl. Phys., v. 36, no. 12, pp. 3811-3815.

_____ and TILLER, W.A. 1963. Ice interface morphology and texture developed during freezing. J. Appl. Phys., v. 34, no. 11, pp. 3349-3355.

HIGASHI, A. 1958. Experimental study of frost heaving. U.S. Army CRREL, Research Report 45, 44 p.

HILLIG, W.B. 1958. The kinetics of freezing of ice in the direction perpendicular to the basal plane, pp. 350-359, in Growth and Perfection of Crystals, ed. by R.H. Doremus, B.W. Roberts and D. Turnbull, J. Wiley, N.Y., 932 p.

_____ and TURNBULL, D. 1956. Theory of crystal growth in undercooled pure liquids. J. Chem. Phys., v. 24, no. 4, p. 914.

HOEKSTRA, P., and MILLER, R.D. 1967. On the mobility of water molecules in the transition layer between ice and solid surface, J. Coll. Sci., v. 25, no. 2, pp. 166-173.

HOOKE, R. LeB., DAHLIN, B.C., and KAUPER, M.T. 1972. Creep of ice containing dispersed fine sand. J. Glac., v. 11, no. 63, pp. 327-336.

JESSOP, A.M. 1970. How to beat permafrost problems. Oilweek, Jan. 12., pp. 22-25.

KAMB, B. 1959. Ice petrofabric observations from Blue Glacier, Washington, in relation to theory and experiment. J. Geoph. Res., v. 64, no. 11, pp. 1891-1909.

_____ 1972. Experimental recrystallization of ice under stress. pp. 211-241, in "Flow and Fracture of Rocks", ed. by H.C. Heard, I.Y. Borg., N.L. Carter, C.B. Raleigh, A.G.U. Monograph 16, 352 p.

KATASONOV, E.M. 1967. Features of deposits formed under permafrost conditions. pp. 237-240, in Arctic and Alpine Environments, ed. by H.E. Wright and W.H. Osburn Jr., Indiana Univ. Press, Bloomington, Ind., 308 p.

KETCHAM, W.M., and HOBBS, P.V. 1967. The preferred orientation in the growth of ice from the melt. J. Crystal Growth, v. 1, pp. 263-270.

KHEISIN, D.H., and CHEREPANOV, N.V. 1969. Modification of the form of gas bubbles in ice. Problemy Arktiki i Antarktiki, v. 32, pp. 100-105 (in Russian).

KNIGHT, C.A. 1962a. Studies of Arctic lake ice. J. Glac., v. 4, no. 33, pp. 319-335.

_____ 1962b. Polygonization of aged sea ice. J. Geol., v. 70, no. 2, pp. 240-245.

KNIGHT, C.A. 1966. Grain boundary migration and other processes in the formation of ice sheets on water. J. Appl. Phys., v. 37, no. 2, pp. 568-574.

_____ 1971. Experiments on the contact angle of water on ice. Phil. Mag. v. 23, no. 181 (8th series), pp. 153-165.

KREITNER, J.D. 1969. The petrofabrics of aufeis in a turbulent Alaskan stream. Unpubl. M.Sc. thesis, Univ. of Alaska, 59 p.

KUON, L.G., and JONAS, J.J. 1973. Effect of strain rate and temperature on the microstructure of polycrystalline ice. pp. 370-376, in Physics and Chemistry of Ice, ed. by E. Whalley, S.J. Jones, L.W. Gold, Roy. Soc. Can., Ottawa, 403 p.

LACHENBRUCH, A.H. 1962. Mechanics of thermal contraction cracks and ice wedge polygons in permafrost. Geol. Soc. Am. Spec. Paper 70, 69 p.

_____ BREWER, M.C., GREENE, G.W., and MARSHALL, B.W. 1962. Temperatures in permafrost. pp. 791-803, in Temperature: Its Measurement and Control in Science and Industry, v. 3, pt. 1, ed. by F.G. Brickwedde, Reinhold Publ. Co., New York, 848 p.

LADANYI, B. 1972. An engineering theory of creep of frozen soils. Can. Geotech. J., v. 9, no. 1, pp. 63-80.

LANGWAY, C.C. 1958. Ice fabrics and the universal stage. U.S. Army CRREL, Technical Report 62, 16 p.

LEES, D.C.G. 1946. The hot-tearing tendencies of aluminum casting alloys. J. Inst. Met., v. 72, pp. 343-364.

LINELL, K.A., and KAPLAR, C.W. 1966. Description and classification of frozen soils. U.S. Army CRREL, Technical Report 150, 10 p.

LYONS, J.B. and STOIBER, R.E. 1962. Orientation fabrics in lake ice. J. Glac., v. 4, no. 33, pp. 367-370.

MACKAY, J.R. 1962. Pingos of the Pleistocene Mackenzie Delta area. Geogr. Bull., no. 18, pp. 21-63.

_____ 1963. The Mackenzie Delta area, N.W.T. Geogr. Branch, Dept. Mines Tech. Surveys, Memoir 8, Ottawa: Queens Printer, 202 p.

_____ 1966. Segregated epigenetic ice and slumps in permafrost, Mackenzie Delta area, N.W.T. Geogr. Bull., no. 8, pp. 59-80.

_____ 1971. The origin of massive icy beds in permafrost, Western Arctic Coast, Canada. Can. J. Earth Sci., v. 8, no. 4, pp. 397-422.

_____ 1972a. Offshore permafrost and ground ice, Southern Beaufort Sea, Canada. Can. J. Earth Sci., v. 9, no. 11, pp. 1550-1561.

MACKAY, J.R.  1972b.  The world of underground ice.  Ann. Ass. Am. Geog.,
     v. 62, no. 1, pp. 1-22.

_____  1972c.  Permafrost and ground ice.  pp. 235-248, in Proceedings,
     Canadian Northern Pipeline Research Conference.  Nat. Res. Counc.
     Can., Assoc. Comm. Geotech. Res., Tech. Man. No. 104, 331 p.

_____  1972d.  Some observations on ice-wedges, Garry Island, N.W.T.
     pp. 131-139, in Mackenzie Delta area monograph, 22nd Int. Geog. Cong.,
     ed. by D.E. Kerfoot, Brock Uni., 174 p.

_____  1972e.  Some observations on the growth of pingos.  pp. 141-148,
     in Mackenzie Delta area monograph, 22nd Int., Geog. Cong., ed. by
     D.E. Kerfoot, Brock Uni., 174 p.

_____  1973a.  The growth of pingos, Western Arctic Coast, Canada.  Can.
     J. Earth Sci., v. 10, no. 6, pp. 979-1004.

_____  1973b.  Problems in the origin of massive ice beds, Western Arctic,
     Canada.  pp. 223-228, in Permafrost:  The North American Contribution
     to the Second International Conference, Nat. Acad. Sci., Washington,
     D.C., 783 p.

_____  1974a.  Ice-wedge cracks, Garry Island, Northwest Territories.
     Can. J. Earth Sci., v. 11, no. 10, pp. 1366-1383.

_____  1974b.  Reticulate ice veins in permafrost, Northern Canada.
     Can. Geotech. J., v. 11, no. 2, pp. 230-237.

_____  1974c.  Seismic shot holes and ground temperatures, Mackenzie Delta
     area, Northwest Territories.  Geol. Surv. Can., Paper 74-1, Part A,
     pp. 389-390.

_____  1974d.  The rapidity of tundra polygon growth and destruction,
     Tuktoyaktuk Peninsula-Richards Island area, N.W.T., Geol. Surv.
     Can., Paper 74-1, Part A, pp. 391-392.

_____  1975a.  Relict ice wedges, Pelly Island, N.W.T. (107C/12).  Geol.
     Surv. Can., Paper 75-1, Part A, pp. 469-470.

_____  1975b.  Freezing processes at the bottom of permafrost, Tuktoyaktuk
     Peninsula area, District of Mackenzie (107C).  Geol. Surv. Can.,
     Paper 75-1, Part A, pp. 471-474.

_____  1975c.  Reticulate ice veins in permafrost, Northern Canada:
     Reply. Can. Geotech. J., v. 12, no. 1, pp. 163-165.

_____  1975d.  The stability of permafrost and recent climatic change in
     the Mackenzie Valley, N.W.T.  Geol. Surv. Can., Paper 75-1, Part B,
     pp. 173-176.

MACKAY, J.R. and BLACK, R.F. 1973. Origin, Composition and Structure of Perennially Frozen Ground and Ground Ice: A Review. pp. 185-192, in Permafrost: The North American Contribution to the Second International Conference. Nat. Acad. Sci., Washington, D.C., 783 p.

_____, RAMPTON, V.N., and FYLES, J.G. 1972. Relic permafrost, Western Arctic, Canada. Science, v. 176, no. 4041, pp. 1321-1323.

_____ and STAGER, J.K. 1966a. Thick tilted beds of segregated ice, Mackenzie Delta area, N.W.T. Biul. Perygl., no. 15, pp. 39-43.

_____, _____ 1966b. The structure of some pingos in the Mackenzie Delta area, N.W.T. Geog. Bull., no. 4, pp. 360-368.

MAENO, N. 1967. Air bubble formation in ice crystals. pp. 207-218, in Int. Conf. on Physics of Snow and Ice, v.1, pt. 1, ed. by H. Ôura, The Inst. of Low Temp. Sci., Hokkaido Univ., Sapporo, Japan, 711 p.

McROBERTS, E.C., and NIXON, J.F. 1975. Reticulate Ice Veins, in Permafrost, Northern Canada: Discussion. Can. Geotech. J., v. 12, no. 1, pp. 159-162.

MICHEL, B., and RAMSEIER, R.O. 1971. Classification of river and lake ice. Can. Geotech. J., v. 8, no. 36, pp. 36-45.

MÜLLER, F. 1963. Observations on pingos. Nat. Res. Counc. Can., Tech. Trans. 1073, 117 p.

PENNER, E. 1961. Ice-grain structure and crystal orientation in an ice lens from Leda clay. Geol. Soc. Am. Bull., v. 72, no. 10, pp. 1575-1578.

PEREY, F.G.J., and POUNDER, E.R. 1958. Crystal orientation in ice sheets. Can. J. Phys., v. 36, no. 4, pp. 494-502.

PÉWÉ, T.L. 1962. Ice wedges in permafrost, Lower Yukon River area near Galena, Alaska. Biul. Perygl. No. 11, pp. 65-76.

POHL, R.G. 1954. Solute redistribution by recrystallization. J. Appl. Phys., v. 25, no. 9, pp. 1170-1178.

POPOV, A.I. 1967. Permafrost phenomena in the earth's crust. Cryolithology (in Russian). Moscow Univ. Press, Moscow, U.S.S.R., 304 p.

PORSILD, A.E. 1938. Earth mounds in unglaciated arctic north-western America. Geog. Rev., v. 28, no. 1, pp. 46-58.

POUNDER, E.R. 1963. Crystal growth rates as a function of orientation. pp. 226-231, in Ice and Snow, ed. by W.D. Kingery, M.I.T. Press, Camb., Mass., 684 p.

RAGLE, R.H. 1963. Formation of lake ice in a temperate climate. U.S. Army CRREL, Research Report 107, 25 p.

RAMPTON, V.N. 1972a. An outline of the Quaternary geology of the lower Mackenzie region. pp. 7-14, in Mackenzie Delta area monograph, 22nd Int. Geog. Cong., ed. by D.E. Kerfoot, Brock Univ., 174 p.

_____ 1972b. Surficial deposits of portions of the Mackenzie Delta (107c), Stanton (107D), Cape Dalhousie (107E) and Malloch Hill (97F) map-sheets. pp. 15-28, in Mackenzie Delta area monograph, 22nd Int. Geog. Cong., ed. D.E. Kerfoot, Brock Univ., 174 p.

_____ and MACKAY, J.R. 1971. Massive ice and icy sediments throughout the Tuktoyaktuk Peninsula, Richards Island, and nearby areas, District of Mackenzie. Geol. Surv. Can., Paper 71-21, 16 p.

_____ and WALCOTT, R.I. 1974. Gravity profiles across ice-cored topography. Can. J. Earth Sci., v. 11, no. 1, pp. 110-122.

RAYBOULD, J.G. 1975. Tectonic control on the formation of some fibrous quartz veins, Mid-Wales. Geol. Mag. v. 112, no. 1, pp. 81-90.

SAVAGE, W.F., and ARONSON, A.H. 1966. Preferred orientation in the weld fusion zone. Weld. Res. Suppl., v. 45, pp. 85-89.

SHUMSKII, P.A. 1958. The mechanism of ice straining and its recrystallization. I.A.S.H., Publ. No. 47, pp. 244-248.

_____ 1964. Principles of structural glaciology (transl. D. Krausz). Dover Publications, N.Y., 497 p.

_____ and VTIURIN, B.I. 1966. Underground Ice. pp. 108-113, in Proc. Permafrost Int. Conf., Lafayette, Indiana, Nov. 1963. Nat. Acad. Sci., N.R.C., Publ. 1287, Washington, D.C., 563 p.

SMITH, C.S. 1953. Measurement of internal boundaries in three-dimensional structures by random sectioning. Trans. A.I.M.E., v. 197, pp. 81-87.

STEHLE, N.S. 1967. Migration of bubbles in ice under a temperature gradient. pp. 219-232, in Physics of Snow and Ice, v.1, pt. 1, ed. by H. Ôura, Inst. of Low Temp. Sci., Hokkaido Univ., Sapporo, Japan, 711 p.

STEINEMANN, S. 1954. Flow and recrystallization of ice. I.U.G.G., I.A.S.H., Rome Gen. Ass., Tome IV, pp. 449-462.

_____ 1958. Experimentelle untersuchungen zur plastizität von eis. Beitr. zur Geologie der Schweiz, Hydrologie, no. 10, 72 p.

SUMGHIN, M.I., 1940. On the formation of perennial ice mounds, bulgunniakhs. Comptes Rendus (Doklady) de l'Academie des Sciences de l'U.R.S.S., v. 28, pp. 156-157.

SWINZOW, G.K. 1966. Ice cover of an arctic proglacial lake. U.S. Army CRREL, Research Report No. 155, 43 p.

TABER, S. 1930. The mechanics of frost heaving. J. Geol., v. 38, no. 4, pp. 303-317.

TILLER, W.A. 1957. The modification of eutectic structures. Acta. Met., v. 5, no. 1, pp. 56-58.

UHLMANN, D.H., CHALMERS, B., and JACKSON, K.A. 1964. Interaction between particles and a solid-liquid interface. J. Appl. Phys., v. 35, no. 10, pp. 2986-2993.

VASCONCELLOS, K.F., and BEECH, J. 1975. The development of blowholes in the ice/water/$CO_2$ system. J. Crystal Growth, v. 28, no. 1, pp. 85-92.

VTIURINA, E.A., and VTIURIN, B.I. 1970. Ice formation in rocks (in Russian). Izdatelstro "Nauka", Moscow, 280 p.

WEEKS, W.F., and ASSUR, A. 1964. Growth, structure and strength of sea ice. U.S. Army CRREL, Research Report 135, 19 p.

WILLIAMS, P.J. 1967. The nature of freezing soil and its field behaviour. Norweg. Geotech. Inst. Publ. no. 72, pp. 91-119.

## Ground Ice Classification (modified from Mackay 1972(b))
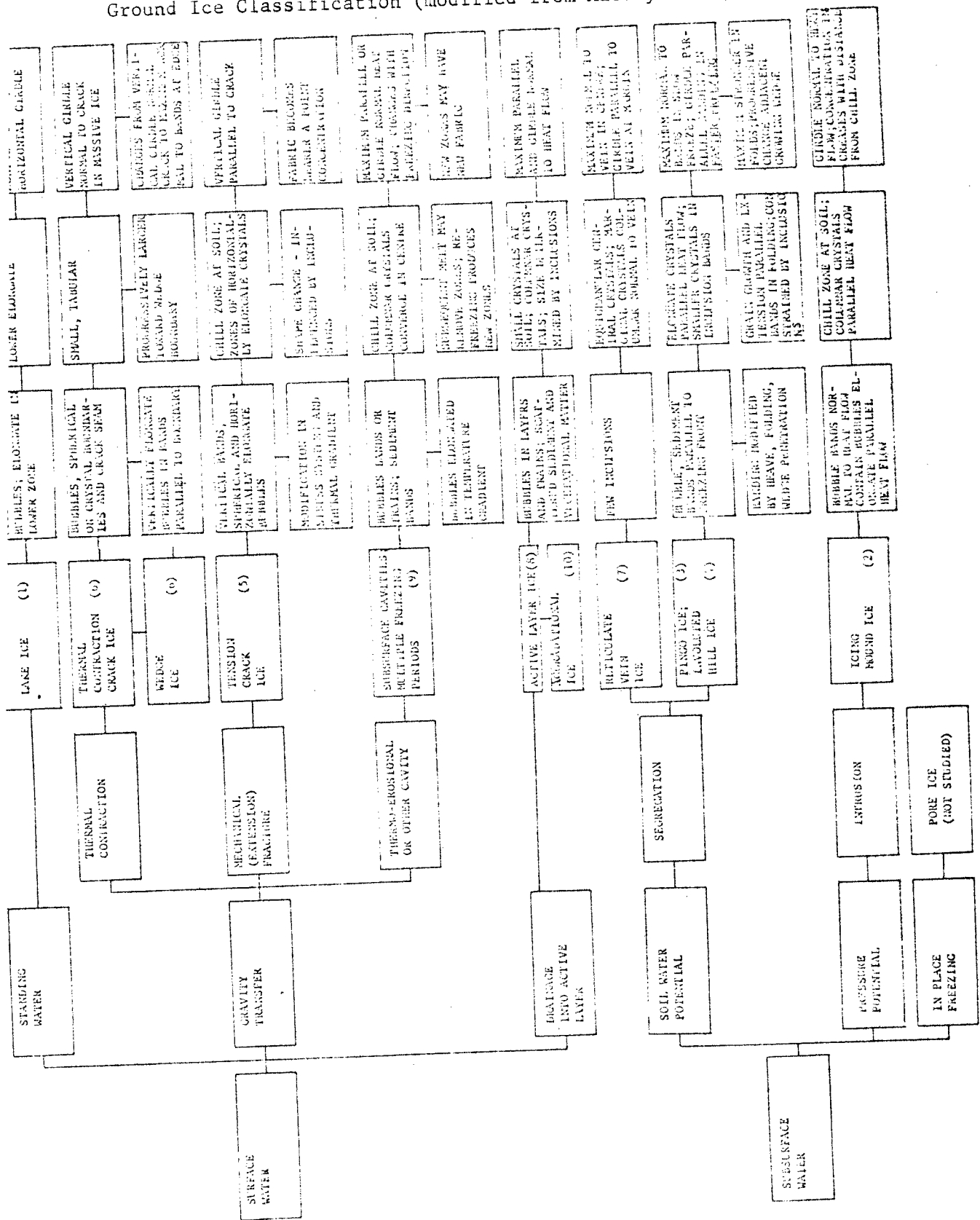
Appendix 2

## GLOSSARY

Anhedral - Descriptive of crystals on which crystal faces are absent.

Annealing - Recovery and recrystallization due to heating of deformed material.

Basal plane - (0001) plane, normal to c-axis or optic axis, in ice crystal.

Chill zone - A boundary layer, adjacent to a cooling surface, of small, equigranular crystals with random orientations.

Columnar crystals - Elongate crystals aligned parallel to the direction of heat flow.

Defect - Imperfection in crystal lattice, e.g. missing or extra atoms, impurities, dislocations.

Deformation band - Deformation-induced crystal layer differing in orientation from remainder.

Dendrites - Lattice controlled projections of crystals at advancing interface.

Dislocation - Linear lattice defect, produced during growth or under subsequent stress; important in deformation (see slip).

Dislocation climb - Movement of dislocation out of its slip plane, e.g. over an obstacle.

Grain boundary migration - Displacement of a boundary perpendicular to its tangent plane.

Grain growth - Increase in grain size of polycrystalline aggregate at elevated temperature under a driving force of reduction in surface energy.

Lineage structure - Dislocation arrays parallel to growth direction, formed during growth.

Polygonization - Formation of low angle boundaries separating unstrained lattice segments during recovery of strained lattice.

Recovery - Removal of residual stresses of deformation.

Recrystallization - Nucleation of new, strain-free grains in a deformed matrix.

Slip - Sliding displacement of one part of a crystal relative to another by dislocation motion parallel to planes of high atomic density.

Subgrains - Lattice segments of a grain, separated by low angle boundaries.